frontiers | Research Topics

Mapping psychopathology with MRI and connectivity analysis

Edited by
Long-Biao Cui, Min Cai, Baojuan Li, Hua-ning Wang, Yongbin Wei and Hong Yin

Published in
Frontiers in Human Neuroscience

ISSN 1664-8714
ISBN 978-2-83251-694-2
DOI 10.3389/978-2-83251-694-2

About Frontiers

Frontiers is more than just an open access publisher of scholarly articles: it is a pioneering approach to the world of academia, radically improving the way scholarly research is managed. The grand vision of Frontiers is a world where all people have an equal opportunity to seek, share and generate knowledge. Frontiers provides immediate and permanent online open access to all its publications, but this alone is not enough to realize our grand goals.

Frontiers journal series

The Frontiers journal series is a multi-tier and interdisciplinary set of open-access, online journals, promising a paradigm shift from the current review, selection and dissemination processes in academic publishing. All Frontiers journals are driven by researchers for researchers; therefore, they constitute a service to the scholarly community. At the same time, the *Frontiers journal series* operates on a revolutionary invention, the tiered publishing system, initially addressing specific communities of scholars, and gradually climbing up to broader public understanding, thus serving the interests of the lay society, too.

Dedication to quality

Each Frontiers article is a landmark of the highest quality, thanks to genuinely collaborative interactions between authors and review editors, who include some of the world's best academicians. Research must be certified by peers before entering a stream of knowledge that may eventually reach the public - and shape society; therefore, Frontiers only applies the most rigorous and unbiased reviews. Frontiers revolutionizes research publishing by freely delivering the most outstanding research, evaluated with no bias from both the academic and social point of view. By applying the most advanced information technologies, Frontiers is catapulting scholarly publishing into a new generation.

What are Frontiers Research Topics?

Frontiers Research Topics are very popular trademarks of the *Frontiers journals series*: they are collections of at least ten articles, all centered on a particular subject. With their unique mix of varied contributions from Original Research to Review Articles, Frontiers Research Topics unify the most influential researchers, the latest key findings and historical advances in a hot research area.

Find out more on how to host your own Frontiers Research Topic or contribute to one as an author by contacting the Frontiers editorial office: frontiersin.org/about/contact

Mapping psychopathology with MRI and connectivity analysis

Topic editors

Long-Biao Cui — Air Force Medical University, China
Min Cai — Fourth Military Medical University, China
Baojuan Li — Massachusetts General Hospital, Harvard Medical School, United States
Hua-ning Wang — Air Force Medical University, China
Yongbin Wei — Beijing University of Posts and Telecommunications (BUPT), China
Hong Yin — Fourth Military Medical University, China

Citation

Cui, L.-B., Cai, M., Li, B., Wang, H.-n., Wei, Y., Yin, H., eds. (2023). *Mapping psychopathology with MRI and connectivity analysis*. Lausanne: Frontiers Media SA. doi: 10.3389/978-2-83251-694-2

Table of contents

frontiers | Frontiers in Human Neuroscience

TYPE Editorial
PUBLISHED 01 February 2023
DOI 10.3389/fnhum.2023.1141569

OPEN ACCESS

EDITED AND REVIEWED BY
Mingzhou Ding,
University of Florida, United States

*CORRESPONDENCE
Baojuan Li
✉ libjuan@fmmu.edu.cn

SPECIALTY SECTION
This article was submitted to Brain Imaging and Stimulation, a section of the journal Frontiers in Human Neuroscience

RECEIVED 10 January 2023
ACCEPTED 13 January 2023
PUBLISHED 01 February 2023

CITATION
Cui L-B, Wei Y, Cai M, Wang H-N, Yin H and Li B (2023) Editorial: Mapping psychopathology with MRI and connectivity analysis.
Front. Hum. Neurosci. 17:1141569.
doi: 10.3389/fnhum.2023.1141569

Editorial: Mapping psychopathology with MRI and connectivity analysis

Long-Biao Cui[1,2], Yongbin Wei[3], Min Cai[4], Hua-Ning Wang[4], Hong Yin[5] and Baojuan Li[6]*

[1]Department of Radiology, The Second Medical Center, Chinese PLA General Hospital, Beijing, China, [2]Schizophrenia Imaging Laboratory, Fourth Military Medical University, Xi'an, China, [3]Complex Traits Genetics Lab, Vrije Universiteit Amsterdam, Amsterdam, Netherlands, [4]Department of Psychiatry, Xijing Hospital, Fourth Military Medical University, Xi'an, China, [5]Department of Radiology, Xi'an People's Hospital, Xi'an, China, [6]School of Biomedical Engineering, Fourth Military Medical University, Xi'an, China

KEYWORDS

psychiatric disorders, neurological diseases, connectivity, mapping, magnetic resonance imaging

Editorial on the Research Topic
Mapping psychopathology with MRI and connectivity analysis

Different connections exist between different neurons and brain regions, constituting a complex and extensive brain network. Modern brain science research shows that the realization of many higher cognitive functions relies on the synergistic cooperation between different brain regions, not just on a specific brain region. The pathogenesis of many neurological and psychiatric disorders (e.g., schizophrenia, depression, etc.) is, to some extent, due to abnormalities in the connections between related brain regions. Brain connections at the macroscale can be classified into three types: structural connectivity, functional connectivity, and effective connectivity. Structural connectivity refers to the anatomical connections between brain regions. Functional connectivity uses signals recorded from different brain regions to calculate a certain index reflecting the strength of the relationship between brain regions. In contrast, effective connectivity is a causal and directional influence. In contrast to functional and structural connectivity, effective connectivity can establish causal relationships between the actions of different brain regions and may provide insights to explore psychopathology's neural mechanisms.

The present Frontiers Research Topic entitled "*Mapping psychopathology with MRI and connectivity analysis*" is part of the article collection series, "*Mapping psychopathology with fMRI and effective connectivity analysis*" (https://www.frontiersin.org/research-topics/3471/mapping-psychopathology-with-fmri-and-effective-connectivity-analysis). This Research Topic aims to introduce the use of magnetic resonance imaging (MRI) to investigate the neural mechanisms underlying neurological and psychiatric disorders (e.g., major depressive disorder, schizophrenia, Parkinson's disease, etc.). In addition, treatment effects were taken as the focus of the Research Topic, which included neuromodulation and psychotropic drugs, on the directional coupling between brain regions and whether alterations in connectivity persisted in subjects in remission.

At the macroscale, the human brain can be considered a complex and large network system consisting of structural and functional connections of different brain regions (Zhao et al.). Neuroimaging techniques have become a powerful method to study the structure, function, and metabolism of the brain in methamphetamine users (Yang et al.). Wang et al. enrolled diffusion weighted imaging (DWI) data of 42 adults with attention-deficit/hyperactivity disorder (ADHD) and 59 typically developing adults to explore the presence of abnormal

connectomes in rich club structures in the brains of adults with ADHD, and the results showed that ADHD patients had reduced density of rich clubs in central structural nodes, mainly located in the insula, bilateral precuneus, left putamen, caudate nucleus, and right calcarine (Wang et al., 2021).

Functional MRI (fMRI) has emerged as an effective technique for the study of psychiatric disorders (Agoalikum et al.). Current neuroimaging findings suggest that major depression is not a dysfunction of a single brain region but associated with brain network dysfunction. An fMRI study of patients with major depressive disorder showed a significant decrease in the amplitude of low-frequency fluctuation and fractional amplitude of low-frequency fluctuation in the right precentral gyrus, a decrease in degree centrality in the left triangular part of the inferior frontal gyrus, and an increase in the left hippocampus after electroconvulsive therapy treatment (Li X. et al.). Agoalikum et al. used resting-state fMRI data to recognize disrupted brain connectivity differences among children, adolescents, and adults with ADHD. Their results showed that abnormal dynamic interactions and connectivity deficits were correlated with different groups and that these abnormalities differed between children, adolescents, and adults with ADHD. Li H. et al. studied changes in the functional connectivity of the vermis and brain regions in subjects with bipolar disorder at the resting state, and patients with bipolar disorder had reduced resting-state functional connectivity in the vermis and ventral prefrontal cortex compared to the HC group. A meta-analysis of patients with obsessive-compulsive disorder showed that the most consistent local connectivity abnormalities in obsessive-compulsive disorder patients occurred in the prefrontal cortex (Qing et al.). Gao et al. selected the striatum as a seed for functional connectivity analysis and found altered functional connectivity in the cortico-striatal network in patients with primary unilateral hemifacial spasm compared to healthy controls. In another study, functional connectivity changes in patients with vestibular migraine were assessed using resting-state functional connectivity analysis and compared with healthy controls. The results found that patients had reduced functional connectivity between the left inferior/middle temporal gyrus and supplementary motor area/the left superior frontal gyrus (Zhe et al.). Previous studies have confirmed that there are some changes in brain structure and function in patients with schizophrenia (Zhao et al.). Studies on local function in schizophrenia have found that cognitive dysfunction in schizophrenia is related to the function of the lentiform nucleus (Li P. et al.). Previous studies reported negative functional connectivity between the right lateral prefrontal cortex and the left putamen (Quide et al., 2013). One study found that quantitative and specific functional connectivity biomarkers may be valid radiomics signatures for individualized diagnosis of schizophrenia (Cui et al., 2018). In another study, Zhang Y. et al. found abnormal connectivity in brain language areas in patients with hallucinations.

However, the changes in the information flow, as measured by effective connectivity, of these distributed systems are still largely unknown. It has been shown that brain connectivity changes dynamically during the development of psychiatric disorders (Insel, 2010). Effective connectivity, as a type of brain connectivity, measures serve as promising biomarkers of schizophrenia (Li et al., 2017; Mastrovito et al., 2018). One study explored changes in causal connections between brain regions in adolescent-onset schizophrenia (AOS) patients and observed effective connectivity between the left superior temporal gyrus and the other four brain regions in the right hemisphere (superior frontal gyrus, angular gyrus, insula, and middle occipital gyrus) was impaired in patients with AOS. The results suggest that altered directional connectivity in the left superior temporal gyrus may have a significant effect on the development of AOS and as a possible biomarker for this disease (Lyu et al., 2021). Xi et al. obtained fMRI from first-degree relatives of patients with schizophrenia and found increased connectivity from the left anterior cingulate cortex to the right hippocampus and decreased connectivity from the right anterior cingulate cortex to the right hippocampus in patients' relatives compared to healthy controls (Xi et al., 2016). In another study, abnormalities in anterior cingulate cortex-related connections in the first schizophrenia *in vivo* were revealed by spectral dynamic causal modeling (Cui et al., 2015).

To summarize, this Research Topic highlights the application of MRI and connectivity analysis in the study of neurological and mental disorders. Furthermore, connectivity analysis using MRI data may provide a deeper understanding of the neural mechanisms of psychopathology.

Author contributions

L-BC, YW, MC, H-NW, HY, and BL drafted and revised the manuscript. All authors contributed to the article and approved the submitted version.

Funding

This work was supported by the grant from National Natural Science Foundation of China (Nos. 61976248 and 82271949).

Acknowledgments

We thank Xiao-Fan Liu for comments on this Editorial. We thank Mingrui Xia and all authors for their contribution to our Research Topic.

Conflict of interest

The authors declare that the research was conducted in the absence of any commercial or financial relationships that could be construed as a potential conflict of interest.

Publisher's note

References

Cui, L. B., Liu, J., Wang, L. X., Li, C., Xi, Y. B., Guo, F., et al. (2015). Anterior cingulate cortex-related connectivity in first-episode schizophrenia: A spectral dynamic causal modeling study with functional magnetic resonance imaging. *Front. Hum. Neurosci.* 9, 589. doi: 10.3389/fnhum.2015.00589

Cui, L. B., Liu, L., Wang, H. N., Wang, L. X., Guo, F., Xi, Y. B., et al. (2018). Disease definition for schizophrenia by functional connectivity using radiomics strategy. *Schizophr. Bull.* 44, 1053–1059. doi: 10.1093/schbul/sby007

Insel, T. R. (2010). Rethinking schizophrenia. *Nature* 468, 187–193. doi: 10.1038/nature09552

Li, B., Cui, L. B., Xi, Y. B., Friston, K. J., Guo, F., Wang, H. N., et al. (2017). Abnormal effective connectivity in the brain is involved in auditory verbal hallucinations in schizophrenia. *Neurosci. Bull.* 33, 281–291. doi: 10.1007/s12264-017-0101-x

Lyu, H., Jiao, J., Feng, G., Wang, X., Sun, B., Zhao, Z., et al. (2021). Abnormal causal connectivity of left superior temporal gyrus in drug-naive first- episode adolescent-onset schizophrenia: A resting-state fMRI study. *Psychiatry Res. Neuroimaging* 315, 111330. doi: 10.1016/j.pscychresns.2021.111330

Mastrovito, D., Hanson, C., and Hanson, S. J. (2018). Differences in atypical resting-state effective connectivity distinguish autism from schizophrenia. *Neuroimage Clin. (2018)* 18, 367–376. doi: 10.1016/j.nicl.01, 014.

Quide, Y., Morris, R. W., Shepherd, A. M., Rowland, J. E., and Green, M. J. (2013). Task-related fronto-striatal functional connectivity during working memory performance in schizophrenia. *Schizophr. Res. (2013)* 150, 468–475. doi: 10.1016/j.schres.08, 009.

Wang, B., Wang, G., Wang, X., Cao, R., Xiang, J., Yan, T., et al. (2021). Rich-club analysis in adults with ADHD connectomes reveals an abnormal structural core network. *J. Atten. Disord.* 25, 1068–1079. doi: 10.1177/1087054719883031

Xi, Y. B., Li, C., Cui, L. B., Liu, J., Guo, F., Li, L., et al. (2016). Anterior cingulate cortico-hippocampal dysconnectivity in unaffected relatives of schizophrenia patients: A stochastic dynamic causal modeling study. *Front. Hum. Neurosci.* 10, 383. doi: 10.3389/fnhum.2016.00383

frontiers in Human Neuroscience

ORIGINAL RESEARCH
published: 16 July 2021
doi: 10.3389/fnhum.2021.711688

Decreased Functional Connectivity of Vermis-Ventral Prefrontal Cortex in Bipolar Disorder

Huanhuan Li[1†], *Hu Liu*[1†], *Yanqing Tang*[2], *Rongkai Yan*[3,4], *Xiaowei Jiang*[1,2,5], *Guoguang Fan*[1*] *and Wenge Sun*[1*]

[1]*Department of Radiology, The First Hospital of China Medical University, Shenyang, China,* [2]*Department of Psychiatry, The First Hospital of China Medical University, Shenyang, China,* [3]*Department of Radiology, The Second Affiliated Hospital of Hainan Medical University, Haikou, China,* [4]*Department of Radiology, Johns Hopkins University School of Medicine, Baltimore, MD, United States,* [5]*Brain Function Research Section, The First Hospital of China Medical University, Shenyang, China*

OPEN ACCESS

Edited by:
Long-Biao Cui, People's Liberation Army General Hospital, China

Reviewed by:
Jie Gong, Xidian University, China
Wen-Jun Wu, Fourth Military Medical University, China

***Correspondence:**
Guoguang Fan
fanguog@sina.com
Wenge Sun
wengesun@sina.com

[†]*These authors have contributed equally to this work*

Specialty section:
This article was submitted to Brain Imaging and Stimulation, a section of the journal Frontiers in Human Neuroscience

Received: *19 May 2021*
Accepted: *25 June 2021*
Published: *16 July 2021*

Citation:
Li H, Liu H, Tang Y, Yan R, Jiang X, Fan G and Sun W (2021) Decreased Functional Connectivity of Vermis-Ventral Prefrontal Cortex in Bipolar Disorder. Front. Hum. Neurosci. 15:711688. doi: 10.3389/fnhum.2021.711688

Objectives: To investigate changes in functional connectivity between the vermis and cerebral regions in the resting state among subjects with bipolar disorder (BD).

Methods: Thirty participants with BD and 28 healthy controls (HC) underwent the resting state functional magnetic resonance imaging (fMRI). Resting-state functional connectivity (rsFC) of the anterior and posterior vermis was examined. For each participant, rsFC maps of the anterior and posterior vermis were computed and compared across the two groups.

Results: rsFC between the whole vermis and ventral prefrontal cortex (VPFC) was significantly lower in the BD groups compared to the HC group, and rsFC between the anterior vermis and the middle cingulate cortex was likewise significantly decreased in the BD group.

Limitations: 83.3% of the BD participants were taking medication at the time of the study. Our findings may in part be attributed to treatment differences because we did not examine the effects of medication on rsFC. Further, the mixed BD subtypes in our current study may have confounding effects influencing the results.

Conclusions: These rsFC differences of vermis-VPFC between groups may contribute to the BD mood regulation.

Keywords: bipolar disorder, resting state, functional connectivity, cerebellum, vermis

Abbreviations: BD, Bipolar disorder; MRI, Magnetic resonance imaging; rsFC, Resting-state functional connectivity; fMRI, functional MRI; ROI, Region of interest; HC, Healthy control; HDRS, Hamilton Depression Rating Scale; YMRS, Young Mania Rating Scale; BOLD, Blood oxygen level dependence; GLM, Generalized linear model; FWHM, Full width at half maximum; VPFC, Ventral prefrontal gyrus.

INTRODUCTION

Bipolar disorder (BD) is a severe psychiatric illness characterized by recurrent disturbances in sleep, behavior, perception, cognition, and mood regulation (Goodwin and Geddes, 2007). The cerebellum has long been regarded as a brain structure involved in motor systems (anterior lobe and lobule VI), there is growing contemporary evidence that it influences cognition (posterior lobe) and mood regulation (the vermis; Schutter and Van Honk, 2005; Schmahmann, 2019). The cerebellum's involvement in mood regulation is consistent with earlier clinical studies that suggested the cerebellum functioned as an emotional pacemaker (Heath, 1977; Heath et al., 1979), as well as contemporary evidence that implicates the cerebellar vermis and fastigial nucleus as the limbic cerebellum (Schmahmann, 2001, 2004). The fastigial nucleus, one of the deep cerebellar nuclei, mediates the connection between the vermis and the cerebellar inferior peduncle and connects to the reticular formation and the limbic system through the inferior peduncle (Schmahmann, 2004). The connections between the vermis and both the reticular and limbic system imply that the vermis plays an important role in the regulation of affect (Stoodley and Schmahmann, 2009; Moulton et al., 2011). Some studies found that multi-episode BD patients have smaller vermal V2 and V3 areas *via* structural magnetic resonance imaging (MRI) compared to first-episode patients (DelBello et al., 1999; Mills et al., 2005). These data suggested that the vermis might therefore be subject to atrophy during BD spells. Moreover, mood disorders such as BD have been linked to impairments in anterior limbic brain structures, wherein the cerebellum may modulate mood (Strakowski et al., 2002).

Recent studies of spontaneous resting-state functional connectivity (rsFC) have focused on the BD brain network abnormalities such as abnormal rsFC in the frontotemporal system (Chepenik et al., 2010; Dickstein et al., 2010) and corticolimbic system (Anand et al., 2009). rsFC between the cerebellum and the whole brain can also be defined as the temporal dependency of their neural activation patterns by their coherence in spontaneous fluctuations in resting-state functional MRI (fMRI) signals (Buckner and Vincent, 2007). One recent MRI study found that the cerebellum and basal ganglia are closely correlated with mood states in BD, representing the altered metabolic activity of BD patients' cerebellum (Johnson et al., 2018). Another resting-state fMRI study also found altered cerebellum-brain region connectivity in unmedicated BD (Chen et al., 2019).

In this study, we utilized a region-of-interest (ROI) based approach to examine rsFC in individuals with BD and healthy control (HC) participants. We selected the vermis as ROI and hypothesized that the BD group would show altered rsFC between vermis and cerebral regions which are involved in mood regulation compared to the HC group.

MATERIALS AND METHODS

Subjects

All BD participants were diagnosed using the Structured Clinical Interview for DSM-IV (Bell, 1994) and fulfilled DSM-IV criteria for BD in this study. Using DSM-IV criteria, psychologists of our working group recruited all BD patients from the outpatient center of the First Hospital of China Medical University and Mental Health Center of Shenyang between June 2010 and August 2018. Enrolled patients were consistently aged 18–50 years right-handed, and exhibited neither neurological illness nor head trauma involving loss of consciousness exceeding 5 min, nor any major physical disorder or contraindication for fMRI scanning. Psychologists systematically evaluated the presence or absence of Axis I Disorder for the recruited patients and assessed patients' mood state at scanning according to the DSM-IV Structured Clinical Interview. Psychological examinations of all HCs recruited from the local community were normal, these examinations confirmed no personal histories of mental illness, mood, psychotic, anxiety, or substance misuse disorders in their first-degree family members. Thirty BD patients and 28 HCs were ultimately included in the study population (matched by age and gender, $p > 0.05$). Symptoms were assessed using the Hamilton Depression Rating Scale (HDRS) and the Young Mania Rating Scale (YMRS). Twenty-five (83.3%) of the BD participants were taking medication at the time of scanning. Some of the participants in this study also participated in our previous study (Xu et al., 2014). Their behavioral assessment was made by XJ. All participants were approved by the ethics committee of the first hospital of China Medical University and provided a signed, written informed consent.

At the time of scanning, five (16.7%) participants with BD met DSM-IV criteria for a depressive episode and six (20.0%) for a manic/mixed or hypomanic episode, whereas the remaining 19 (63.3%) were euthymic. Detailed demographic and clinical characteristics of the participants are presented in **Table 1**.

MRI Scanning and Image Preprocessing

All fMRI scans were performed using a 3.0-T GE Signa System (GE Signa, Milwaukee, Wisconsin, USA) in the Department of Radiology, the First Hospital of China Medical University.

TABLE 1 | Demographic and clinical data of subjects.

	Healthy	Bipolar disorder	*P*
N	28	30	NA
Age (years, mean ± SD)	31.38 ± 8.08	30.51 ± 8.79	0.836
Sex (male: female)	13:15	18:12	0.300
HDRS (mean ± SD)	0.40 ± 0.77	9.71 ± 10.12	<0.001
YMRS (mean ± SD)	0.06 ± 0.35	6.43 ± 9.33	<0.001
Medication(yes/no)	NA	25/5	NA
Typical antipsychotics *(N)*	NA	16	NA
Anticonvulsant *(N)*	NA	14	NA
Lithium salts *(N)*	NA	5	NA
Antidepressants *(N)*	NA	11	NA

SD, standard deviation; HDRS, Hamilton Depression Rating Scale; YMRS, Young Mania Rating Scale; NA, not applicable; N, number.

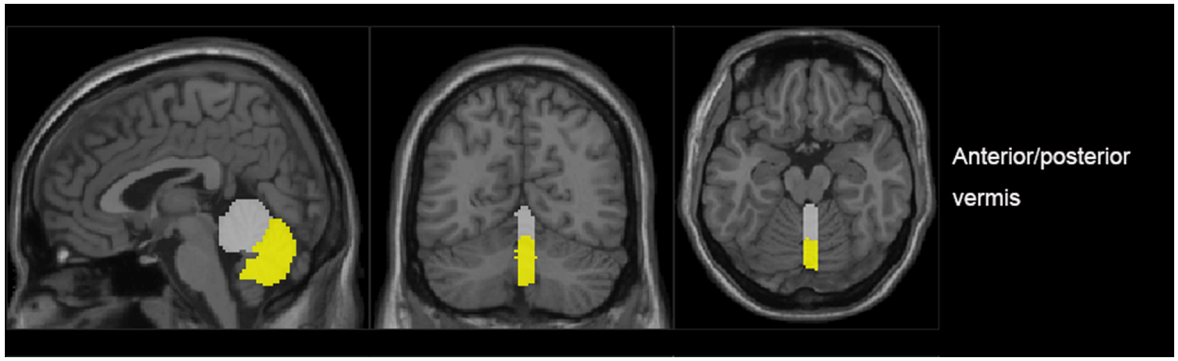

FIGURE 1 | The generated anterior (gray) and posterior (yellow) regions of interest (ROIs) in a representative subject.

The clinician asked the patients to remove any metal jewelry or accessories that might interfere with the machine and briefly introduced the procedure of MRI scanning to reduce the anxiety of patients. Foam pads were provided to reduce head motion and scanner noise when patients were lying down. Technician set the parameter of a 3D-SPGR sequence to acquire three-dimensional T1-weighted images in a sagittal orientation with the repetition time (TR) = 7.1 ms, echo time (TE) = 3.2 ms, field of view (FOV) = 24 cm×24 cm, flip angle = 15°, matrix = 256 × 256, slice thickness = 1.8 mm, no gap. The fMRI scanning was performed in darkness, and an observer stood to one side to ensure the patients kept their eyes closed, relaxing, and moving as little as possible. The slices of functional images were positioned approximately along the AC-PC line using a gradient echo-planar imaging (EPI): TR = 2,000 ms, TE = 30 ms, FOV = 24 cm × 24 cm, flip angle = 90°, matrix = 64 × 64, slice thickness = 3 mm, no gap, slices = 35. For each participant, the fMRI scanning lasted 7 min. Image preprocessing was carried out using SPM8[1] and DPABI (Yan et al., 2016). Preprocessing consisted of slice-time correction, motion correction, spatial normalization, and spatial smoothing full width at half maximum (FWHM = 6 mm). Movement parameters were extracted out by SPM8 for each participant, which can exclude the data sets with more than 2 mm maximum translation along the x, y, or z axes, allowing 2° of maximum rotation about three axes among each image. Further preprocessing consisted of removing linear drift through linear regression and temporal band-pass filtering (0.01–0.08 Hz) to reduce the effects of low-frequency drifts and physiological high-frequency noise.

Definition of ROIs

The vermis was divided into anterior vermis (vermis I-V) and posterior vermis (vermis VI-IX) by AAL (Anatomical automatic labelling; Pfefferbaum et al., 2011; **Figure 1**). For each ROI, the blood oxygen level dependence (BOLD) time series of the voxels within the ROI were averaged to generate the reference time series.

A whole-brain mask was created by taking the intersections of the normalized T1-weighted high-resolution images of all participants, which were stripped using the software BrainSuite2[2].

FC Analysis

A regression generalized linear model (GLM) was created for each participant, including a time series regressor for one of the two vermal subregions, and applied to each of eight nuisance covariates (white matter, cerebrospinal fluid, and six motion parameters). Correlation analysis was performed in a voxel-wise manner between the seed ROIs and the whole brain using DPABI. The correlation coefficients were then transformed to z-values using the Fisher r-to-z transformation for more conforming to Gaussian distribution. A one-sample t-test model was used to delineate the functional connectivity of each vermis ROI in the first-level analysis. Direct comparisons were conducted to identify differences in functional connectivity between BD vs. HC in the second-level random-effects analysis.

Statistical Analyses

Statistical significance was determined by a corrected $P < 0.05$ that combined individual voxel $p_{(\text{uncorrected})} < 0.01$ with GRF (Gaussian random field) correction for cluster-level inference of $p < 0.05$ (Bousse et al., 2012). Additional exploratory analyses (ANCOVA) were performed for effects of medications (overall presence or absence of medication) on the regions that showed significant differences between the HC and BD groups. Finally, significant correlations between HDRS, YMRS in the BD group, and the transformed z-scores showing significant group differences were performed using exploratory correlation analyses to identify the relationship between the symptom severity and the strength of connectivity. A two-tailed p level of 0.05 was used as the criterion of statistical significance.

RESULTS

Regions with changed vermal connectivity between the BD and HC groups are shown in **Table 2**. Compared to the HC

[1]http://www.fil.ion.ucl.ac.uk/spm

[2]http://brainsuite.org

TABLE 2 | Detailed information for clusters showing group connectivity differences in BD at the given threshold (cluster size > 297 mm^3, and $P < 0.00014$).

Voxels	PV_X	PV_Y	PV_Z	H	Brain regions (AAL atlas)	BA	T
Anterior vermis							
104	−6	68	7	L	Ventral prefrontal cortex (Frontal_superior_medial)	10	−5.030
190	7	−16	32	R	Middle cingulate cortex (Cingulum_middle)	23	−4.160
Posterior vermis							
201	−4	69	5	L	Ventral prefrontal cortex (Frontal_superior_medial)	10	−4.430

PV: peak voxel. X, Y, Z: coordinates in the Montreal Neurological Institute space. BA: Brodmann area. T: T values from a t-test of the peak voxel (showing greatest statistical difference within a cluster).

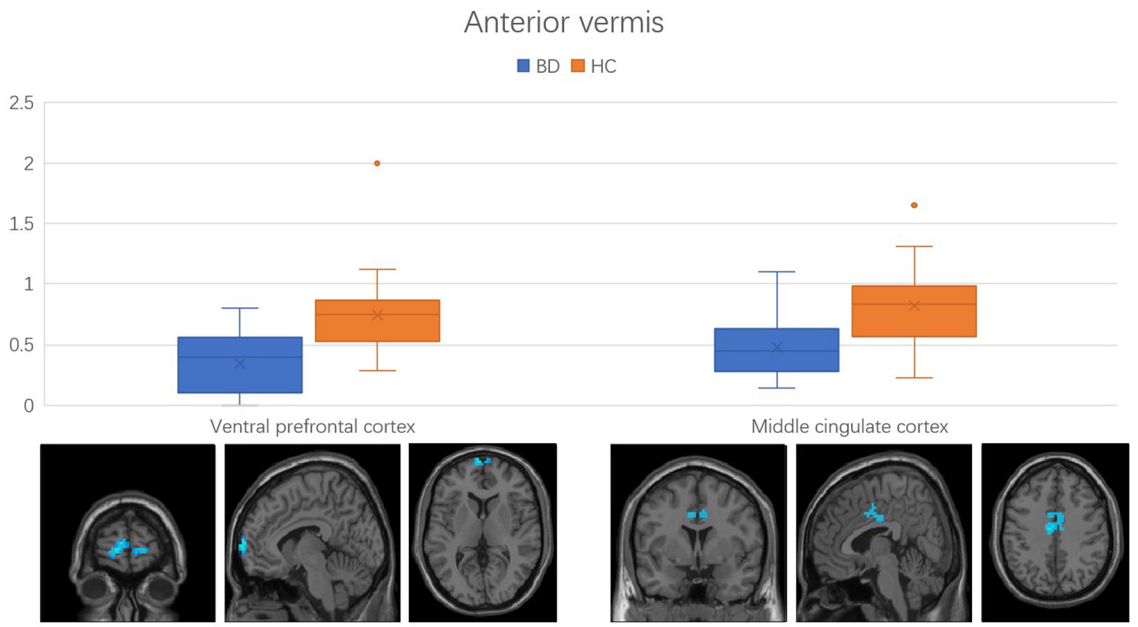

FIGURE 2 | Functional connectivity between anterior vermis and ventral prefrontal cortex, middle cingulate cortex in the comparison between bipolar disorder (BD) and healthy controls (HC) groups. Error bars represent the standard deviation of Z values at the peak voxel. BD, bipolar disorder; HC, healthy control.

group, significant differences in rsFC were observed between the anterior vermis and brain regions that included ventral prefrontal gyrus (VPFC; BA 10) and middle cingulate cortex (BA 24; **Figure 2**), while the posterior vermis showed significant differences in rsFC with VPFC (BA 10) in the BD group (**Figure 3**). In addition, there were no significant effects of medication on FC values in the regions that differed between the HC and BD groups (ANCOVA test, $p > 0.05$). Finally, correlation analysis was performed between the connectivity coefficient within clusters showing significant group differences and behavioral measures as assessed by HDRS, YMRS in the BD group. Analyses of correlations did not show any significant effects between functional connectivity and clinical scores (**Table 3**).

TABLE 3 | The correlation between the strength of these changed connectivity regions and the clinical scores in BD group.

Brain regions	Clinical scores			
	HDRS	P	YMRS	P
Changed connectivity with the anterior vermis				
Ventral prefrontal cortex	−0.307	0.332	−0.434	0.213
Middle cingulate cortex	−0.532	0.143	0.125	0.544
Changed connectivity with the posterior vermis				
Ventral prefrontal cortex	−0.631	0.095	0.154	0.510

The numbers in the table are Pearson's correlation coefficients.

DISCUSSION

The current study examined vermal connectivity in BD patients. We discovered that two cerebral regions (VPFC and middle cingulate cortex) showed decreasing connectivity with the vermis. Previous studies show that these two brain regions exhibited changed neural activity or disturbed connectivity with other cerebral regions. We initially found the connectivity pattern between vermis and these two cerebral regions was similarly disturbed in BD patients.

Previous studies proposed that the vermis can be considered as the "limbic cerebellum," based on its regional connections with limbic structures (Schmahmann, 2001, 2004). Patients with the cerebellar cognitive affective syndrome can show emotional lability, inappropriate laughing or crying, and changes in affection, suggesting that these cerebellar-limbic connections are

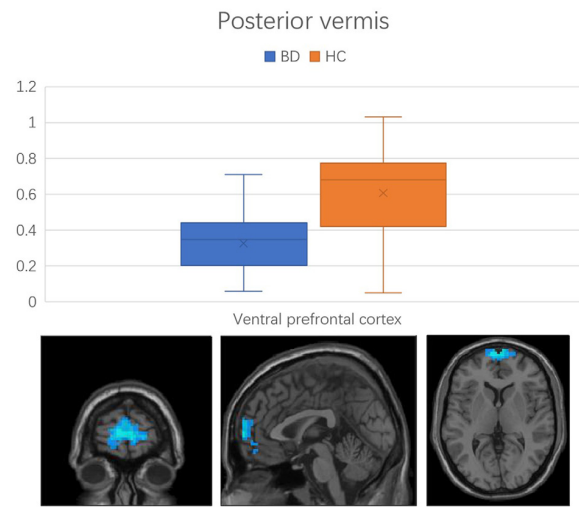

FIGURE 3 | Functional connectivity between the posterior vermis and ventral prefrontal cortex in the comparison between BD and HC groups. Error bars represent the standard deviation of *Z* values at the peak voxel. BD, bipolar disorder; HC, healthy control.

involved in the modulation of emotional processing (Levisohn et al., 2000). What's more, malformations of the posterior vermis have been confirmed to be associated with emotional symptoms (Tavano et al., 2007). These studies implicated the cerebellar vermis, especially the posterior vermis play important roles in mood regulation. Interestingly, the VPFC has now also been shown to play an important role in emotion processes (Kringelbach, 2005). Many fMRI studies have found abnormal activation of the VPFC in BD during tasks (Blumberg et al., 2003; Elliott et al., 2004; Lawrence et al., 2004; Strakowski et al., 2004; Malhi et al., 2005). Abnormal VPFC neural activity and disturbed VPFC-amygdala rsFC were also observed by resting-state studies (Liu et al., 2014; Xu et al., 2014). Trait abnormalities of VPFC in BD are further supported by postmortem histopathological findings such as decreased glial density and reductions in the density of both neurons and glia (Ongur et al., 1998; Rajkowska, 2000, 2002). In our study, the entire vermis showed changed rsFC patterns with the VPFC, establishing that the decreased rsFC of vermis-VPFC plays an important role in the regulation of mood linked to the core psychopathology of BD.

Another changed connectivity region of the anterior vermis, which belongs to the anterior lobe of the cerebellum, is the middle cingulate cortex (BA 24). The function of the anterior cerebellar lobe is mainly associated with motor control (Stoodley and Schmahmann, 2009). The middle cingulate cortex area is the midsection of the cingulate gyrus in its anterior-posterior axis and appears to be involved in both motor control and cognitive tasks such as response selection, error detection, competition monitoring, and working memory (Torta and Cauda, 2011). Previous studies have consistently reported aberrant motor control presentation in BD (Manschreck et al., 2004; Krebs et al., 2010; Deveney et al., 2012; Weathers et al., 2012). Our findings combined with previous studies suggest that the anterior vermis may be involved in the motor control of BD patients, which should be further validated by future studies.

There are several limitations to this study. First, 83.3% of the BD participants were taking medication at the time of the study. Although we did not find significant effects of medication on FC values in this study, our findings may in part be attributed to treatment differences. Second, confounding effects may influence the result of mixed BD subtypes in our current study; future studies that compare subtypes in BD would likely contribute to our understanding of the underlying mechanisms of BD. Thirdly, the sample size is modest. Finally, correlation analyses did not reveal significant relationships between rsFC and symptom measures in BD. In this study, only the HDRS and YMRS symptom measurements were assessed in the BD group. Future studies should include more comprehensive symptom measurements to enhance our understanding of the relationship between symptom severity and functional connectivity as well as state vs. trait-related abnormalities in BD. Because the majority of BD participants in this study were in remitted states, our findings more likely reflect trait-related differences between BD and HC.

CONCLUSION

In summary, BD patients showed decreased rsFC of vermis and VPFC as compared to the HC group. This resting-state fMRI study suggests that the abnormal rsFC of vermis-VPFC may contribute to mood regulation in BD patients. Further work focusing on this field may contribute to our understanding of BD neuropathphysiology.

DATA AVAILABILITY STATEMENT

The raw data supporting the conclusions of this article will be made available by the authors, without undue reservation.

ETHICS STATEMENT

The studies involving human participants were reviewed and approved by The First Hospital of China Medical University. The patients/participants provided their written informed consent to participate in this study.

AUTHOR CONTRIBUTIONS

Conception and design: GF and WS. Development of methodology: HLiu. Data acquisition, analysis, and interpretation: YT and XJ. Writing, review, and/or revision of the manuscript: HLiu, HLi, and RY. Study supervision: YT, GF, and WS. All authors contributed to the article and approved the submitted version.

FUNDING

This work was supported by National Key R&D Program of China (Grant #2018YFC1311600 and 2016YFC1306900 to YT), Liaoning Revitalization Talents Program (Grant

#XLYC1808036 to YT), Science and Technology Plan Program of Liaoning Province (2015225018 to YT), National Science Fund for Distinguished Young Scholars (81725005 to Fei Wang), Liaoning Education Foundation (Pandeng Scholar to Fei Wang), Innovation Team Support Plan of Higher Education of Liaoning Province (LT2017007 to Fei Wang), Major Special Construction Plan of China Medical University (3110117059 and 3110118055 to Fei Wang), Joint Fund of National Natural Science Foundation of China (U1808204 to Feng Wu), and Natural Science Foundation of Liaoning Province (2019-MS-05 to Feng Wu).

REFERENCES

Anand, A., Li, Y., Wang, Y., Lowe, M. J., and Dzemidzic, M. (2009). Resting state corticolimbic connectivity abnormalities in unmedicated bipolar disorder and unipolar depression. *Psychiatry Res.* 171, 189–198. doi: 10.1016/j.pscychresns.2008.03.012

Bell, C. C. (1994). DSM IV: Diagnostic and Statistical Manual of Mental Disorders. *JAMA* 272, 828–829. doi: 10.1001/jama.1994.03520100096046

Blumberg, H. P., Martin, A., Kaufman, J., Leung, H. C., Skudlarski, P., Lacadie, C., et al. (2003). Frontostriatal abnormalities in adolescents with bipolar disorder: preliminary observations from functional MRI. *Am. J. Psychiatry* 160, 1345–1347. doi: 10.1176/appi.ajp.160.7.1345

Bousse, A., Pedemonte, S., Thomas, B. A., Erlandsson, K., Ourselin, S., Arridge, S., et al. (2012). Markov random field and Gaussian mixture for segmented MRI-based partial volume correction in PET. *Phys. Med. Biol.* 57, 6681–6705. doi: 10.1088/0031-9155/57/20/6681

Buckner, R. L., and Vincent, J. L. (2007). Unrest at rest: default activity and spontaneous network correlations. *Neuroimage* 37, 1091–1096. doi: 10.1016/j.neuroimage.2007.01.010

Chen, G., Zhao, L., Jia, Y., Zhong, S., Chen, F., Luo, X., et al. (2019). Abnormal cerebellum-DMN regions connectivity in unmedicated bipolar II disorder. *J. Affect. Disord.* 243, 441–447. doi: 10.1016/j.jad.2018.09.076

Chepenik, L. G., Raffo, M., Hampson, M., Lacadie, C., Wang, F., Jones, M. M., et al. (2010). Functional connectivity between ventral prefrontal cortex and amygdala at low frequency in the resting state in bipolar disorder. *Psychiatry Res.* 182, 207–210. doi: 10.1016/j.pscychresns.2010.04.002

DelBello, M. P., Strakowski, S. M., Zimmerman, M. E., Hawkins, J. M., and Sax, K. W. (1999). MRI analysis of the cerebellum in bipolar disorder: a pilot study. *Neuropsychopharmacology* 21, 63–68. doi: 10.1016/S0893-133X(99)00026-3

Deveney, C. M., Connolly, M. E., Jenkins, S. E., Kim, P., Fromm, S. J., Brotman, M. A., et al. (2012). Striatal dysfunction during failed motor inhibition in children at risk for bipolar disorder. *Prog. Neuropsychopharmacol. Biol. Psychiatry* 38, 127–133. doi: 10.1016/j.pnpbp.2012.02.014

Dickstein, D. P., Gorrostieta, C., Ombao, H., Goldberg, L. D., Brazel, A. C., Gable, C. J., et al. (2010). Fronto-temporal spontaneous resting state functional connectivity in pediatric bipolar disorder. *Biol. Psychiatry* 68, 839–846. doi: 10.1016/j.biopsych.2010.06.029

Elliott, R., Ogilvie, A., Rubinsztein, J. S., Calderon, G., Dolan, R. J., and Sahakian, B. J. (2004). Abnormal ventral frontal response during performance of an affective go/no go task in patients with mania. *Biol. Psychiatry* 55, 1163–1170. doi: 10.1016/j.biopsych.2004.03.007

Goodwin, G. M., and Geddes, J. R. (2007). What is the heartland of psychiatry? *Br. J. Psychiatry* 191, 189–191. doi: 10.1192/bjp.bp.107.036343

Heath, R. G. (1977). Modulation of emotion with a brain pacemaker: treatment for intractable psychiatric illness. *J. Nerv. Ment. Dis.* 165, 300–317.

Heath, R. G., Franklin, D. E., and Shraberg, D. (1979). Gross pathology of the cerebellum in patients diagnosed and treated as functional psychiatric disorders. *J. Nerv. Ment. Dis.* 167, 585–592. doi: 10.1097/00005053-197910000-00001

Johnson, C. P., Christensen, G. E., Fiedorowicz, J. G., Mani, M., Shaffer, J. J., Jr., Magnotta, V. A., et al. (2018). Alterations of the cerebellum and basal ganglia in bipolar disorder mood states detected by quantitative T1ρ mapping. *Bipolar Disord.* 20, 381–390. doi: 10.1111/bdi.12581

Krebs, M. O., Bourdel, M. C., Cherif, Z. R., Bouhours, P., Loo, H., Poirier, M. F., et al. (2010). Deficit of inhibition motor control in untreated patients with schizophrenia: further support from visually guided saccade paradigms. *Psychiatry Res.* 179, 279–284. doi: 10.1016/j.psychres.2009.07.008

Kringelbach, M. L. (2005). The human orbitofrontal cortex: linking reward to hedonic experience. *Nat. Rev. Neurosci.* 6, 691–702. doi: 10.1038/nrn1747

Lawrence, N. S., Williams, A. M., Surguladze, S., Giampietro, V., Brammer, M. J., Andrew, C., et al. (2004). Subcortical and ventral prefrontal cortical neural responses to facial expressions distinguish patients with bipolar disorder and major depression. *Biol. Psychiatry* 55, 578–587. doi: 10.1016/j.biopsych.2003.11.017

Levisohn, L., Cronin-Golomb, A., and Schmahmann, J. D. (2000). Neuropsychological consequences of cerebellar tumour resection in children: cerebellar cognitive affective syndrome in a paediatric population. *Brain* 123, 1041–1050. doi: 10.1093/brain/123.5.1041

Liu, H., Tang, Y., Womer, F., Fan, G., Lu, T., Driesen, N., et al. (2014). Differentiating patterns of amygdala-frontal functional connectivity in schizophrenia and bipolar disorder. *Schizophr. Bull.* 40, 469–477. doi: 10.1093/schbul/sbt044

Malhi, G. S., Lagopoulos, J., Sachdev, P. S., Ivanovski, B., and Shnier, R. (2005). An emotional stroop functional MRI study of euthymic bipolar disorder. *Bipolar Disord.* 7, 58–69. doi: 10.1111/j.1399-5618.2005.00255.x

Manschreck, T. C., Maher, B. A., and Candela, S. F. (2004). Earlier age of first diagnosis in schizophrenia is related to impaired motor control. *Schizophr. Bull.* 30, 351–360. doi: 10.1093/oxfordjournals.schbul.a007084

Mills, N. P., DelBello, M. P., Adler, C. M., and Strakowski, S. M. (2005). MRI analysis of cerebellar vermal abnormalities in bipolar disorder. *Am. J. Psychiatry* 162, 1530–1533. doi: 10.1176/appi.ajp.162.8.1530

Moulton, E. A., Elman, I., Pendse, G., Schmahmann, J., Becerra, L., and Borsook, D. (2011). Aversion-related circuitry in the cerebellum: responses to noxious heat and unpleasant images. *J. Neurosci.* 31, 3795–3804. doi: 10.1523/JNEUROSCI.6709-10.2011

Ongur, D., Drevets, W. C., and Price, J. L. (1998). Glial reduction in the subgenual prefrontal cortex in mood disorders. *Proc. Natl. Acad. Sci. U S A* 95, 13290–13295. doi: 10.1073/pnas.95.22.13290

Pfefferbaum, A., Chanraud, S., Pitel, A. L., Müller-Oehring, E., Shankaranarayanan, A., Alsop, D. C., et al. (2011). Cerebral blood flow in posterior cortical nodes of the default mode network decreases with task engagement but remains higher than in most brain regions. *Cereb. Cortex.* 21, 233–244. doi: 10.1093/cercor/bhq090

Rajkowska, G. (2000). Postmortem studies in mood disorders indicate altered numbers of neurons and glial cells. *Biol. Psychiatry* 48, 766–777. doi: 10.1016/s0006-3223(00)00950-1

Rajkowska, G. (2002). Cell pathology in mood disorders. *Semin. Clin. Neuropsychiatry* 7, 281–292. doi: 10.1053/scnp.2002.35228

Schmahmann, J. D. (2001). The cerebrocerebellar system: anatomic substrates of the cerebellar contribution to cognition and emotion. *Int. Rev. Psychiatry* 13, 247–260. doi: 10.1080/09540260120082092

Schmahmann, J. D. (2004). Disorders of the cerebellum: ataxia, dysmetria of thought and the cerebellar cognitive affective syndrome. *J. Neuropsychiatry Clin. Neurosci.* 16, 367–378. doi: 10.1176/jnp.16.3.367

Schmahmann, J. D. (2019). The cerebellum and cognition. *Neurosci. Lett.* 688, 62–75. doi: 10.1016/j.neulet.2018.07.005

Schutter, D. J., and Van Honk, J. (2005). The cerebellum on the rise in human emotion. *Cerebellum* 4, 290–294. doi: 10.1080/14734220500348584

Stoodley, C. J., and Schmahmann, J. D. (2009). Functional topography in the human cerebellum: a meta-analysis of neuroimaging studies. *Neuroimage* 44, 489–501. doi: 10.1016/j.neuroimage.2008.08.039

Strakowski, S. M., Adler, C. M., and DelBello, M. P. (2002). Volumetric MRI studies of mood disorders: do they distinguish unipolar and bipolar disorder? *Bipolar Disord.* 4, 80–88. doi: 10.1034/j.1399-5618.2002.01160.x

Strakowski, S. M., Adler, C. M., Holland, S. K., Mills, N., and DelBello, M. P. (2004). A preliminary FMRI study of sustained attention in euthymic,

unmedicated bipolar disorder. *Neuropsychopharmacology* 29, 1734–1740. doi: 10.1038/sj.npp.1300492

Tavano, A., Grasso, R., Gagliardi, C., Triulzi, F., Bresolin, N., Fabbro, F., et al. (2007). Disorders of cognitive and affective development in cerebellar malformations. *Brain* 130, 2646–2660. doi: 10.1093/brain/awm201

Torta, D. M., and Cauda, F. (2011). Different functions in the cingulate cortex, a meta-analytic connectivity modeling study. *Neuroimage* 56, 2157–2172. doi: 10.1016/j.neuroimage.2011.03.066

Weathers, J. D., Stringaris, A., Deveney, C. M., Brotman, M. A., Zarate, C. A., Jr., Connolly, M. E., et al. (2012). A developmental study of the neural circuitry mediating motor inhibition in bipolar disorder. *Am. J. Psychiatry* 169, 633–641. doi: 10.1176/appi.ajp.2012.11081244

Xu, K., Liu, H., Li, H., Tang, Y., Womer, F., Jiang, X., et al. (2014). Amplitude of low-frequency fluctuations in bipolar disorder: a resting state fMRI study. *J. Affect. Disord.* 152, 237–242. doi: 10.1016/j.jad.2013.09.017

Yan, C. G., Wang, X. D., Zuo, X. N., and Zang, Y. F. (2016). DPABI: data processing & analysis for (resting-state) brain imaging. *Neuroinformatics* 14, 339–351. doi: 10.1007/s12021-016-9299-4

Conflict of Interest: The authors declare that the research was conducted in the absence of any commercial or financial relationships that could be construed as a potential conflict of interest.

frontiers in Human Neuroscience

ORIGINAL RESEARCH
published: 16 August 2021
doi: 10.3389/fnhum.2021.717130

Cortical Areas Associated With Multisensory Integration Showing Altered Morphology and Functional Connectivity in Relation to Reduced Life Quality in Vestibular Migraine

*Xia Zhe[1†], Li Chen[2†], Dongsheng Zhang[1], Min Tang[1], Jie Gao[1], Kai Ai[3], Weijun Liu[4], Xiaoyan Lei[1] and Xiaoling Zhang[1]**

[1]Department of MRI, Shaanxi Provincial People's Hospital, Xi'an, China, [2]Department of Neurology, Shaanxi Provincial People's Hospital, Xi'an, China, [3]Department of Clinical Science, Philips Healthcare, Xi'an, China, [4]Consumables and Reagents Department, Shaanxi Provincial People's Hospital, Xi'an, China

OPEN ACCESS

Edited by:
Long-Biao Cui,
People's Liberation Army General Hospital, China

Reviewed by:
Chao He,
General Hospital of Northern Theater Command, China
Marianne Dieterich,
LMU Munich University Hospital, Germany

***Correspondence:**
Xiaoling Zhang
zxl.822@163.com

†These authors have contributed equally to this work

Specialty section:
This article was submitted to Brain Imaging and Stimulation, a section of the journal Frontiers in Human Neuroscience

Received: 30 May 2021
Accepted: 26 July 2021
Published: 16 August 2021

Citation:
Zhe X, Chen L, Zhang D, Tang M, Gao J, Ai K, Liu W, Lei X and Zhang X (2021) Cortical Areas Associated With Multisensory Integration Showing Altered Morphology and Functional Connectivity in Relation to Reduced Life Quality in Vestibular Migraine. Front. Hum. Neurosci. 15:717130. doi: 10.3389/fnhum.2021.717130

Background: Increasing evidence suggests that the temporal and parietal lobes are associated with multisensory integration and vestibular migraine. However, temporal and parietal lobe structural and functional connectivity (FC) changes related to vestibular migraine need to be further investigated.

Methods: Twenty-five patients with vestibular migraine (VM) and 27 age- and sex-matched healthy controls participated in this study. Participants completed standardized questionnaires assessing migraine and vertigo-related clinical features. Cerebral cortex characteristics [i.e., thickness (CT), fractal dimension (FD), sulcus depth (SD), and the gyrification index (GI)] were evaluated using an automated Computational Anatomy Toolbox (CAT12). Regions with significant differences were used in a seed-based comparison of resting-state FC conducted with DPABI. The relationship between changes in cortical characteristics or FC and clinical features was also analyzed in the patients with VM.

Results: Relative to controls, patients with VM showed significantly thinner CT in the bilateral inferior temporal gyrus, left middle temporal gyrus, and the right superior parietal lobule. A shallower SD was observed in the right superior and inferior parietal lobule. FD and GI did not differ significantly between the two groups. A negative correlation was found between CT in the right inferior temporal gyrus, as well as the left middle temporal gyrus, and the Dizziness Handicap Inventory (DHI) score in VM patients. Furthermore, patients with VM exhibited weaker FC between the left inferior/middle temporal gyrus and the left medial superior frontal gyrus, supplementary motor area.

Conclusion: Our data revealed cortical structural and resting-state FC abnormalities associated with multisensory integration, contributing to a lower quality of life. These observations suggest a role for multisensory integration in patients with VM pathophysiology. Future research should focus on using a task-based fMRI to measure multisensory integration.

Keywords: vestibular migraine, cortical surface, surface-based morphometry, temporal lobe, parietal lobe, multisensory integration

INTRODUCTION

Vestibular migraine (VM) is considered to be the most common central cause of episodic vertigo, manifesting as moderately to severely intense vestibular symptoms and a migraine history. In 2012, the International Headache Society and the Ba'ra'ny Society proposed criteria for diagnosing VM as a disease entity (Lempert et al., 2012). An estimated 2.7% of adults suffer from vestibular migraines according to a recent population-based survey in the United States (Formeister et al., 2018). Women suffer from VM 2 to 3 times more frequently than do men (Neuhauser et al., 2001; Lempert and Neuhauser, 2009). VM is a disabling disorder that results in a significant burden on healthcare. Therefore, it is important to understand the pathophysiology of VM to help develop treatment plans for patients.

Previous studies indicate that the temporal lobe and the parietal lobe are associated with multisensory integration and vestibular processing (Obermann et al., 2014; Komeilipoor et al., 2017; Messina et al., 2017; Oh et al., 2018). Patients with VM have activity in the temporal and parietal lobes during VM attacks (Shin et al., 2014). Several voxel-based morphometric (VBM) studies have reported that patients with VM exhibit gray matter (GM) volume abnormalities in temporal lobe regions, including the superior temporal gyrus, middle temporal gyrus, and inferior temporal gyrus, as well as the parietal lobe (Obermann et al., 2014; Messina et al., 2017). Together, these findings strongly suggest that structural abnormalities in the temporal lobe are involved in multisensory integration, including visual, auditory, tactile, and vestibular processing (Beauchamp, 2005; Amedi et al., 2007). It is unclear, however, whether cerebral cortex characteristics alter multisensory integration and vestibular processing in brain areas during VM attacks. Surface-based morphometry (SBM) can focus on cortical structural characteristics, yielding more specific information about neurological development as well as changes in cortical function related to thinning of the cortex (Panizzon et al., 2009; Yotter et al., 2011a; Dahnke et al., 2013). Compared with VBM, SBM has been shown to be more sensitive and precise for detecting gray-matter atrophy, and it uses a completely automatic method, which provides the basis for projection-based thickness (PBT) measurement in order to obtain a local measure of GM within the cortex (Lemaitre et al., 2012; Dahnke et al., 2013). The SBM approach has been frequently used as a research method to assess cortical surface characteristics in migraine and other vestibular disorders (Komaromy et al., 2019; Nigro et al., 2019; Lai et al., 2020). However, no study to date has investigated the pattern of cerebral cortex characteristics and their changes in relation to the clinical features of VM.

Resting-state functional connectivity (FC) provides a powerful method to investigate the FC among brain regions, detecting the synchronized blood oxygen level-dependent (BOLD) signals from the seed region to the whole brain so as to locate highly correlated areas with similar characteristics (Xu et al., 2019; Niu et al., 2020). However, previous functional magnetic resonance imaging (fMRI) studies have used the amplitude of low-frequency fluctuation (ALFF) during external stimulation to assess functional changes in patients with VM. Russo et al. (2014) demonstrated that abnormal thalamic function is involved in central vestibular processing. Teggi et al. (2016) reported activation of brain areas related to integrating visual and vestibular cues in patients with VM undergoing fMRI during visual stimulation in vertigo-free periods. A fMRI study to observe treatment effectiveness found ALFF values in the left posterior cerebellum of patients with VM increased significantly after 1 month of vestibular rehabilitation training (Liu et al., 2020). Functional imaging demonstrated the cerebellum can improve vestibular functioning through a vestibular compensation mechanism. Recently, Wang et al. (2021) evaluated resting-state FC alterations in patients with VM during the interictal period. Although several fMRI studies have focused on ALFF or FC, no studies have explored FC alterations based on cortical structural abnormalities in patients with VM.

Given that previous findings have shown that changes in the gray-matter volume of the temporal and parietal lobes are related to multisensory vestibular processing in VM (Obermann et al., 2014; Messina et al., 2017; Zhe et al., 2020), we hypothesized that alterations in cerebral cortex characteristics in patients with VM could be located in brain regions associated with multisensory vestibular processing. And we also hypothesized that changes in cortical regions were accompanied by changes in FC. Therefore, in the current study, we used a whole-brain SBM technique to evaluate cortical surface characteristics in VM patients, during an interictal period, compared with healthy controls. Furthermore, we used seed-based FC to investigate whether cortical regions with structural abnormalities also exhibit FC alterations in a patient with VM. Additionally, we assessed the relationships between brain morphological or FC changes and clinical parameters.

MATERIALS AND METHODS

Subjects

Patients were recruited from the vertigo and dizziness outpatient service center of the Shaanxi Provincial People's Hospital in China between January 2016 and October 2020, who were diagnosed with VM by a neurologist based on the International Classification of Headache Disorder 3rd edition criteria (Lempert et al., 2012). Twenty-five right-handed patients with VM (21 without aura and four with aura) and 27 healthy controls participated in this study. Patients were excluded if they had a history of other neurologic, psychiatric, audiovestibular, or systemic disorders. All patients in a symptom-free interval underwent a routine neurologic and neuro-otological examination, as well as MRI scanning, which were performed on the same day. No peripheral vestibular dysfunction was found in videonystagmography (VNG) recordings. The clinical symptoms of each patient were assessed using a Visual Analog Scale (VAS; 0 = no pain; 10 = worst possible pain), the Migraine Disability Assessment Scale (MIDAS), the Headache Impact Test-6 (HIT-6), and the Dizziness Handicap Inventory (DHI) using face-to-face interviews with a standardized questionnaire and questions (Sauro et al., 2010; Hawker et al., 2011; Balci et al., 2018). Eight of the patients with VM were treated with migraine-preventive

medications and nonsteroidal analgesics. Most patients (n = 17) did not take any medication regularly.

The 27 age-, sex- and handedness-matched healthy controls were from the community. The exclusion criteria were: migraine; chronic pain; previous vestibular neuritis; Meniere's disease; secondary somatoform vertigo; drug abuse; neurologic, mental or systemic disorders; ischemic or hemorrhagic stroke; or severe head trauma. All subjects had no structural abnormalities or white matter (WM) lesions in T2-weighted or FLAIR imaging. This study was approved by the Ethics Committee of the Shaanxi Provincial People's Hospital. All participants provided written informed consent before entering the study.

Imaging Data Acquisition

All the images were obtained using a 3.0 T Philips Ingenia scanner with a 16-channel phased-array head coil. A high-resolution three-dimensional (3D) magnetization-prepared rapid-acquisition gradient echo (MPRAGE) T1-weighted (T1w) sequence covering the whole brain (332 sagittal slices) was collected. The acquisition parameters were: repetition time (TR) = 1,900 ms; echo time (TE) = 2.26 ms; inversion time (TI) = 900 ms; flip angle (FA) = 9°; matrix = 256 × 256; field of view = 220 × 220 mm; and 1.00 mm slice thickness with no interslice gap. Resting-state functional BOLD images were scanned using gradient echo-planar imaging with the following parameters: repetition time = 2,000 s; echo time = 30 ms; slices = 34; slice thickness = 4 mm; slice gap = 0 mm; field of view = 230 × 230 mm; matrix = 128 × 128; flip angle = 90°; and 200 volumes. For the resting-state scan, all subjects were asked to keep their eyes closed and their minds calm, and to stay awake throughout the scan. After the scan, subjects were asked whether or not they remained awake during the entire procedure.

Image Processing

Structural images were processed using CAT12[1] and SPM12 run in MATLAB R2014b (The MathWorks, Inc.). CAT12 provides a volume-based method for estimating regional thickness (CT) without extensive reconstruction of the cortical surface and has been shown to be a fast and reliable alternative to FreeSurfer (Paul et al., 2017; Seiger et al., 2018). Moreover, CAT12 is a fully automated method that allows the measurement of the whole brain cortical surface. For each participant, the processing pipeline included bias-field, noise removal, skull stripping, and segmentation into GM, WM, and cerebrospinal fluid (CSF). The images were finally normalized to MNI space, which uses diffeomorphic anatomical registration using exponentiated Lie algebra (DARTEL) to a 1.5 mm isotropic adult template (Ashburner, 2007). Here, the CT evaluation and reconstruction of the central surface were performed in one step, based on the PBT method (Dahnke et al., 2013). Importantly, the PBT allows the appropriate handing of partial volume information, sulcal blurring, and sulcal asymmetries without explicit sulcus reconstruction (Dahnke et al., 2013). After the initial surface reconstruction, topology correction (Yotter et al., 2011b), spherical mapping (Yotter et al., 2011a), and spherical registration were conducted. In addition, CAT12 allows the estimation of other morphological indices of fractal dimension (FD), sulcus depth (SD), and gyrification index (GI), which were also calculated for each participant with default parameter settings. The calculation of CT, FD, SD, and GI was performed in subject native surface space. The images of cerebral cortex characteristics were checked for homogeneity. As all the images had high correlation values (>0.85), none of them had to be discarded. Finally, the CT images were smoothed using a Gaussian kernel with a full width at half maximum (FWHM) of 15 mm, and three other surface parameters were smoothened with an isotropic 20 mm FWHM Gaussian kernel.

All functional images were preprocessed using Data Processing and Analysis for Brain Imaging 3.0[2], which is based on Statistical Parametric Mapping 12[3]. First, the first 10 volumes were removed to allow subjects to adapt to the magnetic field. Second, slice timing correction was performed to correct for the inter-slice time delay within each volume. Third, head motion >1.5 mm and translation >1.5° of rotation in any direction were excluded. Images were spatially normalized into MNI space using a standard EPI template provided by SPM12 and resliced into a voxel size of 3 × 3 × 3 mm. Finally, data were spatially smoothed using a 6-mm FWHM Gaussian kernel.

Seed-based FC analysis was performed with seeds from the SBM findings. Seeds were defined as 3-mm-radius spheres centered on the peak voxel for the CT and SD clusters showing between-group differences. The averaged time-course of each seed area was extracted, and Pearson's correlation (r) was used to calculate the FC between the extracted time-courses and the time-courses of the entire brain in a voxel-wise manner. The individual r-maps were normalized to Z-maps using Fisher's Z-transformation.

Statistical Analysis

Demographic and Clinical Data

A two-sample t-test was used to estimate the differences in age, sex, and years of education between the VM and healthy control groups. The statistical significance level was set at $P < 0.05$. These statistical analyses were performed using the SPSS software package (version 22.0).

Cortical Surface Characteristics Analysis

Cortical surface characteristics were compared between the VM patients and healthy controls using two-sample t-tests in CAT12 with age and sex as covariates. Family-wise error (FWE) correction was performed to correct for multiple comparisons; $P < 0.05$ was considered statistically significant. Then, the surviving clusters were reported. Finally, based on the Desikan–Killiany (DK40) atlas (Desikan et al., 2006), we extracted the mean cortical surface characteristics (CT, SD, GI, and FD) from the above mentioned significant clusters. Partial correlations adjusted for age and sex were used to analyze differences between the cortical surface characteristics of these

[1]http://dbm.neuro.uni-jena.de/cat12

[2]http://rfmri.org/dpabi

[3]http://www.fil.ion.ucl.ac.uk/spm

TABLE 1 | Demographic and clinical characteristics of patients.

Characteristics	VM (n = 27) Mean ± SD	HC (n = 25) Mean ± SD	P value
Sex (female/male)	27/4	25/4	0.91
Age (years)	38.22 ± 10.58	37.28 ± 11.45	0.76
Education (years)	13.89 ± 3.61	14.40 ± 2.48	0.56
Disease duration (years)	9.15 ± 7.58		
Headache frequency (number)	6.67 ± 4.93		
VAS	4.74 ± 2.75		
MIDAS	54.33 ± 53.13		
HIT-6	51.56 ± 19.94		
DHI	48.93 ± 16.43		

Note: VM, vestibular migraine; HC, healthy control; VAS, Visual Analog Scale (0 = no pain, 10 = worst possible pain); MIDAS, Migraine Disability Assessment Scale; HIT-6, Headache Impact Test-6; DHI, Dizziness Handicap Inventory.

TABLE 2 | Decreased CT in various brain regions in patients with VM.

	Brain regions	Peak MNI			Cluster voxels	T	Z	P
R	Inferior temporal gyrus	63	−36	−22	149	5.38	4.74	0.000
	Superior parietal lobule	24	−63	50	68	5.06	4.60	0.000
L	Inferior temporal gyrus	−56	−38	−14	102	5.19	4.51	0.000
	Middle temporal gyrus	−56	−38	−14	102	5.19	4.51	0.000

Note: MNI, Montreal Neurological Institute; R, right; L, Left; CT, thickness; VM, vestibular migraine.

altered regions and clinical indices (including the VAS score, disease duration, attack frequency, MIDAS score, HIT-6 score, and DHI score). The significance threshold was set at $P < 0.05$.

Seed-Based FC Analysis

A comparison of FC between groups was performed using a two-sample t-test within DPABI, with age and sex as covariates. Correction for multiple comparisons was performed using a Gaussian random field at $P < 0.05$ (voxel $P < 0.001$). Then, the surviving clusters were reported.

Finally, we extracted the average Z-values for each region with significant differences and performed a partial correlation analysis with patients' clinical parameters using SPSS 22.0, controlling for age and sex. The significance threshold was set at $P < 0.05$.

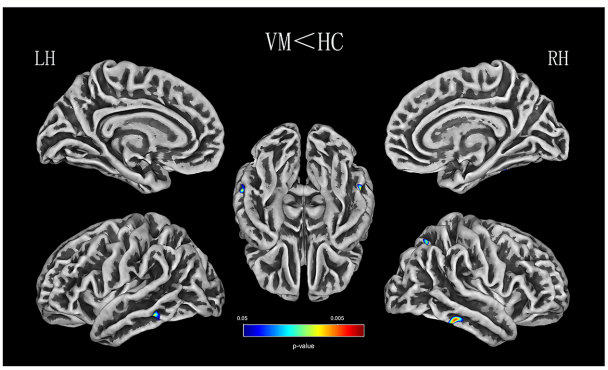

FIGURE 1 | CT (thickness) analysis results of patients with vestibular migraine (VM) compared with healthy controls [$P < 0.05$, family-wise error (FWE)-corrected].

RESULTS

Demographic and Clinical Data

There were no significant differences between the VM patients and healthy controls in age, sex, or years of education. The results are summarized in **Table 1**. VM patients suffered from a moderate and severe migraine burden with a mean VAS score of 4.74 ± 2.75, mean HIT-6 score of 51.56 ± 19.94, and mean MIDAS score of 54.33 ± 53.13. Their scores on the vertigo scale were moderate with a mean DHI score of 48.93 ± 16.43.

Cortical Surface Characteristics Results

Relative to healthy comparison subjects, the VM patients showed significantly thinner CT in the bilateral inferior temporal gyrus, left middle temporal gyrus, and right superior parietal lobule (**Table 2**, **Figure 1**). Reduced SD was found in the right superior and inferior parietal lobule (**Table 3**, **Figure 2**). There was no significant intergroup difference for surface parameters GI and FD. In the VM patients, a significant negative correlation was found between DHI scores and the CT of the right inferior temporal gyrus ($r = -0.542$; $P = 0.005$; **Figure 3A**) and left middle temporal gyrus ($r = -0.553$; $P = 0.004$; **Figure 3B**). No correlation was found between abnormal SD and disease duration, attack frequency, VAS score, MIDAS score, HIT-6 score, or DHI score in the VM patients.

Seed-Based FC Results

Patients with VM showed significantly weaker FC between the left inferior/middle temporal gyrus and the left superior frontal gyrus, supplementary motor area (**Table 4**, **Figure 4**). There were no significant group differences in FC with other seed regions (right inferior temporal gyrus, right superior, and inferior parietal lobule). No significant correlation was observed between FC alterations and clinical characteristics in patients with VM.

TABLE 3 | Decreased SD in various brain regions in patients with VM.

	Brain regions	Peak MNI			Cluster voxels	*T*	*Z*	*P*
R	Superior parietal lobule	28	−51	49	382	5.02	4.48	0.000
	Inferior parietal lobule	32	−60	47	382	4.91	4.39	0.000

Note: MNI, Montreal Neurological Institute; R, right; SD, sulcus depth.

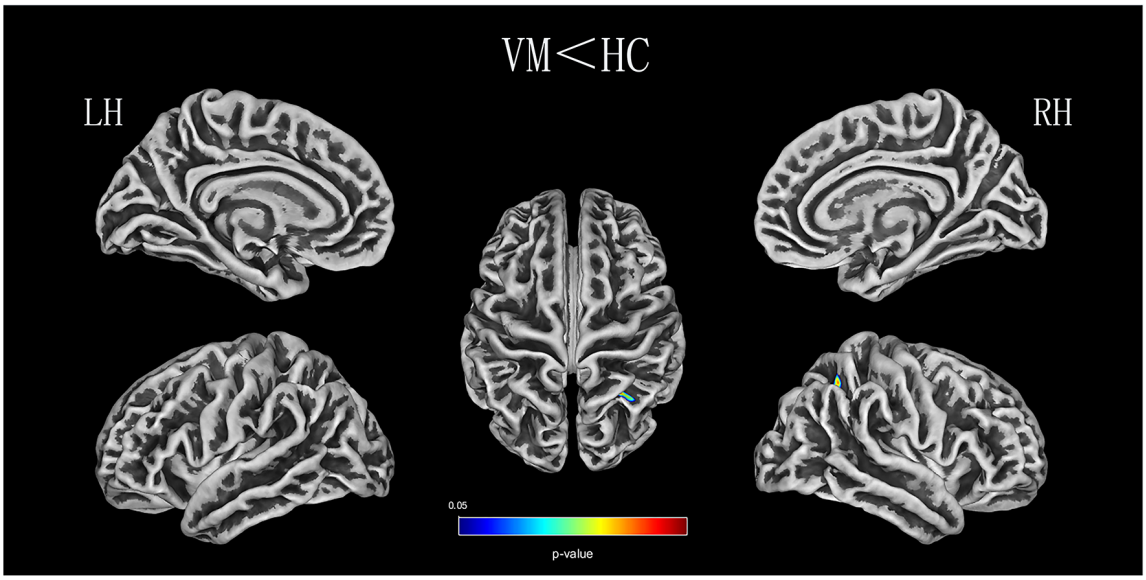

FIGURE 2 | SD (sulcus depth) analysis results of patients with VM compared with healthy controls ($P < 0.05$, FWE-corrected).

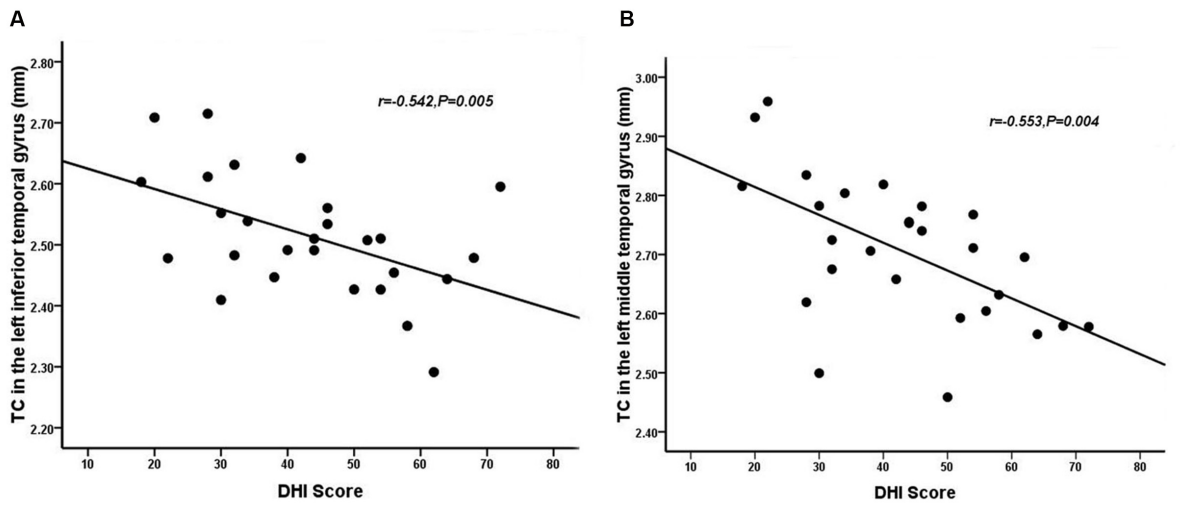

FIGURE 3 | Correlation between the CT of the inferior **(A)** and middle temporal gyrus **(B)** and dizziness handicap inventory (DHI) score in patients with VM ($P < 0.05$).

DISCUSSION

As far as we know, our study is the first to directly investigate cortical surface characteristics and FC changes in patients with VM and healthy controls, as well as associations between cortical surface characteristics or FC and clinical variables. Compared with healthy controls, we found that patients with VM had decreased CT and SD in certain areas, including multisensory

TABLE 4 | Abnormal functional connectivity of the left inferior/middle temporal gyrus in patients with VM.

	Seed points		Brain region	BA	Peak MNI			Cluster voxels	*T*
L	Inferior/middle temporal gyrus	L	Medial superior frontal gyrus	9	−9	51	33	248	−5.54
		L	Supplementary motor area	6	−9	18	69	75	−5.12

Note: MNI, Montreal Neurological Institute; R, right.

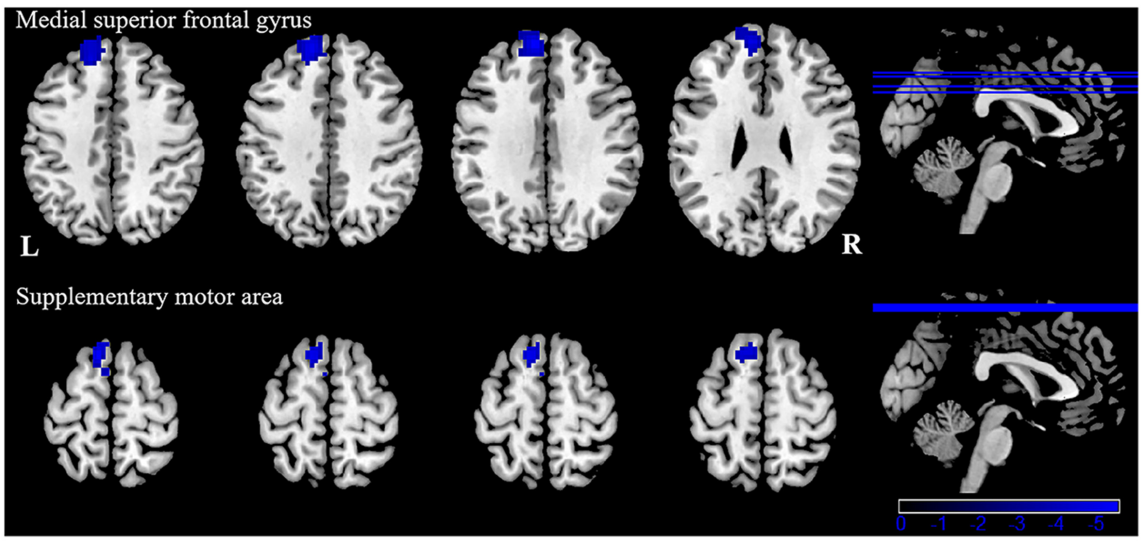

FIGURE 4 | Functional connectivity (FC) analysis results for patients with VM compared with healthy controls ($P < 0.05$, GRF-corrected).

integration and vestibular processing regions. Additionally, we found that DHI scores and CT were significantly correlated in the right inferior temporal gyrus and the left middle temporal gyrus. Using the clusters derived from the SBM analysis as seed regions, we found significantly weaker FC between the left inferior/middle temporal gyrus and the left medial superior frontal gyrus, supplementary motor area. Our data confirmed our hypothesis that VM patients have abnormalities in cortical surface characteristics related to multisensory vestibular processing and that changes in cortical regions are accompanied by changes in FC.

The temporal lobe has been recognized as a region associated with multisensory integration, which involves auditory, olfactory, vestibular, and visual senses and the perception of spoken and written language (Kiernan, 2012). A number of studies on patients with migraine have found that CT was thinning in the temporal lobe, suggesting that the temporal lobe plays an important role in the regulation of pain (Coppola et al., 2017; Jia and Yu, 2017). Several studies have demonstrated greater interregional CT correlations in patients with migraine, specifically over temporal regions (Chong et al., 2020). Schwedt et al. (2015) found that temporal pole correlations distinguished groups of migraine patients from healthy controls. An fMRI study of 12 right-handed patients with VM, which used cold caloric stimulation, found a typical pattern of BOLD signals in temporal-parietal areas in the interictal interval, including patients with migraine without aura and healthy controls (Russo et al., 2014). A recent functional imaging study of two patients reported that the metabolism of the temporoparietal-insular areas increased during a VM attack (Fasold et al., 2002). These results suggest that some modification of structural covariance patterns in the temporal lobe is involved in pain-processing and multisensory integration (Moulton et al., 2011). The VM patients in that study also showed reduced CT in multiple areas of the temporal lobe, including the inferior and middle gyrus, compared with healthy controls, which is in line with the findings of several previous studies. Obermann et al. (2014) found that gray-matter volume was decreased in the inferior temporal gyrus, middle temporal gyrus, and the superior temporal gyrus, the middle cingulate, dorsolateral prefrontal, insular, parietal, and occipital cortices (Obermann et al., 2014). These structurally abnormal brain areas in patients with VM are involved in multisensory vestibular control, as well as pain processing and central vestibular compensation. In contrast, a recent VBM study found an increase in the temporal lobe, frontal lobe, and occipital lobe in VM patients compared with healthy controls (Messina et al., 2017). These inconsistent findings might be due to differences in sample size, attack frequency, medication status, and data acquisition and processing in the various studies.

The inferior temporal gyrus is related to visual processing (Naito et al., 2003). There is some evidence that decreased CT in the inferior temporal gyrus might contribute to abnormalities in multisensory integration of visual processing, such as amplifying vision (photophobia), hearing (phonophobia), or olfactory stimuli, which may induce an attack of VM. Repeated VM attacks over time that seem to lead to an alteration of

multisensory integration of visual processing structures may provide an explanation as to why most VM patients have increased sensitivity to visual, auditory, and olfactory stimuli during VM attacks. Previous studies have also suggested that the middle temporal gyrus plays a key role in interconnecting with other multisensory cortical areas, and it is deemed to form a multisensory integrative network (Helmchen et al., 2014). The middle temporal gyrus, inferior temporal gyrus, and superior temporal gyrus, and the lateral temporal lobe play a role in the underlying connection between migraine and the vestibular system (Rocca et al., 2006; Schwedt et al., 2013; Helmchen et al., 2014). The middle temporal gyrus belongs to the temporal perisylvian vestibular cortex, which is particularly sensitive for dizziness (Kahane et al., 2010). Furthermore, CT in the inferior and middle temporal gyrus is negatively correlated with the severity of vertigo in VM patients. The DHI was used to evaluate the self-perceived handicapping effects of dizziness, which is related to the physical, emotional, and functional aspects of patients. Vertigo attacks result in subjective spatial orientation errors, surrounding environment spiraling around, and complaining of imbalance in patients. That may lead to patients who usually dare not to attempt daily activities, and experience obvious anxiety and depression which reflect the degree of vertigo. In the present study, a mean DHI score of 48.93 points was obtained. In patients with VM, as the DHI score increased, there was a decrease in life quality scales showing moderate disability in DHI. However, we did not evaluate symptoms of depression and anxiety. Thus, it is not clear whether anxiety or depression is associated with DHI in patients with VM. Future studies should clarify this. Correlations revealing a CT decrease in the temporal lobe was associated with an increased subjective intensity of vertigo in VM, which indicated that the temporal lobe is involved in the pathophysiology of patients with VM and is associated with the daily life of the patient. Therefore, CT reduction in the inferior and middle temporal gyrus is a potentially valuable morphological characteristic, which might result in central vestibular syndromes that manifest along with vertigo and dizziness. Based on all of the above discussion, our results indicate that long–term and high-frequency headaches and vertigo attacks may lead to reduced CT in multisensory integrative and vestibular processing areas in VM, reflecting abnormal brain structure due to the effects of brain disease. This has profound implications for our understanding of multisensory integrative networks in patients with VM.

The second finding of the current study is decreased CT in the superior parietal lobule. Furthermore, we found lower SD in the inferior and superior parietal lobule in patients with VM compared with healthy controls. Other studies proposed that the parietal lobule is chiefly involved in discriminating sensory features of pain (Hofbauer et al., 2001; Oshiro et al., 2007, 2009). The superior parietal lobule, as a part of the parietofrontal network, has been found to be related to the perceptual matrix of pain (Garcia-Larrea and Peyron, 2013). It also contains major parts of the sensory cortex that are involved in spatial orientation and sensory information processing and interpretation (Kamali et al., 2014). Studies have confirmed that the inferior parietal lobe belongs to part of the multisensory vestibular cortical network involved in pain and vestibular processing (Dieterich and Brandt, 2008). The parietal lobule has been implicated in VM, and some VBM studies on patients with VM have reported a lower gray-matter volume in the parietal lobes of such patients compared with controls (Obermann et al., 2014; Zhe et al., 2020). A recent fMRI study of two VM patients reported increased activity in the inferior parietal lobule during visual stimulation in a vertigo-free period (Teggi et al., 2016). Correlation analysis also revealed that decreased gray-matter volume in the parietal lobe is associated with illness duration and headache intensity in patients with VM (Obermann et al., 2014). These studies indicate that cortical abnormalities of the parietal lobe are involved in nociception and multisensory vestibular control. Our findings in VM patients implicate the parietal lobe in the modulation of pain perception and dysfunction of sensory integration.

In order to assess if these cortical structural abnormalities also exhibited FC alterations, we performed a resting-state FC study. Our results showed decreased FC between the left inferior/middle temporal gyrus and left medial superior frontal gyrus supplementary motor area in patients with VM, compared to healthy controls. The medial superior frontal gyrus is not only involved in emotional responses and feelings of pain, but also in memory, attention responses, and cognitive reactions related to pain (Bluhm et al., 2007). The study confirmed that the superior frontal gyrus is involved in the integration of somatosensory and vestibular information (Klingner et al., 2016). Our research indicates that the endogenous analgesic mechanism of VM patients is adjusted because some long–term migraine and vertigo attacks occur, altering the emotional response to pain, or reducing pain perception and cognition, which can reduce the input of pain signals. Anatomically, the SMA is located in the dorsomedial frontal cortex, which is involved in executive control (Aron and Roldrack, 2006; Li et al., 2006), pain anticipation (Koyama et al., 2005; Rainville et al., 2009), and an affective component of pain (Apkarian et al., 2005; Geha et al., 2008). Our results indicate that the FC decrease between the left inferior/middle temporal gyrus and left supplementary motor area may be related to deficits in affective pain modulation and affective pain response inhibition. In addition, the SMA is associated with auditory processing (Lima et al., 2016). Phonophobia is reported in about half of patients with VM during a vertigo attack (Neuhauser et al., 2006). Exposure to noise may cause generalized discomfort and increase the pain and vertigo of the patients with VM. Recurrent VM attacks may ultimately result in FC alterations associated with auditory processing. Thus, the FC changes may serve as a possible explanation for phonophobia when vertigo occurs (Wei et al., 2020), which provides a new clue for therapy for this syndrome.

The present study has several limitations. First, our study was conducted with a relatively small sample. Our study should have included a larger sample that was more representative of a pathological population, which would help to assure greater reproducibility of its results. Second, subgroup analyses of migraine (migraine without aura and migraine with aura) were not performed. To better elucidate the cortical morphological difference between them, future studies should compare the two types of VM, and it would be valuable to recruit a larger

sample size to be able to divide participants into the subgroups "migraine without aura" and "migraine with aura." Third, we did not examine subcortical and brain stem structures in this study; therefore, future studies need to be designed to include both. Fourth, because the sample size was relatively small, the correlation analysis was not strictly conducted with Bonferroni corrections. Fifth, we did not use an experimental task to measure multisensory integration. Finally, we did not evaluate symptoms of depression and anxiety, although previous research has reported that patients with VM have high levels of depression and anxiety (Kim et al., 2016). The burden of symptomatology can affect cortical morphology. Assessment of depression and anxiety scores should be performed in future studies.

CONCLUSION

In conclusion, we evaluated cortical structural and FC alterations in patients with VM using SBM and resting-state FC analyses, compared with healthy controls. CT and SD abnormalities were detected in the temporal lobe and parietal lobe. Furthermore, patients with VM displayed decreased FC between the left inferior/middle temporal gyrus and the left superior frontal gyrus, supplementary motor area. These regions are known to be involved in multisensory integration, vestibular processing, and pain modulation, contributing to a lower quality of life. These findings will promote our understanding of the underlying mechanism of VM, but so far an experimental task to measure multisensory integration in patients with VM has not been used. Future studies should identify brain areas associated with multisensory integration using a task-based fMRI. Moreover, further studies focusing on anxiety and depression are needed, which are bound to shed light on emotional states in patients with VM.

DATA AVAILABILITY STATEMENT

The original contributions presented in the study are included in the article, further inquiries can be directed to the corresponding author.

ETHICS STATEMENT

The studies involving human participants were reviewed and approved by the Ethics Committee of the Shaanxi Provincial People's Hospital. The patients/participants provided their written informed consent to participate in this study.

AUTHOR CONTRIBUTIONS

XZhe drafted the manuscript, designed the experiment, and performed the statistical analysis. LC undertook clinical parameters assessments. MT, JG, XL, and DZ collected the data. KA and WL provided technical support. XZha made study supervision or coordination. All authors contributed to the article and approved the submitted version.

FUNDING

This research was supported by the Social Development Science and Technology Research Project of Shaanxi Province of China (2021SF-290).

ACKNOWLEDGMENTS

We would like to thank all patients and healthy controls for their willingness to participate in the present study.

REFERENCES

Amedi, A., Stern, W. M., Camprodon, J. A., Bermpohl, F., Merabet, L., Rotman, S., et al. (2007). Shape conveyed by visual-to-auditory sensory substitution activates the lateral occipital complex. *Nat. Neurosci.* 10, 687–689. doi: 10.1038/nn1912

Apkarian, A. V., Bushnell, M. C., Treede, R. D., and Zubieta, J. K. (2005). Human brain mechanisms of pain perception and regulation in health and disease. *Eur. J. Pain* 9, 463–484. doi: 10.1016/j.ejpain.2004.11.001

Aron, A. R., and Roldrack, R. A. (2006). Cortical and subcortical contributions to stop signal response inhibition: role of the subthalamic nucleus. *J. Neurosci.* 26, 2424–2433. doi: 10.1523/JNEUROSCI.4682-05.2006

Ashburner, J. (2007). A fast diffeomorphic image registration algorithm. *Neuroimage* 38, 95–113. doi: 10.1016/j.neuroimage.2007.07.007

Balci, B., Senyuva, N., and Akdal, G. (2018). Definition of balance and cognition related to disability levels in vestibular migraine patients. *Noro. Psikiyatr Ars.* 55, 9–14. doi: 10.29399/npa.12617

Beauchamp, M. S. (2005). See me, hear me, touch me: multisensory integration in lateral occipital-temporal cortex. *Curr. Opin. Neurobiol.* 15, 145–153. doi: 10.1016/j.conb.2005.03.011

Bluhm, R. L., Miller, J., Lanius, R. A., Osuch, E. A., Boksman, K., Neufeld, R. W., et al. (2007). Spontaneous low-frequency fluctuations in the BOLD signal in schizophrenic patients: anomalies in the default network. *Schizophr. Bull.* 33, 1004–1012. doi: 10.1093/schbul/sbm052

Chong, C. D., Aguilar, M., and Schwedt, T. J. (2020). Altered hypothalamic region covariance in migraine and cluster headache: a structural MRI study. *Headache* 60, 553–563. doi: 10.1111/head.13742

Coppola, G., Petolicchio, B., Di Renzo, A., Tinelli, E., Di Lorenzo, C., Parisi, V., et al. (2017). Cerebral gray matter volume in patients with chronic migraine: correlations with clinical features. *J. Headache Pain* 18:115. doi: 10.1186/s10194-017-0825-z

Dahnke, R., Yotter, R. A., and Gaser, C. (2013). Cortical thickness and central surface estimation. *Neuroimage* 65, 336–348. doi: 10.1016/j.neuroimage.2012.09.050

Desikan, R. S., Segonne, F., Fischl, B., Quinn, B. T., Dickerson, B. C., Blacker, D., et al. (2006). An automated labeling system for subdividing the human cerebral cortex on MRI scans into gyral based regions of interest. *Neuroimage* 31, 968–980. doi: 10.1016/j.neuroimage.2006.01.021

Dieterich, M., and Brandt, T. (2008). Functional brain imaging of peripheral and central vestibular disorders. *Brain* 131, 2538–2552. doi: 10.1093/brain/awn042

Fasold, O., Von Brevern, M., Kuhberg, M., Ploner, C. J., Villringer, A., Lempert, T., et al. (2002). Human vestibular cortex as identified with caloric stimulation in functional magnetic resonance imaging. *Neuroimage* 17, 1384–1393. doi: 10.1006/nimg.2002.1241

Formeister, E. J., Rizk, H. G., Kohn, M. A., and Sharon, J. D. (2018). The epidemiology of vestibular migraine: a population-based survey study. *Otol. Neurotol.* 39, 1037–1044. doi: 10.1097/MAO.0000000000001900

Garcia-Larrea, L., and Peyron, R. (2013). Pain matrices and neuropathic pain matrices: a review. *Pain* 154, S29–S43. doi: 10.1016/j.pain.2013.09.001

Geha, P. Y., Baliki, M. N., Harden, R. N., Bauer, W. R., Parrish, T. B., and Apkarian, A. V. (2008). The brain in chronic CRPS pain: abnormal gray-white matter interactions in emotional and autonomic regions. *Neuron* 60, 570–581. doi: 10.1016/j.neuron.2008.08.022

Hawker, G. A., Mian, S., Kendzerska, T., and French, M. (2011). Measures of adult pain: visual analog scale for pain (VAS Pain), numeric rating scale for pain (NRS Pain), mcgill pain questionnaire (MPQ), short-form mcgill pain questionnaire (SF-MPQ), chronic pain grade scale (CPGS), short form-36 bodily pain scale (SF-36 BPS) and measure of intermittent and constant osteoarthritis pain (ICOAP). *Arthritis Care Res. (Hoboken)* 63, S240–S252. doi: 10.1002/acr.20543

Helmchen, C., Ye, Z., Sprenger, A., and Munte, T. F. (2014). Changes in resting-state fMRI in vestibular neuritis. *Brain Struct. Funct.* 219, 1889–1900. doi: 10.1007/s00429-013-0608-5

Hofbauer, R. K., Rainville, P., Duncan, G. H., and Bushnell, M. C. (2001). Cortical representation of the sensory dimension of pain. *J. Neurophysiol.* 86, 402–411. doi: 10.1152/jn.2001.86.1.402

Jia, Z., and Yu, S. (2017). Grey matter alterations in migraine: a systematic review and meta-analysis. *Neuroimage Clin.* 14, 130–140. doi: 10.1016/j.nicl.2017.01.019

Kahane, P., Hoffmann, D., Minotti, L., Minotti, L., and Berthoz, A. (2010). Reappraisal of the human vestibular cortex by cortical electrical stimulation study. *Ann. Neurol.* 54, 615–624. doi: 10.1002/ana.10726

Kamali, A., Sair, H. I., Radmanesh, A., and Hasan, K. M. (2014). Decoding the superior parietal lobule connections of the superior longitudinal fasciculus/arcuate fasciculus in the human brain. *Neuroscience* 277, 577–583. doi: 10.1016/j.neuroscience.2014.07.035

Kiernan, J. A. (2012). Anatomy of the temporal lobe. *Epilepsy Res. Treat.* 2012:176157. doi: 10.1016/j.cortex.2017.11.006

Kim, S. K., Kim, Y. B., Park, I. S., Hong, S. J., Kim, H., and Hong, S. M. (2016). Clinical analysis of dizzy patients with high levels of depression and anxiety. *J. Audiol. Otol.* 20, 174–178. doi: 10.7874/jao.2016.20.3.174

Klingner, C. M., Axer, H., .Brodoehl, S., and Witte, O. W. (2016). Vertigo and the processing of vestibular information: a review in the context of predictive coding. *Neurosci. Biobehav. Rev.* 71, 379–387. doi: 10.1016/j.neubiorev.2016.09.009

Komaromy, H., He, M., Perlaki, G., Orsi, G., Nagy, S. A., Bosnyak, E., et al. (2019). Influence of hemispheric white matter lesions and migraine characteristics on cortical thickness and volume. *J. Headache Pain* 20:4. doi: 10.1186/s10194-019-0959-2

Komeilipoor, N., Cesari, P., and Daffertshofer, A. (2017). Involvement of superior temporal areas in audiovisual and audiomotor speech integration. *Neuroscience* 343, 276–283. doi: 10.1016/j.neuroscience.2016.03.047

Koyama, T., Mchaffie, J. G., Laurienti, P. G., and Coghill, R. C. (2005). The subjective experience of pain: where expectations become reality. *Proc. Natl. Acad. Sci. U S A* 102, 12950–12955. doi: 10.1073/pnas.0408576102

Lai, K. L., Niddam, D. M., Fuh, J. L., Chen, W. T., Wu, J. C., and Wang, S. J. (2020). Cortical morphological changes in chronic migraine in a Taiwanese cohort: surface- and voxel-based analyses. *Cephalalgia* 40, 575–585. doi: 10.1177/0333102420920005

Lemaitre, H., Goldman, A. L., Sambataro, F., Verchinski, B. A., Meyer-Lindenberg, A., Weinberger, D. R., et al. (2012). Normal age-related brain morphometric changes: nonuniformity across cortical thickness, surface area and gray matter volume. *Neurobiol. Aging* 33, e611.617–e611.619. doi: 10.1016/j.neurobiolaging.2010.07.013

Lempert, T., and Neuhauser, H. (2009). Epidemiology of vertigo, migraine and vestibular migraine. *J. Neurol.* 256, 333–338. doi: 10.1007/s00415-009-0149-2

Lempert, T., Olesen, J., Furman, J., Waterston, J., Seemungal, B., Carey, J., et al. (2012). Vestibular migraine: diagnostic criteria. *J. Vestib. Res.* 22, 167–172. doi: 10.3233/VES-2012-0453

Li, C. S. H., Huang, C., Constable, R. T., and Sinha, R. (2006). Imaging response inhibition in a stop-signal task: neural correlates independent of signal monitoring and post-response processing. *J. Neurosci.* 26, 186–192. doi: 10.1523/JNEUROSCI.3741-05.2006

Lima, C. F., Krishnan, S., and Scott, S. K. (2016). Roles of supplementary motor areas in auditory processing and auditory imagery. *Trends Neurosci.* 39, 527–542. doi: 10.1016/j.tins.2016.06.003

Liu, L., Hu, X., Zhang, Y., Pan, Q., Zhan, Q., Tan, G., et al. (2020). Effect of vestibular rehabilitation on spontaneous brain activity in patients with vestibular migraine: a resting-state functional magnetic resonance imaging study. *Front. Hum. Neurosci.* 14:227. doi: 10.3389/fnhum.2020.00227

Messina, R., Rocca, M. A., Colombo, B., Teggi, R., Falini, A., Comi, G., et al. (2017). Structural brain abnormalities in patients with vestibular migraine. *J. Neurol.* 264, 295–303. doi: 10.1007/s00415-016-8349-z

Moulton, E. A., Becerra, L., Maleki, N., Pendse, G., Tully, S., and Hargreaves, R., et al. (2011). Painful heat reveals hyperexcitability of the temporal pole in interictal and ictal migraine states. *Cereb. Cortex* 21, 435–448. doi: 10.1093/cercor/bhq109

Naito, Y., Tateya, I., Hirano, S., Inoue, M., Funabiki, K., Toyoda, H., et al. (2003). Cortical correlates of vestibulo-ocular reflex modulation: a PET study. *Brain* 126, 1562–1578. doi: 10.1093/brain/awg165

Neuhauser, H., Leopold, M., Von Brevern, M., Arnold, G., and Lempert, T. (2001). The interrelations of migraine, vertigo and migrainous vertigo. *Neurology* 56, 436–441. doi: 10.1212/wnl.56.4.436

Neuhauser, H. K., Radtke, A., von Brevern, M., Feldmann, M., Lezius, F., Ziese, T., et al. (2006). Migrainous vertigo: prevalence and impact on quality of life. *Neurology* 67, 1028–1033. doi: 10.1212/01.wnl.0000237539.09942.06

Nigro, S., Indovina, I., Riccelli, R., Chiarella, G., Petrolo, C., Lacquaniti, F., et al. (2019). Reduced cortical folding in multi-modal vestibular regions in persistent postural perceptual dizziness. *Brain Imaging Behav.* 13, 798–809. doi: 10.1007/s11682-018-9900-6

Niu, X., Xu, H., Guo, C., Yang, T., Dustin, K., Gao, L., et al. (2020). Strengthened thalamoparietal functional connectivity in patients with hemifacial spasm: a cross-sectional resting-state fMRI study. *Br. J. Radiol.* 93:20190887. doi: 10.1259/bjr.20190887

Obermann, M., Wurthmann, S., Steinberg, B. S., Theysohn, N., Diener, H. C., and Naegel, S. (2014). Central vestibular system modulation in vestibular migraine. *Cephalalgia* 34, 1053–1061. doi: 10.1177/0333102414527650

Oh, S. Y., Boegle, R., Ertl, M., Stephan, T., and Dieterich, M. (2018). Multisensory vestibular, vestibular-auditory and auditory network effects revealed by parametric sound pressure stimulation. *Neuroimage* 176, 354–363. doi: 10.1016/j.neuroimage.2018.04.057

Oshiro, Y., Quevedo, A. S., Mchaffie, J. G., Kraft, R. A., and Coghill, R. C. (2009). Brain mechanisms supporting discrimination of sensory features of pain: a new model. *J. Neurosci.* 29, 14924–14931. doi: 10.1523/JNEUROSCI.5538-08.2009

Oshiro, Y., Quevedo, A. S., Mchaffie, J. G., Kraft, R. A., and Coghill, R. C. (2007). Brain mechanisms supporting spatial discrimination of pain. *J. Neurosci.* 27, 3388–3394. doi: 10.1523/JNEUROSCI.5128-06.2007

Panizzon, M. S., Fennema-Notestine, C., Eyler, L. T., Jernigan, T. L., Prom-Wormley, E., Neale, M., et al. (2009). Distinct genetic influences on cortical surface area and cortical thickness. *Cereb Cortex* 19, 2728–2735. doi: 10.1093/cercor/bhp026

Paul, F. R., R. Schmidt, P., Dahnke, R., Biberacher, V., Beer, A., Buck, D., et al. (2017). Volume versus surface-based cortical thickness measurements: a comparative study with healthy controls and multiple sclerosis patients. *PLos One* 12:e0179590. doi: 10.1371/journal.pone.0179590

Rainville, P., Roy, M., Pich, M., Chen, J. I., and Peretz, Z. (2009). Cerebral and spinal modulation of pain by emotions. *Proc. Natl. Acad. Sci. U S A* 106, 20900–20905. doi: 10.1073/pnas.0904706106

Rocca, M. A., Ceccarelli, A., Falini, A., Colombo, B., Tortorella, P., Bernasconi, L., et al. (2006). Brain gray matter changes in migraine patients with T2-visible lesions: a 3-T MRI study. *Stroke* 37, 1765–1770. doi: 10.1161/01.STR.0000226589.00599.4d

Russo, A., Marcelli, V., Esposito, F., Corvino, V., Marcuccio, L., Giannone, A., et al. (2014). Abnormal thalamic function in patients abnormal thalamic function in patients. *Neurology* 82, 2120–2126. doi: 10.1212/WNL.0000000000000496

Sauro, K. M., Rose, M. S., Becker, W. J., Christie, S. N., Giammarco, R., Mackie, G. F., et al. (2010). HIT-6 and MIDAS as measures of headache disability in a headache referral population. *Headache* 50, 383–395. doi: 10.1111/j.1526-4610.2009.01544.x

Schwedt, T. J., Berisha, V., and Chong, C. D. (2015). Temporal lobe cortical thickness correlations differentiate the migraine brain from the healthy brain. *PLoS One* 10:e0116687. doi: 10.1371/journal.pone.0116687

Schwedt, T. J., Schlaggar, B. L., Mar, S., Nolan, T., Coalson, R. S., Nardos, B., et al. (2013). Atypical resting-state functional connectivity of affective pain

regions in chronic migraine. *Headache* 53, 737–751. doi: 10.1111/head.12081

Seiger, R., Ganger, S., Kranz, G. S., Hahn, A., and Lanzenberger, R. (2018). Cortical thickness estimations of freesurfer and the CAT12 toolbox in patients with Alzheimer's disease and healthy controls. *J. Neuroimaging* 28, 515–523. doi: 10.1111/jon.12521

Shin, J. H., Kim, Y. K., Kim, H. J., and Kim, J. S. (2014). Altered brain metabolism in vestibular migraine: comparison of interictal and ictal findings. *Cephalalgia* 34, 58–67. doi: 10.1177/0333102413498940

Teggi, R., Colombo, B., Rocca, M. A., Bondi, S., Messina, R., Comi, G., et al. (2016). A review of recent literature on functional MRI and personal experience in two cases of definite vestibular migraine. *Neurol. Sci.* 37, 1399–1402. doi: 10.1007/s10072-016-2618-6

Wang, S., Wang, H., Liu, X., Yan, W., Wang, M., and Zhao, R. (2021). A resting-state functional MRI study in patients with vestibular migraine during interictal period. *Acta Neurol. Belg.* 121, 1–7. doi: 10.1007/s13760-021-01639-9

Wei, H., Chen, J., Chen, Y., Yu, Y., Zhou, G., Qu, L., et al. (2020). Impaired functional connectivity of limbic system in migraine without aura. *Brain Imaging Behav.* 14, 1805–1814. doi: 10.1007/s11682-019-00116-5

Xu, H, Gao, C., Li, H., Gao, L., Zhang, M., and Wang, Y. (2019). Structural and functional amygdala abnormalities in hemifacial spasm. *Front. Neurol.* 10:393. doi: 10.3389/fneur.2019.00393

Yotter, R. A., Dahnke, R., Thompson, P. M., and Gaser, C. (2011a). Topological correction of brain surface meshes using spherical harmonics. *Hum. Brain Mapp.* 32, 1109–1124. doi: 10.1002/hbm.21095

Yotter, R. A., Thompson, P. M., and Gaser, C. (2011b). Algorithms to improve the reparameterization of spherical mappings of brain surface meshes. *J. Neuroimaging* 21, e134–e147. doi: 10.1111/j.1552-6569.2010.00484.x

Zhe, X., Gao, J., Chen, L., Zhang, D., Tang, M., Yan, X., et al. (2020). Altered structure of the vestibular cortex in patients with vestibular migraine. *Brain Behav.* 10:e01572. doi: 10.1002/brb3.1572

Conflict of Interest: Author KA was employed by the company Philips Healthcare.

The remaining authors declare that the research was conducted in the absence of any commercial or financial relationships that could be construed as a potential conflict of interest.

Publisher's Note: All claims expressed in this article are solely those of the authors and do not necessarily represent those of their affiliated organizations, or those of the publisher, the editors and the reviewers. Any product that may be evaluated in this article, or claim that may be made by its manufacturer, is not guaranteed or endorsed by the publisher.

frontiers in Human Neuroscience

ORIGINAL RESEARCH
published: 30 August 2021
doi: 10.3389/fnhum.2021.705863

The Higher Parietal Cortical Thickness in Abstinent Methamphetamine Patients Is Correlated With Functional Connectivity and Age of First Usage

Ru Yang[1†], Lei He[1,2†], Zhixue Zhang[3], Wenming Zhou[2] and Jun Liu[1]*

[1] Department of Radiology, The Second Xiangya Hospital, Central South University, Changsha, China, [2] Department of Radiology, The First People's Hospital of Yueyang, Yueyang, China, [3] Department of Radiology, The First Hospital of Hunan University of Chinese Medicine, Changsha, China

OPEN ACCESS

Edited by:
Long-Biao Cui, People's Liberation Army General Hospital, China

Reviewed by:
Zhaowen Liu, Massachusetts General Hospital and Harvard Medical School, United States
Fan Guo, Fourth Military Medical University, China

****Correspondence:***
Jun Liu
junliu123@csu.edu.cn

[†] These authors have contributed equally to this work

Specialty section:
This article was submitted to Brain Imaging and Stimulation, a section of the journal Frontiers in Human Neuroscience

Received: *06 May 2021*
Accepted: *09 August 2021*
Published: *30 August 2021*

Citation:
Yang R, He L, Zhang Z, Zhou W and Liu J (2021) The Higher Parietal Cortical Thickness in Abstinent Methamphetamine Patients Is Correlated With Functional Connectivity and Age of First Usage. Front. Hum. Neurosci. 15:705863. doi: 10.3389/fnhum.2021.705863

Aim: This study aimed to explore the changes of cortical thickness in abstinent methamphetamine (MA) patients compared with healthy controls.

Materials and Methods: Three-tesla structural and functional magnetic resonance imaging (MRI) was obtained from 38 abstinent methamphetamine-dependent (AMD) patients and 32 demographically equivalent healthy controls. The cortical thickness was assessed using FreeSurfer software. General linear model was used to get brain regions with significant different cortical thickness between groups ($p < 0.05$, Monte Carlo simulation corrected). The mean cortical thickness value and functional connectivity with all other brain regions was extracted from those significant regions. Moreover, correlation coefficients were calculated in the AMD group to assess the relations between the mean cortical thickness, functional connectivity and age when they first took MA and the duration of both MA use and abstinence.

Results: The AMD group showed significant cortical thickness increase in one cluster located in the parietal cortex, including right posterior central gyrus, supramarginal gyrus, and superior parietal lobule. In addition, cortical thickness values of those regions were all significant and negatively correlated with the age when patients first used MA. The cortical thickness of right posterior gyrus were positively correlated with its functional connectivities with left middle frontal gyrus and both left and right medial orbitofrontal gyrus.

Conclusion: The higher cortical thickness in the parietal cortex of the AMD group is in agreement with findings in related studies of increased glucose metabolism and gray matter volume. Importantly, the negative correlation between parietal cortical thickness and age of first MA suggested that adolescent brains are more vulnerable to MA's neurotoxic effect.

Keywords: methamphetamine, long-term abstinence, cortical thickness, addiction, adolescent

INTRODUCTION

Methamphetamine (MA) is an addictive psychoactive drug that has rapid onset and wreaks havoc on the nervous system. It has been widely abused and has become a global public health problem (Var et al., 2016; Darke et al., 2017). According to the Word Drug Reports in 2017, Amphetamines, including amphetamine and methamphetamine, are the second most abused stimulant group worldwide after cannabis (United Nations Office of Drugs Crime, 2017a). MA has dominated the global amphetamines market, accounting for 72% of the global seizures of amphetamines (United Nations Office of Drugs Crime, 2017b). Moreover, various physical illnesses and psychotic disorders can be caused by methamphetamine abuse (Gonzalez et al., 2004; Woods et al., 2005; Cruickshank and Dyer, 2009; London et al., 2015). Worse of all, patients often relapse when they suffer from stress and come across other high risk environments that may trigger MA relapse even after abstinence or treatment (Volkow et al., 2006; McKetin et al., 2012; Brecht and Herbeck, 2014).

Neuroimaging techniques have become powerful methods to study brain structures, functions, and metabolism in MA users. Comprehensive MA related brain structure and function changes have been found (Chang et al., 2005; Ernst and Chang, 2008; Groman et al., 2012) and some can be restored and improved to a certain extent after treatment or abstinence (Groman et al., 2012; Brooks et al., 2016; Choi et al., 2018). Our previous study investigated the gray matter volume difference between abstinent methamphetamine-dependent (AMD) patients and healthy controls (HC) using the voxel-based morphometry (VBM) method (Zhang et al., 2018). "The increased gray matter volumes in the bilateral cerebellum and decreased volumes in the right calcarine and right cuneus were found and suggested abnormal visual and cognitive functions in the AMD patients" (Zhang et al., 2018). Moreover, "the left cerebellum crus GMV was positively correlated with abstinence duration which signaled the cognitive function recovery along with the abstinence." VBM is an efficient tool to measure structural differences and is sensitive to subtle gray matter alterations. It is more rapid and provides voxel-wise whole brain results compared to manually segmented brain regions in traditional morphometric approaches (Ashburner and Friston, 2000). Therefore, it has been extensively used in psychiatric disorder studies including substance addiction (Morales et al., 2012; Durazzo et al., 2015; Hartwell et al., 2016). As another important structural analysis method, surf-based cortical thickness measurement allows the "regional distribution and quantification of gray matter cortical loss to be specifically assessed in contrast to gyral or lobar volumetric studies which combine gray and white matter within regional volumes" (Rohrer et al., 2009). Hence, cortical thickness can also assess the brain substrates of neurodegenerative disease and provide complementary information to other imaging techniques about neuroanatomy (Rohrer et al., 2009). Therefore it has been commonly used in psychiatry and neural diseases but has not been applied toward the study of MA addiction or abstinence to our knowledge.

In this study, we investigated abnormality of cortical thickness of methamphetamine abstinence patients and its association with functional connectivity and addiction/abstinence variables to provide potential complementary structural biomarkers of MA addiction or abstinence.

MATERIALS AND METHODS

Subjects and MR Imaging Acquisition

Thirty two healthy subjects and 38 AMD subjects were recruited in this study from April 2016 to July 2017. All AMD subjects were recruited from Pingtang Mandatory Detoxification, Changsha City, Hunan Province. The inclusion and exclusion criteria for all subjects in this study were the same as our previous study (Zhang et al., 2018). AMD subjects were diagnosed using the Diagnostic and Statistical Manual on Mental Disorders (DSM-V) and after that had received a long-term (14–25 months) compulsory abstinence. In addition, for all subjects, smoking status, and alcohol consumption were recorded. For every AMD subject, the age when they first used MA, the months of MA use before their most recent abstinence and months of abstinence were also recorded.

Every subject was scanned in a 3T Siemens Skyra MRI scanner equipped with a 32-channel head coil. T1-weighted images and resting-state functional MR images were collected. The detailed MRI scanning sequences and parameters were also identical to the previous study (Zhang et al., 2018).

The study was approved by the Ethics Committees of the Second Xiangya Hospital of Central South University. Confidentiality of personal information and freedom to withdraw from the study were guaranteed.

Imaging Data Analyses

All MRI images were visually inspected by two radiologists for lesions, structural abnormalities and artifacts. No subjects were excluded.

Cortical reconstructions of the T1-weighted images were performed using FreeSurfer (version 5.3.0)[1] on a Linux workstation. The detailed steps have been described by related studies (Collins et al., 2017; Perez et al., 2018). For each subject, the gray and white matter boundary derived from automatic segmentation were visually checked and was then used to identify the pial surface with a deformable surface algorithm. Cortical thickness was measured as the distance between the white matter and pial surfaces. After construction, images were then morphed and registered to an average spherical space where gyral and sulcal features were optimally aligned. Individual measures were then transformed into the average space. Cortical thickness maps were then smoothed with a 15 mm half-maximum full-width Gaussian kernel.

Functional images processing was performed with DPABI (a toolbox for Data Processing and Analysis of Brain Imaging). After preprocessing including slice timing, realign, normalization

[1] https://surfer.nmr.mgh.harvard.edu/

and nuisance covariates regression, functional connectivity was calculated on Anatomic-Automatic-Labeling (AAL) template.

Statistical Analysis

Demographics were compared between AMD and healthy control groups with SPSS 21.0. Age and years of education were compared using two-sample *t*-test while smoking status and alcohol consumption were tested using Fisher exact test. The significance level was set to $p < 0.05$.

QDEC tool in FreeSurfer was utilized to compare cortical thickness between two groups using a 2-class general linear model (GLM). Multiple comparisons were corrected using Monte Carlo simulation method with an initial vertex-wise threshold of $p < 0.01$ and vertex level corrected to $p < 0.05$.

Mean values were then extracted from brain regions which showed significantly different cortical thickness between the two groups. In the AMD group, we calculated the correlation coefficients of those mean cortical thickness values with patients' age when they first used MA, the total months of MA use and abstinence. The significance level was set to $p < 0.05$.

The functional connectivity of significant region to any other regions on AAL template was also extracted. The correlation coefficients between these connectivity values with cortical thickness values were calculated. The significance level was set to $p < 0.05$.

RESULTS

Demographics

Our study included 38 AMD patients and 32 healthy subjects. As showed in **Table 1**, there were no significant differences between the two groups in age, years of education, smoking status or alcohol consumption.

Cortical Thickness Analysis Results

In comparison with the HC group, the AMD group showed significant cortical thickness increase in one cluster in parietal cortex. The detailed location of the cluster was defined by overlapping it with AAL template. It contains three parts including right posterior central gyrus, supramarginal gyrus, and superior parietal lobule (**Table 2** and **Figure 1**).

TABLE 1 | Demographic information and characterization.

Group	AMD	HC	*p*
N	38	32	
Age/year	33.1 ± 6.0	34.5 ± 7.0	0.353[a]
Education/year	8.7 ± 2.1	9.6 ± 2.4	0.113[a]
Smoking (Yes/No)	37/1	30/2	0.589[b]
Drinking (Yes/No)	13/25	8/24	0.443[b]
Age of first MA use	26.0 ± 6.9		
Months of MA use	64.2 ± 34.2		
Months of abstinence	19.1 ± 2.7		

[a] *Two-sample t-test.*
[b] *Fisher exact test. Significant level was set at p < 0.05. There are no statistically significant differences between AMD and HC group based on demographic information and characterization.*

Correlation Analyses

In the AMD group, the mean cortical thickness of all three regions were significantly negatively correlated with the age of first MA usage: right posterior central gyrus, $r = -0.635$, $p < 0.001$; right supramarginal gyrus, $r = -0.652$, $p < 0.001$; right superior parietal lobule, $r = -0.496$, $p = 0.002$. No significant correlations were found between cortical thickness and months of MA use or months of abstinence (**Figure 2**).

Intuitively, the association between cortical thickness of abnormal regions in AMD patients and the age of first MA use could be affected by the duration of MA use. Therefore, partial correlation coefficients were calculated to exclude the effect of MA use duration. Those three mean cortical thicknesses were still strongly correlated to the age of first MA use: Right posterior central gyrus, $r = -0.617$, $p < 0.001$; right supramarginal gyrus, $r = -0.644$, $p < 0.001$; right superior parietal lobule, $r = -0.588$, $p < 0.001$.

Moreover, the cortical thickness of right posterior gyrus were positively correlated with its functional connectivities to three regions including left middle frontal gyrus ($r = 0.324$, $p = 0.047$), right medial orbitofrontal gyrus ($r = 0.397$, $p = 0.014$) and left medial orbitofrontal gyrus ($r = 0.334$, $p = 0.041$).

DISCUSSION

In this study, we adopted the surface-based cortical thickness method to investigate the abnormal brain structure in abstinent methamphetamine-dependent patients. Increased cortical thickness was found in one cluster located in the right parietal cortex, including right posterior central gyrus, supramarginal gyrus, and superior parietal lobule. In addition, mean cortical thickness values of those regions were all strongly negatively correlated with age of first MA use in AMD patients. Moreover, the cortical thickness of right posterior gyrus were positively correlated with its functional connectivities left middle frontal gyrus, right medial orbitofrontal gyrus, and left medial orbitofrontal gyrus.

The higher cortical thickness in parietal cortex of the AMD group agreed with previous studies that observed increased glucose metabolism in both short and long term abstinent MA patients (Volkow et al., 2001; Berman et al., 2008) and increased gray matter (Jernigan et al., 2005) in abstinence methamphetamine patients, and the increased glucose metabolism in high dose MA treatment rats' brains without abstinence (Thanos et al., 2016). The parietal cortex was found to be especially sensitive to methamphetamine neurotoxicity (Volkow et al., 2001). The increased cortical thickness found in this study could be explained by the growing numbers of microglia and astrocytes, which could driven by MA abuse (LaVoie et al., 2004) and were thought to increase the cerebral glucose metabolic. Moreover, the activated microglia were linked to vasculature outside of neurodegeneration regions (Bowyer et al., 2017), which could also increase the cortical thickness in

TABLE 2 | Regions with increased cortical thickness in AMD group compared with HC group.

Brain region (AAL)	Volume (mm^3)	*p*	Peak talairach coordinates		
			X	Y	Z
Right posterior central gyrus (peak location)	1347.13	0.0474*	54.2	−14.6	34.4

*Statistical threshold was $p < 0.05$ corrected for multiple comparisons by Monte Carlo simulation method; Coordinates are located in Talairach space. AAL, Anatomic-Automatic-Labeling template. *$p < 0.05$.*

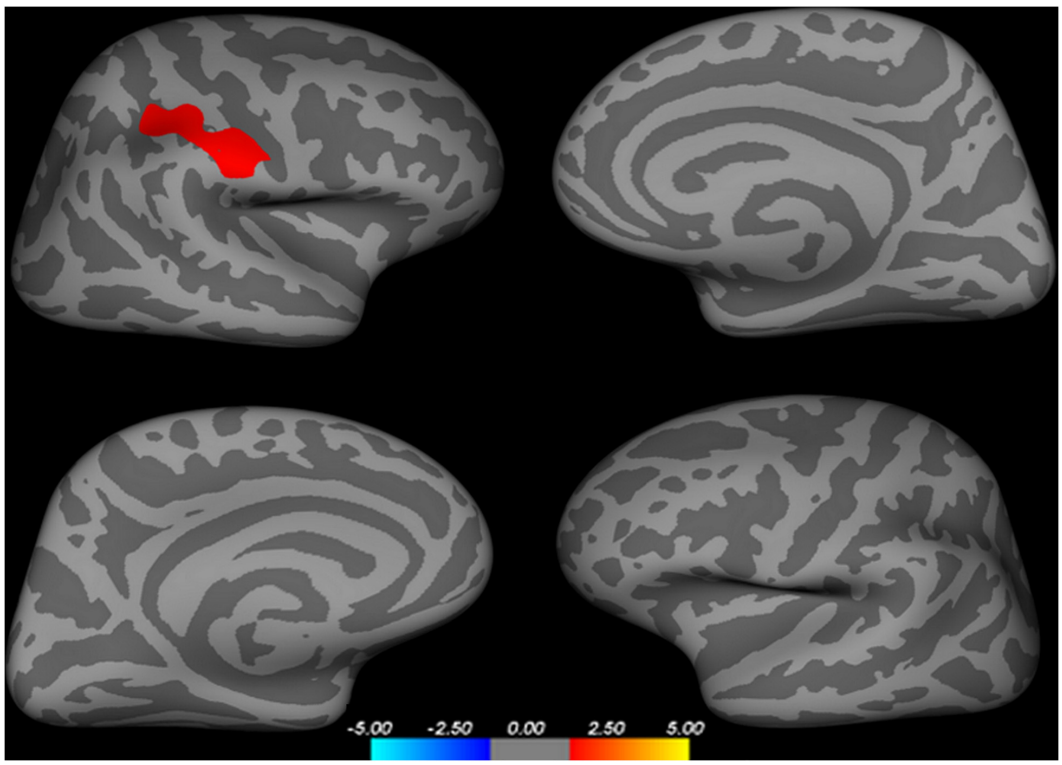

FIGURE 1 | Regions with increased cortex thickness in AMD group.

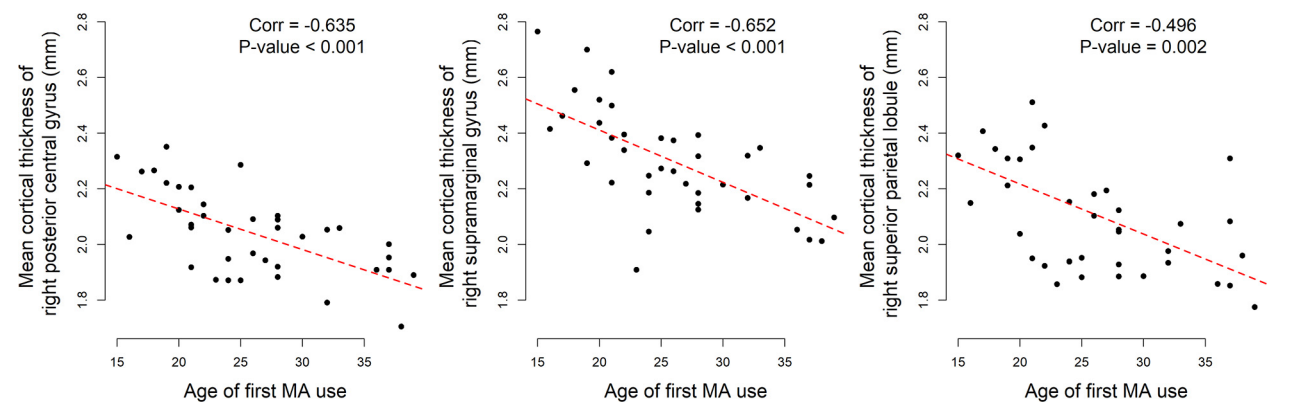

FIGURE 2 | Significant correlations between age of first MA use and mean cortical thickness of abnormal regions in AMD group.

parietal cortex. Although increased microglial activation along with increased brain volume were found after chronic MA treatment (Thanos et al., 2016), their causal relations have not yet been proven.

MA users have varied decision-making changes and the parietal cortex has been shown to be critical for it (Bowyer et al., 2007). Specifically, the parietal cortex activation levels have been found to be correlated to decision making of uncertainty in MA patients (Paulus et al., 2003). The parietal cortex metabolism in MA users was correlated with Grooved pegboard tasks performance, which is also involved with decision-making (Volkow et al., 2001). In addition, gene expression changes related to synaptic plasticity were also found in the parietal cortex and may be related to these behavioral outcomes (Paulus et al., 2001). Moreover, the middle frontal gyrus and medial orbitofrontal cortex are both important areas for decision making. That their connections with right posterior gyrus were positively correlated with its cortical thickness also implied the parietal cortex plays an essential role in MA addiction.

The peak intensity value of the significant cluster in our study was located in the right posterior central gyrus, which contains the primary somatosensory cortex. Besides dopaminergic and serotonergic terminals, a study on adult rats indicated that MA also has the neurotoxic effect on glutamatergic neurons in the somatosensory cortex (Pu et al., 1996). Reactive microgliosis was also observed in the somatosensory cortex (LaVoie et al., 2004).

Importantly, we found that cortical thickness of significant regions located in the parietal cortex were negatively correlated with age of first MA use with or without excluding the effect of MA use duration. In other words, the younger the patient was when starting to abuse MA, the thicker those regions were than in healthy patients no matter how long they used MA. A study by Jernigan et al. (2005) showed that nucleus accumbens volume increase associated with MA dependence has a larger effect on younger MA patients. Also, it was reported that the age when MA was first used was positively related with intracranial volume (Huckans et al., 2010). "Adolescence is a critical period of brain development as the brain undergoes dynamic synaptic reorganization and myelination" (Castellanos et al., 1999). On the one hand, environmental insults can affect brain development and cause irreversible damage to the adolescent brain (Castellanos et al., 1999; Rapoport and Brain, 2008). On the other hand, the adolescent brain can recover more effectively from lesions for its greater neuroplasticity (Lyoo et al., 2015). In the parietal cortex, increased glucose metabolism was found in brains with and without abstinence after MA treatment, and the increased gray matter volume was found in both short and long term MA abstinent patients. We speculated that the abnormal parietal cortex was mainly caused by MA exposure before abstinence. The negative correlation between age of first MA use and the cortical thickness could be interpreted as: adolescent brains are more vulnerable to MA neurotoxic effects that cause irreversible damage even after a long-term abstinence.

LIMITATION

In this study, we found higher cortical thickness in parietal cortex of the AMD group, which is agreed with the increased glucose metabolism and gray matter in related studies. However, the underlying mechanisms are still not clear. Future studies are encouraged to explore the causal relation between increased microglial activation and brain volume change or MA usage. Moreover, that the negative correlation between age of first MA use and the cortical thickness also need to be validated and explained by researches from other modalities.

DATA AVAILABILITY STATEMENT

The raw data supporting the conclusions of this article will be made available by the authors, without undue reservation.

ETHICS STATEMENT

The studies involving human participants were reviewed and approved by the Ethics Committee of the Second Xiangya Hospital, Central South University. The patients/participants provided their written informed consent to participate in this study.

AUTHOR CONTRIBUTIONS

RY, WZ, and JL conceptualized and designed the research. ZZ collected the demographics and MRI data. LH analyzed MRI data and undertook the statistical analysis with RY. RY and LH wrote the first draft. RY contributed to final manuscript including editing figures, tables, and format. All authors critically reviewed the content and approved the final version for publication.

FUNDING

This work was supported by the National Natural Science Foundation of China (Grant No. 81671671), the National Key Research and Development Program of China, (Grant No. 2016YFC0800908), the Clinical Research Center For Medical Imaging In Hunan Province (Grant No. 2020SK4001), and the project of Changsha Science and Technology (Grant No. kq1801115).

REFERENCES

Ashburner, J., and Friston, K. J. (2000). Voxel-based morphometry–the methods. *NeuroImage* 11, 805–821. doi: 10.1006/nimg.2000.0582

Berman, S. M., Voytek, B., Mandelkern, M. A., Hassid, B. D., Isaacson, A., Monterosso, J., et al. (2008). Changes in cerebral glucose metabolism during early abstinence from chronic methamphetamine abuse. *Mol. Psychiatry* 13, 897–908. doi: 10.1038/sj.mp.4002107

Bowyer, J. F., Pogge, A. R., Delongchamp, R. R., O'Callaghan, J. P., Vrana, K. E., and Freeman, W. M. (2007). A threshold neurotoxic amphetamine exposure inhibits parietal cortex expression of synaptic plasticity-related genes. *Neuroscience* 144, 66–76. doi: 10.1016/j.neuroscience.2006.08.076

Bowyer, J. F., Tranter, K. M., Sarkar, S., George, N. I., Hanig, J. P., Kelly, K. A., et al. (2017). Corticosterone and exogenous glucose alter blood glucose levels, neurotoxicity, and vascular toxicity produced by methamphetamine. *J. Neurochem.* 143, 198–213. doi: 10.1111/jnc.14143

Brecht, M. L., and Herbeck, D. (2014). Time to relapse following treatment for methamphetamine use: a long-term perspective on patterns and predictors. *Drug Alcohol Depend.* 139, 18–25. doi: 10.1016/j.drugalcdep.2014.02.702

Brooks, S. J., Burch, K. H., Maiorana, S. A., Cocolas, E., Schioth, H. B., Nilsson, E. K., et al. (2016). Psychological intervention with working memory training increases basal ganglia volume: A VBM study of inpatient treatment for methamphetamine use. *NeuroImage Clin.* 12, 478–491. doi: 10.1016/j.nicl.2016.08.019

Castellanos, F. X., Giedd, J. N., Blumenthal, J., Jeffries, N. O., Castellanos, F. X., Liu, H., et al. (1999). Brain development during childhood and adolescence: a longitudinal MRI study. *Nat. Neurosci.* 2, 861–863. doi: 10.1038/13158

Chang, L., Cloak, C., Patterson, K., Grob, C., Miller, E. N., and Ernst, T. (2005). Enlarged striatum in abstinent methamphetamine abusers: a possible compensatory response. *Biol. Psychiatry* 57, 967–974. doi: 10.1016/j.biopsych.2005.01.039

Choi, J. K., Lim, G., Chen, Y. I., and Jenkins, B. G. (2018). Abstinence to chronic methamphetamine switches connectivity between striatal, hippocampal and sensorimotor regions and increases cerebral blood volume response. *NeuroImage* 174, 364–379. doi: 10.1016/j.neuroimage.2018.02.059

Collins, J. A., Montal, V., Hochberg, D., Quimby, M., Mandelli, M. L., Makris, N., et al. (2017). Focal temporal pole atrophy and network degeneration in semantic variant primary progressive aphasia. *Brain* 140, 457–471. doi: 10.1093/brain/aww313

Cruickshank, C. C., and Dyer, K. R. (2009). A review of the clinical pharmacology of methamphetamine. *Addiction* 104, 1085–1099. doi: 10.1111/j.1360-0443.2009.02564.x

Darke, S., Kaye, S., and Duflou, J. (2017). Methamphetamine-related death is an under-addressed public health problem. *Addiction* 112, 2204–2205. doi: 10.1111/add.14035

Durazzo, T. C., Mon, A., Gazdzinski, S., Yeh, P. H., and Meyerhoff, D. J. (2015). Serial longitudinal magnetic resonance imaging data indicate non-linear regional gray matter volume recovery in abstinent alcohol-dependent individuals. *Addict. Biol.* 20, 956–967. doi: 10.1111/adb.12180

Ernst, T., and Chang, L. (2008). Adaptation of brain glutamate plus glutamine during abstinence from chronic methamphetamine use.. *J. Neuroimmune Pharmacol.* 3, 165–172. doi: 10.1007/s11481-008-9108-4

Gonzalez, R., Rippeth, J. D., Carey, C. L., Heaton, R. K., Moore, D. J., Schweinsburg, B. C., et al. (2004). Neurocognitive performance of methamphetamine users discordant for history of marijuana exposure. *Drug Alcohol Depend.* 76, 181–190. doi: 10.1016/j.drugalcdep.2004.04.014

Groman, S. M., Lee, B., Seu, E., James, A. S., Feiler, K., Mandelkern, M. A., et al. (2012). Dysregulation of D(2)-mediated dopamine transmission in monkeys after chronic escalating methamphetamine exposure. *J. Neurosci.* 32, 5843–5852. doi: 10.1523/jneurosci.0029-12.2012

Hartwell, E. E., Moallem, N. R., Courtney, K. E., Glasner-Edwards, S., and Ray, L. A. (2016). Sex Differences in the association between internalizing symptoms and craving in methamphetamine users. *J. Addict. Med.* 10, 395–401. doi: 10.1097/adm.0000000000000250

Huckans, M. S., Schwartz, D. L., Mitchell, A. D., Lahna, D. L., Luber, H. S., Mitchell, S. H., et al. (2010). Global and local morphometric differences in recently abstinent methamphetamine-dependent individuals. *NeuroImage* 50, 1392–1401. doi: 10.1016/j.neuroimage.2010.01.056

Jernigan, T. L., Gamst, A. C., Archibald, S. L., Fennema-Notestine, C., Mindt, M. R., Marcotte, T. D., et al. (2005). Effects of methamphetamine dependence and HIV infection on cerebral morphology. *The Am. J. Psychiatry* 162, 1461–1467. doi: 10.1176/appi.ajp.162.8.1461

LaVoie, M. J., Card, J. P., and Hastings, T. G. (2004). Microglial activation precedes dopamine terminal pathology in methamphetamine-induced neurotoxicity. *Exp. Neurol.* 187, 47–57. doi: 10.1016/j.expneurol.2004.01.010

London, E. D., Kohno, M., Morales, A. M., and Ballard, M. E. (2015). Chronic methamphetamine abuse and corticostriatal deficits revealed by neuroimaging. *Brain Res.* 1628, 174–185. doi: 10.1016/j.brainres.2014.10.044

Lyoo, I. K., Yoon, S., Kim, T. S., Lim, S. M., Choi, Y., Kim, J. E., et al. (2015). Predisposition to and effects of methamphetamine use on the adolescent brain. *Mol. Psychiatry* 20, 1516–1524. doi: 10.1038/mp.2014.191

McKetin, R., Najman, J. M., Baker, A. L., Lubman, D. I., Dawe, S., Ali, R., et al. (2012). Evaluating the impact of community-based treatment options on methamphetamine use: findings from the Methamphetamine. *Addiction* 107, 1998–2008. doi: 10.1111/j.1360-0443.2012.03933.x

Morales, A. M., Lee, B., Hellemann, G., O'Neill, J., and London, E. D. (2012). Gray-matter volume in methamphetamine dependence: cigarette smoking and changes with abstinence from methamphetamine. *Drug Alcohol Depend.* 125, 230–238. doi: 10.1016/j.drugalcdep.2012.02.017

Paulus, M. P., Hozack, N., Frank, L., Brown, G. G., and Schuckit, M. A. (2003). Decision making by methamphetamine-dependent subjects is associated with error-rate-independent decrease in prefrontal and parietal activation. *Biol. Psychiatry* 53, 65–74. doi: 10.1016/s0006-3223(02)01442-7

Paulus, M. P., Zauscher, B., McDowell, J. E., Frank, L., Brown, G. G., and Braff, D. L. (2001). Prefrontal, parietal, and temporal cortex networks underlie decision-making in the presence of uncertainty. *NeuroImage* 13, 91–100. doi: 10.1006/nimg.2000.0667

Perez, D. L., Matin, N., Williams, B., Tanev, K., Makris, N., LaFrance, W. C., et al. (2018). Cortical thickness alterations linked to somatoform and psychological dissociation in functional neurological disorders. *Hum. Brain Mapp.* 39, 428–439. doi: 10.1002/hbm.23853

Pu, C., Broening, H. W., and Vorhees, C. V. (1996). Effect of methamphetamine on glutamate-positive neurons in the adult and developing rat somatosensory cortex. *Synapse* 23, 328–334. doi: 10.1002/(sici)1098-2396(199608)23:4<328::aid-syn11>3.0.co;2-t

Rapoport, J., and Brain, G. N. (2008). Neuroplasticity in healthy, hyperactive and psychotic children: insights from neuroimaging. *Neuropsychopharmacology* 33, 181–197. doi: 10.1038/sj.npp.1301553

Rohrer, J. D., Warren, J. D., Modat, M., Ridgway, G. R., Douiri, A., Rossor, M. N., et al. (2009). Patterns of cortical thinning in the language variants of frontotemporal lobar degeneration. *Neurology* 72, 1562–1569. doi: 10.1212/wnl.0b013e3181a4124e

Thanos, P. K., Kim, R., Delis, F., Ananth, M., Chachati, G., Gold, M. S., et al. (2016). Chronic methamphetamine effects on brain structure and function in rats. *PLoS One* 11:e0155457. doi: 10.1371/journal.pone.0155457

United Nations Office of Drugs and Crime (2017a). *Global Overview of Drug Demand and Supply: Latest Trends, Cross-Cutting Issues., World Drug Report 2017*. Vienna: United Nations Office on Drugs and Crime.

United Nations Office of Drugs and Crime (2017b). *Market Analysis of Synthetic Drugs: Amphetamine-type Stimulants, New Psychoactive Substances., World Drug Report 2017*. Vienna: United Nations Office on Drugs and Crime.

Var, S. R., Day, T. R., Vitomirov, A., Smith, D. M., Soontornniyomkij, V., Moore, D. J., et al. (2016). Mitochondrial injury and cognitive function in HIV infection and methamphetamine use. *AIDS* 30, 839–848. doi: 10.1097/qad.0000000000001027

Volkow, N. D., Chang, L., Wang, G. J., Fowler, J. S., Franceschi, D., Sedler, M. J., et al. (2001). Higher cortical and lower subcortical metabolism in detoxified methamphetamine abusers. *Am. J. Psychiatry* 158, 383–389. doi: 10.1176/appi.ajp.158.3.383

Volkow, N. D., Wang, G. J., Telang, F., Fowler, J. S., Logan, J., Childress, A. R., et al. (2006). Cocaine cues and dopamine in dorsal striatum: mechanism of craving in cocaine addiction. *J. Neurosci.* 26, 6583–6588. doi: 10.1523/jneurosci.1544-06.2006

Woods, S. P., Rippeth, J. D., Conover, E., Gongvatana, A., Gonzalez, R., Carey, C. L., et al. (2005). Deficient strategic control of verbal encoding and retrieval in individuals with methamphetamine dependence. *Neuropsychology* 19, 35–43. doi: 10.1037/0894-4105.19.1.35

Zhang, Z., He, L., Huang, S., Fan, L., Li, Y., Li, P., et al. (2018). Alteration of brain structure with long-term abstinence of methamphetamine by voxel-based morphometry. *Front. Psychiatry* 9:722. doi: 10.3389/fpsyt.2018.00722

Conflict of Interest: The authors declare that the research was conducted in the absence of any commercial or financial relationships that could be construed as a potential conflict of interest.

frontiers in Human Neuroscience

MINI REVIEW
published: 09 September 2021
doi: 10.3389/fnhum.2021.720239

Shaping the Trans-Scale Properties of Schizophrenia *via* Cerebral Alterations on Magnetic Resonance Imaging and Single-Nucleotide Polymorphisms of Coding and Non-Coding Regions

Shu-Wan Zhao [1,2†], Xian Xu [3†], Xian-Yang Wang [1], Tian-Cai Yan [1], Yang Cao [1], Qing-Hong Yan [4], Kun Chen [5], Yin-Chuan Jin [1], Ya-Hong Zhang [4], Hong Yin [2*] and Long-Biao Cui [1,3*]*

[1] Department of Clinical Psychology, School of Medical Psychology, Fourth Military Medical University, Xi'an, China, [2] Department of Radiology, Xijing Hospital, Fourth Military Medical University, Xi'an, China, [3] Department of Radiology, The Second Medical Center, Chinese PLA General Hospital, Beijing, China, [4] Department of Psychiatry, Xijing Hospital, Fourth Military Medical University, Xi'an, China, [5] Department of Anatomy and K. K. Leung Brain Research Centre, Fourth Military Medical University, Xi'an, China

Schizophrenia is a complex mental illness with genetic heterogeneity, which is often accompanied by alterations in brain structure and function. The neurobiological mechanism of schizophrenia associated with heredity remains unknown. Recently, the development of trans-scale and multi-omics methods that integrate gene and imaging information sheds new light on the nature of schizophrenia. In this article, we summarized the results of brain structural and functional changes related to the specific single-nucleotide polymorphisms (SNPs) in the past decade, and the SNPs were divided into non-coding regions and coding regions, respectively. It is hoped that the relationship between SNPs and cerebral alterations can be displayed more clearly and intuitively, so as to provide fresh approaches for the discovery of potential biomarkers and the development of clinical accurate individualized treatment decision-making.

Keywords: schizophrenia, magnetic resonance imaging, gene, trans-scale, single-nucleotide polymorphism

OPEN ACCESS

Edited by:
Mingrui Xia,
Beijing Normal University, China

Reviewed by:
Zhijiang Wang,
Peking University Sixth Hospital, China
Suping Cai,
Xidian University, China

***Correspondence:**
Ya-Hong Zhang
13572281986@126.com
Hong Yin
yinhong@fmmu.edu.cn
Long-Biao Cui
lbcui@fmmu.edu.cn

[†]These authors have contributed equally to this work

Specialty section:
This article was submitted to Brain Imaging and Stimulation, a section of the journal Frontiers in Human Neuroscience

Received: *04 June 2021*
Accepted: *05 August 2021*
Published: *09 September 2021*

Citation:
Zhao S-W, Xu X, Wang X-Y, Yan T-C, Cao Y, Yan Q-H, Chen K, Jin Y-C, Zhang Y-H, Yin H and Cui L-B (2021) Shaping the Trans-Scale Properties of Schizophrenia via Cerebral Alterations on Magnetic Resonance Imaging and Single-Nucleotide Polymorphisms of Coding and Non-Coding Regions. Front. Hum. Neurosci. 15:720239. doi: 10.3389/fnhum.2021.720239

INTRODUCTION

Schizophrenia is a common and complex multidimensional disease with high heredity, and genetic factors play an important role in its pathophysiological mechanism (McCutcheon et al., 2020). Understanding the genetic basis of schizophrenia is of great help to explore its pathogenesis.

In recent years, the application of trans-scale and multi-omics methods that combine gene and imaging in schizophrenia has promoted the elucidation of gene-related pathogenesis and the exploration of potential biomarkers (Reddaway et al., 2018). Trans-scale analysis is a research strategy for the joint analysis of information between different scales (van den Heuvel et al., 2019). From the macroscopic level, the human brain can be viewed as a complex network system made up of structural and functional connections between brain regions. And, from the microscopic perspective, the neurons containing dendrites and axons form a complex system of wiring

which makes up the structural basis of our brain. Microscale level information, such as genetic, molecular, and cellular, can provide sufficient evidence for the construction of brain phenotypes and mechanisms of brain injury at the macroscale level (van den Heuvel et al., 2019). Multi-omics analysis is a research strategy of integrative analysis that integrates information between different disciplines. Many disciplines, including genomics, epigenomics, transcriptomics, proteomics, metabolomics, gut microbiomics, and connectomics, have made significant contributions to the study of the pathogenesis of schizophrenia (Guan et al., 2021). The multi-omics analysis strategy can provide a more comprehensive perspective on the exploration of schizophrenia pathogenesis.

With the evolvement of functional magnetic resonance imaging (fMRI), structural magnetic resonance imaging (sMRI), diffusion-weighted imaging (DWI), and other sequences, alterations of brain structure and function can be displayed more accurately on MRI. Brain microstructures, such as white matter myelination, can be measured indirectly in a non-invasive manner using magnetization transfer imaging (MTI) technique (Whitaker et al., 2016). MRI plays an increasingly important role in the study of brain phenotypes and differential diagnosis of mental disorders. Previous studies have confirmed that there are some alterations in brain structure and function in patients with schizophrenia (Brown and Thompson, 2010), which may be related to clinical symptoms of schizophrenia (Cui et al., 2017; Liu et al., 2019). Another study has found out that quantitative and specific functional connectivity (FC) biomarkers could be an effective radiomics features for individualized diagnosis for schizophrenia (Cui et al., 2018). The appearance of brain phenotypes on MRI may provide clues to the differential diagnosis of schizophrenia and bipolar disorder, which overlap in risk genes and clinical symptoms. While brain disturbances in patients with bipolar disorder are primarily located in the fronto-limbic subsystems, schizophrenia is characterized by disorders of the small world and rich club and the effects still present in the unaffected offspring (Perry et al., 2019). Therefore, MRI-based imaging study has gradually become the most common method to study mental disorders at macroscale, providing connectomics and radiomics approaches.

Sinlge-nucletode polymorphisms (SNPs) are the most common genetic variation at the genome level, which are caused by the change of a single base pair in the DNA sequence. SNPs are found randomly in the coding region or the non-coding region of the gene and produce corresponding effects by affecting gene expression, mRNA processing, and protein translation (Bush and Moore, 2012; Gurung and Prata, 2015; Roy et al., 2020). According to the research, SNPs account for a large part of the genetic variation associated with schizophrenia (Pardinas et al., 2018). Although recent genome-wide association studies (GWASs) have identified many SNPs loci associated with schizophrenia (Schizophrenia Working Group of the Psychiatric Genomics C., 2014), providing many possible genetic variation resources with biological functions for analyzing the pathogenesis of schizophrenia, the functions behind these mutations still need to be verified. Changes in genes at the molecular level may be the basis that SNPs affect the functional and structural connectivity of the brain, as well as the volume and density of gray matter and white matter.

The effects produced by SNPs represent information at the cellular, molecular, and other microscopic levels, whereas MRI can provide a macroscopic view of brain phenotypes. The approach of combining micro-level and macro-level information for research exemplifies the trans-scale research strategy. Methods that combine genetic information with imaging information fall under the umbrella of multi-omics technologies. On the one hand, the trans-scale and multi-omics analysis strategy that combines genomics, connectomics, and radiomics is instrumental to visualize the link between functional genetic variants associated with schizophrenia and the imaging phenotype. On the other hand, the trans-scale and multi-omics analysis strategy linking gene variation with brain structure and function have further contributed to the advanced studies of molecular biological mechanisms behind brain phenotypes and clinical manifestations of schizophrenia. The goal of trans-scale neuroscience of psychiatric illnesses is to deepen insights of the relationship between alterations at different scales (van den Heuvel et al., 2019). Therefore, an updated overview of trans-scale properties of schizophrenia based on multi-omics research strategies is needed.

The effect of risk genes on structural connectivity and FC during executive tasks was found in a systematic review summarized by Gurung and Prata in 2015 (Gurung and Prata, 2015). In this review, we have carefully categorized the types of brain phenotype alterations and the location of SNPs separately. For alterations in brain phenotype, we address both structural and functional aspects. Based on the location of the SNPs, we have divided them into non-coding regions and coding regions to describe, respectively. The purpose of this article is to summarize the studies on the relationship between specific SNPs loci in schizophrenia-related genes and cerebral alterations based on trans-scale and multi-omics strategies in the past decade, as well as demonstrate the advantages of trans-scale and multi-omics research strategy through the relationship between SNPs and alterations in brain phenotypes. The candidate genes are listed as follows, and the specific SNPs loci and their possible effects on trans-scale properties of schizophrenia will be discussed in detail (zinc finger protein 804A [*ZNF804A*], calcium voltage-gated channel subunit alpha 1C [*CACNA1C*], neurogranin [*NRGN*], cholinergic receptor, muscarinic 3 [*CHRM3*], oligodendrocyte lineage transcription factor 2 [*OLTG2*], D-amino acid oxidase activator [*DAOA*], D-amino acid oxidase [*DAAO*], Disrupted in Schizophrenia Gene 1 [*DISC1*], nitric oxide synthase 1 [*NOS1*], *KIAA0319*, *N*-Methyl D-Aspartate 1 [*GRIN1*], Glutamate receptor 2 [*GRIA2*], microRNA 137 [*MIR137*], metabotropic glutamate receptor 3 [*GRM3*], contactin-associated protein-like 2 [*CNTNAP2*], Neuregulin1 [*NRG1*], glutamate receptor delta 1 [*GRID1*], and cyclin M2 gene [*CNNM2*]) (**Table 1**).

TABLE 1 | MRI studies investigating the impact of SNPs on brain.

SNP ID	Gene	Location	Patients/controls	Findings	References
Functional connectivity					
rs6800381	*CHRM3*	Non-coding region	161/150	FC between the left rectus and right thalamus (as quantitative traits)	Wang et al. (2016)
rs12807809	*NRGN*	Non-coding region	59/99	FC between the hippocampus and bilateral middle cingulate gyri and left anterior cingulate gyrus (TT < CC/CT)	Zhang et al. (2019)
rs11146020	*GRIN1*	Non-coding region	55/0	Causality connections between the left and right dorsolateral prefrontal cortex	Cai et al. (2020b)
rs2038136, rs2038137;	*KIAA0319*	Non-coding region	28/27	Resting-state network in language-related regions (no affection)	Jamadar et al. (2013)
rs1344706	*ZNF804A*	Coding region	52/128	Degree centrality in the precuneus (AA > CC/CA)	Chen et al. (2018)
rs1344706	*ZNF804A*		92/99	FC between the left hippocampus and right DLPFC (AA < CC/CA)	Zhang et al. (2018)
rs1344706	*ZNF804A*		78/153 (working memory)	FC of the right DLPFC and left hippocampal formation (contrast CC > CA > AA)	Rasetti et al. (2011)
rs1059004	*OLIG2*	Coding region	55/53	FC between left olfactory cortex, left parahippocampal gyrus, left middle temporal pole, bilateral hippocampus, and bilateral amygdala (AA/CA < CC)	Cai et al. (2020a)
rs1059004	*OLIG2*		49/47	Nodal efficiency in the right precuneus and left middle temporal pole (CA<CC)	Lv et al. (2020)
rs2391191	*DAOA*	Coding region	11/9	Connectivity density and larger global efficiency (AG > AA)	Liu et al. (2014)
rs1006737	*CACNA1C*	Coding region	54/80 (verbal fluency task)	FC between the left precentral gyrus/inferior frontal gyrus and superior temporal gyrus (AA/AG < GG)	Tecelao et al. (2019)
rs3782206	*NOS1*	Coding region	78/0 (Stroop); 76/0	FC between the right IFG and bilateral DLPFC in the Stroop task and the resting state (TT/CT < CC)	Zhang et al. (2015)
rs821617	*DISC1*	Coding region	46/24	FC between the right precuneus and inferior frontal gyrus (AA < AG/GG)	Gong et al. (2014)
rs3918346	*DAAO*	Coding region	40/48 (verbal fluency task)	FC between the left precuneus and a distributed network (TT/CT < CC) FC between the right posterior cingulate and right precuneus and left insula (TT/CT > CC)	Papagni et al. (2011)
rs4504469	*KIAA0319*	Coding region	28/27	Resting-state network in language-related regions (no affection)	Jamadar et al. (2013)
rs3813296	*GRIA2*	Coding region	55/0	Descending pathway from the prefrontal lobe to the striatum (GT < TT)	Cai et al. (2020b)
rs11146020	*GRIN1*	Non-coding region	55/0	Interaction effect: ascending pathway from the bilateral pallidum to the right caudate and the bilateral dLPFC	Cai et al. (2020b)
rs3813296	*GRIA2*	Coding region			
Structural connectivity					
rs35753505	*NRG1*	Non-coding region	36/31	FA in the anterior cingulum (TT/TC < CC)	Wang et al. (2009)
rs7808623	*GRM3*	Coding region	74/87	FA in the anterior thalamic radiation and corticospinal tract, as well as a series of tracts connecting the frontal cortex to the cerebellum (GG > TG > TT)	Mounce et al. (2014)
rs1625579	*MIR137*	Coding region	83/63	FA in both right orbitofrontal region and left striatum(TT < GT)	Kuswanto et al. (2015)
rs2710126	*CNTNAP2*	Coding region	44/81	FA in the uncinate fasciculus (AA < AG, AA < GG)	Clemm von Hohenberg et al. (2013)
rs1344706	*ZNF804A*	Coding region	100/69	FA, axial diffusivity, radial diffusivity, and mean diffusivity (no association)	Wei et al. (2013)

(Continued)

TABLE 1 | Continued

SNP ID	Gene	Location	Patients/controls	Findings	References
Brain structure					
rs12807809	*NRGN*	Non-coding region	91/65	Cortical thinning: frontal, parietal, and temporal cortices (TT) Thalamic shape abnormalities: regions related to pulvinar and medial dorsal nuclei (TT)	Thong et al. (2013)
			99/263	Gray matter volume in the left anterior cingulate cortex (TT < TC < CC)	Ohi et al. (2012)
rs3814614	*GRID1*	Non-coding region	62/54	Gray matter density in the right medial cerebellum and an area in the medial parietal cortex between the central and precuneal regions (in the cerebellar: CC < CT) (in the parietal: CC > CT)	Nenadic et al. (2012)
rs1344706	*ZNF804A*	Coding region	80/69	White matter density in the left prefrontal lobe and bilateral hippocampus (TT/GT > GG)	Wei et al. (2012)
rs7914558	*CNNM2*	Coding region	173/449	Gray matter volumes in the bilateral inferior frontal gyri (GG < GA/AA)	Ohi et al. (2013)
rs3813296	*GRIA2*	Coding region	55/0	White matter volume in the superior corona radiata (GT > TT)	Cai et al. (2020b)

FC, functional connectivity; FA, fractional anisotropy; CHRM3, cholinergic receptor, muscarinic 3; CNTNAP2, contactin-associated protein-like 2; COMT, catechol-O-methyltransferase; DAAO, D*-amino acid oxidase; DAOA,* D*-amino acid oxidase activator; DISC1, disrupted in schizophrenia gene 1; DLPFC, dorsolateral prefrontal cortex; FA, fractional anisotropy; FC, functional connectivity; IFG, inferior frontal gyrus; NOS1, nitric oxide synthase 1; NRGN, neurogranin; RS, resting state; ZNF804A, zinc finger protein 804A.*

MRI AND SNPs IN SCHIZOPHRENIA

Brain Function and SNPs in Schizophrenia

Single-Nucleotide Polymorphisms of Non-Coding Region

In first-episode treatment-naive schizophrenia, FC network analysis has suggested significant effects of *CHRM3* rs6800381 on the abnormal thalamo-orbital frontal cortex connectivity (Wang et al., 2016). Compared with C allele carriers, *NRGN* gene rs12807809 TT homozygotes in patients with schizophrenia have significantly lower hippocampus-seeded FC values in bilateral middle cingulate gyri and left anterior cingulate gyrus, suggesting that rs12807809 may be involved in the pathophysiological process of abnormal Papez circuit function (Zhang et al., 2019). The effects of *GRIN1* rs11146020 are mainly reflected on the causality connections between the bilateral dorsolateral prefrontal cortex (DLPFC) (Cai et al., 2020b).

However, some SNP genotypes are not associated with changes of FC in patients with schizophrenia, demonstrating the uncertainty of genetic factors at the molecular and cellular levels. For example, left Broca superior/inferior parietal network and bilateral Wernicke-frontoparietal network are related to *KIAA0319* SNPs (rs2038136, rs2038137) only in controls, respectively, but not in schizophrenia (Jamadar et al., 2013).

Single-Nucleotide Polymorphisms of Coding Region

Chen et al. identified that rs1344706 within intron 2 of the *ZNF804A* gene played a role in degree centrality in the precuneus, an important hub of the whole-brain network, in patients with schizophrenia (Chen et al., 2018). The investigation on the relationship between rs1059004 polymorphism which locates in the 3′-untranslated region (3′UTR) intronic region of the *OLIG2* gene and the whole-brain FC in patients with first-episode schizophrenia reveals that the FC strength decreased both in patients with schizophrenia and healthy controls with risk A allele and there is at some level a positive relationship between FC strength and verbal fluency score in patients, suggesting that there are synergistic effects between rs1059004 polymorphism and brain connections (Cai et al., 2020a). Compared with C allele homozygote, patients with schizophrenia with risk A allele have significantly lower nodal efficiency in the right precuneus and left middle temporal pole (Lv et al., 2020). Using brain connectivity network properties, "AG" carriers of *DAOA* rs2391191 have higher connectivity density and larger global efficiency than "AA" carriers (Liu et al., 2014).

For the *CACNA1C* rs1006737, the risk allele carriers (AA/AG) show decreased connectivity between the left precentral gyrus/inferior frontal gyrus and superior temporal gyrus vs. non-risk allele homozygotes (GG) in schizophrenia, thus presenting abnormal verbal fluency (Tecelao et al., 2019). *ZNF804A* rs1344706 seems to play an important role in FC between the left hippocampus and right DLPFC, which may serve as the brain mechanism of rs1344706 in schizophrenia (Zhang et al., 2018). However, during a working memory task, seeded connectivity analysis of the homozygous control group of the risk allele (AA) demonstrate a disruption in right DLPFC–left

hippocampal formation coupling when compared with the other genotype groups, but there is no effect of genotype in patients with schizophrenia (Rasetti et al., 2011). FC between the right inferior frontal gyrus and bilateral DLPFC is reduced in the risk allele carriers (the TT/TC group) of *NOS1* gene rs3782206 in both Stroop task and resting state, suggesting a relevance of rs3782206 to cognitive functions and neural mechanisms at the inferior frontal gyrus (Zhang et al., 2015). Significant association is also detected between the right precuneus inferior frontal gyrus functional connection and the *DISC1* rs821617 in patients with schizophrenia (Gong et al., 2014). For *DAAO* rs3918346 genotype, there are verbal fluency task-dependent changes of FC between the left precuneus and distributed networks including left and right precuneus, left putamen, right posterior cingulate gyrus, left caudate and right angular gyrus, and between the right posterior cingulate and right precuneus and left insula among patients with schizophrenia (Papagni et al., 2011). Similar to the effect of *KIAA0319* SNPs (rs2038136,rs2038137) genotype, the influence of SNP rs4504469 located at the exon of *KIAA0319* coding region on the left Broca upper/lower parietal network and bilateral Wernicke-frontalparietal network is reflected only in controls (Jamadar et al., 2013). In addition to investigating the influences of SNP rs11146020, which is located in the non-coding region of *GRIN1*, Cai et al. (2020b) found that SNP rs3813296 located in the intron region of *GRIA2* also has certain effects on the causality connections which located on the descending pathway from DLPFC to the striatum and thalamus in patients with schizophrenia. In the meantime, the interaction effects of rs11146020 and rs3813296 on causality connectivity are mainly located in the upstream pathway from the bilateral pallidum to the right caudate and the bilateral DLPFC, and negatively correlated with the Mayer–Salovey–Caruso emotional intelligence test, managing emotions score.

Brain Structure and SNPs in Schizophrenia

Single-Nucleotide Polymorphisms of Non-Coding Region

As for structural connectivity and brain structure, MRI studies are helpful to explore biological clues about the genetic underpinnings of structural connectome deficits in schizophrenia (Voineskos, 2015). For the *NRG1* rs35753505 genotype, fractional anisotropy in the anterior cingulum of patients with schizophrenia with the T allele is significantly lower than that of patients with schizophrenia with CC genotype and healthy controls with T allele (Wang et al., 2009). On the basis of previous studies, Nenadic et al. (2012) found that the SNP rs3814614 located in the *GRID1* promoter region affected the gray matter density in the right medial cerebellum and a region of the medial parietal cortex. Moreover, the cerebellar cluster gray matter density of TT homozygous patients was the highest, CT heterozygote was the intermediate, and CC homozygote was the lowest, showing significant interaction effects of group × genotype (Nenadic et al., 2012). These findings contribute to our understanding of the mechanisms of the abnormal cortical–subcortical brain networks in schizophrenia with the involvement of the *NRGN*. Apart from the effect on FC, the *NRGN* rs12807809 genotype is also associated with the morphological and structural changes of the cerebral cortex. The frontal, parietal, and temporal cortices of patients with schizophrenia with TT genotype were extensively thinned, and there are also thalamic shape abnormalities in the regions involving pulvinar and medial dorsal nuclei (Thong et al., 2013). Furthermore, patients with schizophrenia carrying risk T allele have a smaller gray matter volume in the left anterior cingulate cortex, compared to non-risk C allele carriers (Ohi et al., 2012).

Single-Nucleotide Polymorphisms of Coding Region

The minor allele of rs7808623, located in the intronic region of *GRM3* gene, is associated with higher white matter integrity in the anterior thalamic radiation and the corticospinal tract, as well as a series of tracts connecting the frontal cortex to the cerebellum (Mounce et al., 2014). This study indirectly mirrors the importance of *GRM3* in maintaining white matter integrity. For *MIR137* rs1625579 genotype, patients with schizophrenia with risk T allele homozygous genotype decreased fractional anisotropy values in both right orbitofrontal region and left striatum compared to G allele/A allele carriers (Kuswanto et al., 2015). There are some correlations between *CNTNAP2*, also known as Neurexin 4 (*NRXN4*), rs2710126 genotype and fractional anisotropy in the uncinate fasciculus (Clemm von Hohenberg et al., 2013). Despite the lack of association between *ZNF804A* rs1344706 and white matter integrity in schizophrenia (Wei et al., 2013), T allele carriers present higher white matter density in the left prefrontal lobe and bilateral hippocampi (Wei et al., 2012). Compared with non-risk A allele carriers, patients with schizophrenia with G/G genotype of risk variant rs7914558 which is located in intron1 of the *CNNM2* have smaller gray matter volumes in the bilateral inferior frontal gyri, especially the orbital region (Ohi et al., 2013). Among the effects of *GRIA2* gene rs3813296 on white matter (Cai et al., 2020b), the most significant effect is located on the bilateral superior corona radiata fibers. Compared with the TT genotype, patients with GT genotype have a significantly larger volume of the superior corona radiata, which leads to the dispersion of the connection strength between the left DLPFC and the right caudate (Cai et al., 2020b). This is seemingly the factor that patients with GT genotype have a decrease in connection strength between the two areas. All the above research results provide a possible mechanism underlying the association between cerebral abnormalities and schizophrenia at the level of genetic polymorphisms.

DISCUSSION

Based on the genetic variation data provided by GWAS research results, the current research takes the common SNPs in the whole genome as the objects to carry out association analysis at the overall level, and looks for the SNPs and susceptibility genes related to schizophrenia. The discovery of SNPs function increases the understanding of the association between functional genetic variation and imaging phenotypes related to schizophrenia from the gene level, and may also provide important clues about the anatomical heterogeneity of schizophrenia. Microscopic level alterations in gene function provide theoretical support for macroscopic level alterations in

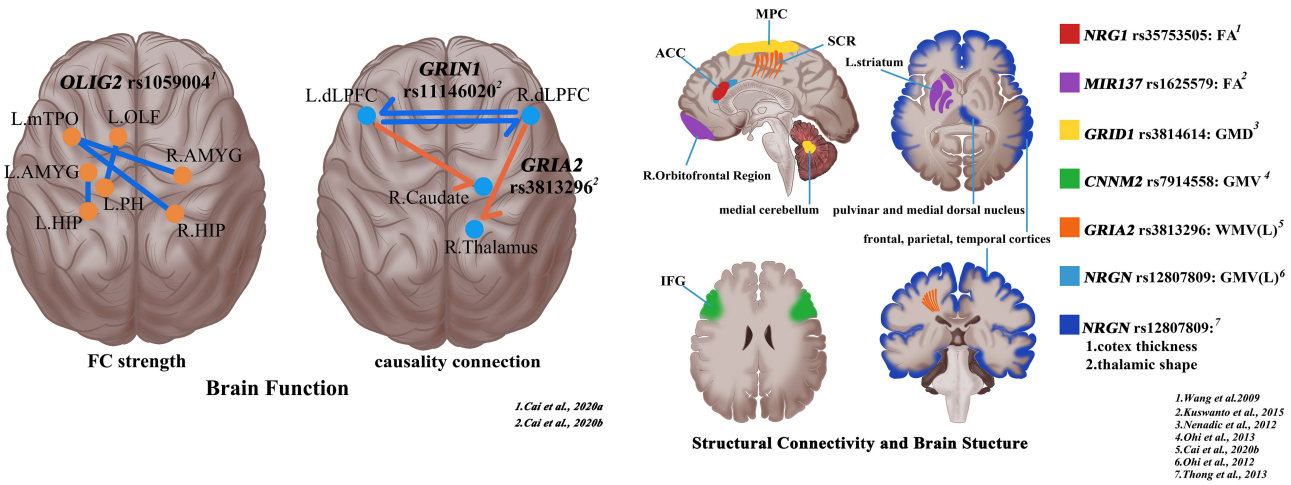

FIGURE 1 | Shaping the trans-scale and multi-omics properties of schizophrenia *via* magnetic resonance imaging and single-nucleotide polymorphisms (SNPs). R, right; L, left; ACC, anterior cingulate cortex; MPC, medial parietal cortex; SCR, superior corona radiata; IFG, inferior frontal gyrus; FA, fractional anisotropy; GMD, gray matter density; GMV, Gray matter volume; WMV, white matter volume.

brain phenotype (van den Heuvel et al., 2019). The application of multi-omics method combining gene and MRI in schizophrenia intuitively reveals the possible pathogenesis related to genes from the perspective of brain structure and function changes (**Figure 1**). In particular, using genetic imaging strategies, especially based on the high-quality images presented by MRI techniques, to investigate the influence of genetic factors on brain phenotypes will help to study schizophrenia in a more integrated perspective. The key of the trans-scale and multi-omics research strategy is to synthesize the information of different scales and different disciplines, so as to provide the most comprehensive way to explain the nature of schizophrenia (Guan et al., 2021). A recent review systematically summarizes the application of multi-omics approaches in schizophrenia in terms of pathogenesis, disease typing, clinical grading, risk prediction, and precision interventions (Guan et al., 2021). Compared to the information provided by a single discipline, the combination of genetic data and imaging data can provide us with more comprehensive information. In other words, the trans-scale information provided by multi-omics methods can deepen the understanding of the pathophysiological mechanism of clinical symptoms of schizophrenia, and can provide new clew for the stratification of patients and high-risk groups and the development of more accurate risk and treatment response biomarkers. The analytical framework that combines clinical data from multi-view biclustering analysis with gene expression levels allows for the accurate identification of subtypes of schizophrenia (Yin et al., 2019). Protein interactome can be used to describe polygenic associations between antipsychotic drug targets and risk genes, and help to develop new targets for the treatment of negative symptoms and cognitive impairment in schizophrenia (Kauppi et al., 2018). Clinical transformation is one of the ultimate goals of all research. The heterogeneity of schizophrenia is indirectly reflected by the multiple imaging features exhibited by patients with schizophrenia. Different genotypes of patients also have different brain phenotypes, which show individualized characteristics in neuroimaging. This heterogeneity between different scales indirectly suggests that clinicians need to design more individualized and precise clinical decisions.

Most recently, functional striatal abnormalities have been developed as a new neuroimaging biomarker for the identification, prognosis, and subtyping of schizophrenia based on brain function (Li et al., 2020). Loci of striatal hyperactivity recapitulate the spatial distribution of dopaminergic function and the expression profiles of polygenic risk for schizophrenia. Furthermore, by applying a novel machine learning method, 413 genetic factors related to schizophrenia across 13 brain regions can be obviously identified (Huckins et al., 2019). The expression of schizophrenia-related genes is reflected in the whole neurodevelopmental process: some during specific stages of pregnancy, and others during adolescence or adulthood. Genetic influence on schizophrenia paves the way for the potential application of MRI in schizophrenia (Jiang et al., 2020). A network fusion-based approach has been applied to integrate three types of data, including genetic, epigenetic, and neuroimaging data, for the diagnosis and prediction of patients with schizophrenia (Su-Ping et al., 2016). For example, adolescents in a high-risk state can be screened by identified risk factors for schizophrenia, so as to predict and intervene at early stage in the future for adolescents who may suffer from schizophrenia. Future research will place more emphasis on integrated analysis of information across different dimensions supported by trans-scale and multi-omics technologies (van den Heuvel et al., 2019; Guan et al., 2021). This new trans-scale and multi-omics methods give us unprecedented power to understand the nature of schizophrenia.

But so far, this combination method has only played a hint and reference role in the pathogenesis of schizophrenia. Most of the studies involved in this article are hypothetical, only with the help of imaging methods to observe changes in brain structure and function in the presence of a specific SNPs. The researchers did not conduct animal experiments to confirm that the changes shown in the images were induced by the specific SNPs. This is a common problem in related research fields. At the same time, due to the complexity and genetic heterogeneity of schizophrenia, there are differences among regions, races, and populations. Therefore, experiments need to reduce the contingency and increase the universality of results. In addition, the sample size of most studies is relatively small, especially the studies on the effects of the relationship between genes and structure on the brain are based on healthy people. It is necessary to increase the sample size for the verification of the results. Furthermore, future research will place more emphasis on integrated analysis of information across different dimensions supported by trans-scale and multi-omics technologies. This is a great challenge to be faced in future research. It is also important to note that the use of antipsychotic drugs can lead to some alterations in the brain phenotype of patients with schizophrenia (Guo et al., 2019; Wang et al., 2019). Future studies need to be aware of whether or not patients with schizophrenia have been treated with antipsychotic medication when discussing changes in their brain phenotypes.

All in all, the new trans-scale and multi-omics methods give us unprecedented power to understand the nature of schizophrenia, which will promote the identification of biomarkers and risk prediction ability, provide help for the multigene strategy of heterogeneous dissection of schizophrenia, and further promote the implementation of individualized accurate diagnosis and treatment.

AUTHOR CONTRIBUTIONS

Y-HZ, HY, and L-BC conceptualized the manuscript. S-WZ, XX, and L-BC wrote the first draft of the manuscript. All authors provided feedback and revised the manuscript.

FUNDING

This work was supported by the grant support of Fourth Military Medical University (2019CYJH) and the Project funded by the China Postdoctoral Science Foundation (2019TQ0130).

ACKNOWLEDGMENTS

We are indebted to Xu-Sha Wu for her helpful suggestions and comments on the manuscript.

REFERENCES

Brown, G. G., and Thompson, W. K. (2010). Functional brain imaging in schizophrenia: selected results and methods. *Curr. Top. Behav. Neurosci.* 4, 181–214. doi: 10.1007/7854_2010_54

Bush, W. S., and Moore, J. H. (2012). Chapter 11: genome-wide association studies. *PLoS Comput. Biol.* 8:e1002822. doi: 10.1371/journal.pcbi.1002822

Cai, S., Lv, Y., Huang, K., Zhang, W., Kang, Y., Huang, L., et al. (2020a). Association of rs1059004 polymorphism in the OLIG2 locus with whole-brain functional connectivity in first-episode schizophrenia. *Behav. Brain Res.* 379:112392. doi: 10.1016/j.bbr.2019.112392

Cai, S., Lv, Y., Huang, K., Zhang, W., Wang, Q., Huang, L., et al. (2020b). Modulation on glutamic pathway of frontal-striatum-thalamus by rs11146020 and rs3813296 gene polymorphism in first-episode negative schizophrenia. *Front. Neurosci.* 14, 351. doi: 10.3389/fnins.2020.00351

Chen, X., Zhang, Z., Zhang, Q., Zhao, W., Zhai, J., Chen, M., et al. (2018). Effect of rs1344706 in the ZNF804A gene on the brain network. *Neuroimage Clin.* 17, 1000–1005. doi: 10.1016/j.nicl.2017.12.017

Clemm von Hohenberg, C., Wigand, M. C., Kubicki, M., Leicht, G., Giegling, I., Karch, S., et al. (2013). CNTNAP2 polymorphisms and structural brain connectivity: a diffusion-tensor imaging study. *J. Psychiatr. Res.* 47, 1349–1356. doi: 10.1016/j.jpsychires.2013.07.002

Cui, L. B., Liu, L., Guo, F., Chen, Y. C., Chen, G., Xi, M., et al. (2017). Disturbed brain activity in resting-state networks of patients with first-episode schizophrenia with auditory verbal hallucinations: a cross-sectional functional MR imaging study. *Radiology* 283, 810–819. doi: 10.1148/radiol.2016160938

Cui, L. B., Liu, L., Wang, H. N., Wang, L. X., Guo, F., Xi, Y. B., et al. (2018). Disease definition for schizophrenia by functional connectivity using radiomics strategy. *Schizophr. Bull.* 44, 1053–1059. doi: 10.1093/schbul/sby007

Gong, X., Lu, W., Kendrick, K. M., Pu, W., Wang, C., Jin, L., et al. (2014). A brain-wide association study of DISC1 genetic variants reveals a relationship with the structure and functional connectivity of the precuneus in schizophrenia. *Hum. Brain Mapp.* 35, 5414–5430. doi: 10.1002/hbm.22560

Guan, F., Ni, T., Zhu, W., Williams, L. K., Cui, L.-B., Li, M., et al. (2021). Integrative omics of schizophrenia: from genetic determinants to clinical classification and risk prediction. *Mol. Psychiatry*. doi: 10.1038/s41380-021-01201-2. [Epub ahead of print].

Guo, F., Zhu, Y.-Q., Li, C., Wang, X.-R., Wang, H.-N., Liu, W.-M., et al. (2019). Gray matter volume changes following antipsychotic therapy in first-episode schizophrenia patients: a longitudinal voxel-based morphometric study. *J. Psychiatric Res.* 116, 126–132. doi: 10.1016/j.jpsychires.2019.06.009

Gurung, R., and Prata, D. P. (2015). What is the impact of genome-wide supported risk variants for schizophrenia and bipolar disorder on brain structure and function? A systematic review. *Psychol. Med.* 45, 2461–2480. doi: 10.1017/S0033291715000537

Huckins, L. M., Dobbyn, A., Ruderfer, D. M., Hoffman, G., Wang, W., Pardinas, A. F., et al. (2019). Gene expression imputation across multiple brain regions provides insights into schizophrenia risk. *Nat. Genet.* 51, 659–674. doi: 10.1038/s41588-019-0364-4

Jamadar, S., Powers, N. R., Meda, S. A., Calhoun, V. D., Gelernter, J., Gruen, J. R., et al. (2013). Genetic influences of resting state fMRI activity in language-related brain regions in healthy controls and schizophrenia patients: a pilot study. *Brain Imaging Behav.* 7, 15–27. doi: 10.1007/s11682-012-9168-1

Jiang, J. B., Cao, Y., An, N. Y., Yang, Q., and Cui, L. B. (2020). Magnetic resonance imaging-based connectomics in first-episode schizophrenia: from preclinical study to clinical translation. *Front. Psychiatry* 11:565056. doi: 10.3389/fpsyt.2020.565056

Kauppi, K., Rosenthal, S. B., Lo, M.-T., Sanyal, N., Jiang, M., Abagyan, R., et al. (2018). Revisiting antipsychotic drug actions through gene networks associated with schizophrenia. *Am. J. Psychiatry* 175, 674–682. doi: 10.1176/appi.ajp.2017.17040410

Kuswanto, C. N., Sum, M. Y., Qiu, A., Sitoh, Y. Y., Liu, J., and Sim, K. (2015). The impact of genome wide supported microRNA-137 (MIR137) risk variants on frontal and striatal white matter integrity, neurocognitive functioning, and negative symptoms in schizophrenia. *Am. J. Med. Genet. B. Neuropsychiatr. Genet.* 168B, 317–326. doi: 10.1002/ajmg.b.32314

Li, A., Zalesky, A., Yue, W., Howes, O., Yan, H., Liu, Y., et al. (2020). A neuroimaging biomarker for striatal dysfunction in schizophrenia. *Nat. Med.* 26, 558–565. doi: 10.1038/s41591-020-0793-8

Liu, A., Chen, X., Wang, Z. J., Xu, Q., Appel-Cresswell, S., and McKeown, M. J. (2014). A genetically informed, group FMRI connectivity modeling approach: application to schizophrenia. *IEEE Trans. Biomed. Eng.* 61, 946–956. doi: 10.1109/TBME.2013.2294151

Liu, L., Cui, L. B., Xi, Y. B., Wang, X. R., Liu, Y. C., Xu, Z. L., et al. (2019). Association between connectivity of hippocampal sub-regions and auditory verbal hallucinations in schizophrenia. *Front. Neurosci.* 13:424. doi: 10.3389/fnins.2019.00424

Lv, Y., Wu, S., Lin, Y., Wang, X., Wang, J., Cai, S., et al. (2020). Association of rs1059004 polymorphism in the OLIG2 locus with functional brain network in first-episode negative schizophrenia. *Psychiatry Res. Neuroimaging* 303:111130. doi: 10.1016/j.pscychresns.2020.111130

McCutcheon, R. A., Reis Marques, T., and Howes, O. D. (2020). Schizophrenia-an overview. *JAMA Psychiatry* 77, 201–210. doi: 10.1001/jamapsychiatry.2019.3360

Mounce, J., Luo, L., Caprihan, A., Liu, J., Perrone-Bizzozero, N. I., and Calhoun, V. D. (2014). Association of GRM3 polymorphism with white matter integrity in schizophrenia. *Schizophr. Res.* 155, 8–14. doi: 10.1016/j.schres.2014.03.003

Nenadic, I., Maitra, R., Scherpiet, S., Gaser, C., Schultz, C. C., Schachtzabel, C., et al. (2012). Glutamate receptor delta 1 (GRID1) genetic variation and brain structure in schizophrenia. *J. Psychiatr. Res.* 46, 1531–1539. doi: 10.1016/j.jpsychires.2012.08.026

Ohi, K., Hashimoto, R., Yamamori, H., Yasuda, Y., Fujimoto, M., Umeda-Yano, S., et al. (2013). The impact of the genome-wide supported variant in the cyclin M2 gene on gray matter morphology in schizophrenia. *Behav. Brain Funct.* 9:40. doi: 10.1186/1744-9081-9-40

Ohi, K., Hashimoto, R., Yasuda, Y., Nemoto, K., Ohnishi, T., Fukumoto, M., et al. (2012). Impact of the genome wide supported NRGN gene on anterior cingulate morphology in schizophrenia. *PLoS ONE* 7:e29780. doi: 10.1371/journal.pone.0029780

Papagni, S. A., Mechelli, A., Prata, D. P., Kambeitz, J., Fu, C. H., Picchioni, M., et al. (2011). Differential effects of DAAO on regional activation and functional connectivity in schizophrenia, bipolar disorder and controls. *Neuroimage* 56, 2283–2291. doi: 10.1016/j.neuroimage.2011.03.037

Pardinas, A. F., Holmans, P., Pocklington, A. J., Escott-Price, V., Ripke, S., Carrera, N., et al. (2018). Common schizophrenia alleles are enriched in mutation-intolerant genes and in regions under strong background selection. *Nat. Genet.* 50, 381–389. doi: 10.1038/s41588-018-0059-2

Perry, A., Roberts, G., Mitchell, P. B., and Breakspear, M. (2019). Connectomics of bipolar disorder: a critical review, and evidence for dynamic instabilities within interoceptive networks. *Mol. Psychiatry* 24, 1296–1318. doi: 10.1038/s41380-018-0267-2

Rasetti, R., Sambataro, F., Chen, Q., Callicott, J. H., Mattay, V. S., and Weinberger, D. R. (2011). Altered cortical network dynamics: a potential intermediate phenotype for schizophrenia and association with ZNF804A. *Arch. Gen. Psychiatry* 68, 1207–1217. doi: 10.1001/archgenpsychiatry.2011.103

Reddaway, J. T., Doherty, J. L., Lancaster, T., Linden, D., Walters, J. T., and Hall, J. (2018). Genomic and imaging biomarkers in schizophrenia. *Curr. Top. Behav. Neurosci.* 40, 325–352. doi: 10.1007/7854_2018_52

Roy, J., Anand, K., Mohapatra, S., Nayak, R., Chattopadhyay, T., and Mallick, B. (2020). Single nucleotide polymorphisms in piRNA-pathway genes: an insight into genetic determinants of human diseases. *Mol. Genet. Genomics* 295, 1–12. doi: 10.1007/s00438-019-01612-5

Schizophrenia Working Group of the Psychiatric Genomics C. (2014). Biological insights from 108 schizophrenia-associated genetic loci. *Nature* 511, 421–427. doi: 10.1038/nature13595

Su-Ping, D., Dongdong, L., Calhoun, V. D., and Yu-Ping, W. (2016). "Predicting schizophrenia by fusing networks from SNPs, DNA methylation and fMRI data," in *2016 38th Annual International Conference of the IEEE Engineering in Medicine and Biology Society (EMBC)* (Orlando, FL: IEEE), 1447–1450.

Tecelao, D., Mendes, A., Martins, D., Fu, C., Chaddock, C. A., Picchioni, M. M., et al. (2019). The effect of psychosis associated CACNA1C, and its epistasis with ZNF804A, on brain function. *Genes Brain Behav.* 18:e12510. doi: 10.1111/gbb.12510

Thong, J. Y., Qiu, A., Sum, M. Y., Kuswanto, C. N., Tuan, T. A., Donohoe, G., et al. (2013). Effects of the neurogranin variant rs12807809 on thalamocortical morphology in schizophrenia. *PLoS ONE* 8:e85603. doi: 10.1371/journal.pone.0085603

van den Heuvel, M. P., Scholtens, L. H., and Kahn, R. S. (2019). Multiscale neuroscience of psychiatric disorders. *Biol. Psychiatry* 86, 512–522. doi: 10.1016/j.biopsych.2019.05.015

Voineskos, A. N. (2015). Genetic underpinnings of white matter 'connectivity': heritability, risk, and heterogeneity in schizophrenia. *Schizophr. Res.* 161, 50–60. doi: 10.1016/j.schres.2014.03.034

Wang, F., Jiang, T., Sun, Z., Teng, S. L., Luo, X., Zhu, Z., et al. (2009). Neuregulin 1 genetic variation and anterior cingulum integrity in patients with schizophrenia and healthy controls. *J. Psychiatry Neurosci.* 34, 181–186. Available online at: http://jpn.ca/vol34-issue3/34-3-181/

Wang, L.-X., Guo, F., Zhu, Y.-Q., Wang, H.-N., Liu, W.-M., Li, C., et al. (2019). Effect of second-generation antipsychotics on brain network topology in first-episode schizophrenia: a longitudinal rs-fMRI study. *Schizophrenia Res.* 208, 160–166. doi: 10.1016/j.schres.2019.03.015

Wang, Q., Cheng, W., Li, M., Ren, H., Hu, X., Deng, W., et al. (2016). The CHRM3 gene is implicated in abnormal thalamo-orbital frontal cortex functional connectivity in first-episode treatment-naive patients with schizophrenia. *Psychol. Med.* 46, 1523–1534. doi: 10.1017/S0033291716000167

Wei, Q., Kang, Z., Diao, F., Guidon, A., Wu, X., Zheng, L., et al. (2013). No association of ZNF804A rs1344706 with white matter integrity in schizophrenia: a tract-based spatial statistics study. *Neurosci. Lett.* 532, 64–69. doi: 10.1016/j.neulet.2012.10.062

Wei, Q., Kang, Z., Diao, F., Shan, B., Li, L., Zheng, L., et al. (2012). Association of the ZNF804A gene polymorphism rs1344706 with white matter density changes in Chinese schizophrenia. *Prog. Neuropsychopharmacol. Biol. Psychiatry* 36, 122–127. doi: 10.1016/j.pnpbp.2011.08.021

Whitaker, K. J., Vértes, P. E., Romero-Garcia, R., Váša, F., Moutoussis, M., Prabhu, G., et al. (2016). Adolescence is associated with genomically patterned consolidation of the hubs of the human brain connectome. *Proc. Natl. Acad. Sci. U. S. A.* 113, 9105–9110. doi: 10.1073/pnas.1601745113

Yin, L., Chau, C. K. L., Sham, P.-C., and So, H.-C. (2019). Integrating clinical data and imputed transcriptome from GWAS to uncover complex disease subtypes: applications in psychiatry and cardiology. *Am. J. Hum. Genet.* 105, 1193–1212. doi: 10.1016/j.ajhg.2019.10.012

Zhang, Y., Gong, X., Yin, Z., Cui, L., Yang, J., Wang, P., et al. (2019). Association between NRGN gene polymorphism and resting-state hippocampal functional connectivity in schizophrenia. *BMC Psychiatry* 19:108. doi: 10.1186/s12888-019-2088-5

Zhang, Y., Yan, H., Liao, J., Yu, H., Jiang, S., Liu, Q., et al. (2018). ZNF804A Variation may affect hippocampal-prefrontal resting-state functional connectivity in schizophrenic and healthy individuals. *Neurosci. Bull.* 34, 507–516. doi: 10.1007/s12264-018-0221-y

Zhang, Z., Chen, X., Yu, P., Zhang, Q., Sun, X., Gu, H., et al. (2015). Evidence for the contribution of NOS1 gene polymorphism (rs3782206) to prefrontal function in schizophrenia patients and healthy controls. *Neuropsychopharmacology* 40, 1383–1394. doi: 10.1038/npp.2014.323

Conflict of Interest: The authors declare that the research was conducted in the absence of any commercial or financial relationships that could be construed as a potential conflict of interest.

frontiers in Human Neuroscience

SYSTEMATIC REVIEW
published: 16 September 2021
doi: 10.3389/fnhum.2021.739175

Abnormalities of Localized Connectivity in Obsessive-Compulsive Disorder: A Voxel-Wise Meta-Analysis

Xiuli Qing[1], *Li Gu*[1]* *and Dehua Li*[2]*

[1] Department of Obstetrics, Key Laboratory of Birth Defects and Related Diseases of Women and Children in Ministry of Education, West China Second University Hospital, Sichuan University, Chengdu, China, [2] Nursing Department, West China Second University Hospital, Sichuan University, Chengdu, China

OPEN ACCESS

Edited by:
Long-Biao Cui,
People's Liberation Army General Hospital, China

Reviewed by:
Di Wu,
Fourth Military Medical University, China
Xun Yang,
Chongqing University, China

***Correspondence:**
Li Gu
2816392866@qq.com
Dehua Li
562372162@qq.com

Specialty section:
This article was submitted to Brain Imaging and Stimulation, a section of the journal Frontiers in Human Neuroscience

Received: 10 July 2021
Accepted: 26 August 2021
Published: 16 September 2021

Citation:
Qing X, Gu L and Li D (2021) Abnormalities of Localized Connectivity in Obsessive-Compulsive Disorder: A Voxel-Wise Meta-Analysis. Front. Hum. Neurosci. 15:739175. doi: 10.3389/fnhum.2021.739175

Background: A large amount of resting-state functional magnetic resonance imaging (rs-fMRI) studies have revealed abnormalities of regional homogeneity (ReHo, an index of localized intraregional connectivity) in the obsessive-compulsive disorder (OCD) in the past few decades, However, the findings of these ReHo studies have remained inconsistent. Hence, we performed a meta-analysis to investigate the concurrence across ReHo studies for clarifying the most consistent localized connectivity underpinning this disorder.

Methods: A systematic review of online databases was conducted for whole-brain rs-fMRI studies comparing ReHo between OCD patients and healthy control subjects (HCS). Anisotropic effect size version of the seed-based d mapping, a voxel-wise meta-analytic approach, was adopted to explore regions of abnormal ReHo alterations in OCD patients relative to HCS. Additionally, meta-regression analyses were conducted to explore the potential effects of clinical features on the reported ReHo abnormalities.

Results: Ten datasets comprising 359 OCD patients and 361 HCS were included. Compared with HCS, patients with OCD showed higher ReHo in the bilateral inferior frontal gyri and orbitofrontal cortex (OFC). Meanwhile, lower ReHo was identified in the supplementary motor area (SMA) and bilateral cerebellum in OCD patients. Meta-regression analysis demonstrated that the ReHo in the OFC was negatively correlated with illness duration in OCD patients.

Conclusions: Our meta-analysis gave a quantitative overview of ReHo findings in OCD and demonstrated that the most consistent localized connectivity abnormalities in individuals with OCD are in the prefrontal cortex. Meanwhile, our findings provided evidence that the hypo-activation of SMA and cerebellum might be associated with the pathophysiology of OCD.

Keywords: obsessive-compulsive disorder, resting-state functional magnetic resonance imaging, localized connectivity, regional homogeneity, meta-analysis, seed-based d mapping

INTRODUCTION

Obsessive-compulsive disorder (OCD), a common mental illness characterized persistent intrusive thoughts (obsessions) and/or ritualized repetitive behaviors (compulsions) (Stein et al., 2019), has a lifetime prevalence rate of 2 to 3% (Ruscio et al., 2010). OCD usually has an onset in childhood and turns into a chronic course (Ruscio et al., 2010). Despite its high disability rate and the resultant social burden, the neuropathology of OCD is still not fully understood. Thus, identifying the neural correlates of OCD is of paramount significance to elevate the diagnostic specificity and improve the treatment efficacy of this disorder.

The development of multimodal magnetic resonance imaging (MRI) techniques and neuroimage analytical approaches have greatly advanced our understanding of the neurobiological substrates regarding OCD in the past few decades (Dougherty et al., 2018). Previous structural MRI meta- and meta- analytical publications have indicated the key role of the cortico-striato-thalamo-cortical (CSTC) network in the pathophysiology of OCD (Radua and Mataix-Cols, 2009; Rotge et al., 2010; de Wit et al., 2014; Fouche et al., 2017; Hu et al., 2017). Meanwhile, it is reported that multiple phenotypic subtypes of OCD might have different structural neural substrates (Dougherty et al., 2018). For example, Hirose et al. found a negative association between washing symptom dimension score and the right thalamic gray matter as well as a significant negative correlation between hoarding symptom dimension score and the left angular white matter in OCD patients (Hirose et al., 2017). In terms of the functional MRI (fMRI) researches in OCD, the results appear to be highly heterogeneous. For example, patients with OCD showed abnormal activation of mesolimbic and ventral striatal circuitry during reward-based spatial learning (Marsh et al., 2015). One experiment testing the error monitoring function revealed hyperactivation of the right amygdala and the subgenual anterior cingulate cortex in OCD patients compared with healthy control subjects (HCS) (Grutzmann et al., 2016). Another fMRI study examining decision making function found that OCD patients showed hypo-activation in the ventromedial orbitofrontal cortex (Norman et al., 2018). The discrepancies between these fMRI studies might be attributed to sample size, clinical heterogeneity (such as medication strategies and comorbidity profiles) and experimental paradigm, which dramatically affected the fMRI findings.

Rather than traditional task-based fMRI, the resting-state fMRI (rs-fMRI) is a commonly used neuroimaging approach to explore the brain function alterations in normal and disease states without performing any task (Biswal, 2012). The amplitude low-frequency Puctuation (ALFF) is a commonly used rs-fMRI parameter that could provide information of regional activation of brain (Fox and Raichle, 2007) while an improved measure named fractional amplitude of low-frequency fluctuation (fALFF) has been put forward as a normalized version of ALFF (Zou et al., 2008). Previous investigations have demonstrated alterations of (f)ALFF in a range of brain regions including the classical CSTC circuits and some newly found brain areas such as the parietal lobe, temporal lobe and the cerebellum (Hou et al., 2012; Fan et al., 2017; Gimenez et al., 2017; Qiu et al., 2017). Besides the (f)ALFF, functional connectivity (FC), a valid rs-fMRI index reflecting the level of integration of local activity across brain regions (Buckner et al., 2013), has been widely adopted to investigate the neural pathogenesis of OCD (Gursel et al., 2018). Previous FC studies have identified that, besides the classical CSTC circuitry, the between-network hypoconnectivity of triple-network (salience, frontoparietal and default-mode networks) might also get involved in the psychopathology in OCD (Gursel et al., 2018). Though explorations of network-level neural function abnormalities in OCD have achieved remarkable progress, the local neural dysfunction of this disorder received less attention.

Regional Homogeneity (ReHo), a rs-fMRI parameter characterizing the local synchronization of spontaneous blood oxygen level-dependent signal fluctuation among neighboring voxels within a given cluster, offered new chance to investigate the localized connectivity disruptions in patients without a priori constraints (Zang et al., 2004). A large amount of rs-fMRI studies have revealed abnormalities of ReHo in OCD, However, the findings of these ReHo studies have remained inconsistent and controversial. For example, one study reported that OCD patients exhibited higher ReHo in the right cerebellum (Ping et al., 2013) while another study identified lower ReHo in the bilateral cerebellum of OCD patients (Hu et al., 2019). Thus, it was necessary to perform a quantitative overview of ReHo findings in OCD.

To our knowledge, Hao et al. published a meta-analysis concerning ReHo alterations in OCD via seed-based d mapping (SDM) approach (Hao et al., 2019). Nevertheless, there were two major shortcomings in their study. First, according to SDM designers' suggestion, the minimum of 10 studies was recommended for SDM meta-analyses (Carlisi et al., 2017; Muller et al., 2018). However, only eight datasets were included in their meta-analysis (Hao et al., 2019). Second, Hao et al. did not to evaluate the association between the clinical variables and ReHo alterations because the included studies were too few (less than 9 studies) to perform meta-regression analysis (Radua and Mataix-Cols, 2009). Therefore, we conducted an updated voxel wise meta-analysis to identify the most robust ReHo abnormalities in OCD patients compared with the controls using the Anisotropic effect size version of the seed-based d mapping (AES-SDM). This new version of SDM method has several advantages such as: (i) avoiding any voxel appearing significant in opposite directions; (ii) reconstructing both positive and negative differences in the same signed differential map; (iii) combining the reported peak coordinates with statistical parametric maps. Additionally, we performed meta-regression to explore the potential effects of clinical features on reported ReHo alterations.

MATERIALS AND METHODS

Data Source

Systematic searches of the online database including PubMed, EMBASE and Web of Science (from January 2000 to December 2020) were conducted. The keyword searches were performed using the following terms: ("obsessive-compulsive disorder" or "OCD") plus ("resting-state functional magnetic resonance

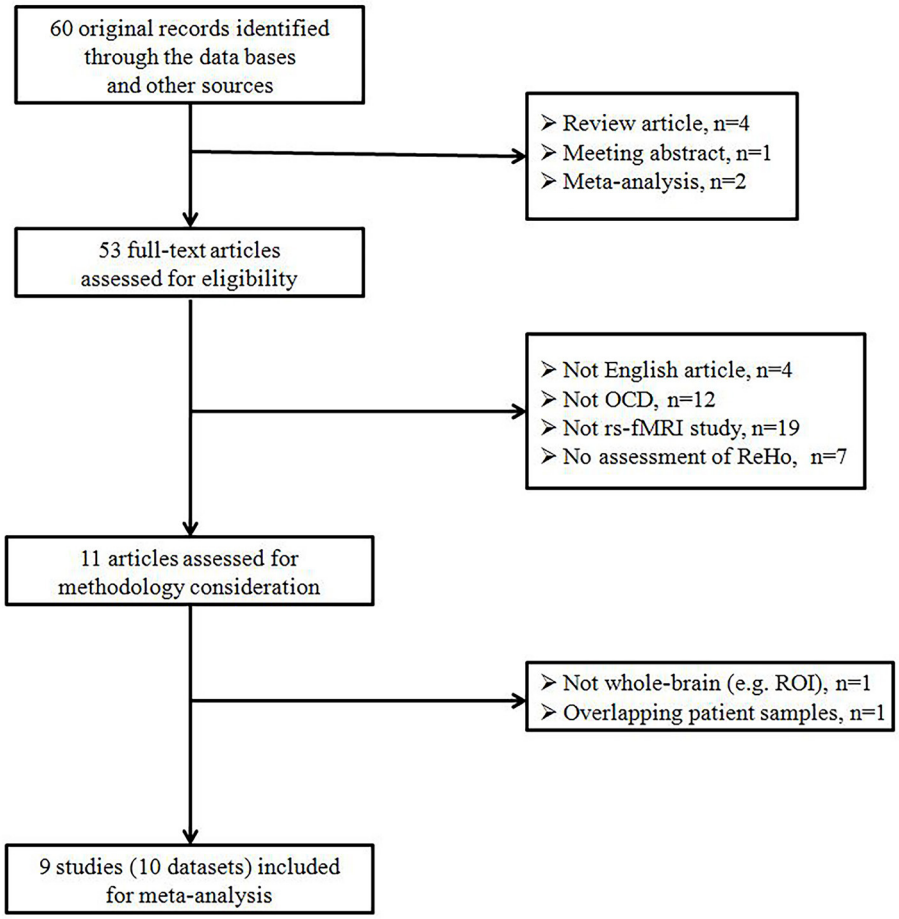

FIGURE 1 | Flow diagram regarding the identification and attrition of studies. OCD, obsessive-compulsive disorder; ReHo, regional homogeneity; ROI, region of interest; rs-fMRI, resting-state functional magnetic resonance imaging.

imaging" or "rs-fMRI") or ("regional homogeneity" or " ReHo") or ("localized connectivity"). We also screened the reference lists of relevant articles in order to obtain additional literature.

Studies Selection and Data Extraction

A study was considered for inclusion if it (i) was a research paper and published in English; (ii) reported ReHo comparison between patients with OCD and HCS; (iii) provided 3-dimensional coordinates of ReHo abnormalities in stereotactic space at the whole-brain level; (iv) adopted significance thresholds for data that were corrected for multiple comparisons. In some cases, we obtained additional details which were essential for the meta-analysis by contacting the corresponding authors. Exclusion criteria were: (i) the article type of the study is not original investigation; (ii) the peak coordinates of the ReHo alterations could not be retrieved; (iii) the study was based on region of interest (ROI) analytical approach; (iv) the data overlapped with those of another publication. We performed the current meta-analysis based on the guidelines of Preferred Reporting Items for Systematic Reviews and Meta-Analysis (PRISMA) (Radua, 2021). The coordinates regarding the ReHo changes between OCD patients and HCS in each included study were independently extracted by two investigators. Meanwhile, clinical features (including the sample size, age, gender, illness duration, symptom severity and medication status) and methodological issues (such as the MRI scanner, analytical software, smoothing kernel, number of foci and the threshold for multiple comparison correction) were extracted. If agreement was not obtained, then another author mediated.

Voxel-Wise Meta-Analysis

Using the AES-SDM software, we conducted the voxel-wise meta-analysis to explore the most robust ReHo abnormalities in patients with OCD compared with HCS based on the selected studies. Meanwhile, we performed a whole-brain jackknife sensitivity analyses to evaluate the reliability of the main effect. Afterwards, we conducted subgroup meta-analysis of unmedicated OCD patients and the subgroup meta-analysis regarding the threshold for correction was also performed. Subsequently, between-study variance was analyzed in order to assess significant heterogeneity of ReHo abnormalities. The kernel size and thresholds for the main

TABLE 1 | Demographic and clinical characteristics of ReHo studies on OCD in the current meta-analysis.

Study	Sociodemographic characteristics						Clinical characteristics: OCD participants only				
	No. of subjects		Mean age (yrs)		Female (%)		Mean illness duration (yrs)	Mean Y-BOCS score	Mean HAMA score	Mean HAMD score	Medication status (%)
	OCD	HCS	OCD	HCS	OCD	HCS					
Yang et al., 2010	22	22	31.18	30.86	63.6	63.6	3.88	32.27	8.5	6.36	Drug-naïve
Ping et al., 2013	20	20	27.1	27.6	20	20	7.34	23.5	12.9	11.2	0.7
Yang et al., 2015	22	22	30.95	29.52	45.5	45.5	8.22	24.43	11.81	8.52	Drug-free
Chen et al., 2016a	30	30	26.23	28.17	20	23.3	5.54	23.77	12.8	10.8	0.67
Niu et al., 2017	26	25	24.19	22.68	30.8	52	5.49	22.92	14.35	15.58	Drug-naïve
Bu et al., 2019	54	54	30.41	28.39	37.1	37.1	8.15	20.72	9.24	8.19	Drug-free
Hu et al., 2019	88	88	29.16	27.88	36.4	36.4	7.32	21.47	8.78	8.74	Drug-free
Yang et al., 2019	15	30	28.77	28.23	60	33.3	7.15	25	6.54	7.23	Drug-free
Xia et al., 2020#	40	70	22.48	20.93	45	55.7	4.08	21.63	NA	NA	Drug-free
Xia et al., 2020*	42	70	22.76	20.93	50	55.7	4.33	22.6	NA	NA	Drug-free

HAMA, Hamilton Anxiety Rating Scale; HAMD, Hamilton Depression Rating Scale; HCS, healthy control subjects; OCD, obsessive-compulsive disorder; ReHo, regional homogeneity; Y-BOCS, Yale-Brown Obsessive Compulsive Scale.
#Subgroup of autogenous-type OCD patients.
**Subgroup of reactive-type OCD patients.*

TABLE 2 | Technical details of ReHo studies on OCD in the current meta-analysis.

Study	MRI Scanner	Software	Smoothing (FWHM)	Coordinate System	Foci	*p*-value (correction)
Yang et al., 2010	1.5T (GE)	SPM8	10 mm	MNI	3	$p < 0.05$ (AlphaSim corrected)
Ping et al., 2013	3.0T (Siemens)	SPM5	4 mm	MNI	20	$p < 0.05$ (AlphaSim corrected)
Yang et al., 2015	3.0T (Siemens)	SPM5	4 mm	MNI	11	$p < 0.05$ (AlphaSim corrected)
Chen et al., 2016a	3.0T (GE)	SPM8	4 mm	MNI	10	$p < 0.05$ (AlphaSim corrected)
Niu et al., 2017	3.0T (GE)	SPM8	4 mm	MNI	5	$p < 0.005$ (AlphaSim corrected)
Bu et al., 2019	3.0T (GE)	SPM8	8 mm	MNI	0	$p < 0.05$ (FDR corrected)
Hu et al., 2019	3.0T (GE)	SPM8	8 mm	MNI	16	$p < 0.05$ (FWE corrected)
Yang et al., 2019	3.0T (Siemens)	DPABI-V	4 mm	MNI	7	$p < 0.05$ (GRF corrected)
Xia et al., 2020#	3.0T (Siemens)	SPM12	6 mm	MNI	5	$p < 0.05$ (FDR corrected)
Xia et al., 2020*	3.0T (Siemens)	SPM12	6 mm	MNI	3	$p < 0.05$ (FDR corrected)

DPABI, data processing and analysis for brain imaging; FDR, false discovery rate; FWE, family wise error; FWHM, full width at half maximum; GRF, Gaussian random field; MNI, Montreal Neurological Institute; OCD, obsessive-compulsive disorder; ReHo, regional homogeneity; SPM, statistical parametric mapping; T, Tesla.
#Subgroup of autogenous-type OCD patients.
**Subgroup of reactive-type OCD patients.*

effect and heterogeneity analysis were set as follows: full-width at half-maximum = 20 mm; anisotropy = 1.0, voxel $P = 0.005$, peak height threshold = 1, cluster extent = 100 voxels. We also performed Egger's test for the evaluation of publication bias. Finally, the meta-regression analyses were performed to examine the potential effects of clinical variables (such as symptom severity and illness duration) on the reported ReHo changes. It should be noted that a more conservative threshold ($P < 0.0005$) was used for meta-regression analysis in order to achieve the optimal balance of sensitivity and specificity as suggested by previous publication (Wise et al., 2016). All the analyses are performed according to the AES-SDM tutorial (http://www.sdmproject.com/software/Tutorial.pdf).

RESULTS

Included Studies and Sample Characteristics

Our search strategy identified a total of 60 studies. Of these, 11 ReHo studies were chosen for further consideration after primary screening. Among the 11 ReHo investigations, One study adopted an ROI analytical method instead of a whole-brain approach (Chen et al., 2016c). Another study recruited samples that were overlapped with previous publication (Chen et al., 2016b). Therefore, these two studies were excluded from the current meta-analysis. Ultimately, 9 original investigations (Yang et al., 2010, 2015, 2019; Ping et al., 2013; Chen et al., 2016a; Niu et al., 2017; Bu et al., 2019; Hu et al., 2019; Xia et al., 2020) met the

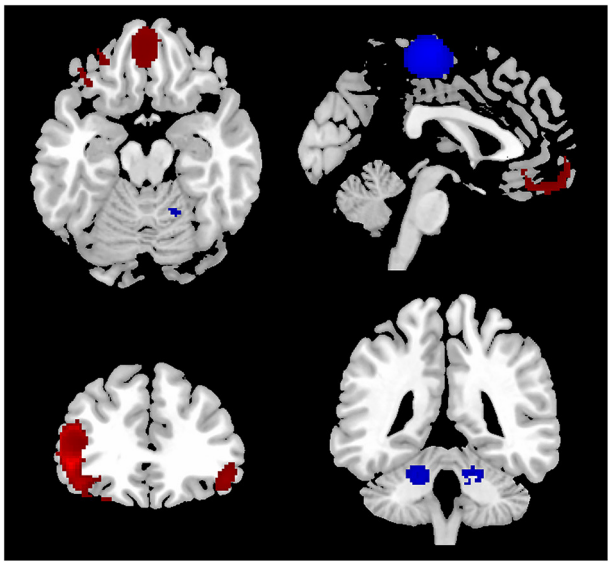

FIGURE 2 | Results of the meta-analysis of whole-brain ReHo studies in patients with OCD. Regions of ReHo alterations in patients with OCD relative to HCS were shown on the three-dimensional T1-weighted template images from software (MRIcroN). Higher ReHo was shown in red color while lower ReHo was displayed in blue color. HCS, healthy control subjects; OCD, obsessive-compulsive disorder; ReHo, regional homogeneity.

inclusion criteria (see **Figure 1** for details). No additional articles were found in the reference lists of the included studies. One investigation included two different subgroups of OCD patients (autogenous-type OCD and reactive-type OCD, two different types of obsessions in OCD proposed by Lee and Kwon, 2003; Xia et al., 2020). We treated this investigation as two unique datasets, with each patient subgroup selected independently in the current meta-analysis. Therefore, a total of 10 datasets comprising 359 OCD patients and 361 HCS were included in our meta-analysis, along with 80 coordinates extracted from these 10 datasets. There was no significant difference between the two groups in terms of age and sex. The mean age was 27.35 years in the OCD patient group vs. 26.56 years in the HCS group while there were 142 (39.6%) female OCD patients vs. 149 (41.2%) female HCS. The demographic details from all recruited studies were well-described in the **Table 1** while the technical details of the included studies were available in the **Table 2**.

Regional ReHo Differences Between Patients With OCD and HCS

Compared with HCS, patients with OCD showed higher ReHo in the bilateral inferior frontal gyri (IFG) and orbitofrontal cortex (OFC). Meanwhile, lower ReHo was identified in the supplementary motor area (SMA) and bilateral cerebellum in OCD patients (see **Figure 2** and **Table 3** for details). All aforementioned clusters did not reveal significant statistical heterogeneity between studies ($p > 0.005$). Additionally, none of the clusters showed significant publication bias in the Egger's test ($p > 0.05$).

Subgroup Meta-Analyses

The subgroup meta-analyses showed that the main findings above remained highly reproducible when only the 8 unmedicated OCD datasets or only the 9 datasets using the threshold of 0.05 for multiple comparison corrections were analyzed (**Table 4**). Unfortunately, we failed to perform the subgroup meta-analyses regarding other clinical subtypes or imaging methodologies because there were not enough primary datasets.

Sensitivity Analyses

As displayed in the **Table 3**, the whole brain jackknife sensitivity analyses indicated that higher ReHo in the left IFG and lower ReHo in the SMA were highly replicable, because these two findings were consistent throughout all the 10 combinations of 9 datasets. The lower ReHo in the bilateral cerebellum failed to emerge in one of the study combinations while the higher ReHo in the right IFG and OFC failed to emerge in two of the study combinations. The detailed results of the whole brain jackknife sensitivity analyses were shown in the **Table 4**.

Meta-Regression Analysis

The clinical Information of the patients with OCD including the age, gender, symptom severity and illness duration was available for all the 10 datasets. Using a stringent threshold of $P < 0.0005$ to minimize spurious findings, our meta regression revealed that samples with longer illness duration of OCD patients had more decreased ReHo in the OFC, which had been found as anomalous in the main effect. That is, the illness duration was negatively associated with the ReHo in the OFC ($x = 0$, $y = 46$, $z = -2$; SDM-$Z = -3.304$, $P = 0.000005677$; 428 voxels) (**Figure 3**). Other relevant clinical variables were not correlated, at least linearly, with OCD-related ReHo alterations.

DISCUSSION

The current study integrated rs-fMRI publications for a meta-analysis of ReHo differences between OCD patients and HCS. Using AES-SDM approach, our meta-analysis identified that patients with OCD showed higher ReHo in the bilateral IFG and OFC. Meanwhile, lower ReHo was identified in the SMA and bilateral cerebellum in OCD patients. These findings remained stable when jackknife sensitivity analyses were performed, which suggested that the results of our meta-analysis were robust and reliable.

In line with the classical CSTC model of OCD, we identified higher ReHo in the bilateral IFG and OFC in OCD patients relative to the HCS. The prefrontal dysfunction is widely considered to be implicated in the psychopathology of OCD (Pauls et al., 2014). Localized connectivity dysfunction in bilateral IFG might be associated with impairments of cognitive control, which had been consistently reported in OCD patients (Shin et al., 2014). Previous multicenter mega-analytical publication has demonstrated smaller gray matter volume in bilateral IFG in OCD patients while the current study revealed higher ReHo in the bilateral IFG (de Wit et al., 2014). We speculated that the hyper-activation of bilateral IFG is a compensatory response

TABLE 3 | Statistical concurrence observed across ReHo studies on OCD.

Region	Local maximum					Cluster		Jackknife sensitivity analysis (combination of studies detecting the differences)
	MNI Coordinates			SDM-Z	*P*	Number of voxels	Breakdown (number of voxel)	
Higher ReHo (OCD > HCS)								
Left inferior frontal gyrus	−48	34	0	3.203	∼0	2023	Left inferior frontal gyrus (1663) Left middle frontal gyrus (202) Left insula (158)	10 out of 10
Right inferior frontal gyrus	48	36	−10	1.942	0.000668841	408	Right inferior frontal gyrus (370) Right middle frontal gyrus (38)	8 out of 10
Left orbitofrontal gyrus	−10	50	−16	1.792	0.001478572	587	Left orbitfrontal gyrus (339) Right orbitfrontal gyrus (248)	8 out of 10
Lower ReHo (OCD < HCS)								
Right supplementary motor area	6	−20	66	−1.996	0.000082057	1443	Left paracentral lobule (327) Left supplementary motor area (129) Right paracentral lobule (363) Right precentral gyrus (96) Right supplementary motor area (528)	10 out of 10
Left cerebellum	−14	−52	−24	−1.605	0.001129702	269	Left cerebellum (269)	9 out of 10
Right cerebellum	20	−58	−26	−1.604	0.001129702	160	Left cerebellum (160)	9 out of 10

HCS, healthy control subjects; MNI, Montreal Neurological Institute; OCD, obsessive-compulsive disorder; ReHo, regional homogeneity; SDM, seed-based d mapping.

TABLE 4 | Sensitivity analyses of clusters with altered ReHo between OCD patients and controls from 9 included studies (10 datasets) in the current meta-analysis.

Analysis	Left IFG	Right IFG	Left OFG	Right SMA	Left cerebellum	Right cerebellum
Jackknife sensitivity analysis (discarded study)						
Yang et al., 2010	Y	Y	Y	Y	Y	Y
Ping et al., 2013	Y	Y	Y	Y	Y	Y
Yang et al., 2015	Y	N	Y	Y	Y	Y
Chen et al., 2016a	Y	N	Y	Y	Y	Y
Niu et al., 2017	Y	Y	Y	Y	Y	Y
Bu et al., 2019	Y	Y	Y	Y	Y	Y
Hu et al., 2019	Y	Y	Y	Y	N	N
Yang et al., 2019	Y	Y	Y	Y	Y	Y
Xia et al., 2020#	Y	Y	N	Y	Y	Y
Xia et al., 2020*	Y	Y	N	Y	Y	Y
Subgroup analysis						
Studies including unmedicated OCD patients ($N = 8$)	Y	N	Y	Y	Y	Y
Studies corrected using threshold of 0.05 ($N = 9$)	Y	Y	Y	Y	Y	Y

IFG, inferior frontal gyrus; N, no; OCD, obsessive-compulsive disorder; OFG, orbitofrontal gyrus; ReHo, regional homogeneity;. SMA, supplementary motor area; Y, yes.
#Subgroup of autogenous-type OCD patients.
**Subgroup of reactive-type OCD patients.*

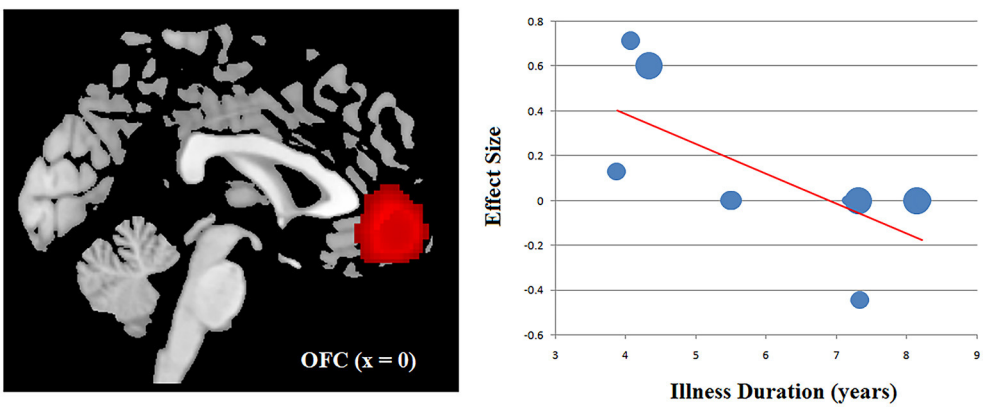

FIGURE 3 | Results of meta-regression analysis illustrating a negative association between the ReHo in the OFC and the illness duration in patients with OCD. The effects sizes were extracted to create the plots in the graph and each study is represented as a dot, with dot size reflecting sample size: large dots indicate samples with over 40 patients; medium dots, samples with 20–40 patients; and small dots, samples with under 20 patients. OCD, obsessive-compulsive disorder; OFC, orbitofrontal cortex; ReHo, regional homogeneity.

to the gray matter structural deficits of IFG. It is reported that the OFC plays an essential role in reward processing (Milad and Rauch, 2012). Recent meta-analysis has demonstrated lower fractional anisotropy in the left orbitofrontal white matter of OCD patients, which was negatively and independently associated with symptom severity and illness duration in patients with OCD (Hu et al., 2020). One animal experiment indicated that giving repeated stimulation to the OFC of the mice could lead to persistent OCD-like behaviors (Ahmari et al., 2013). Grover et al. found that high-frequency neuromodulation of OFC could improve obsessive-compulsive behavior (Grover et al., 2021). In the current study, higher ReHo in the OFC may be related the behavioral deficits of OCD patients since OCD patients perform poorly on tasks that require adjusting responses based on changing reward feedback (Marsh et al., 2015). Additionally, our meta-regression analysis showed a negative correlation between the illness duration and the ReHo in the OFC. Previous study demonstrated a negative association between disease duration and ReHo value in the bilateral OFC in OCD patients at the whole-brain level (Niu et al., 2017). Yun et al. performed a multicenter study and found the centrality of orbito-frontal cortical surface areas was negatively correlated with OCD illness duration (Yun et al., 2020). Based on the evidence above, we proposed that the OFC might be related to the illness chronicity in OCD. However, this meta-regression finding should be interpreted with caution since two datasets (Ping et al., 2013; Chen et al., 2016a) in the current meta-analysis included OCD patients who were on stable doses of serotonin

reuptake inhibitors at the time of the MRI scanning. Beucke et al. reported that antidepressant medication might affect the neural function within the CSTC circuits in OCD (Beucke et al., 2013). Therefore, further studies would be warranted to clarify our meta-regression finding.

It should be noted that prior meta-analysis reported decreased ReHo in the left caudate nucleus (Hao et al., 2019) while our meta analysis identified no ReHo alterations in the striatum. One possible reason accounting for the inconsistency is the differences of included datasets. A larger number of datasets was included in the current meta analysis ($N = 10$) than in the previous publication ($N = 8$). As suggested by Radua and his colleagues, the minimum of 10 studies was essential for the reliability of performing the SDM meta-analysis (Carlisi et al., 2017; Muller et al., 2018). Therefore, we confirmed the validity of the current meta-analysis.

The SMA is considered to be implicated in movement initiation and inhibition, response selection, and motor planning (Bonini et al., 2014). A task-based MRI study demonstrated that OCD patients and their siblings showed greater activity in the left SMA during successful inhibition paradigm relative to HCS, indicating that the SMA hyperactivity is a neurocognitive endophenotype of OCD (de Wit et al., 2012). Another study found that increased correlation of the error-related negativity in the event-related potential and activation of SMA might indicate stronger recruitment of proactive control in OCD (Grutzmann et al., 2016). Our meta-analysis revealed lower ReHo in the SMA, suggesting that hypo-activation of the SMA might be involved the pathophysiology of OCD.

Another interesting finding is that we identified lower ReHo in the bilateral cerebellum in OCD patients. Besides the traditional role of motor control, researches have proved that the cerebellum is involved in cognitive control (Buckner, 2013) and information processing (Ramnani, 2006). In fact, the cerebellum offers output to the cerebral cortex and tunes sensory input for facilitating behavioral adjustment in response to feedback (Gao et al., 2018). Sha et al. reported greater somatomotor-cerebellar connectivity in OCD patients and highlighted somatomotor-cerebellar circuits as potential targets for novel treatments in OCD (Sha et al., 2020). One study demonstrated decreased dynamic amplitude of low-frequency fluctuation (dALFF) of cerebellum in drug-naive OCD patients using the sliding-window approach (Liu et al., 2021). Meanwhile, another rs-fMRI study identified decreased cerebellar-cerebral functional connectivity in executive control and emotion processing networks in OCD patients (Xu et al., 2019). Taken collectively, our meta analysis emphasized the role of cerebellum in the pathogenesis of OCD.

In terms of the significance of ReHo alterations, previous investigations suggested that the index of ReHo could contribute the blood oxygenation level dependent (BOLD) fluctuations at the baseline (Anderson et al., 2014). An elevation of prefrontal ReHo might suggest an pronounced participation of this brain region in the neurophysiological functions such as the rumination (Dar and Iqbal, 2015) while a reduction of ReHo usually occurs alongside an increase in distributed connectivity during late neurodevelopment (Fair et al., 2007; Supekar et al., 2009).

Several limitations of the current meta-analysis should be addressed. First, our meta-analysis was performed on the basis of stereotactic coordinates extracted from each included dataset instead of raw brain maps (Radua et al., 2012), which might result in less accurate findings. Second, as the number of datasets included in our meta analysis was small, we failed to perform subgroup meta-analyses. Third, the potential effects of drug treatment could not be fully ruled out since a majority of studies employing OCD patients who were on drug treatment. Future ReHo studies recruiting unmedicated OCD patients are still needed to verify the reproducibility of the findings in the current meta analysis. Forth, it should be pointed out that all the included studies were conducted in China, which limited the generalizability of the our findings to other populations. Finally, the meta-regression results should be regarded as preliminary finding rather than conclusive evidence because the number of eligible studies for meta-regression analysis is limited.

In summary, the current meta-analysis presented a quantitative overview of ReHo findings in OCD and demonstrated that the most consistent localized connectivity abnormalities in individuals with OCD are in the prefrontal cortex. Additionally, our findings provided evidence that the hypo-activation of SMA and cerebellum might be associated with the pathophysiology of OCD, which might give additional explanation to the well known CSTC model of OCD.

DATA AVAILABILITY STATEMENT

The original contributions presented in the study are included in the article/Supplementary Material, further inquiries can be directed to the corresponding author/s.

AUTHOR CONTRIBUTIONS

LG and DL designed the study. XQ and LG acquired the data and wrote the article, which DL reviewed. XQ, LG, and DL analyzed the data. All authors approved the final version for publication.

REFERENCES

Ahmari, S. E., Spellman, T., Douglass, N. L., Kheirbek, M. A., Simpson, H. B., Deisseroth, K., et al. (2013). Repeated cortico-striatal stimulation generates persistent OCD-like behavior. *Science* 340, 1234–1239. doi: 10.1126/science.1234733

Anderson, J. S., Zielinski, B. A., Nielsen, J. A., and Ferguson, M. A. (2014). Complexity of low-frequency blood oxygen level-dependent fluctuations covaries with local connectivity. *Hum. Brain Mapp.* 35, 1273–1283. doi: 10.1002/hbm.22251

Beucke, J. C., Sepulcre, J., Talukdar, T., Linnman, C., Zschenderlein, K., Endrass, T., et al. (2013). Abnormally high degree connectivity of the orbitofrontal cortex in obsessive-compulsive disorder. *JAMA Psychiatry* 70, 619–629. doi: 10.1001/jamapsychiatry.2013.173

Biswal, B. B. (2012). Resting state fMRI: a personal history. *Neuroimage* 62, 938–944. doi: 10.1016/j.neuroimage.2012.01.090

Bonini, F., Burle, B., Liégeois-Chauvel, C., Régis, J., Chauvel, P., and Vidal, F. (2014). Action monitoring and medial frontal cortex: leading role of supplementary motor area. *Science* 343, 888–891. doi: 10.1126/science.1247412

Bu, X., Hu, X., Zhang, L., Li, B., Zhou, M., Lu, L., et al. (2019). Investigating the predictive value of different resting-state functional MRI parameters in obsessive-compulsive disorder. *Transl. Psychiatry* 9:17. doi: 10.1038/s41398-018-0362-9

Buckner, R. L. (2013). The cerebellum and cognitive function: 25 years of insight from anatomy and neuroimaging. *Neuron* 80, 807–815. doi: 10.1016/j.neuron.2013.10.044

Buckner, R. L., Krienen, F. M., and Yeo, B. T. (2013). Opportunities and limitations of intrinsic functional connectivity MRI. *Nat. Neurosci.* 16, 832–837. doi: 10.1038/nn.3423

Carlisi, C. O., Norman, L. J., Lukito, S. S., Radua, J., Mataix-Cols, D., and Rubia, K. (2017). Comparative multimodal meta-analysis of structural and functional brain abnormalities in autism spectrum disorder and obsessive-compulsive disorder. *Biol. Psychiatry* 82, 83–102. doi: 10.1016/j.biopsych.2016.10.006

Chen, Y., Juhás, M., Greenshaw, A. J., Hu, Q., Meng, X., Cui, H., et al. (2016a). Abnormal resting-state functional connectivity of the left caudate nucleus in obsessive-compulsive disorder. *Neurosci. Lett.* 623, 57–62. doi: 10.1016/j.neulet.2016.04.030

Chen, Y., Juhas, M., Greenshaw, A. J., Hu, Q., Meng, X., Cui, H., et al. (2016b). Data on the impact of SSRIs and depression symptoms on the neural activities in obsessive-compulsive disorder at rest. *Data Brief* 8, 324–328. doi: 10.1016/j.dib.2016.05.061

Chen, Y., Meng, X., Hu, Q., Cui, H., Ding, Y., Kang, L., et al. (2016c). Altered resting-state functional organization within the central executive network in obsessive-compulsive disorder. *Psychiatry Clin. Neurosci.* 70, 448–456. doi: 10.1111/pcn.12419

Dar, K. A., and Iqbal, N. (2015). Worry and rumination in generalized anxiety disorder and obsessive compulsive disorder. *J. Psychol.* 149, 866–880. doi: 10.1080/00223980.2014.986430

de Wit, S. J., Alonso, P., Schweren, L., Mataix-Cols, D., Lochner, C., Menchon, J. M., et al. (2014). Multicenter voxel-based morphometry mega-analysis of structural brain scans in obsessive-compulsive disorder. *Am. J. Psychiatry* 171, 340–349. doi: 10.1176/appi.ajp.2013.13040574

de Wit, S. J., de Vries, F. E., van der Werf, Y. D., Cath, D. C., Heslenfeld, D. J., Veltman, E. M., et al. (2012). Presupplementary motor area hyperactivity during response inhibition: a candidate endophenotype of obsessive-compulsive disorder. *Am. J. Psychiatry* 169, 1100–1108. doi: 10.1176/appi.ajp.2012.12010073

Dougherty, D. D., Brennan, B. P., Stewart, S. E., Wilhelm, S., Widge, A. S., and Rauch, S. L. (2018). Neuroscientifically informed formulation and treatment planning for patients with obsessive-compulsive disorder: a review. *JAMA Psychiatry* 75, 1081–1087. doi: 10.1001/jamapsychiatry.2018.0930

Fair, D. A., Dosenbach, N. U., Church, J. A., Cohen, A. L., Brahmbhatt, S., Miezin, F. M., et al. (2007). Development of distinct control networks through segregation and integration. *Proc. Natl. Acad. Sci. U.S.A.* 104, 13507–13512. doi: 10.1073/pnas.0705843104

Fan, J., Zhong, M., Gan, J., Liu, W., Niu, C., Liao, H., et al. (2017). Spontaneous neural activity in the right superior temporal gyrus and left middle temporal gyrus is associated with insight level in obsessive-compulsive disorder. *J. Affect. Disord.* 207, 203–211. doi: 10.1016/j.jad.2016.08.027

Fouche, J. P., du Plessis, S., Hattingh, C., Roos, A., Lochner, C., Soriano-Mas, C., et al. (2017). Cortical thickness in obsessive-compulsive disorder: multisite mega-analysis of 780 brain scans from six centres. *Br. J. Psychiatry* 210, 67–74. doi: 10.1192/bjp.bp.115.164020

Fox, M. D., and Raichle, M. E. (2007). Spontaneous fluctuations in brain activity observed with functional magnetic resonance imaging. *Nat. Rev. Neurosci.* 8, 700–711. doi: 10.1038/nrn2201

Gao, Z., Davis, C., Thomas, A. M., Economo, M. N., Abrego, A. M., Svoboda, K., et al. (2018). A cortico-cerebellar loop for motor planning. *Nature* 563, 113–116. doi: 10.1038/s41586-018-0633-x

Gimenez, M., Guinea-Izquierdo, A., Villalta-Gil, V., Martinez-Zalacain, I., Segalas, C., Subira, M., et al. (2017). Brain alterations in low-frequency fluctuations across multiple bands in obsessive compulsive disorder. *Brain Imaging Behav.* 11, 1690–1706. doi: 10.1007/s11682-016-9601-y

Grover, S., Nguyen, J. A., Viswanathan, V., and Reinhart, R. M. G. (2021). High-frequency neuromodulation improves obsessive-compulsive behavior. *Nat. Med.* 27, 232–238. doi: 10.1038/s41591-020-01173-w

Grutzmann, R., Endrass, T., Kaufmann, C., Allen, E., Eichele, T., and Kathmann, N. (2016). Presupplementary Motor Area Contributes to Altered Error Monitoring in Obsessive-Compulsive Disorder. *Biol. Psychiatry* 80, 562–571. doi: 10.1016/j.biopsych.2014.12.010

Gursel, D. A., Avram, M., Sorg, C., Brandl, F., and Koch, K. (2018). Frontoparietal areas link impairments of large-scale intrinsic brain networks with aberrant fronto-striatal interactions in OCD: a meta-analysis of resting-state functional connectivity. *Neurosci. Biobehav. Rev.* 87, 151–160. doi: 10.1016/j.neubiorev.2018.01.016

Hao, H., Chen, C., Mao, W., Xia, W., Yi, Z., Zhao, P., et al. (2019). Alterations in resting-state local functional connectivity in obsessive-compulsive disorder. *J. Affect. Disord.* 245, 113–119. doi: 10.1016/j.jad.2018.10.112

Hirose, M., Hirano, Y., Nemoto, K., Sutoh, C., Asano, K., Miyata, H., et al. (2017). Relationship between symptom dimensions and brain morphology in obsessive-compulsive disorder. *Brain Imaging Behav.* 11, 1326–1333. doi: 10.1007/s11682-016-9611-9

Hou, J., Wu, W., Lin, Y., Wang, J., Zhou, D., Guo, J., et al. (2012). Localization of cerebral functional deficits in patients with obsessive-compulsive disorder: a resting-state fMRI study. *J. Affect. Disord.* 138, 313–321. doi: 10.1016/j.jad.2012.01.022

Hu, X., Du, M., Chen, L., Li, L., Zhou, M., Zhang, L., et al. (2017). Meta-analytic investigations of common and distinct grey matter alterations in youths and adults with obsessive-compulsive disorder. *Neurosci. Biobehav. Rev.* 78, 91–103. doi: 10.1016/j.neubiorev.2017.04.012

Hu, X., Zhang, L., Bu, X., Li, H., Gao, Y., Lu, L., et al. (2020). White matter disruption in obsessive-compulsive disorder revealed by meta-analysis of tract-based spatial statistics. *Depress. Anxiety* 37, 620–631. doi: 10.1002/da.23008

Hu, X., Zhang, L., Bu, X., Li, H., Li, B., Tang, W., et al. (2019). Localized connectivity in obsessive-compulsive disorder: an investigation combining univariate and multivariate pattern analyses. *Front. Behav. Neurosci.* 13:122. doi: 10.3389/fnbeh.2019.00122

Lee, H. J., and Kwon, S. M. (2003). Two different types of obsession: autogenous obsessions and reactive obsessions. *Behav. Res. Ther.* 41, 11–29. doi: 10.1016/S0005-7967(01)00101-2

Liu, J., Bu, X., Hu, X., Li, H., Cao, L., Gao, Y., et al. (2021). Temporal variability of regional intrinsic neural activity in drug-naïve patients with obsessive-compulsive disorder. *Hum. Brain Mapp.* 42, 3792–3803. doi: 10.1002/hbm.25465

Marsh, R., Tau, G. Z., Wang, Z., Huo, Y., Liu, G., Hao, X., et al. (2015). Reward-based spatial learning in unmedicated adults with obsessive-compulsive disorder. *Am. J. Psychiatry* 172, 383–392. doi: 10.1176/appi.ajp.2014.13121700

Milad, M. R., and Rauch, S. L. (2012). Obsessive-compulsive disorder: beyond segregated cortico-striatal pathways. *Trends Cogn. Sci.* 16, 43–51. doi: 10.1016/j.tics.2011.11.003

Muller, V. I., Cieslik, E. C., Laird, A. R., Fox, P. T., Radua, J., Mataix-Cols, D., et al. (2018). Ten simple rules for neuroimaging meta-analysis. *Neurosci. Biobehav. Rev.* 84, 151–161. doi: 10.1016/j.neubiorev.2017.11.012

Niu, Q., Yang, L., Song, X., Chu, C., Liu, H., Zhang, L., et al. (2017). Abnormal resting-state brain activities in patients with first-episode obsessive-compulsive disorder. *Neuropsychiatr. Dis. Treat.* 13, 507–513. doi: 10.2147/NDT.S117510

Norman, L. J., Carlisi, C. O., Christakou, A., Murphy, C. M., Chantiluke, K., Giampietro, V., et al. (2018). Frontostriatal dysfunction during decision making in attention-deficit/hyperactivity disorder and obsessive-compulsive disorder. *Biol. Psychiatry Cogn. Neurosci Neuroimaging.* 3, 694–703. doi: 10.1016/j.bpsc.2018.03.009

Pauls, D. L., Abramovitch, A., Rauch, S. L., and Geller, D. A. (2014). Obsessive-compulsive disorder: an integrative genetic and neurobiological perspective. *Nat. Rev. Neurosci.* 15, 410–424. doi: 10.1038/nrn3746

Ping, L., Su-Fang, L., Hai-Ying, H., Zhang-Ye, D., Jia, L., Zhi-Hua, G., et al. (2013). Abnormal spontaneous neural activity in obsessive-compulsive disorder: a resting-state functional magnetic resonance imaging study. *PLoS ONE* 8:e67262. doi: 10.1371/journal.pone.0067262

Qiu, L., Fu, X., Wang, S., Tang, Q., Chen, X., Cheng, L., et al. (2017). Abnormal regional spontaneous neuronal activity associated with symptom severity in treatment-naive patients with obsessive-compulsive disorder

revealed by resting-state functional MRI. *Neurosci. Lett.* 640, 99–104. doi: 10.1016/j.neulet.2017.01.024

Radua, J. (2021). PRISMA 2020 - An updated checklist for systematic reviews and meta-analyses. *Neurosci. Biobehav. Rev.* 124, 324–325. doi: 10.1016/j.neubiorev.2021.02.016

Radua, J., and Mataix-Cols, D. (2009). Voxel-wise meta-analysis of grey matter changes in obsessive-compulsive disorder. *Br. J. Psychiatry* 195, 393–402. doi: 10.1192/bjp.bp.108.055046

Radua, J., Mataix-Cols, D., Phillips, M. L., El-Hage, W., Kronhaus, D. M., Cardoner, N., et al. (2012). A new meta-analytic method for neuroimaging studies that combines reported peak coordinates and statistical parametric maps. *Eur. Psychiatry* 27, 605–611. doi: 10.1016/j.eurpsy.2011.04.001

Ramnani, N. (2006). The primate cortico-cerebellar system: anatomy and function. *Nat. Rev. Neurosci.* 7, 511–522. doi: 10.1038/nrn1953

Rotge, J. Y., Langbour, N., Guehl, D., Bioulac, B., Jaafari, N., Allard, M., et al. (2010). Gray matter alterations in obsessive-compulsive disorder: an anatomic likelihood estimation meta-analysis. *Neuropsychopharmacology* 35, 686–691. doi: 10.1038/npp.2009.175

Ruscio, A. M., Stein, D. J., Chiu, W. T., and Kessler, R. C. (2010). The epidemiology of obsessive-compulsive disorder in the National Comorbidity Survey Replication. *Mol. Psychiatry* 15, 53–63. doi: 10.1038/mp.2008.94

Sha, Z., Edmiston, E. K., Versace, A., Fournier, J. C., Graur, S., Greenberg, T., et al. (2020). Functional disruption of cerebello-thalamo-cortical networks in obsessive-compulsive disorder. *Biol. Psychiatry Cogn. Neurosci. Neuroimaging* 5, 438–447. doi: 10.1016/j.bpsc.2019.12.002

Shin, N. Y., Lee, T. Y., Kim, E., and Kwon, J. S. (2014). Cognitive functioning in obsessive-compulsive disorder: a meta-analysis. *Psychol. Med.* 44, 1121–1130. doi: 10.1017/S0033291713001803

Stein, D. J., Costa, D. L. C., Lochner, C., Miguel, E. C., Reddy, Y. C. J., Shavitt, R. G., et al. (2019). Obsessive-compulsive disorder. *Nat. Rev. Dis. Primers* 5:52. doi: 10.1038/s41572-019-0102-3

Supekar, K., Musen, M., and Menon, V. (2009). Development of large-scale functional brain networks in children. *PLoS Biol.* 7:e1000157. doi: 10.1371/journal.pbio.1000157

Wise, T., Radua, J., Nortje, G., Cleare, A. J., Young, A. H., and Arnone, D. (2016). Voxel-based meta-analytical evidence of structural disconnectivity in major depression and bipolar disorder. *Biol. Psychiatry* 79, 293–302. doi: 10.1016/j.biopsych.2015.03.004

Xia, J., Fan, J., Liu, W., Du, H., Zhu, J., Yi, J., et al. (2020). Functional connectivity within the salience network differentiates autogenous- from reactive-type obsessive-compulsive disorder. *Prog. Neuropsychopharmacol. Biol. Psychiatry* 98:109813. doi: 10.1016/j.pnpbp.2019.109813

Xu, T., Zhao, Q., Wang, P., Fan, Q., Chen, J., Zhang, H., et al. (2019). Altered resting-state cerebellar-cerebral functional connectivity in obsessive-compulsive disorder. *Psychol. Med.* 49, 1156–1165. doi: 10.1017/S0033291718001915

Yang, T., Cheng, Y., Li, H., Jiang, H., Luo, C., Shan, B., et al. (2010). Abnormal regional homogeneity of drug-naïve obsessive-compulsive patients. *Neuroreport* 21, 786–790. doi: 10.1097/WNR.0b013e32833cadf0

Yang, X., Luo, J., Zhong, Z., Yao, S., Wang, P., Gao, J., et al. (2019). Abnormal regional homogeneity in patients with obsessive-compulsive disorder and their unaffected siblings: a resting-state fMRI study. *Front. Psychiatry* 10:452. doi: 10.3389/fpsyt.2019.00452

Yang, X. Y., Sun, J., Luo, J., Zhong, Z. X., Li, P., Yao, S. M., et al. (2015). Regional homogeneity of spontaneous brain activity in adult patients with obsessive-compulsive disorder before and after cognitive behavioural therapy. *J. Affect. Disord.* 188, 243–251. doi: 10.1016/j.jad.2015.07.048

Yun, J. Y., Boedhoe, P. S. W., Vriend, C., Jahanshad, N., Abe, Y., Ameis, S. H., et al. (2020). Brain structural covariance networks in obsessive-compulsive disorder: a graph analysis from the ENIGMA Consortium. *Brain* 143, 684–700. doi: 10.1093/brain/awaa001

Zang, Y., Jiang, T., Lu, Y., He, Y., and Tian, L. (2004). Regional homogeneity approach to fMRI data analysis. *Neuroimage* 22, 394–400. doi: 10.1016/j.neuroimage.2003.12.030

Zou, Q. H., Zhu, C. Z., Yang, Y., Zuo, X. N., Long, X. Y., Cao, Q. J., et al. (2008). An improved approach to detection of amplitude of low-frequency fluctuation (ALFF) for resting-state fMRI: fractional ALFF. *J. Neurosci. Methods* 172, 137–141. doi: 10.1016/j.jneumeth.2008.04.012

Conflict of Interest: The authors declare that the research was conducted in the absence of any commercial or financial relationships that could be construed as a potential conflict of interest.

The reviewer XY declared a shared affiliation, with no collaboration, with the authors to the handling editor at the time of the review.

frontiers in Human Neuroscience

ORIGINAL RESEARCH
published: 05 October 2021
doi: 10.3389/fnhum.2021.697696

Differences in Disrupted Dynamic Functional Network Connectivity Among Children, Adolescents, and Adults With Attention Deficit/Hyperactivity Disorder: A Resting-State fMRI Study

*Elijah Agoalikum[1], Benjamin Klugah-Brown[1], Hang Yang[1], Pan Wang[1], Shruti Varshney[2], Bochao Niu[1] and Bharat Biswal[1,2]**

[1] MOE Key Laboratory for Neuroinformation, School of Life Sciences and Technology, The Clinical Hospital of Chengdu Brain Science Institute, University of Electronic Science and Technology of China, Chengdu, China, [2] Department of Biomedical Engineering, New Jersey Institute of Technology, Newark, NJ, United States

OPEN ACCESS

Edited by:
Long-Biao Cui,
People's Liberation Army General Hospital, China

Reviewed by:
Mingrui Xia,
Beijing Normal University, China
Xiao Chang,
King's College London, United Kingdom

***Correspondence:**
Bharat Biswal
bbiswal@gmail.com

Specialty section:
This article was submitted to Brain Imaging and Stimulation, a section of the journal Frontiers in Human Neuroscience

Received: 20 April 2021
Accepted: 26 July 2021
Published: 05 October 2021

Citation:
Agoalikum E, Klugah-Brown B, Yang H, Wang P, Varshney S, Niu B and Biswal B (2021) Differences in Disrupted Dynamic Functional Network Connectivity Among Children, Adolescents, and Adults With Attention Deficit/Hyperactivity Disorder: A Resting-State fMRI Study. Front. Hum. Neurosci. 15:697696. doi: 10.3389/fnhum.2021.697696

Attention deficit hyperactivity disorder (ADHD) is one of the most widespread mental disorders and often persists from childhood to adulthood, and its symptoms vary with age. In this study, we aim to determine the disrupted dynamic functional network connectivity differences in adult, adolescent, and child ADHD using resting-state functional magnetic resonance imaging (rs-fMRI) data consisting of 35 children (8.64 ± 0.81 years), 40 adolescents (14.11 ± 1.83 years), and 39 adults (31.59 ± 10.13 years). We hypothesized that functional connectivity is time-varying and that there are within- and between-network connectivity differences among the three age groups. Nine functional networks were identified using group ICA, and three FC-states were recognized based on their dynamic functional network connectivity (dFNC) pattern. Fraction of time, mean dwell time, transition probability, degree-in, and degree-out were calculated to measure the state dynamics. Higher-order networks including the DMN, SN, and FPN, and lower-order networks comprising the SMN, VN, SC, and AUD were frequently distributed across all states and were found to show connectivity differences among the three age groups. Our findings imply abnormal dynamic interactions and dysconnectivity associated with different ADHD, and these abnormalities differ between the three ADHD age groups. Given the dFNC differences between the three groups in the current study, our work further provides new insights into the mechanism subserved by age difference in the pathophysiology of ADHD and may set the grounds for future case-control studies in the individual age groups, as well as serving as a guide in the development of treatment strategies to target these specific networks in each age group.

Keywords: ADHD, brain connectivity, dynamic functional brain network, fMRI, brain networks and dynamic connectivity, resting state—fMRI

INTRODUCTION

Attention deficit hyperactivity disorder (ADHD) is one of the most common mental disorders worldwide, characterized by inattentive, hyperactive, or impulsive behaviors (American Psychiatric Association., 2000). ADHD mostly affects children, but often persists to adulthood (Danielson et al., 2018). The Diagnostic and Statistical Manual of Mental Disorders-IV (DSM-IV) classified ADHD into 3 sub-types, namely; hyperactive/impulsive (HI), inattentive (IA), and combined (C) type. ADHD prevalence in children, adolescents, and adults is 9.5, 11.4, and 4.4%, respectively (Gimpel and Kuhn, 2000; Barbaresi et al., 2002; Kessler et al., 2006; Wolraich et al., 2011), with its symptoms varying from one age group to the other (Katragadda and Schubiner, 2007).

Functional magnetic resonance imaging (fMRI) has become a popular technique for studying brain diseases or disorders such as ADHD. The majority of these ADHD fMRI studies have followed a task-based approach, aiming to examine how brain function may be modulated by group status during cognitive task performance. This approach is designed to isolate specific cognitive processes that may be linked to or modified by ADHD symptoms or treatment. In recent times, however, there has been an overwhelming interest in an alternative method called resting-state functional magnetic resonance imaging (rs-fMRI). The term "resting state" is misleading because the brain is never at rest (Stark and Squire, 2001; Raichle, 2006). It is often used to denote a task-free procedure where participants are asked to lie still in a scanner, with their eyes either opened or closed, and not think about anything specific. Resting-state fMRI gives a measure of brain neurophysiology that is not dependent on task-directed cognitive processes. Moreover, the discovery of the default mode network of brain structures, which is said to be active during the resting state and show dynamic negative correlations with task-related regions, has opened up new areas of investigation (Raichle et al., 2001; Greicius et al., 2003) and has raised interesting questions with regards to abnormal patterns of brain activation in patients with ADHD.

Under resting-state conditions, intrinsic networks obtained from rs-fMRI correlate with low frequency BOLD signal fluctuations between regions of the brain (Biswal et al., 1995; Fox and Raichle, 2007; Khundrakpam et al., 2016). It has been demonstrated that the human brain is functionally organized into a hierarchy of large-scale connectivity networks (Meunier et al., 2009). Abnormal functional connectivity (FC) within the default mode, executive control, salience, and attention-related networks were observed in ADHD patients (Sidlauskaite et al., 2016; Bos et al., 2017). These networks are said to be associated with symptoms of ADHD, such as impairment of executive function processing and distractibility (Francx et al., 2015; Zhao et al., 2017). Significant differences were also observed between child and adolescent ADHD patients within the default mode and frontoparietal networks (Park et al., 2016), which are also said to be highly associated with ADHD symptoms (Buckner et al., 2008; Andrews-Hanna, 2012; Ptak, 2012). These and several other studies have found significant differences both between ADHD patients and healthy control subjects and also among ADHD patient groups, but most of these studies are based on the assumption that FC is static throughout the whole scan time and, therefore, calculate FC using the entire time course. Even though static functional network connectivity (sFNC) has been used to successfully determine brain abnormalities in ADHD and other neurological diseases, it has ignored the fact that different neural activities can occur at different points in time.

Having proven that FC of the resting brain is indeed dynamic (Fox et al., 2005), methods have been in development since 2010 to depict the time-varying network connectivity in rs-fMRI and to capture the network activity of the brain in more detail (Chang and Glover, 2010; Sakoğlu et al., 2010).

In recent times, some researchers have observed time-varying connectivity patterns among intrinsic networks in mental disorders, such as schizophrenia and bipolar disorder, that cannot be detected using sFNC (Damaraju et al., 2014; Rashid et al., 2014). Dynamic functional network connectivity (dFNC) has yielded fascinating results in several brain disorders, showing the within and between network disconnections that may be unknown or uncertain (Damaraju et al., 2014; de Lacy et al., 2017; de Lacy and Calhoun, 2018). Previous works using task-based regions of interest suggest lagging strength in frontal-parietal-striatal-cerebellar connections in ADHD, with implications mainly in the frontoparietal, ventral attention, and default mode networks (Cortese et al., 2012; Hart et al., 2012, 2013).

Even though dFNC has been employed to study the differences between healthy control subjects and patients in several mental disorders including ADHD, no study has employed dFNC to access network connectivity differences between child, adolescent, and adult ADHD patients. Given that ADHD symptoms vary among the three age groups, identifying network disruptions specific to each age group will provide new insights into the pathophysiology of ADHD and may set the grounds for future case-control studies in the individual age groups, as well as serving as a guide in the development of treatment strategies to target these specific networks in each age group. We, therefore, performed dFNC using group independent component analysis (GICA), sliding window correlation, and K-means clustering to explore network connectivity differences in ADHD between these three age groups. We hypothesized that dFNC can capture the time-varying characteristics of fMRI data perculiar to the three ADHD age groups.

MATERIALS AND METHODS

Data Acquisition

Unprocessed resting-state fMRI data of ADHD patients (158 subjects) were obtained from the New York University Child Study Center for the ADHD-200 Global Competition and UCLA dataset (Bilder et al., 2016). The NYU dataset is made up of 45 child ADHD patients, and 73 adolescent ADHD patients. The UCLA dataset is made up of 40 adult ADHD patients. Both datasets are made openly to researchers online. All participants used in the current study were diagnosed with ADHD and their symptom scores have been used for the correlation analysis in

TABLE 1 | Data demographics.

ADHD group	Adults ($n = 39$)	Adolescents ($n = 40$)	Adolescents ($n = 40$)	*P*-value
Gender (M/F) 0.026224	(20/19)	(31/9)	(26/9)	
Age (years)	31.59 ± 10.13	14.11 ± 1.83	8.64 ± 0.81	<0.00001
Data range (years)	21–50	11.41–17.61	7.24–9.98	
OA score	63.49 ± 4.99	70.18 ± 46	70.74 ± 7.81	
H score	31.57 ± 4.63	65.95 ± 11.89	66.69 ± 12.69	
IA score	35.77 ± 2.78	68.88 ± 9.16	69.89 ± 8.87	

One-ANOVA was used to determine group differences. OA, Overall severity; H, Hyperactivity severity; IA, Inattentive severity.

the current study. Detailed information about the subjects can be found in **Table 1**.

For the adult dataset, MRI data were acquired on one of two 3T Siemens Trio scanners, located at the Ahmanson-Lovelace Brain Mapping Center (Siemens version syngo MR B15) and the Staglin Center for Cognitive Neuroscience (Siemens version syngo MR B17) at UCLA. Functional MRI data were collected using a T2*-weighted echo-planar imaging (EPI) sequence with the following parameters: slice thickness = 4 mm, slices = 34, TR = 2 s, TE = 30 ms, flip angle = 90°, matrix 64 × 64, FOV = 192 mm. Additionally, a T2-weighted matched-bandwidth high-resolution anatomical scan (with the same slice prescription as the fMRI scan) and MPRAGE were collected. The parameters for the high-resolution scan were: 4 mm slices, TR/TE = 5,000/34 ms, 4 averages, matrix = 128 × 128, 90-degree flip angle. The parameters for MPRAGE were the following: TR = 1.9 s, TE = 2.26 ms, FOV = 250 mm, matrix = 256 × 256, sagittal plane, slice thickness = 1 mm, 176 slices. For the child and adolescent datasets, MRI data were obtained using Siemens Magnetom Allegra Syngo Mr 2004a. FMRI data were collected using an echo-planar imaging sequence with the following parameters: slice thickness: 4 mm, Slices: 33, TR: 2,000 ms, TE: 15 ms, Rotation = 90°, FoV phase: 80.0%, FoV read = 240 mm. In addition, T1-weighted images were acquired using the following parameters: Slice thickness = 1.33 ms, TR = 2,530,ms, TE = 3.25,ms, rotation = 0 degrees, FoV phase = 100.0%, FoV read = 256 mm.

Data Preprocessing

For the adult dataset, the first 2 time points were removed, leaving final time points of 150. For the pediatric (adolescent and child) datasets, the first 26 time points were removed to ensure that all the data have equal time points since the time courses are used in the dFNC calculations. The same preprocessing steps were done for all subjects, including slice time correction, realignment, co-registration of T1 images to corresponding functional images, segmentation, normalization by Diffeomorphic Anatomical Registration using Exponentiated Lie algebra (DARTEL) (Ashburner, 2007), and resampling to 3 × 3 × 3 mm voxels, nuisance covariates regression using Friston 24 (Friston et al., 1996), and spatial smoothing with a 6 mm full width half maximum (FWHM) Gaussian kernel. Pediatric and adult datasets were preprocessed separately to ensure that the right template is generated for normalization. Subjects with a maximum translation > 2 mm or rotation > 2° were excluded from further analysis, leaving a total of 114 subjects. The final data used for further analysis included 35 children (8.64 ± 0.81 years), 40 adolescents (14.11 ± 1.83 years), and 39 adults (31.59 ± 10.13 years). All preprocessing steps were performed using the data processing assistant for resting-state fMRI, advanced edition (DPARSFA) in the DPABI toolbox (Yan et al., 2016).

Group Spatial Independent Component Analysis

Data were decomposed into functional networks using a group-level spatial ICA as implemented in the GIFT toolbox.[1] A relatively high model order with 60 components was performed using the Infomax algorithm with a best-run selection from 10 randomly initialized analyses to achieve a functional parcellation of refined cortical and subcortical components corresponding to known anatomical and functional segmentations (Himberg et al., 2004; Li et al., 2007; de Lacy and Calhoun, 2018). To make sure that all components selected were intrinsic component networks (ICNs), sorting was performed using a combination of visual inspection and quantitative metrics. For each of the 60 components, spectral metrics of (1) fractional amplitude of low-frequency fluctuations (fALFF) and (2) dynamic range were generated. Generally, independent components representing brain networks are said to have higher values in these spectral metrics, whereas noise components are said to have lower values (Allen et al., 2011, 2012). Hence, we checked the spectral metrics of each component, and only components with high values in these spectral metrics were retained for further scrutiny. Components were also visually inspected, and their peak coordinates were used to determine their correspondence with gray matter. Components with poor overlap with the cerebral gray matter or low spectral metrics were discarded. The remaining 50 components represented the intrinsic networks (INs) used in this study.

dFNC Analysis

The selected components underwent additional post-processing (linear detrending, despiking, and low-pass filtering with a high-frequency cutoff at 0.15 Hz) to remove any remaining sources of noise. DFNC was estimated based on the sliding window approach. Based on previous studies (Allen et al., 2014; Klugah-Brown et al., 2019; Sanfratello et al., 2019), we selected a window width size of 22 TRs = 44 s, and sliding steps of 1 TR, resulting in 128 windows. This was obtained for all 114 subjects to give a total of 14,592 instances (114 subjects × 128 windows). For each window, FNC was estimated between ICNs from a regularized inverse covariance matrix using the graphical LASSO method (Friedman et al., 2008). An L1 norm was placed on the inverse covariance matrix to promote sparsity, and the regularization parameter (lambda) was optimized for each subject. The dFNC values were Fisher-Z transformed. In brief, the graphical LASSO method is a method used for learning

[1] http://mialab.mrn.org/software/gift/

the structure in an undirected Gaussian graphical model, which uses L1 regularization in controlling the number of zeros in the precision matrix $\Theta = \Sigma^{-1}$. Kindly refer to Meinshausen and Bühlmann (2006); Yuan and Lin (2007), and Banerjee et al. (2008) for more information.

K-means clustering was used to cluster all dFNC windows based on the correlation distance. Clustering numbers from 2 to 10 were selected, representing cluster states. For each k, the clustering algorithm was repeated 500 times to increase the chances of escaping local minima, with random initialization used to obtain the state cluster centroids. The optimal number of clusters was estimated using the elbow criterion and silhouette algorithms. An optimal K = 3 was obtained using these two methods. Also, subjects were well distributed among these three clusters, which is better for pattern evaluation. Only the selected 50 ICNs were used in the clustering, resulting in a total of [50 × (50–1)]/2 = 1,225 features. These features were then used for the dynamic FNC analysis between the three groups.

Functional network connectivity, fraction of time, mean dwell time, transition probability, degree-in, and degree-out were compared between the three age groups in each state. Correlation analyses were also performed to determine the impact of age, overall ADHD severity, hyperactivity severity, and inattentive severity on fraction of time and mean dwell time of each age group in each cluster state. All statistical analyses were performed using MATLAB (Mathworks Inc., United States). Age, gender, and mean framewise displacement (mean FD) were used as covariates for statistical analyses. Furthermore, given that our data was obtained from different sites, and several studies have shown the effect of multi-site in different ADHD age groups (Hong et al., 2017; Zhou et al., 2019), we regressed out the effect of site in our analyses. In brief, the NYU dataset (consisting of the pediatric dataset) was represented as site one (1), whiles the UCLA dataset (consisting of the adult dataset) was represented as site two (2). Thus, each subject in the NYU and UCLA datasets were labeled 1 and 2, respectively, and used as covariates in our statistical analysis to regress out site effects. False discovery rate (FDR) was used for multiple comparison corrections. **Figure 1** shows the schematic diagram of the analysis pipeline.

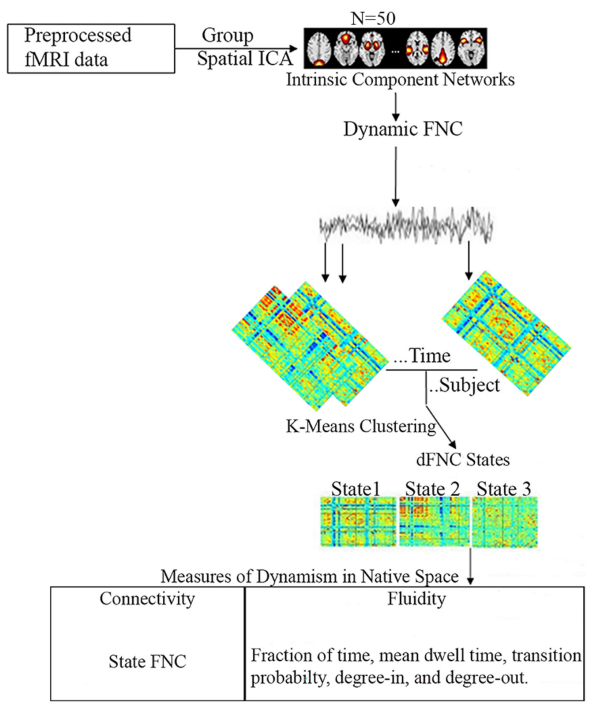

FIGURE 1 | Schematic diagram of the analysis pipeline. Rs-fMRI data was preprocessed and subjected to spatial group ICA resulting in 50 intrinsic component networks. Static FNC was then estimated. For dFNC, the sliding window approach was adopted and clustered using K-means to obtain 3 cluster states. Based on these three cluster states, five measures of dynamism were computed in native space.

RESULTS

Spatial ICA and ICNs

Spatial maps of the ICNs and their time courses were decomposed using GICA. The selected 50 ICNs were further categorized into nine networks based on their anatomical and functional properties, including the sensorimotor network (SMN), visual network (VN), default-mode network (DMN), central executive network (CEN), cerebellum network (CBN), subcortical network (SC), auditory network (AUD), frontoparietal network (FPN), and salience network (SN). The identified ICNs with their activation peaks primarily fell on the gray matter (**Supplementary Figure 2**).

Dynamic FNC States

Three reoccurring dFNC states over time were identified using K-means clustering and the cluster centroid of each dFNC state is shown in **Figure 2**. All three states showed positive connectivity within the VN. States 1 and 3 showed positivity connectivity within the DMN, with state 1 distinguishing itself with negative connectivity between some ICNS of the CBN, AUD, and VN with other networks. States 2 and 3 showed positive connectivity within the VN and SMN, with state 2 showing strong positive connectivity within these two networks than state 3, but some ICNs showed strong negative connectivity within these two networks. State 2 also showed strong positive connectivity between the SMN and VN, with the CBN showing antagonism with other networks in this state.

Group Differences in dFNC States

To find out if there are significant dFNC differences between the three age groups, two-sample *t*-tests were done between 1. Adolescents vs. children 2. Adults vs. children 3. Adults vs. adolescents.

Adolescents vs. Children

Figure 3A demonstrates significant differences ($p < 0.01$, FDR corrected) between adolescent and child ADHD groups. Relative to child ADHD patients, adolescent ADHD patients showed increased network connectivity between the DMN and CEN, DMN and SC, and DMN and SN in state 1. Compared to Child

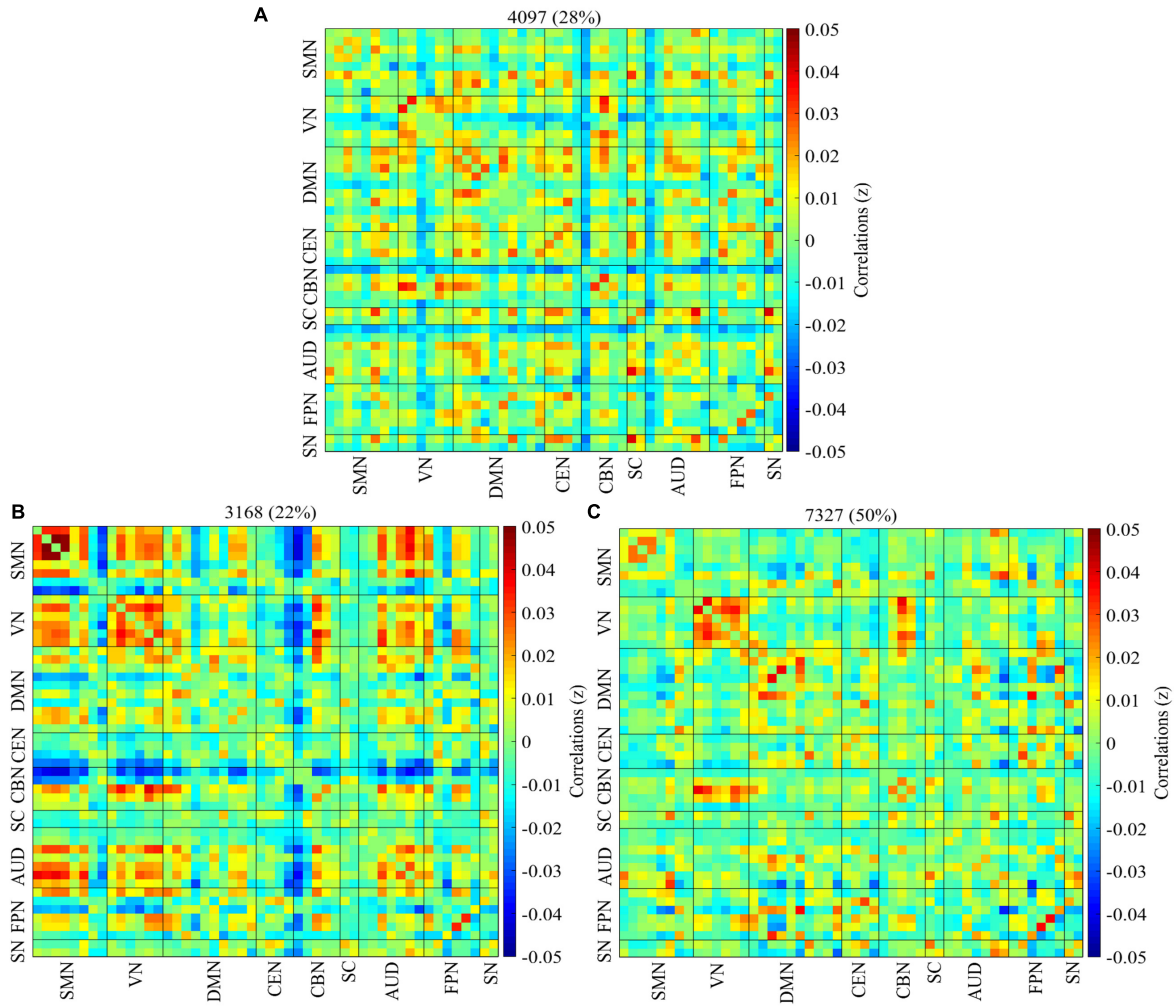

FIGURE 2 | Percentage of occurrence. The median of all subjects together with the total number and percentage of occurrences are displayed in each state. **(A–C)** Represent states 1–3. The connectivity pattern varies among the three cluster states with state 2 showing more connectivity than states 1 and 3.

ADHD patients, adolescent ADHD patients exhibited increased network connectivity between the SMN and SC in state 2.

Adults vs. Children

The results of the two-sample *t*-test between adults and children are shown in **Figure 3B**. All three clusters were found to show significant differences between the two groups ($p < 0.01$, FDR corrected). Relative to child ADHD patients, adult ADHD patients showed increased network connectivity between the SMN and VN, SMN and DMN, SMN and SC, and between the AUD and SC, AUD and DMN, AUD and SN, AUD and FPN, and FPN and CBN in state 1. In state 2, the connectivity pattern changed, with increased network connectivity between the DMN and SMN, DMN and VN, DMN and CBN, DMN and AUD, DMN and FPN, and DMN and SN in adult ADHD patients relative to child ADHD patients. The connectivity pattern again changed in state 3 with more network connectivity differences between the two groups. The DMN showed increased connectivity with the CEN, SC, AUD, FPN, and SN, whiles the VN showed decreased connectivity with the SC in adult ADHD patients relative to child ADHD patients. Compared to the child group, increased connectivity was found within the SMN and AUD, and between the SMN and AUD, SMN and SN, AUD and CBN, AUD and FPN, and AUD and SN in the adult group in state 3.

Adults vs. Adolescents

All three cluster states showed significant differences between the 2 groups ($p < 0.01$, FDR corrected) (**Figure 3C**). In state 1, adult ADHD patients showed increased network connectivity within the AUD, and between the AUD and DMN relative to their adolescent counterparts. Compared to adolescent ADHD patients, increased network connectivity was found within the VN in adult ADHD patients in state 2. Relative to adolescents ADHD patients, adult ADHD patients again showed increased network connectivity within the AUD, between the DMN and SMN, DMN and CBN, and between the DMN and SN in state 3. Also, in state 3, increased network connectivity was observed between the FPN and VN, FPN and CBN, and FPN and SC

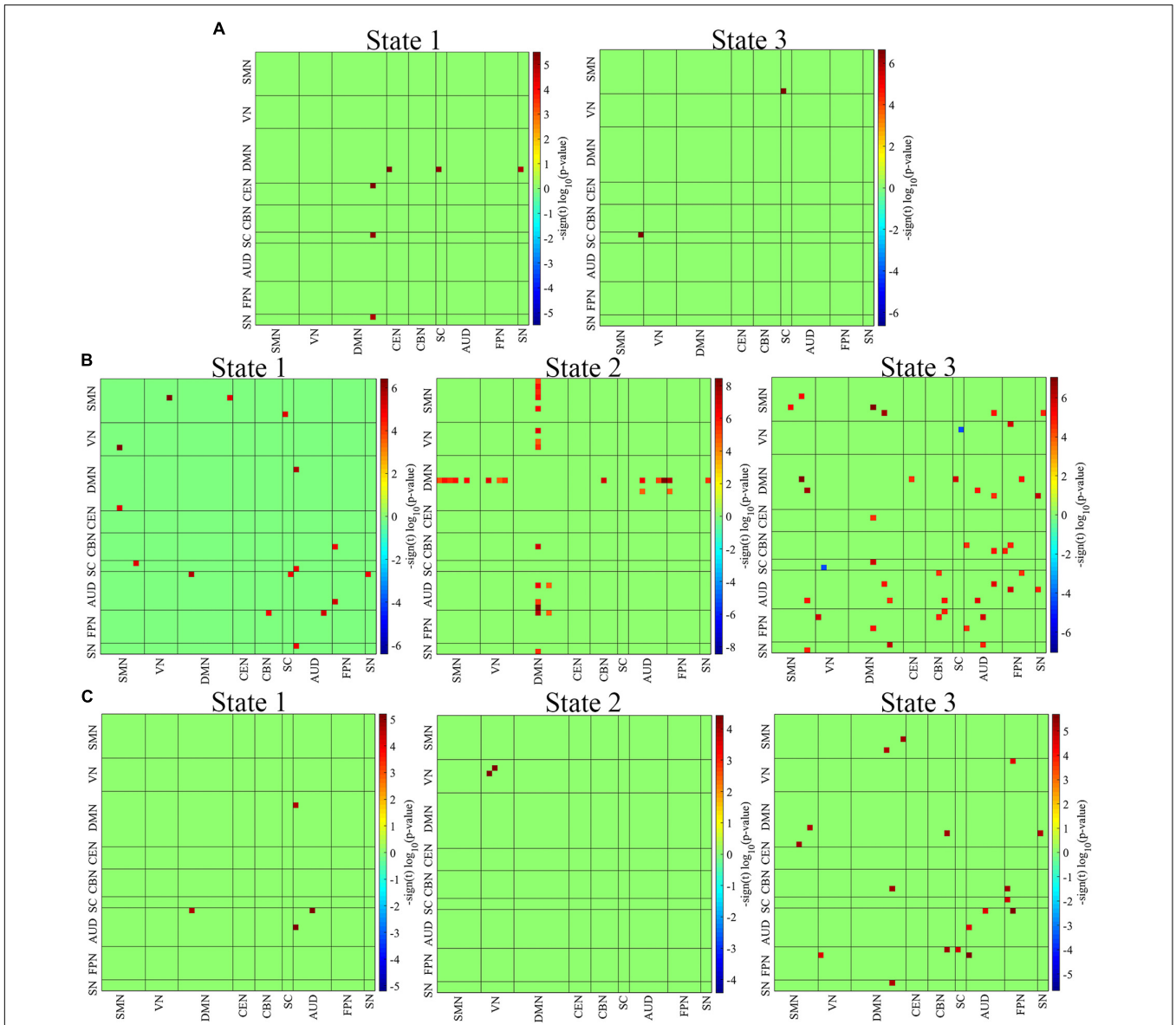

FIGURE 3 | Group differences among the three age groups. **(A)** Adolescent vs. Child ADHD patients. **(B)** Adult vs. Child ADHD patients. **(C)** Adult vs. Adolescent ADHD patients. Two out of the three clusters showed significant differences between child and adolescent ADHD patients, whiles all three clusters showed significant differences between child/adolescent and adult ADHD patients ($P < 0.01$, FDR corrected). The red squares indicate increased network connectivity whiles the blue squares indicate decreased network connectivity.

in adult ADHD patients relative to adolescent ADHD patients. The DMN connectivity difference between the two groups varies across the 3 states. Interestingly, the FPN showed no significant connectivity differences between the 2 groups in states 1 and 2 but showed significant connectivity differences with the VN, CBN, and SC in state 3.

Fluidity Measures

The mean dwell time, which is the mean time spent in one state before moving to the next state, was compared between the three age groups using two-sample *t*-tests (**Figure 4A**). In state 1, the child group showed the highest mean dwell time, whiles the adult and adolescent groups showed the highest mean dwell times in states 2 and 3, respectively. However, significant differences were observed between only adult and adolescent, and adult and child ADHD pairs in states 1 and 2 (FDR corrected), with no significant mean dwell time differences between adolescent and child ADHD patients in all three cluster states.

The proportion of time each subject stayed in each state within the whole scan duration was defined as the fraction of time in that state. **Figure 4B** shows the fraction of time spent in each state over the whole time series. Two-sample *t*-tests were performed to determine the differences in fraction of time between the three age groups. Significant differences in fraction of time were found

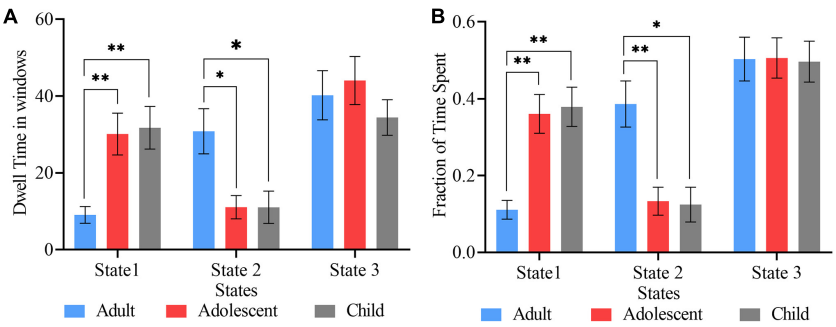

FIGURE 4 | State vectors for temporal analysis. **(A)** Mean dwell times in the three cluster states. **(B)** Fraction of time spent by each group in the three states. The blue, red, and ash bars represent adult, adolescent, and child ADHD patients, respectively. Asterisk indicates $P < 0.05$, FDR corrected and two asterisks indicate $P < 0.001$, FDR corrected.

between adult and adolescent, and adult and child pairs in only states 1 and 2 (FDR corrected). There was no significant fraction of time difference between adolescent and child ADHD pair in any of the three cluster states.

The average transition matrices and transition probabilities of each age group are shown in **Figure 5**, which represent the probability of changing from one state to the other. The red squares along the main diagonals represent a high probability of staying in a particular state, hence, the deeper the red square, the higher the probability of staying in a particular state. The blue squares represent the probability of moving between states, hence, the lighter the blue square, the higher the probability for subjects to move between states. The light blue square in the column of state 2 and the row of state 3 (**Figure 5A**), indicates a high probability of adult subjects moving between these two states, which is evident in the adult mean dwell time and fraction of time spent in these two states. Likewise, adolescent and child patients have high probabilities of moving between states 1 and 3 (**Figures 5B,C**), which is evident in the mean dwell time and the fraction of time they spent in these two states.

The total frequency of transitions from other states into a particular state (referred to as degree-in) (**Figure 6A**) and the total frequency of transitions from a particular state into other states (referred to as degree-out) (**Figure 6B**) was calculated for the three groups in all three states and two-sample *t*-tests were used to determine the differences between the three groups. Significant degree-in differences were found between adult and adolescent, and adult and child pairs in state 1 ($P < 0.05$, FDR corrected), whiles state 2 shows significant differences between only adult and child pair ($P < 0.001$, FDR corrected) (**Figure 6A**). However, both states 1 and 2 showed significant degree-out differences between adult and adolescent, and adult and child ADHD pairs (**Figure 6B**). No significant differences were found between adolescent and child ADHD patients in both degree-in and degree-out.

Correlation Analyses

Correlation analyses were performed to determine the impact of age, overall ADHD severity, hyperactivity severity, and inattentive severity on fraction of time and mean dwell time for each age group in each cluster state using gender and age as covariates. No significant correlations were found between fractions of time and mean dwell time for the above-mentioned measures in all three states in adult ADHD patients. A significant positive correlation was found between overall disease severity and fraction of time in state 2 in the child group (**Figure 7A**). In the adolescent group, mean dwell time in state 1 was positively correlated with overall disease severity and hyperactivity severity (**Figures 7B,D**), whiles faction of time in this same state was positively correlated with only hyperactivity severity (**Figure 7C**).

DISCUSSION

In this study, we investigated time-varying network connectivity patterns and network disruptions in child, adolescent, and adult ADHD patients using ICA, sliding windows, and K-means clustering. Our analysis revealed the following results: (1) unique state network alterations between the resting-state networks were found in all the three groups of ADHD patients with disruption occurring mainly in lower-order functional networks including SMN, AUD, VN, and CBN, while higher-order networks (DMN, SN, CEN, and FPN) showed rather sparse and low connectivity; (2) changes in state vectors as a measure of dynamic changes were obtained for the three groups including mean dwell time, fraction of time spent, number of transitions across states, and total transition measure by the degree in and out of state; (3) mean dwell time was positively correlated with overall disease severity and hyperactivity severity in only the adolescent group, whiles fraction of time was positively correlated with overall severity in the child group and hyperactivity severity in the adolescent group.

To the best of our knowledge, our work is the first to explore dFNC of the three ADHD age groups, adding to the increasing literature on the evidence of dFNC (Chang and Glover, 2010; Sakoğlu et al., 2010; Allen et al., 2014; Damaraju et al., 2014; Rashid et al., 2014; Klugah-Brown et al., 2019) and how it can capture disruption among ADHD patient across different age ranges. The implications of functional interconnections between resting-state networks have gained full attention over the years

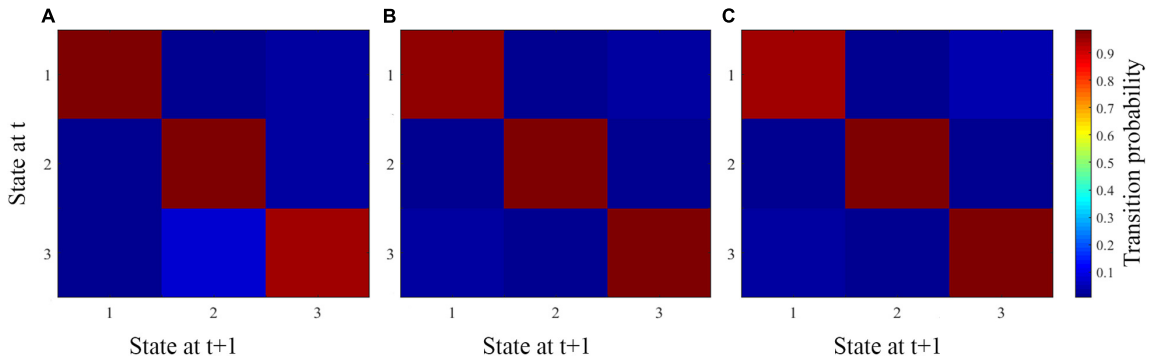

FIGURE 5 | The average transition matrix and transition probabilities of each age group. **(A–C)** Represent the average matrix for adult, adolescent, and child ADHD patients, respectively.

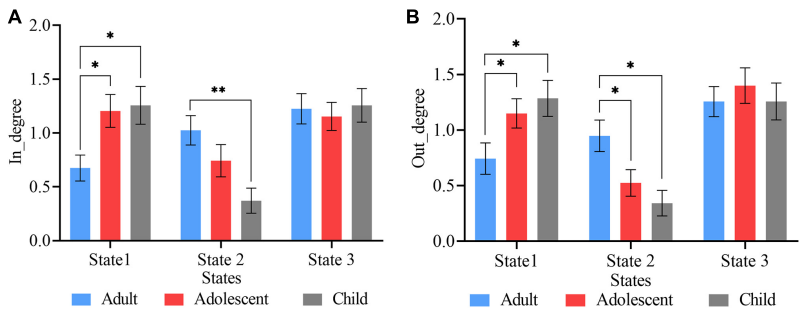

FIGURE 6 | State vectors degree of transitions. **(A)** Frequency of transitions into each state. State 1 showed significant differences in both adult vs. adolescent, and adult vs. child pairs, whereas, state 2 showed significant differences between only adult vs. child ADHD patients. **(B)** Frequency of transitions out of each state. States 1 and 2 showed significant differences between both adult vs. adolescent, and adult vs. child pairs. Asterisk indicates significant states ($p < 0.05$, FDR corrected), two asterisks indicate significant differences with threshold $p < 0.001$, FDR corrected.

and have become a robust tool to investigate brain disorders (find extensive review and meta-analysis in Cortese et al., 2021). However, these studies rely on the assumption that the FC derived static throughout scanning time. In contrast to this assumption, it's been since 2010 that the brain states are more dynamic across time and that a time-varying approach may provide a better view of this phenomenon (Chang and Glover, 2010; Sakoğlu et al., 2010), as well as being able to capture the dynamic connectivity patterns across time.

Three reoccurring states were found using K means clustering, and the connectivity patterns were relatively similar across the groups in all three states (**Supplementary Figure 3**). We observed varying connectivity patterns across states with each state exhibiting different occurrences denoted by a percentage of the total instances for all groups and subjects (**Figure 2**). The measurement taken over longer time windows summarize anatomical connectivity, which reflects RSNs. However, measurements taken over shorter window times accentuate the small departure from the RSN pattern, forming new functional networks from different nodes for a short period and then returning to the RSN pattern. Even though certain functional networks are often repeated in time, their exact organization or arrangement at a particular point depends on the part of the dynamic repertoire being explored (Deco et al., 2011), this results in the differences in the dynamic patterns of the three cluster states. The connectivity patterns within and between lower-order networks was in contrast with disruption expected suggested to occur within and between FPN and other higher-order networks in ADHD (Gao et al., 2019) networks including DMN, FPN, and CEN, this suggests that although altered differences occurred, it did not represent case-control patterns but rather reflected age-driven association among the ADHD groups. The higher-order networks on the contrary showed a rather weaker hyperconnectivity among the groups for all three states. The hyperconnectivity found within and between the SMN, VN, and AUD in the highly connected state 2, highly synchronous patterns were different, with generally more sparse connections in state 3 within the DMN, and between the DMN and FPN compared to state 2. The DMN which is involved in self-referencing and abrupt inattentiveness (Buckner et al., 2008; Fox et al., 2015; Bozhilova et al., 2018) exhibited weaker within and between connectivity is consistent with previous studies in ADHD reflected declining capacity to integrate within network activities similar to those found in case-control groups (Lin and Gau, 2015). In addition, the relatively low connectivity between the FPN and DMN resonates with Castellanos et al. (2008) study in which using resting-state fMRI they showed an anticorrelation between the above networks and suggested that the observed

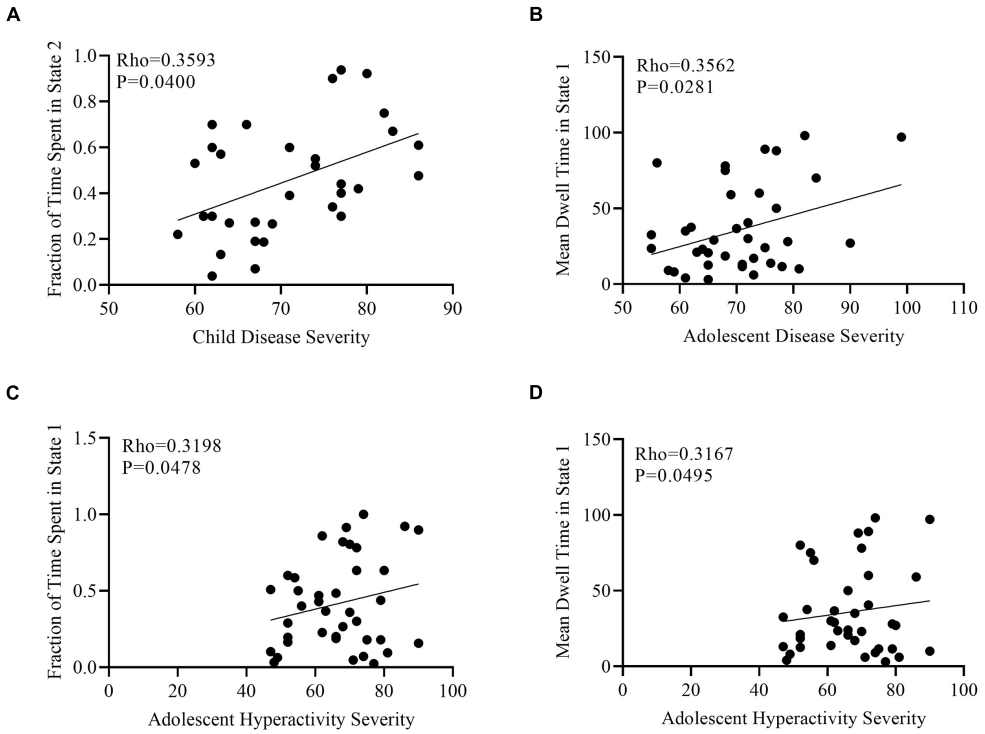

FIGURE 7 | Scatter plots of the correlation analyses. **(A)** Positive correlation between fraction of time spent in state 2 and child disease severity. **(B)** Positive correlation between mean dwell time in state 2 and adolescent disease severity. **(C)** Positive correlation between fraction of time spent in state 1 and adolescent hyperactivity severity. **(D)** Positive correlation between mean dwell time in state 1 and adolescent hyperactivity severity.

pattern reflected a decline in the attention processes in ADHD which is subserved by the higher-order network in FPN.

On the group comparing of the k-mean clusters and the group level connectivity difference, we found different state patterns peculiar to each group. **Supplementary Figure 3** shows the group-specific centroids indication the number of subjects contributing to each state. Following the clusters for each state, the group spatial group differences were generally hyperconnected, **Figure 3A** demonstrates two significant states between adolescents and child ADHD with increased connectivity between the DMN and CEN, SC, and SN. As indicated in the above paragraph, the inattention modulated by DMN is linked with the FPN, however, in both states, the connectivity with the CEN only re-echoed the control networks which are altered involving SN and SC. Inattention has been suggested to be increased in DMN with lower-order networks such as the SC in a task-based study (Oldehinkel et al., 2016) which is parallel with our result. **Figure 3B** shows connectivity differences between adult and child ADHD, in all three states we found the DMN hyperconnection with yet the lower-order networks including AUD and SMN, and also between the lower-order network (SC, VN), altered activation in the occipital regions and disconnections between the occipital cortex and frontal cortex in child and adolescent ADHD patients has been reported in previous studies (Mazaheri et al., 2010; Kröger et al., 2014). Disruptions of the VN have also been reported in ADHD patients (Benli et al., 2018), indicating that the VN plays an important role in ADHD. In state 2, the DMN connected with the FPN, AUD, and within the DMN, which is evident in the task-positive network relating to disrupted attention maintenance, and signifying inattention was revealed in the following review (Luman et al., 2010). Relative to adolescent ADHD patients, increased connectivity was found within the VN in adult ADHD patients. In state 3, Adult ADHD showed increased connectivity between the SMN and DMN relative to child ADHD patients. The connectivity pattern was similar to the state but had a widespread connection between the lower-order networks. Both DMN and FPN were also present, however, there was no connection between them, which is in contrast with the previous notion that these networks provided the core role in the attention and self-referential system in children and adolescents (Houck et al., 2011). For adults and adolescents, we also found all the three states were significant with less connectivity within each state, **Figure 3C**. All connections were in the low-order networks; AUD and VN, in states 1 and 2, respectively. State 3 expressing comparatively more connectivity and was between DMN and the lower-order networks. The phenomenon is similar to those found in the other age groups, however, adults compared to adolescents seem to have a less significant connection across all networks. This may suggest that the transition from adolescence to adulthood had little influence on the overall connectivity pattern in ADHD. In brief for the spatial connectivity difference between each pair of groups, the DMN representing a higher-order network was disrupted. Also,

FPN connectivity was most evident between the adolescent and children relative to adults and other groups. This pattern of connectivity suggests that DMN or self-referential modulated inattention in all groups. thus, the DMN has been reported to be disrupted in several ADHD studies (Cortese et al., 2012; Hart et al., 2013; Park et al., 2016; Qian et al., 2019), and significant connectivity differences across the three age groups found in the current study completed the previous studies.

In our state vector analysis, several temporal measures were captured across all states for each group. Firstly, both the dwell time and fraction of time showed significance between each pair of groups in states 1 and 2 except state 3 **Figure 4**, which reflected correspondence with the spatial results in which for each paired group the connectivity was more in tasks negative network (DMN) and signifies that mental state was not fully represented over all states. Similarly, the likelihood of transition among states showed a corresponding temporal pattern as shown in **Figure 5**. In addition, to further characterize the temporal dynamics with the disease scores, we performed a correlation between each score and the transition vectors. As displayed in **Figure 7**, the adolescent group disease severity and hyperactivity positively correlated with state 1 vectors (mean dwell time and a fraction of time spent), suggesting that duration of occupied state corresponded to disease, and as the mental state changes the severity increases. Also, child disease severity exhibited a positive relationship with the proportion of time spent in state 2. Adults group showed no significance for all measures across groups in each state. These finding implied that the disruption in children and adolescents were more prevalent and showed more dynamic relations relative to adults. Although not clear, we posit that adult ADHD is reduced, reflecting symptom decline in this age group (Katragadda and Schubiner, 2007; Volkow and Swanson, 2011; McCarthy et al., 2012).

Although we showed both temporal and spatial dFNC among the three groups, the result should be interpreted carefully. Firstly, the sample size was a limitation in this study, as connectivity tend to be more stable with an increasing number of participants, we were not able to investigate whether our relatively small sample influence the result presented, we suggest that future studies use larger sample sizes to determine the dFNC differences between the three ADHD age groups. Secondly, albeit the control of sex variable in the individual group analysis, the male to female ratio in the adult dataset was not the same as relative to child and adolescent datasets, which may interfere with brain state, future studies may consider recruiting more samples to include balanced sex ratio.

In sum, this study investigated the temporal and spatial dynamics of ADHD patients. Nine networks were identified using group ICA. Higher-order networks including the DMN and FPN and lower-order networks comprising the SMN, VN, and AUD were frequently distributed across all states and were connected within and between networks. We also found significant differences in measures such as mean dwell time, fraction of time, degree-in, and degree-out among the three age groups. Generally, all groups did not make full significant temporal transitions, only states 1 and 2 exhibited dynamic variability among the three groups. Our findings imply abnormal dynamic interactions and disconnectivity associated with ADHD. However, these abnormalities differ between the three ADHD age groups, especially when compared between child/adolescent and adults. Overall, the current work highlighted the dynamic properties of the brain captured through sliding window correlations. Furthermore, given the dFNC differences among the three groups, our work provides new insights into the mechanism subserved by age difference in the pathophysiology of ADHD and may set the grounds for future case-control studies in the individual age groups, as well as serving as a guide in the development of treatment strategies to target these specific networks in each age group.

DATA AVAILABILITY STATEMENT

The original contributions presented in the study are included in the article/**Supplementary Material**, further inquiries can be directed to the corresponding author/s.

ETHICS STATEMENT

Ethical review and approval was not required for the study on human participants in accordance with the local legislation and institutional requirements. Written informed consent to participate in this study was provided by the participants' legal guardian/next of kin.

AUTHOR CONTRIBUTIONS

EA, BK-B, and BB designed the study. EA organized the data and performed the analysis. EA, BK-B, and PW performed the statistical analysis. EA, BK-B, BB, HY, and SV reviewed the results. EA, BK-B, HY, and BN worked on the figures. EA and BK-B wrote the manuscript. All authors read, contributed to the revision of the manuscript, and approved the submitted version.

FUNDING

This work was supported by the National Natural Science Foundation of China (grant no. 61871420).

ACKNOWLEDGMENTS

We will like to acknowledge Ms. Lydia Fusieni for her advice and support. We will also like to acknowledge Mr. Chen Shuai, Dr. Chen Meng, and all members of the brain connectivity lab for their support.

SUPPLEMENTARY MATERIAL

The Supplementary Material for this article can be found online at: https://www.frontiersin.org/articles/10.3389/fnhum.2021.697696/full#supplementary-material

REFERENCES

Allen, E. A., Damaraju, E., Plis, S. M., Erhardt, E. B., Eichele, T., and Calhoun, V. D. (2014). Tracking whole-brain connectivity dynamics in the resting state. *Cereb. Cortex* 24, 663–676. doi: 10.1093/cercor/bhs352

Allen, E. A., Erhardt, E. B., Damaraju, E., Gruner, W., Segall, J. M., Silva, R. F., et al. (2011). A baseline for the multivariate comparison of resting-state networks. *Front. Syst. Neurosci.* 5:2. doi: 10.3389/fnsys.2011.00002

Allen, E. A., Erhardt, E. B., Wei, Y., Eichele, T., and Calhoun, V. D. (2012). Capturing inter-subject variability with group independent component analysis of fMRI data: A simulation study. *Neuroimage* 59, 4141–4159. doi: 10.1016/j.neuroimage.2011.10.010

Andrews-Hanna, J. R. (2012). The brain's default network and its adaptive role in internal mentation. *Neuroscientist* 18, 251–270. doi: 10.1177/1073858411403316

Ashburner, J. (2007). A fast diffeomorphic image registration algorithm. *Neuroimage* 38, 95–113. doi: 10.1016/j.neuroimage.2007.07.007

American Psychiatric Association. (2000). *Diagnostic and Statistical Manual of Mental Disorders. 4th text revision ed*. Washington, DC: American Psychiatric Association, 553–557.

Banerjee, O., El Ghaoui, L., and D'Aspremont, A. (2008). Model selection through sparse maximum likelihood estimation for multivariate Gaussian or binary data. *J. Mach. Learn. Res.* 9, 485–516. doi: 10.1145/1390681.1390696

Barbaresi, W. J., Katusic, S. K., Colligan, R. C., Shane Pankratz, V., Weaver, A. L., Weber, K. J., et al. (2002). How common is attention-deficit/hyperactivity disorder? Incidence in a population-based birth cohort in Rochester, Minn. *Arch. Pediatr. Adolesc. Med.* 156, 217–224. doi: 10.1001/archpedi.156.3.217

Benli, ŞG., Içer, S., and Ozmen, S. (2018). "Changes of Visual Networks at Resting State in Children with Attention Deficit Hyperactivity Disorder". in *2018 Medical Technologies National Congress. TIPTEKNO*. Magusa: IEEE. 1–4. doi: 10.1109/TIPTEKNO.2018.8597144

Bilder, R., Poldrack, R., Cannon, T., London, E., Freimer, N., Congdon, E., et al. (2016). *UCLA consortium for neuropsychiatric phenomics LA5c Study*. doi: 10.18112/openneuro.ds000030.v1.0.0

Biswal, B., Zerrin Yetkin, F., Haughton, V. M., and Hyde, J. S. (1995). Functional connectivity in the motor cortex of resting human brain using echo−planar mri. *Magn. Reson. Med.* 34, 537–541. doi: 10.1002/mrm.1910340409

Bos, D. J., Oranje, B., Achterberg, M., Vlaskamp, C., Ambrosino, S., de Reus, M. A., et al. (2017). Structural and functional connectivity in children and adolescents with and without attention deficit/hyperactivity disorder. *J. Child Psychol. Psychiatry Allied Discip.* 58, 810–818. doi: 10.1111/jcpp.12712

Bozhilova, N. S., Michelini, G., Kuntsi, J., and Asherson, P. (2018). Mind wandering perspective on attention-deficit/hyperactivity disorder. *Neurosci. Biobehav. Rev.* 92, 464–476. doi: 10.1016/j.neubiorev.2018.07.010

Buckner, R. L., Andrews-Hanna, J. R., and Schacter, D. L. (2008). The brain's default network: Anatomy, function, and relevance to disease. *Ann. N. Y. Acad. Sci.* 1124, 1–38. doi: 10.1196/annals.1440.011

Castellanos, F. X., Margulies, D. S., Kelly, C., Uddin, L. Q., Ghaffari, M., Kirsch, A., et al. (2008). Cingulate-precuneus interactions: a new locus of dysfunction in adult attention-deficit/hyperactivity disorder. *Biol. Psychiatry* 63, 332–337. doi: 10.1016/j.biopsych.2007.06.025

Chang, C., and Glover, G. H. (2010). Time-frequency dynamics of resting-state brain connectivity measured with fMRI. *Neuroimage* 50, 81–98. doi: 10.1016/j.neuroimage.2009.12.011

Cortese, S., Aoki, Y. Y., Itahashi, T., Castellanos, F. X., and Eickhoff, S. B. (2021). Systematic Review and Meta-analysis: resting-state functional magnetic resonance imaging studies of attention-deficit/hyperactivity disorder. *J. Am. Acad. Child Adolesc. Psychiatry* 60, 61–75. doi: 10.1016/j.jaac.2020.08.014

Cortese, S., Kelly, C., Chabernaud, C., Proal, E., Di Martino, A., Milham, M. P., et al. (2012). Toward systems neuroscience of ADHD: A meta-analysis of 55 fMRI sudies. *Am. J. Psychiatry* 169, 1031–1043. doi: 10.1176/appi.ajp.2012.11101521

Damaraju, E., Allen, E. A., Belger, A., Ford, J. M., McEwen, S., Mathalon, D. H., et al. (2014). Dynamic functional connectivity analysis reveals transient states of dysconnectivity in schizophrenia. *NeuroImage Clin.* 5, 298–308. doi: 10.1016/j.nicl.2014.07.003

Danielson, M. L., Bitsko, R. H., Ghandour, R. M., Holbrook, J. R., Kogan, M. D., and Blumberg, S. J. (2018). Prevalence of parent-reported adhd diagnosis and associated treatment among U.S. children and adolescents, 2016. *J. Clin. Child Adolesc. Psychol.* 47, 199–212. doi: 10.1080/15374416.2017.1417860

de Lacy, N., and Calhoun, V. D. (2018). Dynamic connectivity and the effects of maturation in youth with attention deficit hyperactivity disorder. *Netw. Neurosci.* 3, 195–216. doi: 10.1162/netn_a_00063

de Lacy, N., Doherty, D., King, B. H., Rachakonda, S., and Calhoun, V. D. (2017). Disruption to control network function correlates with altered dynamic connectivity in the wider autism spectrum. *NeuroImage Clin.* 15, 513–524. doi: 10.1016/j.nicl.2017.05.024

Deco, G., Jirsa, V. K., and McIntosh, A. R. (2011). Emerging concepts for the dynamical organization of resting-state activity in the brain. *Nat. Rev. Neurosci.* 12, 43–56. doi: 10.1038/nrn2961

Fox, K. C. R., Spreng, R. N., Ellamil, M., Andrews-Hanna, J. R., and Christoff, K. (2015). The wandering brain: Meta-analysis of functional neuroimaging studies of mind-wandering and related spontaneous thought processes. *Neuroimage* 111, 611–621. doi: 10.1016/j.neuroimage.2015.02.039

Fox, M. D., and Raichle, M. E. (2007). Spontaneous fluctuations in brain activity observed with functional magnetic resonance imaging. *Nat. Rev. Neurosci.* 8, 700–711. doi: 10.1038/nrn2201

Fox, M. D., Snyder, A. Z., Vincent, J. L., Corbetta, M., Van Essen, D. C., and Raichle, M. E. (2005). The human brain is intrinsically organized into dynamic, anticorrelated functional networks. *Proc. Natl. Acad. Sci. USA*. 102, 9673–9678. doi: 10.1073/pnas.0504136102

Francx, W., Oldehinkel, M., Oosterlaan, J., Heslenfeld, D., Hartman, C. A., Hoekstra, P. J., et al. (2015). The executive control network and symptomatic improvement in attention-deficit/hyperactivity disorder. *Cortex* 73, 62–72. doi: 10.1016/j.cortex.2015.08.012

Friedman, J., Hastie, T., and Tibshirani, R. (2008). Sparse inverse covariance estimation with the graphical lasso. *Biostatistics* 9, 432–441. doi: 10.1093/biostatistics/kxm045

Friston, K. J., Williams, S., Howard, R., Frackowiak, R. S. J., and Turner, R. (1996). Movement-related effects in fMRI time-series. *Magn. Reson. Med.* 35, 346–355. doi: 10.1002/mrm.1910350312

Gao, Y., Shuai, D., Bu, X., Hu, X., Tang, S., Zhang, L., et al. (2019). Impairments of large-scale functional networks in attention-deficit/hyperactivity disorder: A meta-analysis of resting-state functional connectivity. *Psychol. Med.* 49, 2475–2485. doi: 10.1017/S003329171900237X

Gimpel, G. A., and Kuhn, B. R. (2000). Maternal report of attention deficit hyperactivity disorder symptoms in preschool children. *Child. Care. Health Dev.* 26, 163–176. doi: 10.1046/j.1365-2214.2000.00126.x

Greicius, M. D., Krasnow, B., Reiss, A. L., and Menon, V. (2003). Functional connectivity in the resting brain: A network analysis of the default mode hypothesis. *Proc. Natl. Acad. Sci. USA*. 100, 253–258. doi: 10.1073/pnas.0135058100

Hart, H., Radua, J., Mataix-Cols, D., and Rubia, K. (2012). Meta-analysis of fMRI studies of timing in attention-deficit hyperactivity disorder (ADHD). *Neurosci. Biobehav. Rev.* 36, 2248–2256. doi: 10.1016/j.neubiorev.2012.08.003

Hart, H., Radua, J., Nakao, T., Mataix-Cols, D., and Rubia, K. (2013). Meta-analysis of functional magnetic resonance imaging studies of inhibition and attention in attention-deficit/hyperactivity disorder: Exploring task-specific, stimulant medication, and age effects. *JAMA Psychiatry* 70, 185–198. doi: 10.1001/jamapsychiatry.2013.277

Himberg, J., Hyvärinen, A., and Esposito, F. (2004). Validating the independent components of neuroimaging time series via clustering and visualization. *Neuroimage* 22, 1214–1222. doi: 10.1016/j.neuroimage.2004.03.027

Hong, J., Park, B. Y., Cho, H. H., and Park, H. (2017). Age-related connectivity differences between attention deficit and hyperactivity disorder patients and typically developing subjects: A resting-state functional MRI study. *Neural Regen. Res.* 12, 1640–1647. doi: 10.4103/1673-5374.217339

Houck, G., Kendall, J., Miller, A., Morrell, P., and Wiebe, G. (2011). Self-Concept in children and adolescents with attention deficit hyperactivity disorder. *J. Pediatr. Nurs.* 26, 239–247. doi: 10.1016/j.pedn.2010.02.004

Katragadda, S., and Schubiner, H. (2007). ADHD in children. Adolescents, and Adults. *Prim. Care Clin. Pract.* 34, 317–341. doi: 10.1016/j.pop.2007.04.012

Kessler, R. C., Adler, L., Berkley, R., Biederman, J., Conners, C. K., Demler, O., et al. (2006). The prevalence and correlates of adult ADHD in the United States: results from the national comorbidity survey replication. *Am. J. Psychiatry* 163, 716–723. doi: 10.1176/ajp.2006.163.4.716

Khundrakpam, B. S., Lewis, J. D., Zhao, L., Chouinard-Decorte, F., and Evans, A. C. (2016). Brain connectivity in normally developing children and adolescents. *Neuroimage* 134, 192–203. doi: 10.1016/j.neuroimage.2016.03.062

Klugah-Brown, B., Luo, C., He, H., Jiang, S., Armah, G. K., Wu, Y., et al. (2019). Altered dynamic functional network connectivity in frontal lobe epilepsy. *Brain Topogr.* 32, 394–404. doi: 10.1007/s10548-018-0678-z

Kröger, A., Hof, K., Krick, C., Siniatchkin, M., Jarczok, T., Freitag, C. M., et al. (2014). Visual processing of biological motion in children and adolescents with attention-deficit/hyperactivity disorder: An event related potential-study. *PLoS One* 9:e88585. doi: 10.1371/journal.pone.0088585

Li, Y. O., Adali, T., and Calhoun, V. D. (2007). Estimating the number of independent components for functional magnetic resonance imaging data. *Hum. Brain Mapp.* 28, 1251–1266. doi: 10.1002/hbm.20359

Lin, H. Y., and Gau, S. S. F. (2015). Atomoxetine treatment strengthens an anti-correlated relationship between functional brain networks in medication-naïve adults with attention-deficit hyperactivity disorder: a randomized double-blind placebo-controlled clinical trial. *Int. J. Neuropsychopharmacol.* 19, 1–15. doi: 10.1093/ijnp/pyv094

Luman, M., Tripp, G., and Scheres, A. (2010). Identifying the neurobiology of altered reinforcement sensitivity in ADHD: a review and research agenda. *Neurosci. Biobehav. Rev.* 34, 744–754. doi: 10.1016/j.neubiorev.2009.11.021

Mazaheri, A., Coffey-Corina, S., Mangun, G. R., Bekker, E. M., Berry, A. S., and Corbett, B. A. (2010). Functional disconnection of frontal cortex and visual cortex in attention-deficit/hyperactivity disorder. *Biol. Psychiatry* 67, 617–623. doi: 10.1016/j.biopsych.2009.11.022

McCarthy, S., Wilton, L., Murray, M. L., Hodgkins, P., Asherson, P., and Wong, I. C. K. (2012). The epidemiology of pharmacologically treated attention deficit hyperactivity disorder (ADHD) in children, adolescents and adults in UK primary care. *BMC Pediatr.* 12:78. doi: 10.1186/1471-2431-12-78

Meinshausen, N., and Bühlmann, P. (2006). High-dimensional graphs and variable selection with the Lasso. *Ann. Stat.* 34, 1436–1462. doi: 10.1214/009053606000000281

Meunier, D., Lambiotte, R., Fornito, A., Ersche, K. D., and Bullmore, E. T. (2009). Hierarchical modularity in human brain functional networks. *Front. Neuroinform.* 3:37. doi: 10.3389/neuro.11.037.2009

Oldehinkel, M., Beckmann, C. F., Franke, B., Hartman, C. A., Hoekstra, P. J., Oosterlaan, J., et al. (2016). Functional connectivity in cortico-subcortical brain networks underlying reward processing in attention-deficit/hyperactivity disorder. *NeuroImage Clin.* 12, 796–805. doi: 10.1016/j.nicl.2016.10.006

Park, B. Y., Kim, J., and Park, H. (2016). "Differences in connectivity patterns between child and adolescent attention deficit hyperactivity disorder patients". in *Proceedings of the Annual International Conference of the IEEE Engineering in Medicine and Biology Society. EMBS*. Manhattan N.Y: IEEE. 1127–1130. doi: 10.1109/EMBC.2016.7590902

Ptak, R. (2012). The frontoparietal attention network of the human brain: Action, saliency, and a priority map of the environment. *Neuroscientist* 18, 502–515. doi: 10.1177/1073858411409051

Qian, X., Castellanos, F. X., Uddin, L. Q., Loo, B. R. Y., Liu, S., Koh, H. L., et al. (2019). Large-scale brain functional network topology disruptions underlie symptom heterogeneity in children with attention-deficit/hyperactivity disorder. *NeuroImage Clin.* 21:101600. doi: 10.1016/j.nicl.2018.11.010

Raichle, M. E. (2006). Neuroscience: the brain's dark energy. *Science* 314, 1249–1250. doi: 10.1126/science.1134405

Raichle, M. E., MacLeod, A. M., Snyder, A. Z., Powers, W. J., Gusnard, D. A., and Shulman, G. L. (2001). A default mode of brain function. *Proc. Natl. Acad. Sci. USA.* 98, 676–682. doi: 10.1073/pnas.98.2.676

Rashid, B., Damaraju, E., Pearlson, G. D., and Calhoun, V. D. (2014). Dynamic connectivity states estimated from resting fMRI Identify differences among Schizophrenia, bipolar disorder, and healthy control subjects. *Front. Hum. Neurosci.* 8:897. doi: 10.3389/fnhum.2014.00897

Sakoğlu, U., Pearlson, G. D., Kiehl, K. A., Wang, Y. M., Michael, A. M., and Calhoun, V. D. (2010). A method for evaluating dynamic functional network connectivity and task-modulation: Application to schizophrenia. *MAGMA* 23, 351–366. doi: 10.1007/s10334-010-0197-8

Sanfratello, L., Houck, J. M., and Calhoun, V. D. (2019). Dynamic functional network connectivity in schizophrenia with magnetoencephalography and functional magnetic resonance imaging: do different timescales tell a different story? *Brain Connect.* 9, 251–262. doi: 10.1089/brain.2018.0608

Sidlauskaite, J., Sonuga-Barke, E., Roeyers, H., and Wiersema, J. R. (2016). Altered intrinsic organisation of brain networks implicated in attentional processes in adult attention-deficit/hyperactivity disorder: a resting-state study of attention, default mode and salience network connectivity. *Eur. Arch. Psychiatry Clin. Neurosci.* 266, 349–357. doi: 10.1007/s00406-015-0630-0

Stark, C. E. L., and Squire, L. R. (2001). When zero is not zero: The problem of ambiguous baseline conditions in fMRI. *Proc. Natl. Acad. Sci. USA*. 98, 12760–12766. doi: 10.1073/pnas.221462998

Volkow, N. D., and Swanson, J. M. (2011). Adult attention deficit hyperactivity disorder. *J. Mens Health* 8, 299–305. doi: 10.1016/j.jomh.2011.08.001

Wolraich, M., Brown, L., Brown, R. T., DuPaul, G., Earls, M., Feldman, H. M., et al. (2011). ADHD: Clinical practice guideline for the diagnosis, evaluation, and treatment of attention-deficit/ hyperactivity disorder in children and adolescents. *Pediatrics* 128, 1007–1022. doi: 10.1542/peds.2011-2654

Yan, C. G., Wang, X., Di Zuo, X. N., and Zang, Y. F. (2016). DPABI: data processing & analysis for (resting-state) brain imaging. *Neuroinformatics* 14, 339–351. doi: 10.1007/s12021-016-9299-4

Yuan, M., and Lin, Y. (2007). Model selection and estimation in the Gaussian graphical model. *Biometrika* 94, 19–35. doi: 10.1093/biomet/asm018

Zhao, Q., Li, H., Yu, X., Huang, F., Wang, Y., Liu, L., et al. (2017). Abnormal resting-state functional connectivity of insular subregions and disrupted correlation with working memory in adults with attention deficit/hyperactivity disorder. *Front. Psychiatry* 8:200. doi: 10.3389/fpsyt.2017.00200

Zhou, Z. W., Fang, Y. T., Lan, X. Q., Sun, L., Cao, Q. J., Wang, Y. F., et al. (2019). Inconsistency in abnormal functional connectivity across datasets of ADHD-200 in children with attention deficit hyperactivity disorder. *Front. Psychiatry* 10:692. doi: 10.3389/fpsyt.2019.00692

Conflict of Interest: The authors declare that the research was conducted in the absence of any commercial or financial relationships that could be construed as a potential conflict of interest.

Publisher's Note: All claims expressed in this article are solely those of the authors and do not necessarily represent those of their affiliated organizations, or those of the publisher, the editors and the reviewers. Any product that may be evaluated in this article, or claim that may be made by its manufacturer, is not guaranteed or endorsed by the publisher.

frontiers in Human Neuroscience

ORIGINAL RESEARCH
published: 21 October 2021
doi: 10.3389/fnhum.2021.777043

The Association Between Lentiform Nucleus Function and Cognitive Impairments in Schizophrenia

Ping Li[1], Shu-Wan Zhao[2], Xu-Sha Wu[2], Ya-Juan Zhang[3], Lei Song[3], Lin Wu[3], Xiao-Fan Liu[2], Yu-Fei Fu[2], Di Wu[4], Wen-Jun Wu[4], Ya-Hong Zhang[4], Hong Yin[2], Long-Biao Cui[3,5] and Fan Guo[2]**

[1] Medical Imaging Department 1, Xi'an Mental Health Center, Xi'an, China, [2] Department of Radiology, Xijing Hospital, The Fourth Military Medical University, Xi'an, China, [3] Department of Clinical Psychology, School of Medical Psychology, The Fourth Military Medical University, Xi'an, China, [4] Department of Psychiatry, Xijing Hospital, The Fourth Military Medical University, Xi'an, China, [5] Department of Radiology, The Second Medical Center, Chinese PLA General Hospital, Beijing, China

OPEN ACCESS

Edited by:
Mingrui Xia,
Beijing Normal University, China

Reviewed by:
Teng Xie,
Peking University Sixth Hospital, China
Xinyu Hu,
Sichuan University, China
Xiao Chang,
King's College London, United Kingdom

***Correspondence:**
Long-Biao Cui
lbcui@fmmu.edu.cn
orcid.org/0000-0002-0784-181X
Fan Guo
guofan0602@hotmail.com

Specialty section:
This article was submitted to Brain Imaging and Stimulation, a section of the journal Frontiers in Human Neuroscience

Received: 14 September 2021
Accepted: 29 September 2021
Published: 21 October 2021

Citation:
Li P, Zhao S-W, Wu X-S, Zhang Y-J, Song L, Wu L, Liu X-F, Fu Y-F, Wu D, Wu W-J, Zhang Y-H, Yin H, Cui L-B and Guo F (2021) The Association Between Lentiform Nucleus Function and Cognitive Impairments in Schizophrenia. Front. Hum. Neurosci. 15:777043. doi: 10.3389/fnhum.2021.777043

Introduction: Cognitive decline is the core schizophrenia symptom, which is now well accepted. Holding a role in various aspects of cognition, lentiform nucleus (putamen and globus pallidus) dysfunction contributes to the psychopathology of this disease. However, the effects of lentiform nucleus function on cognitive impairments in schizophrenia are yet to be investigated.

Objectives: We aim to detect the fractional amplitude of low-frequency fluctuation (fALFF) alterations in patients with schizophrenia, and examine how their behavior correlates in relation to the cognitive impairments of the patients.

Methods: All participants underwent magnetic resonance imaging (MRI) and cognitive assessment (digit span and digit symbol coding tests). Screening of brain regions with significant changes in fALFF values was based on analysis of the whole brain. The data were analyzed between Jun 2020 and Mar 2021. There were no interventions beyond the routine therapy determined by their clinicians on the basis of standard clinical practice.

Results: There were 136 patients (75 men and 61 women, 24.1 ± 7.4 years old) and 146 healthy controls (82 men and 64 women, 24.2 ± 5.2 years old) involved in the experiments seriatim. Patients with schizophrenia exhibited decreased raw scores in cognitive tests ($p < 0.001$) and increased fALFF in the bilateral lentiform nuclei (left: 67 voxels; x = −24, y = −6, z = 3; peak t-value = 6.90; right: 16 voxels; x = 18, y = 0, z = 3; peak t-value = 6.36). The fALFF values in the bilateral lentiform nuclei were positively correlated with digit span-backward test scores (left: $r = 0.193$, $p = 0.027$; right: $r = 0.190$, $p = 0.030$), and the right lentiform nucleus was positively correlated with digit symbol coding scores ($r = 0.209$, $p = 0.016$).

Conclusion: This study demonstrates that cognitive impairments in schizophrenia are associated with lentiform nucleus function as revealed by MRI, involving working memory and processing speed.

Keywords: schizophrenia, lentiform nucleus, cognition, magnetic resonance imaging, phenotype

INTRODUCTION

Schizophrenia is a chronic mental illness affecting more than 20 million people all over the world (James et al., 2018). In schizophrenia, cognitive decline is a phenomenon related to the disorder. Schizophrenia has been considered to be a cognitive illness (Kahn and Keefe, 2013), in which cognitive decline is the core symptom (Kahn, 2019). Most recent longitudinal studies have shown 10- and 20-year progressive decline in cognitive functioning in patients with schizophrenia and other psychotic disorders (Zanelli et al., 2019; Fett et al., 2020). Cognitive function is impaired across almost all domains (Kern et al., 2011; Georgiades et al., 2017; Zhang et al., 2019) and contributes substantially to the long-term outcome associated with schizophrenia (Lepage et al., 2014; Mucci et al., 2021), highlighting cognitive symptoms as important targets for treatment.

Previous studies have demonstrated that patients with first-episode schizophrenia showed cognitive deficits across all cognitive domains, particularly in processing speed (Kern et al., 2011; Georgiades et al., 2017; Zhang et al., 2019). Working memory is the impaired cognitive domain that enters most frequently in the second position (Kern et al., 2011; Georgiades et al., 2017), and it is a neurocognitive impairment that differs between first-episode and chronic schizophrenia (McCleery et al., 2014). Taken together, we selected digit span (working memory) and digit symbol coding tests (processing speed) in this study. Taking the dysconnection hypothesis (Friston et al., 2016) and the therapeutic value of neuromodulation (Guan et al., 2020; Xiu et al., 2020) into consideration, neuroimaging study is urgently needed. However, the underlying brain structural and functional mechanisms for the cognitive symptoms remain to be identified (McCutcheon et al., 2020).

As a part of the basal ganglia, the lentiform nucleus (LN) is a lens-shaped, bilateral structure in the basal ganglia bounded by the internal and external capsules and has three components: the internal and external globus pallidus and the putamen (Hibar et al., 2013). The LN is implicated in several degenerative and psychiatric disorders (Obeso et al., 2000; Ellison-Wright et al., 2008). The housing of dopaminergic neurons in the LN explains its involvement in the neuropathology of schizophrenia, as a dopaminergic disorder (Brisch et al., 2014). Basal ganglia dysfunction has been suggested to be involved in the cognitive impairments of schizophrenia, as the dysfunction of cortical, striatal, and thalamocortical dopamine signaling circuits could lead to cognitive deficits (Simpson et al., 2010; Krabbe et al., 2015). Although the studies have suggested that the LN might be functionally linked to cognitive function in schizophrenia including attention, working memory, reward, and executive functions (Vatansever et al., 2016), the direct evidence remains unclear and has yet to be determined, especially in *in vivo* study with patients.

Magnetic resonance imaging (MRI) techniques provide promising tools to allow for exploring neural underpinnings behind this disease. Among these studies, the basal ganglia attracted particular attention, as it seems to be associated not only with the clinical manifestation of the disease but also cognitive information processing (Delvecchio et al., 2018). Previous studies prefer to focus on the structural changes of the LN area, but a few studies have shown a significant correlation between subcortical regions of interest in function (Luo et al., 2018; Fan et al., 2019; Tikasz et al., 2019). Hartberg et al. (2011) have proved that there is a negative correlation between putamen volume and verbal memory in patients with schizophrenia. Previous studies have been focused on either the functional striatal abnormalities instead of LN function in schizophrenia patients or exploring the correlation between striatal structural changes and working memory function. Further studies are needed to show the direct relationship between LN and cognitive function in schizophrenia patients.

Both the amplitude of low frequency fluctuations (ALFF) and the fraction amplitude of low frequency fluctuations (fALFF) can reflect the intensity of spontaneous activity in brain areas. The fALFF is a modified index of the ALFF, being less likely to produce any noise and more sensitive and specific to the detection of spontaneous brain activities in comparison to the ALFF (Chai et al., 2020). Many studies have found that the fALFF is associated with cognitive symptoms of schizophrenia (Fryer et al., 2015; Sui et al., 2015). A recent study, aimed to identify multimodal biomarkers for quantifying and predicting cognitive performance in individuals with schizophrenia and healthy controls, has found that fALFF features were more sensitive to cognitive domain differences (Sui et al., 2018).

Therefore, we aim to detect fALFF alterations in patients with schizophrenia. Specifically, given the involvement of the LN in the pathophysiology of schizophrenia, abnormal functioning of the LN can be strongly associated with the development of cognitive impairment. In the current study, we used the fALFF to determine the relevance of abnormal LN function on cognitive impairments in schizophrenia.

MATERIALS AND METHODS

Participants

This study was approved by the Institutional Ethics Committee, First Affiliated Hospital (Xijing Hospital) of the Fourth Military Medical University. Each participant gave written informed consent after receiving a complete description of this study. Between April 8, 2015 and June 18, 2020, 141 patients with schizophrenia were recruited from the Department of Psychiatry at Xijing Hospital. There were also 146 matched healthy controls, who were enrolled through advertising. The participants were diagnosed on the basis of the Diagnostic and Statistical Manual of Mental Disorders, Fifth Edition (DSM-5), and consensus diagnoses were made by two experienced clinical psychiatrists using all the available information. At the time of scanning, all the subjects underwent the Positive and Negative Syndrome Scale (PANSS) and cognitive assessment (digit span and digit symbol coding test). They were all right-handed, and their biological parents were of the Han Chinese ethnic group. The exclusion criteria for patients were as follows: (1) the presence of another psychiatric disorder; (2) a history of

repetitive transcranial magnetic stimulation, transcranial current stimulation, or behavioral treatment; (3) a history of clinically significant neurological, neurosurgical, or medical illnesses; (4) substance abuse within the prior 30 days or substance dependence within the prior 6 months; (5) pregnancy or any other MRI contraindications, e.g., cardiac pacemakers and other metallic implants; (6) unwillingness to undertake the scanning. Exclusion criteria for healthy controls were as follows: (1) the presence of any psychotic syndrome; (2) a history of receiving antipsychotics, repetitive transcranial magnetic stimulation, transcranial current stimulation, or behavioral treatment; the remaining (3), (4), (5), and (6) were the same as the exclusion criteria for patients.

Cognitive Assessment

We used the Wechsler Adult Intelligence Scale revised in China (WAIS-RC) to assess cognition by digit span (forward and backward) and digit symbol coding tests. For the forward digit span task, the subject was initially required to repeat a string of numbers after the researcher read them out. If the subject is able to repeat the string correctly, then they would be asked to proceed to the next string, which would have its length increased by one; if not, a second test would be conducted with a different string of digits of the same length. If the subject is correct, the test continues with a longer string, otherwise, the test stops and the length of the string is recorded. With the backward digit span test, the subjects were asked to repeat from the last number to the first after hearing a string of numbers, and the rest of the process was consistent with the forward test. In the digit symbol coding test, the subject is required to define 10 different symbols for 10 numbers from 0 to 9. The subject is asked to write the corresponding symbols under disordered numbers within 90 s, and the number of characters written correctly is recorded. Ultimately, digit symbol coding and digit span-forward data were available for 132 patients and 56 healthy controls. In addition, one patient rejected the digit span-backward test.

Image Acquisition

A General Electric (GE) Discovery MR750 3.0 T scanner was used to acquire images at the Department of Radiology at Xijing Hospital with a standard 8-channel head coil. A T1-weighted anatomical imaging (TR = 8.2 ms, TE = 3.2 ms, slice thickness = 1.0 mm, field of view [FOV] = 256 mm × 256 mm, matrix = 256 × 256, and flip angle = 12°) and resting-state functional MRI (TR = 2,000 ms, TE = 30 ms, slice thickness = 3.5 mm, FOV = 240 mm × 240 mm, matrix = 64 × 64, and flip angle = 90°) were performed. Further details about image acquisition are detailed in previous articles (Cui et al., 2019b; Liu et al., 2019). Participants were instructed to relax with their eyes closed but keep from falling asleep during their MRI scan.

Data Processing

The data processing was performed using the Data Processing Assistant for Resting-State fMRI Advanced Edition (DPARSFA) V4.4[1] with the previously published protocols (Cui et al., 2019a). First, the first 10 time points were discarded to ensure the stability of the magnetic field. Second, slice timing correction and realignment (subjects with maximum motion > 2 mm or 2° were excluded) were performed. Five patients were excluded from the study because of excessive head motion, resulting in 136 patients who were included in the following analysis. Third, the nuisance covariates that included six head motion parameters, cerebrospinal fluid signals, white matter signals, and global mean signals were regressed from the data as corrected values. Fourth, T1-weighted images were coregistered to the realigned functional images. Fifth, the coregistered images were normalized to Montreal Neurological Institute space and resampled to 3 mm × 3 mm × 3 mm voxels. Sixth, the volumes were smoothed with a Gaussian kernel (8 mm full-width half-maximum, FWHM).

Fractional Amplitude of Low Frequency Fluctuations Analysis

We used the ALFF for directly observing local field spontaneous neural activity (Logothetis et al., 2001). The ALFF values of the subjects were calculated using the DPARSFA V4.4 (see text footnote 1). The ALFF calculation was performed using previously published protocols (Cui et al., 2019a). Finally, a filtering band-pass (0.01–0.08 Hz) was performed after calculating the ALFF. To overcome the limits of the ALFF approach, a ratio of the power of each frequency at a low-frequency range to that of the entire frequency range, known as fALFF, was obtained for the following statistical analysis (Yang et al., 2018).

Statistical Analysis

For voxel-based comparison of the fALFF, a two-sample *t*-test in SPM12 software[2] was used to test the statistical significance between patients and controls. A $p < 0.05$ (FWE correction) with a cluster size of more than 15 was considered as the statistical significance for the fALFF analysis. The comparison of demographical data and correlation analyses were performed in the Statistical Product and Service Solutions (SPSS, version 22.0). Demographical characteristics (age, gender, and education) and Jenkinson's mean frame-wise displacement were regarded as covariates. A region of interest was created using the significant clusters of group comparison to extract the fALFF values. We used Pearson correlation coefficients to assess the clinical relevance between the fALFF value of the LN (putamen and globus pallidus) and cognitive capacity in patients (significance was set at $p < 0.05$).

[1] http://rfmri.org/DPARSF

[2] http://www.fil.ion.ucl.ac.uk/spm/software/spm12/

TABLE 1 | Demographical and clinical characteristics.

	Schizophrenia patients (n = 136)	Healthy controls (n = 146)	p-values
Age, y[a]	24.1 (7.4)	24.2 (5.2)	0.922
Gender, M/F[b]	75/61	82/64	0.864
Education, y[a]	12 (3)	15 (3)	<0.001
Status, FE/NFE	101/35	/	
Medication, U/T	27/109	/	
Illness duration, mon	14.7 (22.7)	/	
PANSS score		/	
Positive	21.7 (5.3)	/	
Negative	20.2 (7.3)	/	
General	43.7 (8.3)	/	
Total	85.6 (14.3)	/	

Data are shown in mean (standard deviation).
FE, first episode; NFE, non-first episode; U, untreated; T, treated.
[a]*Two-sample t-test.*
[b]*Pearson Chi-Square test.*

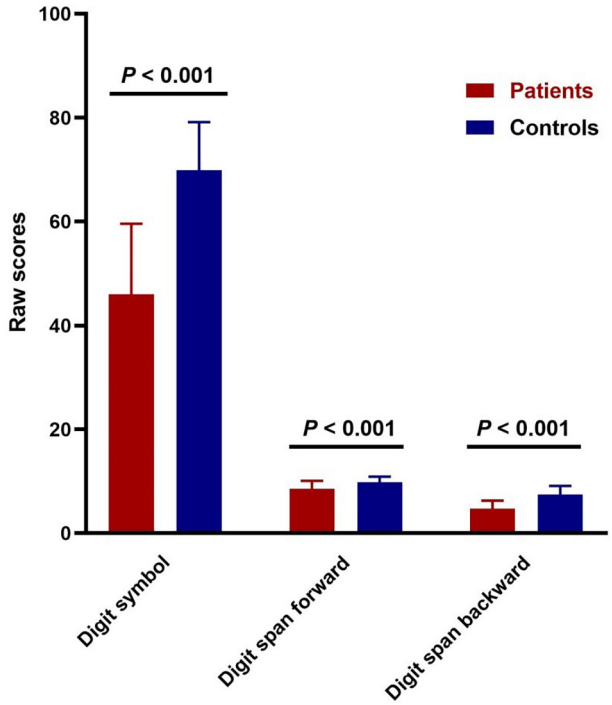

FIGURE 1 | Cognitive impairments in patients with schizophrenia. Comparison of digit symbol coding test (t = –13.985, p = 3.503E-29) and digit span raw scores (forward: t = –5.745, p = 4.7247E-8; backward: t = –10.225, p = 9.7559E-20) between patients and controls.

RESULTS

Demographical and Clinical Characteristics

Table 1 presents the demographic and clinical characteristics of the participants. Apart from the level of education, there was no statistically significant difference in other characteristics between patients and healthy controls.

Cognitive Impairments

The digit symbol coding and digit span-forward data for 132 patients and 56 controls were available. As for digit span-backward, there was one patient who refused to take the test. Two-sample t-testing showed significant differences in the cognitive tests (digit symbol coding, digit span-forward, and digit span-backward) between the two groups ($p < 0.001$; **Figure 1**).

Disrupted Fractional Amplitude of Low-Frequency Fluctuation

In the whole-brain analysis, the regions with altered fALFF values are shown in **Figure 2**. Briefly, schizophrenia patients exhibited increased fALFF in the left LN (67 voxels; x = −24, y = −6, z = 3; peak t-value = 6.90) and the right LN (16 voxels; x = 18, y = 0, z = 3; peak t-value = 6.36). The brain regions with decreased fALFF values included the right anterior occipital gyrus (36 voxels; x = 33, y = −84, z = −12; peak t-value = 6.42), left middle occipital gyrus (17 voxels; x = −30, y = −90, z = −3; peak t-value = 5.93), left superior occipital gyrus (16 voxels; x = −9, y = −90, z = 9; peak t-value = 5.83), and right lingual gyrus (20 voxels; x = 12, y = −84, z = −9; peak t-value = 5.55).

Correlation Between Fractional Amplitude of Low-Frequency Fluctuation and Cognitive Function

The fALFF values were extracted according to the mask of the bilateral LN (significant clusters of group comparison). We calculated the correlation between the cognitive scores and fALFF values in the LN of the patients and reported the (uncorrected) p-values because our hypothesis directly concerned these two selected regions of interest (**Figure 3**), as previously performed (Li et al., 2017). Considering that the scaled score tends to decrease the diversity of data, we used the raw score to present the subtle discrepancies among subjects (Xie et al., 2021). Correlation analysis showed that the digit span-backward test was positively correlated with the fALFF values (the left LN: r = 0.193, p = 0.027; the right LN: r = 0.190, p = 0.030). In addition, a positive correlation between the right LN and digit symbol coding was also demonstrated (r = 0.209, p = 0.016). However, when assessing the correlation between the digit span-forward test and the fALFF values of the LN, there was no significant association.

DISCUSSION

In the current study, we observed that patients and healthy controls had statistically significant differences in cognitive function. Schizophrenia patients exhibited increased fALFF in the bilateral LN. On the contrary, the brain regions with decreased fALFF included the bilateral occipital gyrus and the right lingual gyrus. Furthermore, the digit span-backward test was positively correlated with the fALFF values of the bilateral LN, and the fALFF values

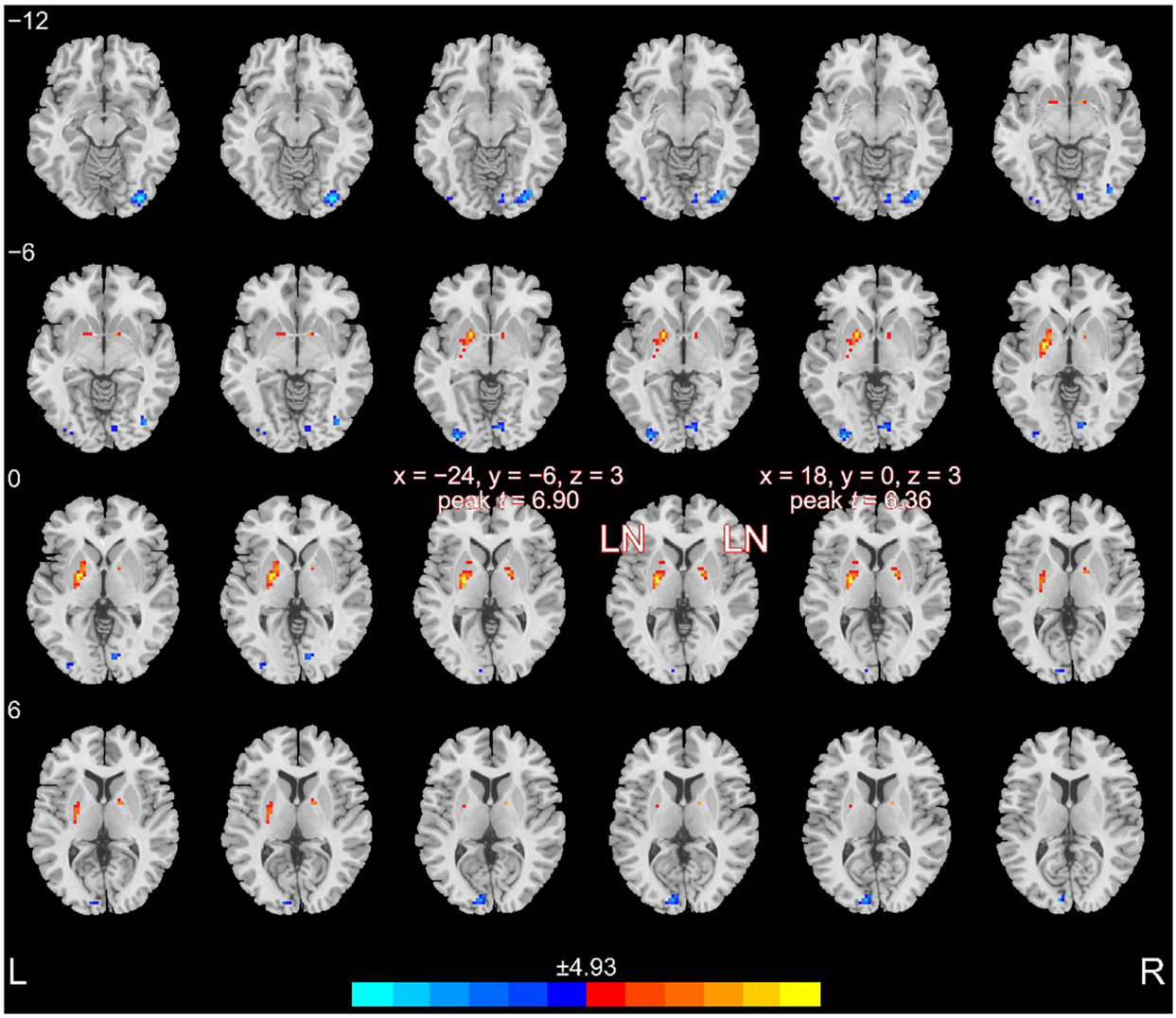

FIGURE 2 | Altered fALFF in patients compared to healthy controls. Patients with schizophrenia exhibited increased fALFF in the bilateral LN.

of the right LN were positively correlated with the digit symbol coding test.

Previous studies have shown that cognitive function is decreased in schizophrenia patients, including memory impairment, deficits in attention, and general cognition (Koshiyama et al., 2018). Although there are several neuropsychological tests for measuring processing speed impairment, which is the largest single deficit in cognitive function in schizophrenia, a meta-analysis has demonstrated that a digit symbol coding task is the most sensitive test to apply to patients with schizophrenia (Dickinson et al., 2007), and that it reflects processing speed. Moreover, digit span (forward and backward) could reflect the function of cognition especially with working memory (Conklin et al., 2000). It has been reported that memory impairment is a severe cognitive dysfunction in schizophrenia (Toulopoulou et al., 2003). Our study is consistent with previous studies showing the dysfunctional changes in cognitive function, especially in the memory of schizophrenia patients (Chen et al., 2016).

Among the different brain structures, the basal ganglia, as the subcortical nuclei rich in dopaminergic neurons, is an important structure for the neuropathology of schizophrenia, as a well-established dopaminergic disorder (Brisch et al., 2014). The basal ganglia are composed of the caudate nucleus, the LN (putamen and the globus pallidus), and the substantia nigra. The LN, as part of the basal ganglia, is not only important for the motor system but also plays a role in cognitive functions, including working memory, executive function, reward, and learning (Schroll et al., 2015). Dopamine is known to play a major part in regulating a number of cognitive functions that are impaired in schizophrenia, and research should now shift focus toward a better understanding of the role of specific striatal pathways in cognition (Conn et al., 2020;

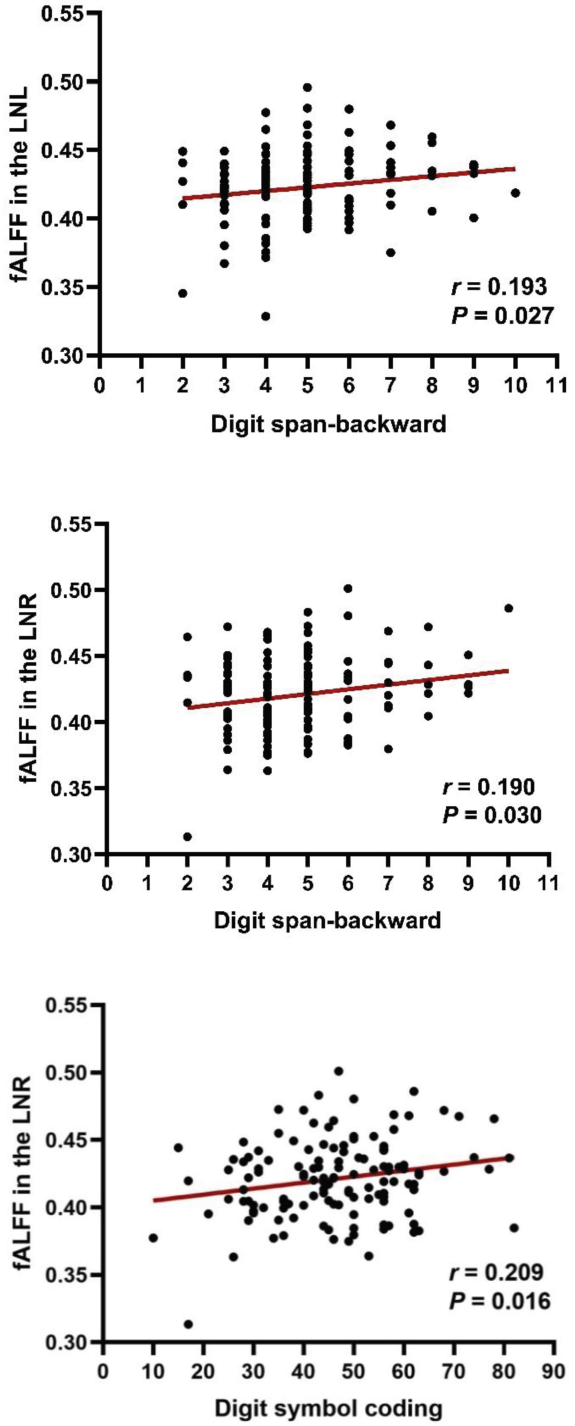

FIGURE 3 | Correlation between fALFF and cognitive impairments in patients with schizophrenia. Digit span-backward test and digit symbol coding were positively correlated with fALFF values in the LN. LNL, left LN; LNR, right LN.

Martel and Gatti McArthur, 2020). A recent study concluded that striatal dysfunction contributes to cognitive difficulties in schizophrenia, which is supported by previous histological and neuroimaging evidence (Avram et al., 2019). Many previous studies have focused on the structural changes of LN in schizophrenia (Luo et al., 2018; Takahashi et al., 2020). Hashimoto et al. (2009) showed that schizophrenia patients had significantly lower fractional anisotropy values in the bilateral globus pallidus and left thalamus compared to controls, suggesting that schizophrenics might have microstructural abnormalities in the globus pallidus and thalamus. However, the functional role of the LN and how it affects cognitive function remains largely unknown. Several similar studies have been focused on the basal ganglia but not on the LN. And some studies have focused on the symptoms assessed by PANSS but not on cognitive function. Therefore, the direct evidence remains unclear whether the LN is linked to certain cognitive functions and has yet to be determined, especially in *in vivo* studies with patients. The purpose of the present study was to provide this evidence.

One of the main results of our study showed increased fALFF in the bilateral LN. Gong et al. (2020) also showed increased ALFF in the LN in schizophrenia patients compared with healthy controls. Another previous study found that the ALFF increased in the parietal lobule and was correlated with decreased social cognition (Sui et al., 2015). Moreover, our result showed decreased fALFF in the bilateral occipital gyrus, which is consistent with a previous study, showing that the decreased fALFF were mainly in the posterior parietal cortex and occipital cortex (Xu et al., 2015). In addition, schizophrenia patients had greater thalamic connectivity with the occipital gyrus (Ferri et al., 2018). Furthermore, abnormal morphology of the occipital gyrus may be a marker of psychiatric illness (Maller et al., 2017). A pronounced decline in gray matter volume was observed in the bilateral occipital lobe in genetic high-risk individuals and first-episode schizophrenia patients (Zhao et al., 2018). Therefore, the regional functional changes of certain brain areas, especially in the LN, might be important brain neuroimaging markers for schizophrenia patients.

Another major result of our study was the correlation between the bilateral LN and the digit span-backward test. The LN, as part of the cortico-striato-thalamocortical circuits, is important for cognitive functions, especially the attention, working memory, reward, and executive functions (Rabinovici et al., 2015; Vatansever et al., 2016). As mentioned above, the digit span backward test could reflect the function of working memory. Our result indicated the LN is correlated with working memory. In previous schizophrenia studies, there have been reports of negative performance-related functional connectivity between the left putamen and the right ventrolateral prefrontal cortices (Quide et al., 2013). Our previous study also proved the importance of putamen in positive symptoms (Cui et al., 2016, 2017), and in disease identification and the treatment response prediction of schizophrenia (Cui et al., 2018, 2020). Thus, our results add to the importance of the LN in schizophrenia, especially in cognitive function. Of note, our

current results did not show a significant correlation between the digit span-forward test and the fALFF values of the LN. Our observation of the results may reflect the unique disease-related abnormalities of the LN.

Our study reflects some limitations. First, a previous study has demonstrated cognitive impairment in schizophrenia as a mediator to influence the association between negative symptoms and hippocampal morphometry (Duan et al., 2021). However, our study only focused on the relationship between the fALFF of the LN and cognitive impairments, and we were not able to answer how the LN contributes to cognitive impairments in schizophrenia. Further MRI-guidance and navigation studies combined with neuromodulation will be needed for answering this question (Wu et al., 2021). Second, antipsychotic treatments modify abnormal cerebral function in schizophrenia (Duan et al., 2020), but the effects of medication and whether the other cognitive function was affected were not investigated in the current study.

CONCLUSION

In conclusion, the present investigation found the association between increased fALFF values in the bilateral LN and cognitive performance in schizophrenia patients. These findings may contribute to our understanding of the LN in schizophrenia and shed light on the development of psychological strategies to improve cognitive function *via* the new target.

DATA AVAILABILITY STATEMENT

The original contributions presented in the study are included in the article/supplementary material, further inquiries can be directed to the corresponding author/s.

ETHICS STATEMENT

The studies involving human participants were reviewed and approved by the Medical Ethics Committee of the First Affiliated Hospital of the Fourth Military Medical University. The patients/participants provided their written informed consent to participate in this study.

AUTHOR CONTRIBUTIONS

FG and L-BC conceptualized the manuscript. PL, FG, and L-BC designed the study, wrote the first draft of the manuscript, and conducted the statistical analyses. S-WZ, X-SW, Y-JZ, LS, LW, X-FL, Y-FF, DW, W-JW, and Y-HZ collected and organized the primary data. L-BC and FG provided supervision in the implementation of the study. All authors provided feedback and revised the manuscript.

FUNDING

L-BC was supported by the grant support of the Fourth Military Medical University (2019CYJH) and the Project funded by the China Postdoctoral Science Foundation (2019TQ0130).

ACKNOWLEDGMENTS

We thank an English teaching professional, Mr. Pengfei Wu, for his kind help to edit and proofread the manuscript.

REFERENCES

Avram, M., Brandl, F., Cabello, J., Leucht, C., Scherr, M., Mustafa, M., et al. (2019). Reduced striatal dopamine synthesis capacity in patients with schizophrenia during remission of positive symptoms. *Brain* 142, 1813–1826. doi: 10.1093/brain/awz093

Brisch, R., Saniotis, A., Wolf, R., Bielau, H., Bernstein, H. G., Steiner, J., et al. (2014). The role of dopamine in schizophrenia from a neurobiological and evolutionary perspective: old fashioned, but still in vogue. *Front. Psychiatry* 5:47. doi: 10.3389/fpsyt.2014.00047

Chai, X., Zhang, R., Xue, C., Li, Z., Xiao, W., Huang, Q., et al. (2020). Altered patterns of the fractional amplitude of low-frequency fluctuation in drug-naive first-episode unipolar and bipolar depression. *Front. Psychiatry* 11:587803. doi: 10.3389/fpsyt.2020.587803

Chen, X. J., Wang, Y., Wang, Y., Yang, T. X., Zou, L. Q., Huang, J., et al. (2016). Neural correlates of prospective memory impairments in schizophrenia. *Neuropsychology* 30, 169–180. doi: 10.1037/neu0000225

Conklin, H. M., Curtis, C. E., Katsanis, J., and Iacono, W. G. (2000). Verbal working memory impairment in schizophrenia patients and their first-degree relatives: evidence from the digit span task. *Am. J. Psychiatry* 157, 275–277. doi: 10.1176/appi.ajp.157.2.275

Conn, K.-A., Burne, T. H. J., and Kesby, J. P. (2020). Subcortical dopamine and cognition in schizophrenia: looking beyond psychosis in preclinical models. *Front. Neurosci.* 14:542. doi: 10.3389/fnins.2020.00542

Cui, L. B., Wei, Y., Xi, Y. B., Griffa, A., De Lange, S. C., Kahn, R. S., et al. (2019b). Connectome-based patterns of first-episode medication-naive patients with schizophrenia. *Schizophr. Bull.* 45, 1291–1299. doi: 10.1093/schbul/sbz014

Cui, L. B., Cai, M., Wang, X. R., Zhu, Y. Q., Wang, L. X., Xi, Y. B., et al. (2019a). Prediction of early response to overall treatment for schizophrenia: a functional magnetic resonance imaging study. *Brain Behav.* 9:e01211. doi: 10.1002/brb3.1211

Cui, L. B., Fu, Y. F., Liu, L., Wu, X. S., Xi, Y. B., Wang, H. N., et al. (2020). Baseline structural and functional magnetic resonance imaging predicts early treatment response in schizophrenia with radiomics strategy. *Eur. J. Neurosci.* 53, 1961–1975. doi: 10.1111/ejn.15046

Cui, L. B., Liu, K., Li, C., Wang, L. X., Guo, F., Tian, P., et al. (2016). Putamen-related regional and network functional deficits in first-episode schizophrenia with auditory verbal hallucinations. *Schizophr. Res.* 173, 13–22. doi: 10.1016/j.schres.2016.02.039

Cui, L. B., Liu, L., Guo, F., Chen, Y. C., Chen, G., Xi, M., et al. (2017). Disturbed brain activity in resting-state networks of patients with first-episode schizophrenia with auditory verbal hallucinations: a cross-sectional functional MR imaging study. *Radiology* 283, 810–819. doi: 10.1148/radiol.2016160938

Cui, L. B., Liu, L., Wang, H. N., Wang, L. X., Guo, F., Xi, Y. B., et al. (2018). Disease definition for schizophrenia by functional connectivity using radiomics strategy. *Schizophr. Bull.* 44, 1053–1059. doi: 10.1093/schbul/sby007

Delvecchio, G., Pigoni, A., Perlini, C., Barillari, M., Versace, A., Ruggeri, M., et al. (2018). A diffusion weighted imaging study of basal ganglia in schizophrenia. *Int. J. Psychiatry Clin. Pract.* 22, 6–12. doi: 10.1080/13651501.2017.1340650

Dickinson, D., Ramsey, M. E., and Gold, J. M. (2007). Overlooking the obvious: a meta-analytic comparison of digit symbol coding tasks and other cognitive measures in schizophrenia. *Arch. Gen. Psychiatry* 64, 532–542. doi: 10.1001/archpsyc.64.5.532

Duan, X., He, C., Ou, J., Wang, R., Xiao, J., Li, L., et al. (2021). Reduced hippocampal volume and its relationship with verbal memory and negative symptoms in treatment-naive first-episode adolescent-onset schizophrenia. *Schizophr. Bull.* 47, 64–74. doi: 10.1093/schbul/sbaa092

Duan, X., Hu, M., Huang, X., Su, C., Zong, X., Dong, X., et al. (2020). Effect of risperidone monotherapy on dynamic functional connectivity of insular subdivisions in treatment-naive, first-episode schizophrenia. *Schizophr. Bull.* 46, 650–660. doi: 10.1093/schbul/sbz087

Ellison-Wright, I., Ellison-Wright, Z., and Bullmore, E. (2008). Structural brain change in attention deficit hyperactivity disorder identified by meta-analysis. *BMC Psychiatry* 8:51. doi: 10.1186/1471-244X-8-51

Fan, F., Xiang, H., Tan, S., Yang, F., Fan, H., Guo, H., et al. (2019). Subcortical structures and cognitive dysfunction in first episode schizophrenia. *Psychiatry Res. Neuroimaging* 286, 69–75. doi: 10.1016/j.pscychresns.2019.01.003

Ferri, J., Ford, J. M., Roach, B. J., Turner, J. A., van Erp, T. G., Voyvodic, J., et al. (2018). Resting-state thalamic dysconnectivity in schizophrenia and relationships with symptoms. *Psychol. Med.* 48, 2492–2499. doi: 10.1017/S003329171800003X

Fett, A. J., Velthorst, E., Reichenberg, A., Ruggero, C. J., Callahan, J. L., Fochtmann, L. J., et al. (2020). Long-term changes in cognitive functioning in individuals with psychotic disorders: findings from the suffolk county mental health project. *JAMA Psychiatry* 77, 387–396. doi: 10.1001/jamapsychiatry.2019.3993

Friston, K., Brown, H. R., Siemerkus, J., and Stephan, K. E. (2016). The dysconnection hypothesis (2016). *Schizophr. Res.* 176, 83–94.

Fryer, S. L., Roach, B. J., Ford, J. M., Turner, J. A., van Erp, T. G. M., Voyvodic, J., et al. (2015). Relating intrinsic low-frequency BOLD cortical oscillations to cognition in schizophrenia. *Neuropsychopharmacology* 40, 2705–2714. doi: 10.1038/npp.2015.119

Georgiades, A., Davis, V. G., Atkins, A. S., Khan, A., Walker, T. W., Loebel, A., et al. (2017). Psychometric characteristics of the MATRICS consensus cognitive battery in a large pooled cohort of stable schizophrenia patients. *Schizophr. Res.* 190, 172–179.

Gong, J., Wang, J., Luo, X., Chen, G., Huang, H., Huang, R., et al. (2020). Abnormalities of intrinsic regional brain activity in first-episode and chronic schizophrenia: a meta-analysis of resting-state functional MRI. *J. Psychiatry Neurosci.* 45, 55–68. doi: 10.1503/jpn.180245

Guan, H. Y., Zhao, J. M., Wang, K. Q., Su, X. R., Pan, Y. F., Guo, J. M., et al. (2020). High-frequency neuronavigated rTMS effect on clinical symptoms and cognitive dysfunction: a pilot double-blind, randomized controlled study in Veterans with schizophrenia. *Transl. Psychiatry* 10:79. doi: 10.1038/s41398-020-0745-6

Hartberg, C. B., Sundet, K., Rimol, L. M., Haukvik, U. K., Lange, E. H., Nesvag, R., et al. (2011). Subcortical brain volumes relate to neurocognition in schizophrenia and bipolar disorder and healthy controls. *Prog. Neuropsychopharmacol. Biol. Psychiatry* 35, 1122–1130. doi: 10.1016/j.pnpbp.2011.03.014

Hashimoto, R., Mori, T., Nemoto, K., Moriguchi, Y., Noguchi, H., Nakabayashi, T., et al. (2009). Abnormal microstructures of the basal ganglia in schizophrenia revealed by diffusion tensor imaging. *World J. Biol. Psychiatry* 10, 65–69. doi: 10.1080/15622970701762536

Hibar, D. P., Stein, J. L., Ryles, A. B., Kohannim, O., Jahanshad, N., Medland, S. E., et al. (2013). Genome-wide association identifies genetic variants associated with lentiform nucleus volume in N = 1345 young and elderly subjects. *Brain Imaging Behav.* 7, 102–115. doi: 10.1007/s11682-012-9199-7

James, S. L., Abate, D., Abate, K. H., Abay, S. M., Abbafati, C., Abbasi, N., et al. (2018). Global, regional, and national incidence, prevalence, and years lived with disability for 354 diseases and injuries for 195 countries and territories, 1990–2017: a systematic analysis for the Global Burden of Disease Study 2017. *Lancet* 392, 1789–1858. doi: 10.1016/s0140-6736(18)32279-7

Kahn, R. S. (2019). On the Specificity of Continuous Cognitive Decline in Schizophrenia. *Am J Psychiatry* 176, 774–776. doi: 10.1176/appi.ajp.2019.19080794

Kahn, R. S., and Keefe, R. S. (2013). Schizophrenia is a cognitive illness: time for a change in focus. *JAMA Psychiatry* 70, 1107–1112. doi: 10.1001/jamapsychiatry.2013.155

Kern, R. S., Gold, J. M., Dickinson, D., Green, M. F., Nuechterlein, K. H., Baade, L. E., et al. (2011). The MCCB impairment profile for schizophrenia outpatients: results from the MATRICS psychometric and standardization study. *Schizophr. Res.* 126, 124–131. doi: 10.1016/j.schres.2010.11.008

Koshiyama, D., Fukunaga, M., Okada, N., Yamashita, F., Yamamori, H., Yasuda, Y., et al. (2018). Subcortical association with memory performance in schizophrenia: a structural magnetic resonance imaging study. *Transl. Psychiatry* 8:20. doi: 10.1038/s41398-017-0069-3

Krabbe, S., Duda, J., Schiemann, J., Poetschke, C., Schneider, G., Kandel, E. R., et al. (2015). Increased dopamine D2 receptor activity in the striatum alters the firing pattern of dopamine neurons in the ventral tegmental area. *Proc. Natl. Acad. Sci. U.S.A.* 112, E1498–E1506. doi: 10.1073/pnas.1500450112

Lepage, M., Bodnar, M., and Bowie, C. R. (2014). Neurocognition: clinical and functional outcomes in schizophrenia. *Can. J. Psychiatry* 59, 5–12. doi: 10.1177/070674371405900103

Li, B., Cui, L. B., Xi, Y. B., Friston, K. J., Guo, F., Wang, H. N., et al. (2017). Abnormal Effective connectivity in the brain is involved in auditory verbal hallucinations in schizophrenia. *Neurosci. Bull.* 33, 281–291. doi: 10.1007/s12264-017-0101-x

Liu, L., Cui, L. B., Xi, Y. B., Wang, X. R., Liu, Y. C., Xu, Z. L., et al. (2019). Association between connectivity of hippocampal sub-regions and auditory verbal hallucinations in schizophrenia. *Front. Neurosci.* 13:424. doi: 10.3389/fnins.2019.00424

Logothetis, N. K., Pauls, J., Augath, M., Trinath, T., and Oeltermann, A. (2001). Neurophysiological investigation of the basis of the fMRI signal. *Nature* 412, 150–157.

Luo, N., Sui, J., Chen, J., Zhang, F., Tian, L., Lin, D., et al. (2018). A schizophrenia-related genetic-brain-cognition pathway revealed in a large chinese population. *EBioMedicine* 37, 471–482. doi: 10.1016/j.ebiom.2018.10.009

Maller, J. J., Anderson, R. J., Thomson, R. H., Daskalakis, Z. J., Rosenfeld, J. V., and Fitzgerald, P. B. (2017). Occipital bending in schizophrenia. *Aust. N. Z. J. Psychiatry* 51, 32–41. doi: 10.1177/0004867416642023

Martel, J. C., and Gatti McArthur, S. (2020). Dopamine receptor subtypes, physiology and pharmacology: new ligands and concepts in schizophrenia. *Front. Pharmacol.* 11:1003. doi: 10.3389/fphar.2020.01003

McCleery, A., Ventura, J., Kern, R. S., Subotnik, K. L., Gretchen-Doorly, D., Green, M. F., et al. (2014). Cognitive functioning in first-episode schizophrenia: MATRICS Consensus Cognitive Battery (MCCB) profile of impairment. *Schizophr. Res.* 157, 33–39. doi: 10.1016/j.schres.2014.04.039

McCutcheon, R. A., Reis Marques, T., and Howes, O. D. (2020). Schizophrenia-An Overview. *JAMA Psychiatry* 77, 201–210. doi: 10.1001/jamapsychiatry.2019.3360

Mucci, A., Galderisi, S., Gibertoni, D., Rossi, A., Rocca, P., Bertolino, A., et al. (2021). Factors associated with real-life functioning in persons with schizophrenia in a 4-year follow-up study of the italian network for research on psychoses. *JAMA Psychiatry* 78, 550–559. doi: 10.1001/jamapsychiatry.2020.4614

Obeso, J. A., Rodríguez-Oroz, M. C., Rodríguez, M., Lanciego, J. L., Artieda, J., Gonzalo, N., et al. (2000). Pathophysiology of the basal ganglia in Parkinson,s disease. *Trends Neurosci.* 23 (10Suppl.), S8–S19.

Quide, Y., Morris, R. W., Shepherd, A. M., Rowland, J. E., and Green, M. J. (2013). Task-related fronto-striatal functional connectivity during working memory performance in schizophrenia. *Schizophr. Res.* 150, 468–475. doi: 10.1016/j.schres.2013.08.009

Rabinovici, G. D., Stephens, M. L., and Possin, K. L. (2015). Executive dysfunction. *Continuum (Minneap Minn)* 21(3 Behavioral Neurology and Neuropsychiatry), 646–659. doi: 10.1212/01.CON.0000466658.05156.54

Schroll, H., Horn, A., Groschel, C., Brucke, C., Lutjens, G., Schneider, G. H., et al. (2015). Differential contributions of the globus pallidus and ventral thalamus to stimulus-response learning in humans. *Neuroimage* 122, 233–245. doi: 10.1016/j.neuroimage.2015.07.061

Simpson, E. H., Kellendonk, C., and Kandel, E. (2010). A possible role for the striatum in the pathogenesis of the cognitive symptoms of schizophrenia. *Neuron* 65, 585–596. doi: 10.1016/j.neuron.2010.02.014

Sui, J., Pearlson, G. D., Du, Y., Yu, Q., Jones, T. R., Chen, J., et al. (2015). In search of multimodal neuroimaging biomarkers of cognitive deficits in schizophrenia. *Biol. Psychiatry* 78, 794–804. doi: 10.1016/j.biopsych.2015.02.017

Sui, J., Qi, S., van Erp, T. G. M., Bustillo, J., Jiang, R., Lin, D., et al. (2018). Multimodal neuromarkers in schizophrenia *via* cognition-guided MRI fusion. *Nat. Commun.* 9:3028. doi: 10.1038/s41467-018-05432-w

Takahashi, T., Tsugawa, S., Nakajima, S., Plitman, E., Chakravarty, M. M., Masuda, F., et al. (2020). Thalamic and striato-pallidal volumes in schizophrenia patients and individuals at risk for psychosis: a multi-atlas segmentation study. *Schizophr. Res.* 2020:S0920-9964(20)30223-1. doi: 10.1016/j.schres.2020.04.016

Tikasz, A., Dumais, A., Lipp, O., Stip, E., Lalonde, P., Laurelli, M., et al. (2019). Reward-related decision-making in schizophrenia: a multimodal neuroimaging study. *Psychiatry Res. Neuroimaging* 286, 45–52. doi: 10.1016/j.pscychresns.2019.03.007

Toulopoulou, T., Morris, R. G., Rabe-Hesketh, S., and Murray, R. M. (2003). Selectivity of verbal memory deficit in schizophrenic patients and their relatives. *Am. J. Med. Genet. B Neuropsychiatr. Genet.* 116B, 1–7. doi: 10.1002/ajmg.b.10027

Vatansever, D., Manktelow, A. E., Sahakian, B. J., Menon, D. K., and Stamatakis, E. A. (2016). Cognitive Flexibility: A Default Network and Basal Ganglia Connectivity Perspective. *Brain Connect.* 6, 201–207. doi: 10.1089/brain.2015.0388

Wu, X. S., Yan, T. C., Wang, X. Y., Cao, Y., Liu, X. F., Fu, Y. F., et al. (2021). Magnetic Resonance Imaging-Guided and Navigated Individualized Repetitive Transcranial Magnetic Stimulation for Cognitive Impairment in Schizophrenia. *Neurosci. Bull.* 37, 1365–1369. doi: 10.1007/s12264-021-00727-3

Xie, Y. J., Xi, Y. B., Cui, L. B., Guan, M. Z., Li, C., Wang, Z. H., et al. (2021). Functional connectivity of cerebellar dentate nucleus and cognitive impairments in patients with drug-naive and first-episode schizophrenia. *Psychiatry Res.* 300:113937.

Xiu, M. H., Guan, H. Y., Zhao, J. M., Wang, K. Q., Pan, Y. F., Su, X. R., et al. (2020). Cognitive enhancing effect of high-frequency neuronavigated rTMS in chronic schizophrenia patients with predominant negative symptoms: a double-blind controlled 32-week follow-up study. *Schizophr. Bull.* 46, 1219–1230.

Xu, Y., Zhuo, C., Qin, W., Zhu, J., and Yu, C. (2015). Altered spontaneous brain activity in schizophrenia: a meta-analysis and a large-sample study. *BioMed. Res. Int.* 2015:204628. doi: 10.1155/2015/204628

Yang, L., Yan, Y., Wang, Y., Hu, X., Lu, J., Chan, P., et al. (2018). Gradual disturbances of the amplitude of low-frequency fluctuations (ALFF) and fractional ALFF in alzheimer spectrum. *Front. Neurosci.* 12:975. doi: 10.3389/fnins.2018.00975

Zanelli, J., Mollon, J., Sandin, S., Morgan, C., Dazzan, P., Pilecka, I., et al. (2019). Cognitive change in schizophrenia and other psychoses in the decade following the first episode. *Am. J. Psychiatry* 176, 811–819. doi: 10.1176/appi.ajp.2019.18091088

Zhang, H., Wang, Y., Hu, Y., Zhu, Y., Zhang, T., Wang, J., et al. (2019). Meta-analysis of cognitive function in Chinese first-episode schizophrenia: MATRICS Consensus Cognitive Battery (MCCB) profile of impairment. *Gen. Psychiatr.* 32:e100043. doi: 10.1136/gpsych-2018-100043

Zhao, C., Zhu, J., Liu, X., Pu, C., Lai, Y., Chen, L., et al. (2018). Structural and functional brain abnormalities in schizophrenia: A cross-sectional study at different stages of the disease. *Prog. Neuropsychopharmacol. Biol. Psychiatry* 83, 27–32. doi: 10.1016/j.pnpbp.2017.12.017

Conflict of Interest: The authors declare that the research was conducted in the absence of any commercial or financial relationships that could be construed as a potential conflict of interest.

Publisher's Note: All claims expressed in this article are solely those of the authors and do not necessarily represent those of their affiliated organizations, or those of the publisher, the editors and the reviewers. Any product that may be evaluated in this article, or claim that may be made by its manufacturer, is not guaranteed or endorsed by the publisher.

frontiers in Human Neuroscience

ORIGINAL RESEARCH
published: 22 October 2021
doi: 10.3389/fnhum.2021.770107

Altered Cortical-Striatal Network in Patients With Hemifacial Spasm

Wenwen Gao[1,2†], Dong Yang[3†], Zhe Zhang[3], Lei Du[1], Bing Liu[1], Jian Liu[4], Yue Chen[1], Yige Wang[1], Xiuxiu Liu[1], Aocai Yang[1], Kuan Lv[1], Jiajia Xue[5] and Guolin Ma[1,2]*

[1] Department of Radiology, China-Japan Friendship Hospital, Beijing, China, [2] Peking University China-Japan Friendship School of Clinical Medicine, Beijing, China, [3] Department of Neurosurgery, China-Japan Friendship Hospital, Beijing, China, [4] Department of Ultrasound Diagnosis, China-Japan Friendship Hospital, Beijing, China, [5] Beijing Laboratory of Biomedical Materials, Beijing University of Chemical Technology, Beijing, China

Objective: Hemifacial spasm (HFS) is a kind of motor disorder, and the striatum plays a significant role in motor function. The purpose of this study was to explore the alterations of the cortical-striatal network in HFS using resting-state functional magnetic resonance imaging (fMRI).

Methods: The fMRI data of 30 adult patients with primary unilateral HFS (15 left-side and 15 right-side) and 30 healthy controls were collected. Six subregions of the striatum in each hemisphere were selected for functional connectivity (FC) analysis. One-sample *t*-test was used to analyze the intragroup FC of the HFS group and the control group. Two-sample *t*-test was used to compare the difference of FC between the two groups. The correlation between the abnormal FC and severity of HFS was evaluated by using the Spearman correlation analysis.

Results: Compared with the controls, the striatal subregions had altered FC with motor and orbitofrontal cortex in patients with HFS. The altered FC between striatal subregions and motor cortex was correlated with the spasm severity in patients with HFS.

Conclusion: The FC of the cortical-striatal network was altered in primary HFS, and these alterations were correlated with the severity of HFS. This study indicated that the cortical-striatal network may play different roles in the underlying pathological mechanism of HFS.

Keywords: hemifacial spasm (HFS), striatum, functional connectivity, motor disorder, resting-state fMRI

OPEN ACCESS

Edited by:
Long-Biao Cui, People's Liberation Army General Hospital, China

Reviewed by:
Maria Angelique Di Biase, The University of Melbourne, Australia
Yahong Zhang, Fourth Military Medical University, China

***Correspondence:**
Guolin Ma
maguolin1007@qq.com

† These authors have contributed equally to this work

Specialty section:
This article was submitted to Brain Imaging and Stimulation, a section of the journal Frontiers in Human Neuroscience

Received: *03 September 2021*
Accepted: *29 September 2021*
Published: *22 October 2021*

Citation:
Gao W, Yang D, Zhang Z, Du L, Liu B, Liu J, Chen Y, Wang Y, Liu X, Yang A, Lv K, Xue J and Ma G (2021) Altered Cortical-Striatal Network in Patients With Hemifacial Spasm. Front. Hum. Neurosci. 15:770107. doi: 10.3389/fnhum.2021.770107

INTRODUCTION

Hemifacial spasm (HFS) is a syndrome of involuntary contraction of facial muscles innervated by ipsilateral facial nerves (Palacios et al., 2008), which can gradually affect facial expressive muscles and platysma muscles (Lu et al., 2014). Primary HFS is believed to be caused by vascular compression of the facial nerve at its root exit zone (Hermier, 2018), but the central mechanism is still not clear. Studies have found that depression and anxiety are more common in patients with HFS (Huang et al., 2009; Rudzińska et al., 2012). Striatum plays a prominent role in modulating motor activity and higher cognitive function (Rosen and Williams, 2001). However, the exact neural

mechanism of the striatum in the regulation of motor in patients with HFS still remains unexplored. Early identification of functional changes in the cortical-striatal loop of patients with HFS can help to understand disease pathogenesis and achieve early diagnosis as well as effective treatments. This study was aimed to investigate the altered cortical-striatal network in patients with primary HFS, using resting-state functional magnetic resonance imaging (fMRI).

As part of the extrapyramidal system, the striatum is integral to the motor, cognitive, and emotion regulation functions (Di Martino et al., 2008). The subregions of the striatum, such as putamen, caudate, and ventral striatum, also are associated with different brain functions. Previous anatomical and neuroimaging studies of the striatum have shown that the putamen mainly receives projections from the sensorimotor cortex, and the caudate receives projections from the associated cortex, while the ventral striatum receives projections from the medial prefrontal cortex, orbitofrontal cortex (OFC), and limbic system (Lehericy et al., 2004; Draganski et al., 2008; Choi et al., 2012).

Based on these facts, striatum would be able to exhibit profound influences in motor disorders. For example, as one part of the striatum, putamen can regulate the amplitude and velocity of muscle contraction *via* the cortical-striatal loop and the dopamine system, and therefore plays a significant role in some motor disorders, including Parkinson's disease and Huntington's disease (Grillner et al., 2005; Loonen and Ivanova, 2013). The abnormal functional connectivity (FC) between the striatum and the motor cortex was also found in patients with motor disorders (Hacker et al., 2012; Unschuld et al., 2012; Luo et al., 2014). In Parkinson's disease, after the substantia nigra degeneration, the content of dopamine in the striatum is also decreased (Schroeder et al., 2020), and in addition to the abnormal striatum-substantia nigra loop, the cortex-striatum loop may also be abnormal (Helmich et al., 2010). These results further highlight the significance of the striatum in the development of motor disorders. Besides, the researchers have used FC analysis to study the function of striatal subregions in healthy people (Di Martino et al., 2008), patients with Parkinson's disease (Helmich et al., 2010; Hacker et al., 2012), depression (Gabbay et al., 2013; Felger et al., 2016), autism (Padmanabhan et al., 2013), and obsessive-compulsive disorder (Harrison et al., 2009), and the mechanisms of central alterations in different subregions of the striatum have been revealed.

Current resting-state fMRI studies of HFS are limited, and the results are diverse. The regional homogeneity (ReHo) index has been used in most previous studies to indicate time-domain coherence between neighboring voxels in the brain. Researchers have found ReHo abnormalities in the motor cortex, frontal lobes, and cerebellum in patients with HFS (Tu et al., 2015; Wei et al., 2015; Lu et al., 2018), and no ReHo alterations in the striatum, probably due to the small sample size and the different meanings between the analysis indexes, i.e., ReHo and FC. However, one study reported that patients after infarction of the caudate, one of the subregions of the striatum, presented with HFS, suggesting that the striatum may play an important role in the development of HFS (Arunabh, Jain and Maheshwari, 1992). In addition, another study on facial nerve palsy found altered FC between the striatum and motor cortex after facial muscle paralysis, further affirming the relationship between the striatum and facial muscle movement (Song et al., 2017). To the best of our knowledge, there are few earlier studies on HFS using the FC analysis method. One study showed abnormalities in FC between the thalamus and parietal cortex in patients with HFS (Niu et al., 2020), but it did not explore the central changes of the striatum in this dyskinesia. HFS is a kind of facial movement disorder, it is not clear that how the striatum regulates the motor function of patients with HFS before and after the onset of its symptoms, and in this study, we focused on striatal function in patients with HFS.

In this study, we performed FC analysis of 12 striatal subregions in patients with HFS. We hypothesized that in patients with chronic primary HFS, the FC between the striatum and motor cortex and FC between striatal subregions will be changed. Since long-term HFS may result in psychological problems, such as depression and anxiety (Bao et al., 2015), we also hypothesized that the FC between the striatum subregions and the emotion-related cortex will be altered in patients with HFS. Furthermore, we explored the relationship between altered FC and clinical characteristics in patients with HFS.

MATERIALS AND METHODS

Subjects

A total of 60 subjects were selected from a total of 64 participants, and 4 subjects (3 patients with HFS and 1 healthy control) were excluded from the analysis due to excessive head motion (translational movement > 2 mm or rotation $> 2°$). Then, 30 patients with HFS (15 left-side HFS, 15 right-side HFS, 12 men, 18 women, age 48.87 ± 10.61 years) were enrolled from 2017 to 2019 in the Department of Neurosurgery, China-Japan Friendship Hospital. HFS was diagnosed by two experienced neurologists based on clinical symptoms and history. The severity of HFS was assessed using the Cohen spasm scale (0–4 scores, with higher scores indicating more severe spasm) (Cohen et al., 1986). The inclusion criteria for patients were as follows: (1) adult patients with primary unilateral HFS, (2) without craniocerebral lesions and mental disorders, no use of psychotropic drugs, and (3) being right-handed. The exclusion criteria for patients were as follows: (1) with bilateral HFS, (2) having contraindications to MRI examination, and (3) with excessive head motion. Notably, 30 age-, sex-, education-matched healthy controls (12 men, 18 women, age 47.63 ± 13.29 years) were recruited from the society. The inclusion criteria for healthy controls are as follows: (1) aged 18 years old or above, (2) absence of neurological and mental disorders, and (3) being right-handed. The demographic and clinical characteristics of participants are shown in **Table 1**. This study was approved by the Ethics Committee of our hospital, and all subjects have given informed consent before the experiment.

Magnetic Resonance Imaging Data Acquisition

The experiment was carried out on the 3.0 T MRI scanner (GE, Discovery MR750, Milwaukee, United States) with an 8-channel phased-array head coil. The resting-state fMRI with a single-shot

TABLE 1 | Demographic and clinical characteristics of participants.

Variable	HFS (n = 30) (mean ± SD)	HC (n = 30) (mean ± SD)	Two-sample t test
			P value
Sex (male/female)	12/18	12/18	–
Age (years)	48.87 ± 10.61	47.63 ± 13.29	0.693
Education (years)	11.57 ± 4.24	13.50 ± 4.35	0.087
Duration (years)	5.70 ± 5.24	N/A	–
Cohen spasm severity (scores)	2.57 ± 0.73	N/A	–

HFS, hemifacial spasm; HC, healthy control; SD, standard deviation.

gradient recalled echo-planar imaging sequence was performed with the following recipe. The repetition time (TR) was 2,000 ms, while the echo time (TE) was set to 30 ms. The slice thickness was chosen to be 3.5 mm with a spacing of 0.7 mm. The matrix of the image was 64 × 64, while the field of view (FOV) was 224 mm × 224 mm. The flip angle was 90°, and the number of excitations (NEX) was set to 1. A total of 8 min were consumed for each data with 34 slices and 240 time points. T2WI scan was used to exclude the cerebral organic lesions. 3D T1WI anatomic images were reconstructed using three-dimensional fast spoiled gradient-echo sequences (3D FSPGR), and the TR of which was 6.7 ms, while the TE was set to minimum full. The matrix was changed to 256 × 256 with a FOV of 256 mm × 256 mm. Furthermore, the slice thickness was chosen as 1.0 mm, while the NEX remained to be 1.

Data Preprocessing

To unify the affected side of the patients, the T1WI and fMRI data with left HFS (15 cases) and matched controls (15 cases) were flipped from left to right before preprocessing (Song et al., 2017). In this study, "right" was defined as the ipsilateral side, and "left" was defined as the contralateral side for the flipped data. The preprocessing was conducted using the software of Data Processing Assistant for Resting-State fMRI (DPARSF) (Yan et al., 2016) in the following steps. First, the DICOM data were converted to NIFTI format and the first 10 time points for each file were removed. Second, the timing correction and realignment were carried out, the T1WI to the mean functional image was co-registered, and the DARTEL tool to compute transformations from individual native space to Montreal Neurological Institute (MNI) space was used (Yan et al., 2017). The subjects with head motion exceeding 2 mm or 2° were excluded. Then, the spatial smoothing using a 4-mm Gaussian kernel was performed and the low-frequency drift and high-frequency noise using band-pass filtering (0.01–0.1 Hz) were removed. Finally, the Friston 24-parameter model was used to regress out head motion effects. In this step, the white matter signal, cerebrospinal fluid signal, and global signal were regressed as covariates.

Definition of the Region of Interest

The regions of interest (ROIs) were determined by the "Define ROI" module using DPARSF software, based on the radius and MNI spatial coordinates. According to the previous study, six striatal subregions of each hemisphere were selected as ROIs, and the radius of each ROI was set to 3 mm. The MNI coordinates of the ROIs were as follows: dorsal caudal putamen (DCP, ± 28, 1, 3), dorsal rostral putamen (DRP, ± 25, 8, 6), ventral rostral putamen (VRP, ± 20, 12, − 3), dorsal caudate (DC, ± 13, 15, 9), inferior ventral striatum (VSi, ± 9, 9, −8), and superior ventral striatum (VSs, ± 10, 15, 0) (Song et al., 2017). The diagram of ROIs is shown in **Figure 1**.

Analysis of Functional Connectivity Based on Voxel-Wise

First, the time course of the average BOLD signal was extracted from each ROI. Then, the Pearson's correlation between the time course of each ROI and the time course of all other voxels in the brain was calculated. Fisher z transformation was performed to improve the normal distribution of the data. Then,

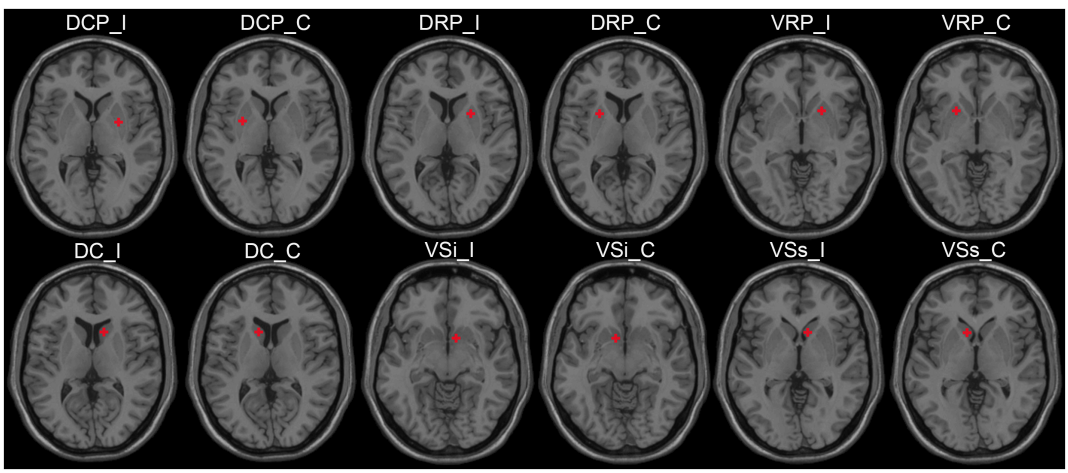

FIGURE 1 | The ROI schematic diagrams of striatal subregions. ROI, region of interest; I, ipsilateral; C, contralateral; DCP, dorsal caudal putamen; DRP, dorsal rostral putamen; VRP, ventral rostral putamen; DC, dorsal caudate; VSi, inferior ventral striatum; VSs, superior ventral striatum.

the correlation map, that is, the FC map of the whole brain was generated for further statistical analysis.

Intragroup Functional Connectivity Analysis

To explore the intragroup FC patterns of the cortical-striatal network, one-sample *t*-tests (default mask) were performed in the HFS group and the HC group. The statistical threshold was set at $z > 3.6594$ and cluster size of >6 mm^3, which corresponded to a corrected $P < 0.001$. This correction threshold was determined using Monte Carlo simulations with the program AlphaSim in AFNI (Ledberg et al., 1998).

Between-Group Functional Connectivity Analysis

To determine the FC differences of the cortical-striatal network between the two groups, two-sample *t*-tests were performed at each FC map of 12 ROIs (default mask). The Gaussian random field (GRF) method was used for multiple comparison corrections, and the statistical threshold was set at voxel-level $P < 0.005$ and cluster-level $P < 0.05$. The DPABI software was used to perform the statistical analysis of FC.

Correlation Analysis

The *z* value of brain regions with significant changes in the HFS group was extracted to explore the relationship between the severity of HFS and altered connectivity. Then, the Spearman correlation analysis was performed using GraphPad Prism 6.0 software to evaluate the correlation between abnormal FC and spasm severity in patients with HFS. The age, sex, education, and duration were regressed as covariates. We also explored the relationship between duration and spasm severity through Spearman correlation analysis, and the age, sex, and education level were regressed as covariates as well. A total of 14 correlations were performed, with 13 abnormal FCs correlating with spasm severity, and, finally, 1 correlation was performed between spasm severity and disease duration. The false discovery rate (FDR) method was used to correct the results of the correlation analysis for multiple comparisons.

Analysis of Functional Connectivity Based on Regions of Interest-Wise

The FC between the striatal ROIs was also calculated. After Fisher *z* transformation, a 12×12 FC matrix was generated for every subject. A total of 66 *z* values were constructed, and each *z* value stands for the FC between two brain regions. Two-sample *t*-tests were performed using SPSS 20.0 software (SPSS Inc., Chicago, IL, United States) to compare the difference of FC between the HFS group and the HC group. Age, gender, and education were regressed as covariates. FDR correction was used to control false positives for multiple comparisons, and the statistical threshold was set at $P < 0.05$.

RESULTS

Clinical Results

There were no significant differences in sex, age, and education level between the HFS group and the HC group ($P > 0.05$) (**Table 1**).

Intragroup Functional Connectivity in the Cortical-Striatal Network

The intragroup FC maps of the cortical-striatal network were similar in the HC and HFS groups, which is consistent with previous studies (Di Martino et al., 2008; Song et al., 2017; Dong et al., 2019). The putamen ROIs had strengthened connectivity with the insula, middle cingulate cortex (MCC), precuneus, and supplementary motor area (SMA) (**Figure 2A**). The DC ROIs had strengthened connectivity with the anterior cingulate cortex (ACC) and superior frontal gyrus (SFG). The ventral striatum ROIs had strengthened connectivity with ACC and OFC (**Figure 2B**). In this study, these intragroup maps were merely for visualizing FC in the two groups.

Group Differences of Functional Connectivity in the Cortical-Striatal Network

Dorsal Caudal Putamen

The contralateral DCP had significantly decreased FC with ipsilateral SFG, SMA, and precentral gyrus, respectively, in the HFS group compared with the HC group (**Figures 3A**, **4A** and **Table 2**).

Dorsal Rostral Putamen

The contralateral DRP had significantly increased FC with contralateral middle frontal gyrus (MFG) and SFG, in the HFS group compared with the HC group (**Figures 3B**, **4A** and **Table 2**).

Ventral Rostral Putamen

There was no significant alteration in FC between VRP and cerebral cortex in the HFS group compared with the HC group.

Dorsal Caudate

The contralateral DC had significantly decreased FC with bilateral cerebellar lobule VIII, IX, and contralateral cerebellar crus II, in patients with HFS than that in controls (**Figures 3C**, **4A** and **Table 2**).

Inferior Ventral Striatum

In the HFS group compared with the HC group, the ipsilateral VSi had significantly increased FC with bilateral OFC, paracentric lobule, and SMA (**Figures 3D,E**, **4B** and **Table 3**), while the FC between ipsilateral VSi and superior marginal gyrus (SMG) was significantly decreased (**Figures 4B**, **5A** and **Table 3**); the FC between contralateral VSi and bilateral OFC was significantly increased (**Figures 4C**, **5B** and **Table 3**), while the FC between contralateral VSi and ipsilateral superior occipital gyrus (SOG) was significantly decreased (**Figures 4C**, **5C** and **Table 3**).

Superior Ventral Striatum

The ipsilateral VSs showed significantly increased FC with bilateral SMA and paracentric lobule, in the HFS group compared with the HC group (**Figures 4C**, **5D** and **Table 3**). The FC between contralateral VSs and ipsilateral SOG in patients with HFS was significantly increased than that in controls (**Figures 4C**, **5E** and **Table 3**).

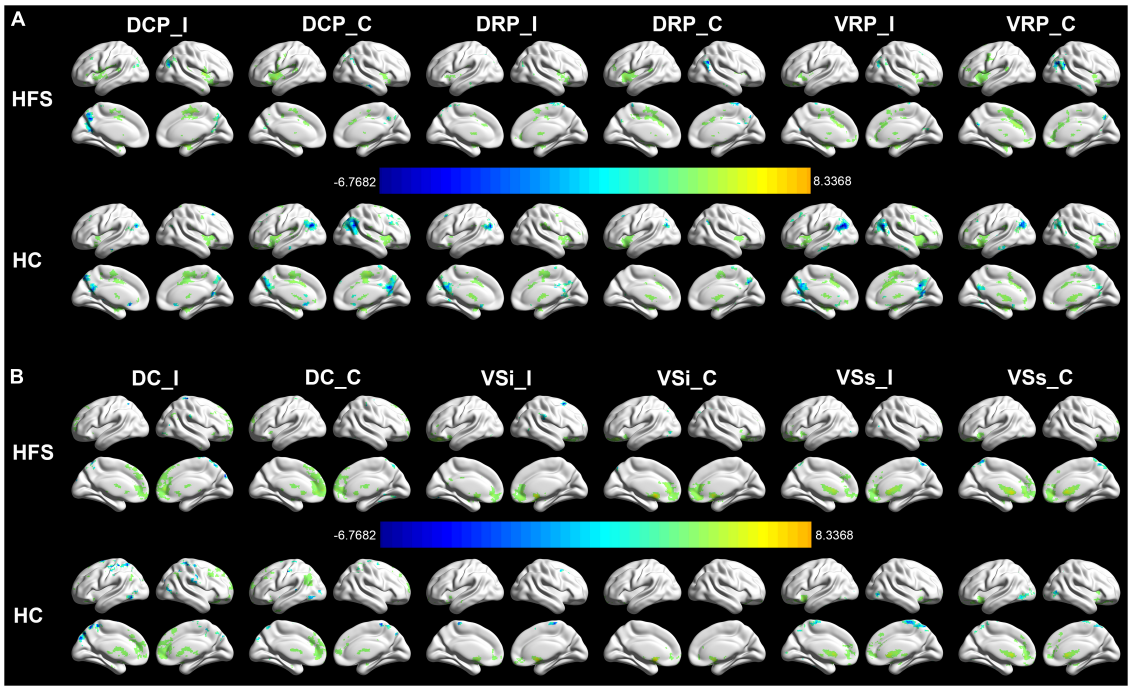

FIGURE 2 | Intragroup FC in the cortical-striatal network. The FC maps of the cortical-striatal network in the HC group and HFS group were similar (AlphaSim correction, $P < 0.001$, cluster size > 6 mm^3). **(A)** The putamen ROIs had strengthened connectivity with the insula, MCC, precuneus, and SMA. **(B)** The dorsal caudate ROIs had strengthened connectivity with the ACC and SFG. The ventral striatum ROIs had strengthened connectivity with ACC and OFC. The color bar represents the *t* value. FC, functional connectivity; HC, healthy control; HFS, hemifacial spasm; MCC, middle cingulate cortex; SMA, supplementary motor area; ACC, anterior cingulate cortex; SFG, superior frontal gyrus; OFC, orbitofrontal cortex; I, ipsilateral; C, contralateral; DCP, dorsal caudal putamen; DRP, dorsal rostral putamen; VRP, ventral rostral putamen; DC, dorsal caudate; VSi, inferior ventral striatum; VSs, superior ventral striatum.

Correlation Between Spasm Severity and Functional Connectivity and Duration

The FC between contralateral DCP and ipsilateral SFG was negatively correlated with the Cohen spasm scores ($r = -0.433$, $P = 0.0168$ uncorrected) (**Figure 6A**). Furthermore, the FC between ipsilateral VSi and contralateral OFC showed positive correlation with the Cohen spasm scores ($r = 0.6739$, $P < 0.0001$ uncorrected) (**Figure 6B**). There was no correlation between the duration and the spasm severity ($r = -0.2327$, $P = 0.2158$ uncorrected) (**Figure 6C**). After FDR correction, there was no significant correlation between abnormal FCs and spasm severity.

Within the Striatal Network

Compared with the HC group, the ipsilateral DCP in the HFS group showed increased FC with ipsilateral DRP and VRP ($P = 0.0053$, $P = 0.0272$ uncorrected), and the FC between contralateral DCP and contralateral VRP was also increased ($P = 0.017$ uncorrected) (**Figure 7**). After FDR correction, there was no significant difference in FC within the striatal network between the HFS group and the HC group.

DISCUSSION

This study investigated the functional alterations of the cortical-striatal network in patients with HFS and their relationship with clinical manifestations. Compared with the controls, the striatal subregions had altered FC with motor and OFC in patients with HFS. Furthermore, the FC between the ventral striatum and motor cortex was positively associated with the severity of HFS. Finally, our results suggest that the cortical-striatal network may play differential roles in the underlying pathological mechanism of HFS.

Increased Functional Connectivity of the Cortical-Striatal Network in Patients With Hemifacial Spasm

As we know, this is the first resting-state fMRI study to examine intrinsic cortical-striatal connectivity in HFS. The emotion-related cortex showed significantly increased FC with the ventral striatum and putamen, in patients with HFS compared with the controls. The orbitofrontal lobe and the VSi are involved in emotional activities (Di Martino et al., 2008; Accolla et al., 2016). The structural and functional abnormalities of those regions were found to be widespread in patients with depression (Botteron et al., 2002; Bremner et al., 2002; Taylor et al., 2003; Ballmaier et al., 2004). Long-term HFS may lead to anxiety and depression (Bao et al., 2015). The increased connectivity between the VSi and orbitofrontal lobe may be associated with the poor mental

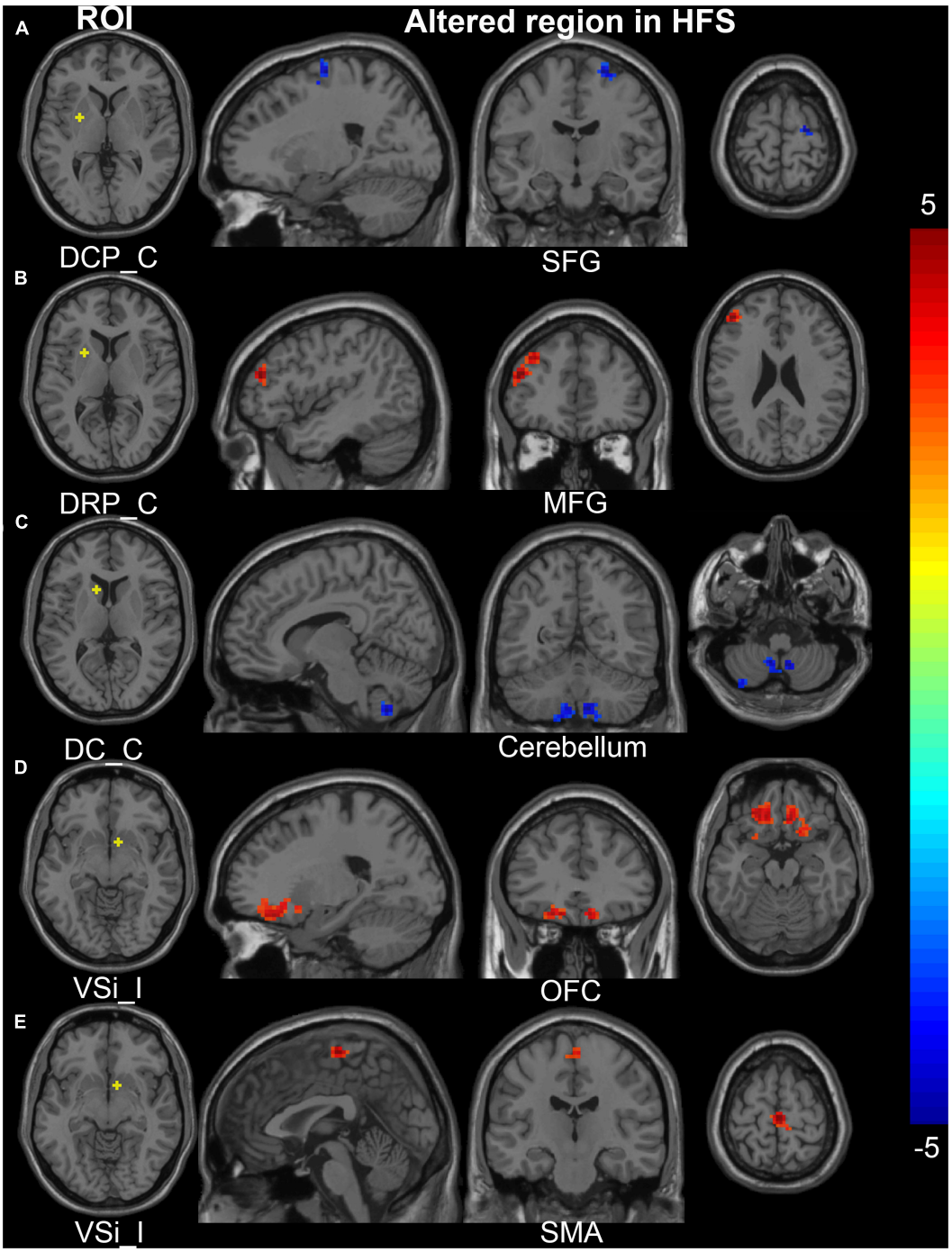

FIGURE 3 | Altered FC in the cortical-striatal network (putamen, caudate, and inferior ventral striatum ROIs). In the HFS group compared with the HC group: **(A)** The FC between contralateral DCP and ipsilateral SFG was decreased. **(B)** The FC between contralateral DRP and contralateral MFG was increased. **(C)** The FC between contralateral DC and bilateral cerebellum was decreased. **(D)** and **(E)** The ipsilateral VSi showed increased FC with bilateral OFC and SMA. The color bar represents the *t* value. FC, functional connectivity; ROIs, regions of interest; HFS, hemifacial spasm; HC, healthy control; C, contralateral; I, ipsilateral; DCP, dorsal caudal putamen; DRP, dorsal rostral putamen; DC, dorsal caudate; VSi, inferior ventral striatum; SFG, superior frontal gyrus; MFG, middle frontal gyrus; OFC, orbitofrontal cortex; SMG, supramarginal gyrus; SMA, supplementary motor area.

status of patients with HFS. The SOG was located in the visual network, and studies have found that this area was involved in facial expression and emotion processing (Tao et al., 2013). We speculated that the increased functional activity of these regions in patients with HFS may be related to abnormal facial expressions. In addition, the putamen had increased

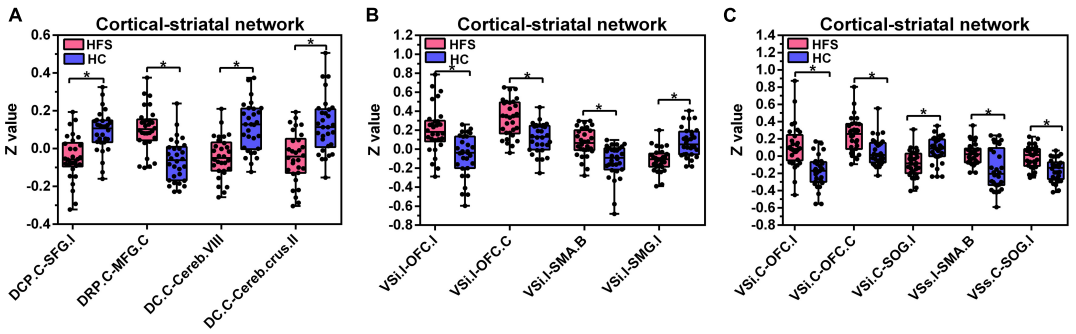

FIGURE 4 | Altered FC in the cortical-striatal network. Boxplots with between-group differences for 13 significant cluster. In the HFS group compared with the HC group: **(A)** The FC between contralateral DCP and ipsilateral SFG was decreased. The FC between contralateral DRP and contralateral MFG was increased. The FC between contralateral DC and bilateral cerebellum was decreased. **(B)** The ipsilateral VSi showed increased FC with bilateral OFC and SMA. The FC between ipsilateral VSi and ipsilateral SMG was decreased. **(C)** The FC between contralateral VSi and bilateral OFC was increased. The FC between contralateral VSi and ipsilateral SOG was decreased. The FC between ipsilateral VSs and bilateral SMA was increased. The FC between contralateral VSs and ipsilateral SOG was increased. FC, functional connectivity; HFS, hemifacial spasm; HC, healthy control; C, contralateral; I, ipsilateral; B, bilateral; DCP, dorsal caudal putamen; SFG, superior frontal gyrus; DRP, dorsal rostral putamen; MFG, middle frontal gyrus; DC, dorsal caudate; Cereb, cerebellum; VSi, inferior ventral striatum; OFC, orbitofrontal cortex; SMA, supplementary motor area; SMG, supramarginal gyrus; SOG, superior occipital gyrus; VSs, superior ventral striatum.

TABLE 2 | Altered FC in the putamen and caudate ROIs between two groups.

ROIs	Contrast	Brain region	Cluster size	Peak *t* value	MNI coordinates (mm)		
					x	y	z
DCP_C	HFS < HC	I superior frontal gyrus	55	−4.8035	21	−12	69
DRP_C	HFS > HC	C middle frontal gyrus	64	5.0707	−45	42	24
DC_C	HFS < HC	B cerebellum posterior lobe	165	−4.8075	9	−57	−51
	HFS < HC	C cerebellum crus2	76	−4.4086	−42	−75	−48

FC, functional connectivity; ROIs, regions of interest; C, contralateral; DCP, dorsal caudal putamen; DRP, dorsal rostral putamen; DC, dorsal caudate; HFS, hemifacial spasm; HC, healthy control; MNI, Montreal Neurological Institute.

TABLE 3 | Altered FC in the ventral striatum ROIs between two groups.

ROIs	Contrast	Brain region	Cluster size	Peak *t* value	MNI coordinates (mm)		
					x	y	z
VSi_I	HFS > HC	I orbitofrontal cortex	107	4.681	9	30	−18
	HFS > HC	C orbitofrontal cortex	166	4.4424	−21	33	−18
	HFS > HC	B supplementary motor area	56	5.0717	3	−21	66
	HFS < HC	I supramarginal gyrus	71	-5.2399	54	−30	24
VSi_C	HFS > HC	I orbitofrontal cortex	94	4.6397	9	27	−24
	HFS > HC	C orbitofrontal cortex	58	4.0489	−12	36	−15
	HFS < HC	I superior occipital gyrus	71	-4.3179	33	−78	45
VSs_I	HFS > HC	B supplementary motor area, paracentral lobe	76	4.534	−3	−21	66
VSs_C	HFS > HC	I superior occipital gyrus	59	4.629	21	−87	3

FC, functional connectivity; ROIs, regions of interest; I, ipsilateral; C, contralateral; VSi, inferior ventral striatum; VSs, superior ventral striatum; HFS, hemifacial spasm; HC, healthy control; MNI, Montreal Neurological Institute.

FC with MFG and SFG, which may be associated with the depression and other adverse emotions of the patients with HFS, and it is consistent with previous studies in patients with depression (Fitzgerald et al., 2006). In summary, the ventral striatum was mainly involved in emotional activities, while the putamen may also involve in emotional activities in addition to motor function.

Decreased Functional Connectivity of the Cortical-Striatal Network in Patients With Hemifacial Spasm

We also found that the FC between the putamen and the ipsilateral motor cortex was decreased in the HFS group, and so does the FC between the caudate and the cerebellum. It

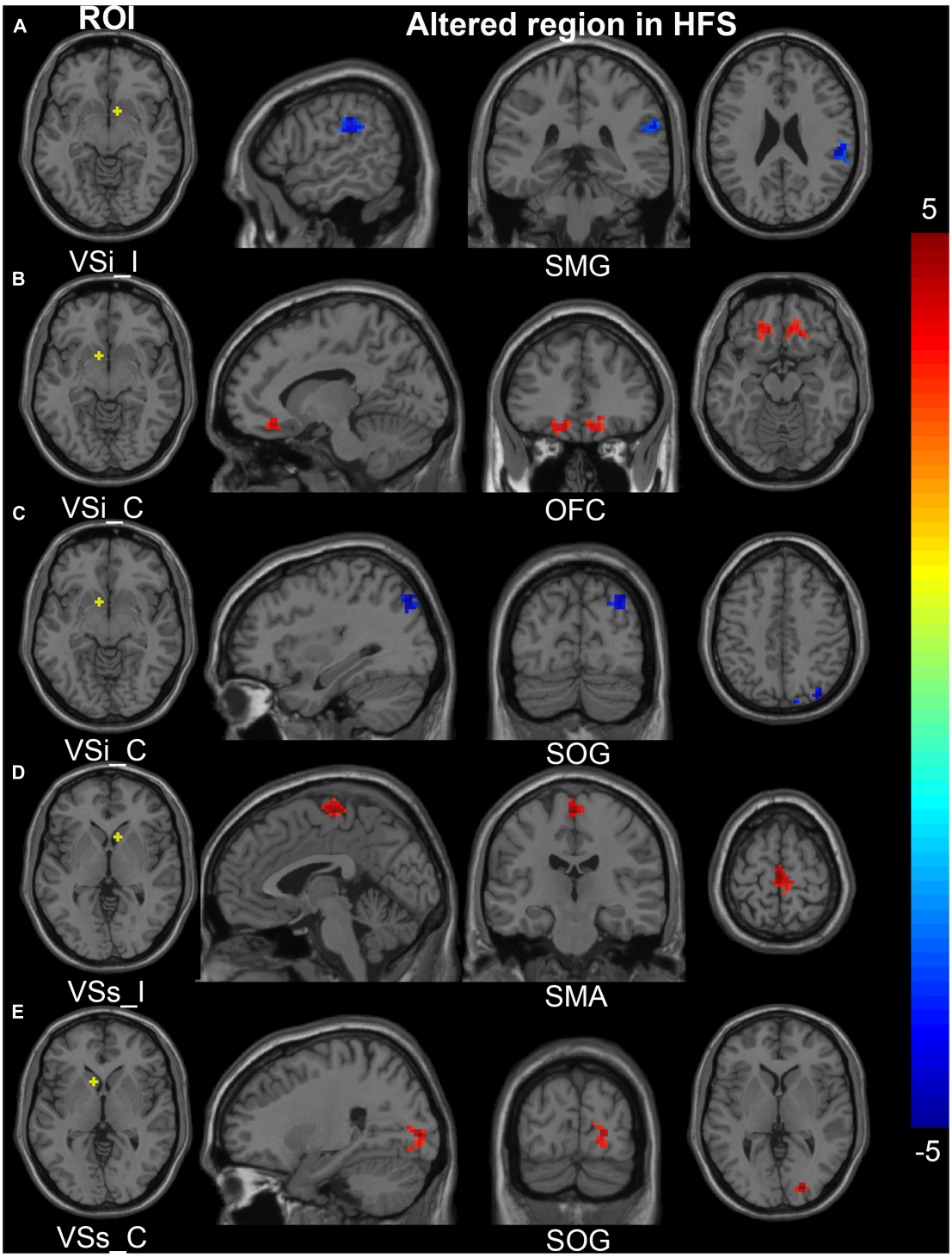

FIGURE 5 | Altered FC in the cortical-striatal network (inferior and superior ventral striatum ROIs). In the HFS group compared with the HC group: **(A)** The FC between ipsilateral VSi and ipsilateral SMG was decreased. **(B)** The FC between contralateral VSi and bilateral OFC was increased. **(C)** The FC between contralateral VSi and ipsilateral SOG was decreased. **(D)** The FC between ipsilateral VSs and bilateral SMA was increased. **(E)** The FC between contralateral VSs and ipsilateral SOG was increased. The color bar represents the *t* value. FC, functional connectivity; ROIs, regions of interest; HFS, hemifacial spasm; HC, healthy control; I, ipsilateral; C, contralateral; VSi, inferior ventral striatum; VSs, superior ventral striatum; SMG, supramarginal gyrus; OFC, orbitofrontal cortex; SOG, superior occipital gyrus; SMA, supplementary motor area.

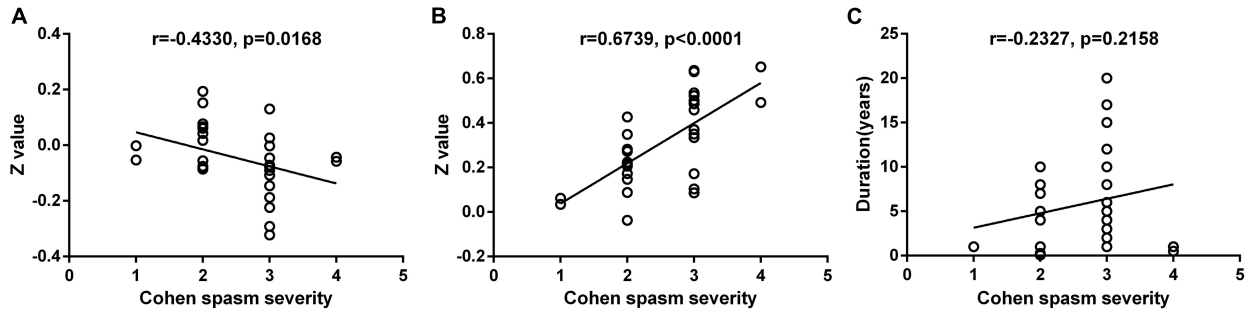

FIGURE 6 | The correlation relationship between spasm severity and altered FC and duration. **(A)** The FC between contralateral DCP and ipsilateral SFG was negatively correlated with the Cohen spasm scores ($r = -0.433$, $P = 0.0168$ uncorrected). **(B)** The FC between ipsilateral VSi and contralateral OFC showed positive correlation with the Cohen spasm scores ($r = 0.6739$, $P < 0.0001$ uncorrected). **(C)** There was no correlation between the duration and the spasm severity ($r = -0.2327$, $P = 0.2158$ uncorrected). FC, functional connectivity; DCP, dorsal caudal putamen; SFG, superior frontal gyrus; VSi, inferior ventral striatum; OFC, orbitofrontal cortex.

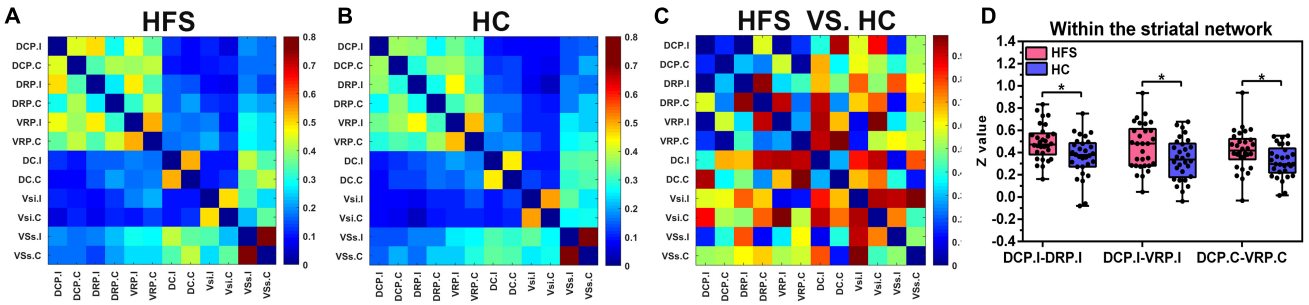

FIGURE 7 | The FC maps of the striatal network. **(A)** and **(B)** The FC matrix map of the striatal network in the HFS group and the HC group. The color bar represented the mean *z* value. **(C)** The group differences of the FC within the striatal network between the two groups. The color bar represents the *P* value. **(D)** In the HFS group compared with the HC group: The ipsilateral DCP showed increased FC with ipsilateral DRP and VRP. In addition, the FC between contralateral DCP and contralateral VRP was increased. * indicates $P < 0.05$ (uncorrected). FC, functional connectivity; HFS, hemifacial spasm; HC, healthy control; DCP, dorsal caudal putamen; DRP, dorsal rostral putamen; VRP, ventral rostral putamen.

was known that the precentral gyrus was the first somatic motor area, and the SFG was the premotor area. One side of the cerebral motor area dominates the contralateral body movement, but the muscles involved in associated movement are dominated by bilateral motor areas, such as extraocular muscles and masticatory muscles (Desai et al., 2013). The decrease of FC between the putamen and ipsilateral motor area may be a compensatory mechanism to inhibit facial muscle spasms. In addition, the cerebellum is an important motor regulation center. The cerebellum may be involved in the processing of movement, cognition, and emotion by forming loops with the brain, and structural or functional abnormalities in these loops may contribute to the development of motor disorders (e.g., ataxia) (D'Angelo and Casali, 2013). Abnormalities in the connectivity between brain regions within the loops can lead to disorders that are associated with loop dysfunction. The cerebellum may form a loop with the cortical-caudate, which is involved in the motor regulation of HFS, and the diminished connectivity may be a consequence of the dysfunction of the caudate-cerebellar loop. To sum up, in addition to the putamen, other parts of the striatum, such as the caudate, may be involved in the pathological process of HFS. Different cortical-striatal loops may be involved in motion monitoring, error detection, and correction (Song et al., 2017).

Increased Functional Connectivity Within the Striatal Network in Patients With Hemifacial Spasm (Uncorrected, $P < 0.05$)

In this study, we found no significant differences in FC within the striatal network between the two groups (FDR correction, threshold $P < 0.05$). However, using a less conservative threshold ($P < 0.05$), we found that the FC between the putamen ROIs was increased in patients with HFS compared with the controls. Interestingly, a study of the striatal network in facial palsy found the decreased FC between the putamen and the ventral striatum (uncorrected) (Song et al., 2017), which is the opposite of our results. We know that facial palsy and facial spasm are two motor disorders with opposite manifestations, the former shows reduced or no movement of the affected facial muscles and the latter shows excessive movement. In addition, the connectivity within the striatal network is also consistent with clinical manifestations, i.e., being diminished in facial palsy

and increased in facial spasm. Therefore, we speculated that the putamen plays an important role in the motor function of facial muscles, and the increased or decreased FC between the putamen and other seeds within the striatum may respond to the increased or decreased motor signals in this neural circuit, thus resulting in different motor states of the facial muscles.

Limitations

There were several limitations in this study. First, the sample size of this study was small, including patients with left HFS and right HFS. To control the problem on the different sides of the lesion, we flipped the left HFS group from left to right. In the future, the changes of brain functional networks in patients with left and right HFS can be studied separately on the basis of expanding the sample size. Second, this study used a cross-sectional study design to explore the changes of the cortical-striatal network in patients with HFS. Longitudinal studies can be conducted in the future to explore the mechanism of brain network changes in different stages of HFS. Finally, previous studies and our study have all found functional abnormalities in the emotion-related cortex in patients with HFS. Therefore, increasing the evaluation of the psychological status of patients may make the results more reliable, which can be added in further studies.

CONCLUSION

Primary unilateral HFS induces several FC alterations in the cortical-striatal network, specifically, the striatal subregions have altered connectivity with motor and OFC in patients with HFS, respectively. The severity of HFS is associated with these functional alterations. This study provides significant evidence that the altered cortical-striatal connectivity is involved in differential neural mechanisms of motor and emotional dysfunction in patients with HFS.

DATA AVAILABILITY STATEMENT

The original contributions presented in the study are included in the article/supplementary material, further inquiries can be directed to the corresponding author.

ETHICS STATEMENT

The studies involving human participants were reviewed and approved by the Ethics Committee of China-Japan Friendship Hospital. The patients/participants provided their written informed consent to participate in this study.

AUTHOR CONTRIBUTIONS

GM conceived and designed the experiments. WG and DY performed the experiments. WG and ZZ analyzed the data. WG, LD, BL, JL, YC, YW, XL, AY, KL, and JX discussed the data. WG wrote the manuscript. DY revised the manuscript. All authors read and approved the final manuscript.

FUNDING

This study was supported by grants from the National Natural Science Foundation of China (NSFC) (No. 81971585) and the National Key Research and Development Program of China (Nos. 2020YFC2003903 and 2020YFC2007301).

ACKNOWLEDGMENTS

We thank Lizhi Xie from GE Healthcare for the help in solving MR technical problems.

REFERENCES

Accolla, E. A., Aust, S., Merkl, A., Schneider, G. H., Kuhn, A. A., Bajbouj, M., et al. (2016). Deep brain stimulation of the posterior gyrus rectus region for treatment resistant depression. *J. Affect. Disord.* 194, 33–37. doi: 10.1016/j.jad.2016.01.022

Arunabh, Jain, S., and Maheshwari, M. C. (1992). Blepharospasm hemifacial spasm and tremors possibly due to isolated caudate nucleus lesions. *J. Assoc. Physicians India* 40, 687–689.

Ballmaier, M., Toga, A. W., Blanton, R. E., Sowell, E. R., Lavretsky, H., Peterson, J., et al. (2004). Anterior cingulate, gyrus rectus, and orbitofrontal abnormalities in elderly depressed patients: an MRI-based parcellation of the prefrontal cortex. *Am. J. Psychiatry* 161, 99–108. doi: 10.1176/appi.ajp.161.1.99

Bao, F., Wang, Y., Liu, J., Mao, C., Ma, S., Guo, C., et al. (2015). Structural changes in the CNS of patients with hemifacial spasm. *Neuroscience* 289, 56–62. doi: 10.1016/j.neuroscience.2014.12.070

Botteron, K. N., Raichle, M. E., Drevets, W. C., Heath, A. C., and Todd, R. D. (2002). Volumetric reduction in left subgenual prefrontal cortex in early onset depression. *Biol. Psychiatry* 51, 342–344. doi: 10.1016/s0006-3223(01)01280-x

Bremner, J. D., Vythilingam, M., Vermetten, E., Nazeer, A., Adil, J., Khan, S., et al. (2002). Reduced volume of orbitofrontal cortex in major depression. *Biol. Psychiatry* 51, 273–279. doi: 10.1016/s0006-3223(01)01336-1

Choi, E. Y., Yeo, B. T. T., and Buckner, R. L. (2012). The organization of the human striatum estimated by intrinsic functional connectivity. *J. Neurophysiol.* 108, 2242–2263. doi: 10.1152/jn.00270.2012

Cohen, D. A., Savino, P. J., Stern, M. B., and Hurtig, H. I. (1986). Botulinum injection therapy for blepharospasm - a review and report of 75 patients. *Clin. Neuropharmacol.* 9, 415–429. doi: 10.1097/00002826-198610000-00002

D'Angelo, E., and Casali, S. (2013). Seeking a unified framework for cerebellar function and dysfunction: from circuit operations to cognition. *Front. Neural. Circuits* 6:116. doi: 10.3389/fncir.2012.00116

Desai, S. D., Patel, D., Bharani, S., and Kharod, N. (2013). Opercular syndrome: a case report and review. *J. Pediatr. Neurosci.* 8, 123–125. doi: 10.4103/1817-1745.117842

Di Martino, A., Scheres, A., Margulies, D. S., Kelly, A. M., Uddin, L. Q., Shehzad, Z., et al. (2008). Functional connectivity of human striatum: a resting state FMRI study. *Cereb. Cortex* 18, 2735–2747.

Dong, C., Yang, Q., Liang, J., Seger, C. A., Han, H., Ning, Y., et al. (2019). Impairment in the goal-directed corticostriatal learning system as a biomarker for obsessive-compulsive disorder. *Psychol. Med.* 50, 1490–1500. doi: 10.1017/s0033291719001429

Draganski, B., Kherif, F., Kloeppel, S., Cook, P. A., Alexander, D. C., Parker, G. J. M., et al. (2008). Evidence for segregated and integrative connectivity patterns in the human basal ganglia. *J. Neurosci.* 28, 7143–7152. doi: 10.1523/jneurosci.1486-08.2008

Felger, J. C., Li, Z., Haroon, E., Woolwine, B. J., Jung, M. Y., Hu, X., et al. (2016). Inflammation is associated with decreased functional connectivity within corticostriatal reward circuitry in depression. *Mol. Psychiatry* 21, 1358–1365. doi: 10.1038/mp.2015.168

Fitzgerald, P., Maller, J., Hoy, K., Oxley, T., Daskalakis, Z., and Laird, A. (2006). A meta-analytic study of changes in brain activation in depression. *Acta Neuropsychiatr.* 18, 286–287. doi: 10.1017/s0924270800031173

Gabbay, V., Ely, B. A., Li, Q., Bangaru, S. D., Panzer, A. M., Alonso, C. M., et al. (2013). Striatum-based circuitry of adolescent depression and Anhedonia. *J. Am. Acad. Child Adolesc. Psychiatry* 52, 628–641. doi: 10.1016/j.jaac.2013.04.003

Grillner, S., Helligren, J., Menard, A., Saitoh, K., and Wikstrom, M. A. (2005). Mechanisms for selection of basic motor programs - roles for the striatum and pallidum. *Trends Neurosci.* 28, 364–370. doi: 10.1016/j.tins.2005.05.004

Hacker, C. D., Perlmutter, J. S., Criswell, S. R., Ances, B. M., and Snyder, A. Z. (2012). Resting state functional connectivity of the striatum in Parkinson's disease. *Brain* 135, 3699–3711. doi: 10.1093/brain/aws281

Harrison, B., Soriano-Mas, C., Pujol, J., Ortiz, H., Lopez-Sola, M., Hernandez-Ribas, R., et al. (2009). Altered cortico-striatal functional connectivity in obsessive-compulsive disorder. *Neuroimage* 47:S49.

Helmich, R. C., Derikx, L. C., Bakker, M., Scheeringa, R., Bloem, B. R., and Toni, I. (2010). Spatial remapping of cortico-striatal connectivity in Parkinson's disease. *Cereb. Cortex* 20, 1175–1186.

Hermier, M. (2018). Imaging of hemifacial spasm. *Neurochirurgie* 64, 117–123.

Huang, Y. C., Fan, J. Y., Ro, L. S., Lyu, R. K., Chang, H. S., Chen, S. T., et al. (2009). Validation of a Chinese version of disease specific quality of life scale (HFS-36) for hemifacial spasm in Taiwan. *Health Qual. Life Outcomes* 7:104.

Ledberg, A., Akerman, S., and Poland, P. F. (1998). Estimation of the probabilities of 3D clusters in functional brain images. *Neuroimage* 8, 113–128. doi: 10.1006/nimg.1998.0336

Lehericy, S., Ducros, M., Van de Moortele, P. F., Francois, C., Thivard, L., Poupon, C., et al. (2004). Diffusion tensor fiber tracking shows distinct Corticostriatal circuits in humans. *Ann. Neurol.* 55, 522–529. doi: 10.1002/ana.20030

Loonen, A. J. M., and Ivanova, S. A. (2013). New insights into the mechanism of drug-induced dyskinesia. *CNS Spectr.* 18, 15–20. doi: 10.1017/s1092852912000752

Lu, A. Y., Yeung, J. T., Gerrard, J. L., Michaelides, E. M., Sekula, R. F. Jr., and Bulsara, K. R. (2014). Hemifacial spasm and neurovascular compression. *ScientificWorldJournal* 2014:349319.

Lu, H., Zhang, Q., Zhang, J., Wang, M., Xu, S., Qin, Z., et al. (2018). A research using resting-state fMRI and VBM for HFS. *Chin. J. Magn. Reson. Imaging* 9, 38–42.

Luo, C., Song, W., Chen, Q., Zheng, Z., Chen, K., Cao, B., et al. (2014). Reduced functional connectivity in early-stage drug-naive Parkinson's disease: a resting-state fMRI study. *Neurobiol. Aging* 35, 431–441. doi: 10.1016/j.neurobiolaging.2013.08.018

Niu, X., Xu, H., Guo, C., Yang, T., Kress, D., Gao, L., et al. (2020). Strengthened thalamoparietal functional connectivity in patients with hemifacial spasm: a cross-sectional resting-state fMRI study. *Br. J. Radiol.* 93:20190887. doi: 10.1259/bjr.20190887

Padmanabhan, A., Lynn, A., Foran, W., Luna, B., and O'Hearn, K. (2013). Age related changes in striatal resting state functional connectivity in autism. *Front. Hum. Neurosci.* 7:814. doi: 10.3389/fnhum.2013.00814

Palacios, E., Breaux, J., and Alvernia, J. E. (2008). Hemifacial spasm. *Ear Nose Throat J.* 87, 368–370.

Rosen, G. D., and Williams, R. W. (2001). Complex trait analysis of the mouse striatum: independent QTLs modulate volume and neuron number. *BMC Neurosci.* 2:5. doi: 10.1186/1471-2202-2-5

Rudzińska, M., Wójcik, M., Malec, M., Grabska, N., Szubiga, M., Hartel, M., et al. (2012). Factors affecting the quality of life in hemifacial spasm patients. *Neurol. Neurochir. Pol.* 46, 121–129. doi: 10.5114/ninp.2012.28254

Schroeder, S., Thu Hang, L., Toussaint, M., Kranz, M., Chovsepian, A., Shang, Q., et al. (2020). PET Imaging of the Adenosine A(2A) Receptor in the Rotenone-based mouse model of Parkinson's disease with F-18 FESCH synthesized by a simplified two-step one-pot Radiolabeling strategy. *Molecules* 25:1633. doi: 10.3390/molecules25071633

Song, W., Cao, Z., Lang, C., Dai, M., Xuan, L., Lv, K., et al. (2017). Disrupted functional connectivity of striatal sub-regions in Bell's palsy patients. *Neuroimage Clin.* 14, 122–129.

Tao, H., Guo, S., Ge, T., Kendrick, K. M., Xue, Z., Liu, Z., et al. (2013). Depression uncouples brain hate circuit. *Mol. Psychiatry* 18, 101–111. doi: 10.1038/mp.2011.127

Taylor, W. D., Steffens, D. C., McQuoid, D. R., Payne, M. E., Lee, S. H., Lai, T. J., et al. (2003). Smaller orbital frontal cortex volumes associated with functional disability in depressed elders. *Biol. Psychiatry* 53, 144–149. doi: 10.1016/s0006-3223(02)01490-7

Tu, Y., Wei, Y., Sun, K., Zhao, W., and Yu, B. (2015). Altered spontaneous brain activity in patients with hemifacial spasm: a resting-state functional MRI study. *PLoS One* 10:e0116849. doi: 10.1371/journal.pone.0116849

Unschuld, P. G., Joel, S. E., Liu, X., Shanahan, M., Margolis, R. L., Biglan, K. M., et al. (2012). Impaired cortico-striatal functional connectivity in prodromal Huntington's Disease. *Neurosci. Lett.* 514, 204–209. doi: 10.1016/j.neulet.2012.02.095

Wei, Y., Zhao, W., and Tu, Y. (2015). Resting-state functional magnetic resonance imaging study of the pathogenesis of hemifacial spasm. *Chin. J. Neurosur.* 31, 482–486.

Yan, C. G., Wang, X. D., Zuo, X. N., and Zang, Y. F. (2016). DPABI: data processing & analysis for (resting-state) brain imaging. *Neuroinformatics* 14, 339–351. doi: 10.1007/s12021-016-9299-4

Yan, C. G., Yang, Z., Colcombe, S. J., Zuo, X. N., and Milham, M. P. (2017). Concordance among indices of intrinsic brain function: insights from inter-individual variation and temporal dynamics. *Sci. Bull.* 62, 1572–1584. doi: 10.1016/j.scib.2017.09.015

Conflict of Interest: The authors declare that the research was conducted in the absence of any commercial or financial relationships that could be construed as a potential conflict of interest.

Publisher's Note: All claims expressed in this article are solely those of the authors and do not necessarily represent those of their affiliated organizations, or those of the publisher, the editors and the reviewers. Any product that may be evaluated in this article, or claim that may be made by its manufacturer, is not guaranteed or endorsed by the publisher.

frontiers in Human Neuroscience

ORIGINAL RESEARCH
published: 11 November 2021
doi: 10.3389/fnhum.2021.762343

Alteration of Whole Brain ALFF/fALFF and Degree Centrality in Adolescents With Depression and Suicidal Ideation After Electroconvulsive Therapy: A Resting-State fMRI Study

*Xiao Li[1], Renqiang Yu[2], Qian Huang[1], Xiaolu Chen[3], Ming Ai[1], Yi Zhou[1], Linqi Dai[1], Xiaoyue Qin[4] and Li Kuang[1]**

[1]Department of Psychiatry, The First Affiliated Hospital of Chongqing Medical University, Chongqing, China, [2]Department of Radiology, The First Affiliated Hospital of Chongqing Medical University, Chongqing, China, [3]The First Branch, The First Affiliated Hospital of Chongqing Medical University, Chongqing, China, [4]Department of the First Clinical Medicine, Chongqing Medical University, Chongqing, China

OPEN ACCESS

Edited by:
Min Cai,
Fourth Military Medical University, China

Reviewed by:
Fan Guo,
Fourth Military Medical University, China
Xinyu Hu,
Sichuan University, China
Huawei Tan,
Renmin Hospital of Wuhan University, China

***Correspondence:**
Li Kuang
kuangli0308@163.com

Specialty section:
This article was submitted to Brain Imaging and Stimulation, a section of the journal Frontiers in Human Neuroscience

Received: 21 August 2021
Accepted: 18 October 2021
Published: 11 November 2021

Citation:
Li X, Yu R, Huang Q, Chen X, Ai M, Zhou Y, Dai L, Qin X and Kuang L (2021) Alteration of Whole Brain ALFF/fALFF and Degree Centrality in Adolescents With Depression and Suicidal Ideation After Electroconvulsive Therapy: A Resting-State fMRI Study. Front. Hum. Neurosci. 15:762343. doi: 10.3389/fnhum.2021.762343

Major depressive disorder (MDD) is one of the most widespread mental disorders and can result in suicide. Suicidal ideation (SI) is strongly predictive of death by suicide, and electroconvulsive therapy (ECT) is effective for MDD, especially in patients with SI. In the present study, we aimed to determine differences in resting-state functional magnetic resonance imaging (rs-fMRI) in 14 adolescents aged 12–17 with MDD and SI at baseline and after ECT. All participants were administered the Hamilton Depression Scale (HAMD) and Beck Scale for Suicide Ideation (BSSI) and received rs-fMRI scans at baseline and after ECT. Following ECT, the amplitude of low frequency fluctuation (ALFF) and fractional ALFF (fALFF) significantly decreased in the right precentral gyrus, and the degree centrality (DC) decreased in the left triangular part of the inferior frontal gyrus and increased in the left hippocampus. There were significant negative correlations between the change of HAMD (△HAMD) and ALFF in the right precentral gyrus at baseline, and between the change of BSSI and the change of fALFF in the right precentral gyrus. The △HAMD was positively correlated with the DC value of the left hippocampus at baseline. We suggest that these brain regions may be indicators of response to ECT in adolescents with MDD and SI.

Keywords: MDD, adolescent, ALFF, degree centrality, resting-state fMRI, suicidal ideation, electroconvulsive therapy

INTRODUCTION

Suicide is an important global health concern cited as the 20th leading cause of death worldwide. Major depressive disorder (MDD) is a major risk factor for suicide (Kessler et al., 2005); previous research has reported that approximately 15% of patients with MDD die by suicide (Chen and Dilsaver, 1996; Angst et al., 2013). Moreover, suicide in adolescents has become a severe public health and social dilemma. A 2013 survey of thousands of teenagers found that one in eight demonstrated suicidal ideation (SI; Nock et al., 2013).

SI is defined as "thoughts about death, dying, plans for suicide, or desire for death" (Miller et al., 2018; Levi-Belz et al., 2019), it is strongly predictive of death by suicide (Klonsky et al., 2016). Additionally, MDD with SI is related to higher rates of poor treatment response (Szanto et al., 2003), and is thought to have different neuropsychological correlates compared to MDD without SI (Marzuk et al., 2005). Therefore, measuring SI in patients with MDD is necessary and may help determine the risk of suicide.

There are many challenges in the treatment of MDD in adolescents. Importantly, adolescents do not exhibit the same symptoms as adults, resulting in difficulties in diagnosis (Lee et al., 2019). Some adolescents with depressive symptoms develop bipolar disorder (BD; Egeland et al., 2000), comorbid borderline personality disorder (Horesh et al., 2003), SI, or non-suicidal self-injury (NSSI; Huang et al., 2021); all of which increase the difficulty of treatment.

Electroconvulsive therapy (ECT) has been found to be effective in schizophrenia, depression, and eating disorders (Pagnin et al., 2004; Sanghani et al., 2018; Pacilio et al., 2019). For different psychiatric illnesses or age groups with SI, ECT can be an effective and appropriate treatment option (Ghaziuddin et al., 2020; Meyer et al., 2020). ECT is also considered a treatment option for adolescents with MDD, especially for adolescents with MDD and SI or related behaviors (Puffer et al., 2016; Mitchell et al., 2018). A previous study has found that adolescents with mood disorders who were administered ECT demonstrated a reduction in SI and NSSI (Ghaziuddin et al., 2020).

MRI is widely used to evaluate brain change in MDD patients after ECT, Wilkinson et al. (2017) found ECT induced hippocampal volume changes in MDD patients, a systematic review of fMRI showed the amplitude of low frequency fluctuations (ALFF) changed widely across the brain, such as orbital gyrus, inferior frontal gyrus, precentral gyrus, etc. (Porta-Casteràs et al., 2020). ALFF is an rs-fMRI-derived measure that reflects the magnitude of spontaneous blood-oxygen-level-dependent (BOLD) signal (Nugent et al., 2015). The fractional ALFF (fALFF) is one of the most common metrics used to quantify these oscillations (Zou et al., 2008); however, both have been used to infer brain activity in psychiatric disorders with or without suicidal behaviors (Bu et al., 2019; Lan et al., 2019; Zhang et al., 2020). One recent study investigated ALFF in depressed patients with SI and found higher ALFF values in the right hippocampus and bilateral thalamus and caudate compared to patients without SI (Lan et al., 2019). In addition, Liu et al. (2015) found that a reduction in depressive symptoms was negatively correlated with increased ALFF in the left hippocampus after eight ECT sessions. Degree centrality (DC), which focuses on the relation of a voxel with the connectivity of the entire network (Buckner et al., 2009), can also be used to measure brain function. Gao et al. (2016) found compared with controls, depressive subjects showed decreased DC in the right parahippocampal gyrus, and elevated DC in the left inferior frontal gyrus.

In the present study, we examined whole brain ALFF/fALFF and DC among adolescents with MDD and SI. We hypothesized that: (1) ECT would make ALFF/fALFF and DC changes in adolescents MDD with SI; (2) ECT-induced brain function changes may be the treatment mechanism for MDD with SI.

MATERIALS AND METHODS

Participants

The present study included 14 adolescents with MDD and SI aged 12–17 years. The participants were recruited from the inpatient clinics at the Department of Psychiatry, First Affiliated Hospital of Chongqing Medical University, China. The presence or absence of diagnoses was independently determined by two experienced psychiatrists using the Mini International Neuropsychiatric Interview for Children and Adolescents (MINI-KID).

Clinical symptoms were assessed with the 17-item Hamilton Depression Rating Scale (HAMD-17; Hamilton, 1960). The Chinese version of the instrument has been found to be reliable and valid (Zhao and Zheng, 1992). SI intensity was assessed with the Beck Scale for Suicide Ideation (BSSI; Beck et al., 1979). The BSSI is a 19-item self-report measure designed to assess the current attitude, behaviors, and plan to commit suicide. All items are rated on a 3-point scale of intensity and generate a total score from 0 to 38. The results of the BSSI were confirmed by two psychiatrists through a clinical interview. The Chinese version of the BSSI shows acceptable reliability and validity (Li et al., 2010).

Participants were excluded if they: (1) had a neurological or serious physical condition, any history of alcohol or drug abuse, any other somatic diseases, or morphological anomalies of the brain; (2) had any surgically placed electronic or metal materials that might interfere with fMRI assessment; (3) took medications in recent five drug half-life; or (4) had head motion exceeding 3 mm in translation or 3° in rotation.

The present study protocol was approved by the Human Research and Ethics Committee of the First Affiliated Hospital of Chongqing Medical University (no. 2017-157). Written informed consent was obtained from all adolescents and their caregivers.

Electroconvulsive Therapy

All patients underwent modified bi-fronto-temporal ECT that was conducted using a Thymatron DGx (Somatics, LLC, Lake Bluff, IL, USA) at the First Affiliated Hospital of Chongqing Medical University (Du et al., 2016). The first three courses of ECT took place on continuous days; the remaining courses of ECT were performed every 2 days, with a break on weekends. After 2 weeks, the ECT was complete. The first energy for ECT was determined according to the patient's age: energy percent = age × 0.5%. The stimulation energy was adjusted based on the seizure time. The energy was increased by 5% in the subsequent treatment if the seizure time was <25 s. Anesthesia was induced with succinylcholine (0.5–1 mg/kg) and diprivan (1.5–2 mg/kg). All the patients received antidepressants, with sertraline (n = 9, 64.3%), fluoxetine (n = 5, 35.7%). Ten patients received antipsychotics, with quetiapine (n = 4, 28.6%), olanzapine (n = 4, 28.6%), aripiprazole (n = 2, 14.3%). Two patients received propranolol (n = 2; 29.5%).

Acquisition of rs-fMRI Data

MR images were obtained using a 3T GE Signa HDxt scanner (General Electric Healthcare, Chicago, IL, USA) with an 8-channel head coil. Participants were instructed to relax with their eyes closed, stay awake, and avoid thinking as much as possible. None of the patients reported falling asleep during the scan. Foam pads and earplugs were used to fix their heads to minimize head motion and reduce machine noise, respectively. The echo-planar imaging pulse sequence parameters were as follows: repetition time (TR) = 2,000 ms; echo time (TE) = 40 ms; field of view (FOV) = 240 × 240 mm^2; matrix = 64 × 64; flip angle = 90°; slice number = 33; slice thickness/gap = 4.0/0 mm; scanner time = 8 min; and 240 volumes. Three-dimensional T1-weighted MR images were used for rs-fMRI co-registration *TR* = 24 ms; *TE* = 9 ms; *FOV* = 240 × 240 mm^2; matrix = 256 × 256; flip angle = 90°; and slice thickness/gap = 1.0/0 mm.

Image Preprocessing

All data preprocessing was performed in MATLAB (MathWorks, Natick, MA, USA) using DPARSF (version 4.3; Data Processing Assistant for Resting-State fMRI[1]), which is based on SPM12[2]. The first five time points were discarded to allow for signal equilibration. Images were then corrected for slice timing and head motion. Functional images were spatially normalized to the Montreal Neurological Institute space and resampled at 3 × 3 × 3 mm^3. Nuisance regression was performed using the 24 head motion parameters, white matter, and cerebrospinal fluid signals as covariates. Linear trends were removed. Finally, the images were bandpass filtered (0.01–0.1 Hz) to reduce low-frequency drift and high-frequency physiological noise.

Calculation of rs-fMRI Measures

The ALFF measures regional spontaneous neural activity (Zang et al., 2007). Each preprocessed fMRI data set was transformed to a frequency domain with a fast Fourier transformation. The square root of the power spectrum was calculated, and the ALFF was obtained as the averaged square root across 0.01–0.1 Hz. The ALFF value of each voxel was then divided by the global mean ALFF value for each participant to reduce the global effects. ALFF was computed as the mean power spectrum in a specific low-frequency band (0.01–0.1 Hz; Zang et al., 2007), and the fALFF was the ratio of the power spectrum in the low-frequency band (0.01–0.1 Hz) to the entire frequency range (Zou et al., 2008). The fALFF value of each voxel was then divided by the global mean fALFF value for each participant to reduce the global effects.

The DC measures the mean correlation between a given region of interest (ROI) and all other ROIs in the functional brain network (Zang et al., 2004). An ROI with a higher DC value suggests that it is more functionally connected with other ROIs than one with a lower DC value. In graph theory, DC is defined as the number (binary graph) or the sum of weights (weighted graph) of edges connecting to a node. Here, we computed Pearson's correlation coefficients between the BOLD time courses of all pairs of voxels and obtained a whole gray matter functional connectivity matrix for each participant. For a given voxel, DC was computed as the sum of positive functional connectivity above a threshold of 0.25 between that voxel and all other voxels within the gray matter (Buckner et al., 2009; Zuo et al., 2012). The individual level DC map was converted into a z-score map by subtracting the mean of the brain mask DC and dividing by the standard deviation of the whole brain mask DC.

[1]http://www.restfmri.net

[2]http://www.fil.ion.ucl.ac.uk/spm

Statistical Analysis

To investigate the differences in the demographics and clinical characteristics of the patients, pre/post-treatment, the paired sample t-test was used for continuous variables. The paired sample t-test was performed in SPM12 to examine differences in ALFF, fALFF, and DC between participants pre/post-treatment. All other statistical analyses were conducted using SPSS (version 25.0; IBM, Armonk, NY, USA) with a statistical significance of $P < 0.05$ [false discovery rate (FDR) corrected].

At baseline, Pearson correlation analyses were performed to examine the correlations between the mean value of measures in the brain regions showing significant differences and clinical symptoms (HAMD/BSSI). After treatment, Pearson correlation analyses were used to examine whether the changes of these measures were correlated with the changes in clinical symptoms. Changes in HAMD (△HAMD) and BSSI (△BSSI) were calculated using the following equations:

$$\triangle \mathrm{HAMD} = \frac{\mathrm{preHAMD} - \mathrm{postHAMD}}{\mathrm{preHAMD}}$$

$$\triangle \mathrm{BSSI} = \frac{\mathrm{preBSSI} - \mathrm{postBSSI}}{\mathrm{preBSSI}}$$

Pearson correlation analyses were also used to examine whether these measures at baseline were correlated with changes in clinical symptoms (△HAMD/△BSSI).

RESULTS

The psychological measurements and demographic data are listed in **Table 1**. Compared to post-treatment, participants pre-treatment demonstrated more severe symptoms according to HAMD and BSSI scores. There were significant improvements in HAMD scores ($P < 0.001$) and BSSI scores ($P < 0.001$; **Table 1**).

Compared to pre-treatment, adolescents post-treatment exhibited decreased ALFF and fALFF in the right precentral gyrus (Precentral_R; **Figures 1**, **2A**, **3**, **4A**; **Table 2**). Moreover, post-treatment, decreased DC values were found in the left triangular part of the inferior frontal gyrus (Frontal_Inf_Tri_L) and increased DC values in the left hippocampus (Hippocampus_L; **Figures 5**, **6A,B**; **Table 2**).

We found significantly negative correlations between the △HAMD and ALFF of the Precentral_R at baseline ($r = -0.5990$, $P = 0.0236$; **Figure 2B**) and between the △BSSI and the change of fALFF in the Precentral_R ($r = -0.6302$, $P = 0.0157$;

TABLE 1 | Demographics and clinical characteristics pre/post-treatment.

Characteristic	Pre-treatment (*n* = 14)	Post-treatment (*n* = 14)	*P*
Age, mean (SD), y	14.57 (1.45)	/	
Sex (Male/Female)	5/9	5/9	
Education years, mean (SD), y	8.35 (1.39)	/	
HAMD, mean (SD)	30.14 (3.78)	11.36 (3.13)	<0.001
BSSI, mean (SD)	21.43 (3.67)	6.93 (3.58)	<0.001

Note: HAMD, Hamilton depression scale; BSSI, Beck scale for suicide ideation; SD, Standard deviation.

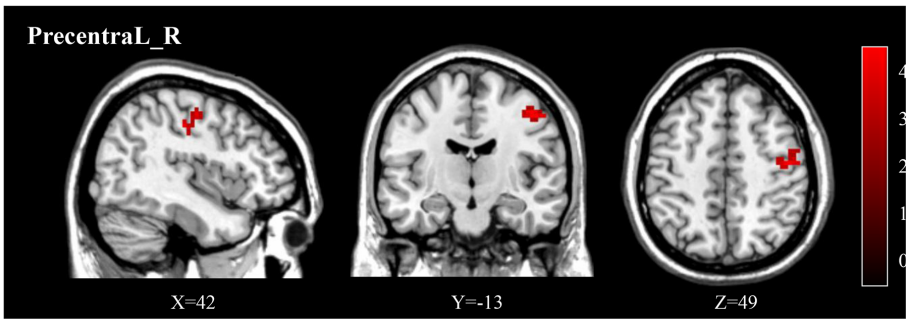

FIGURE 1 | The post-treatment adolescents with MDD exhibited a significantly decreased ALFF in the right precentral gyrus (Precentral_R). ALFF, amplitude of low frequency fluctuation; MDD, Major depressive disorder.

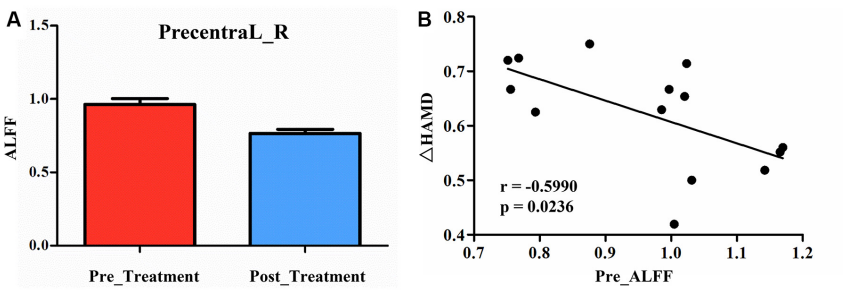

FIGURE 2 | **(A)** Post-treatment, adolescents exhibited a significantly decreased ALFF in the right precentral gyrus (Precentral_R). **(B)** The negative correlations between △HAMD and ALFF of the Precentral_R at baseline. HAMD, Hamilton depression scale.

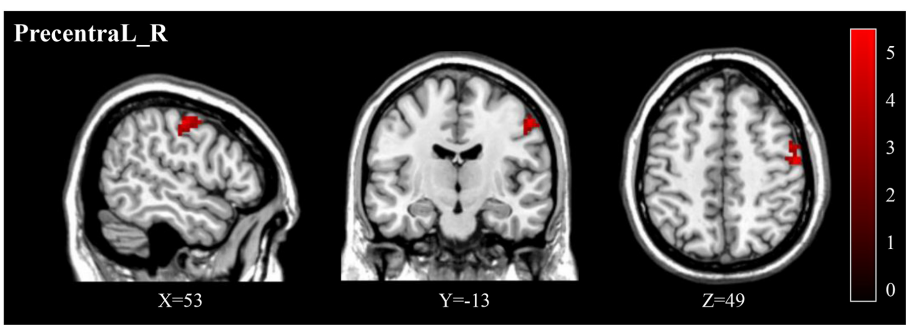

FIGURE 3 | Post-treatment, adolescents exhibited a significantly decreased fALFF in the right precentral gyrus (Precentral_R). fALFF, fractional ALFF.

Figure 4B). In addition, correlation analysis demonstrated that △HAMD was positively correlated with the DC value of the Hippocampus_L at baseline (r = 0.5480, P = 0.0425; **Figure 6C**).

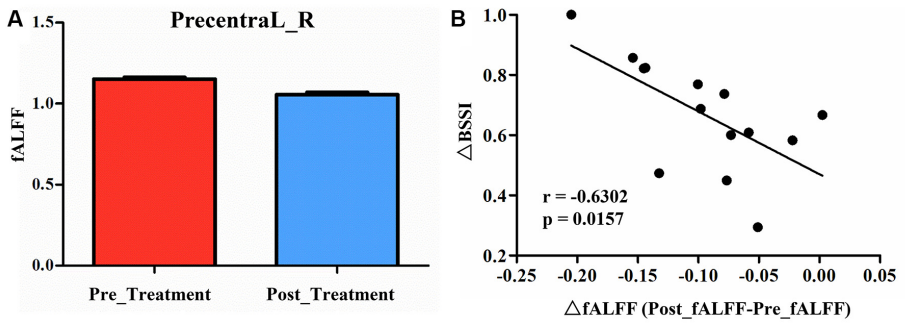

FIGURE 4 | (A) Post-treatment, adolescents exhibited a significantly decreased fALFF in the right precentral gyrus (Precentral_R). **(B)** The negative correlations between the △BSSI and △fALFF in the Precentral_R.

TABLE 2 | Significant differences in ALFF, fALFF, and DC between depression adolescents pre/post-treatment.

Measures	Brain regions	Voxel size	Peak T value	MNI coordinates		
Decreased						
ALFF	PrecentraL_R	71	4.40	46	−12	46
fALFF	PrecentraL_R	52	5.10	51	−9	51
DC	Frontal_Inf_Tri_L	70	5.65	−45	42	6
Increased						
DC	Hippocampus_L	105	6.40	−27	−39	0

Note: DC, degree centrality; MNI, Montreal Neurological Institute.

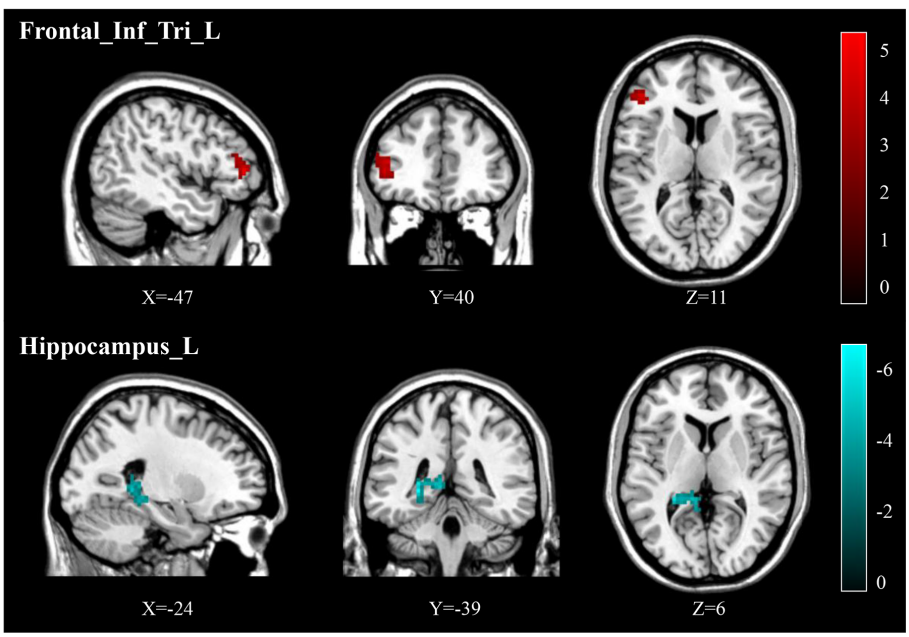

FIGURE 5 | Post-treatment, adolescents exhibited decreased DC in the triangular part of the left inferior frontal gyrus (Frontal_Inf_Tri_L) and increased DC in the left hippocampus (Hippocampus_L).

DISCUSSION

In our present study, in a sample of adolescent patients with MDD and SI, the severity of both MDD and SI substantially decreased after 2 weeks of ECT. Previous studies have found that 2 weeks of repetitive transcranial magnetic stimulation could decrease HAMD scores significantly in adults with increased regional function in the left dorsolateral

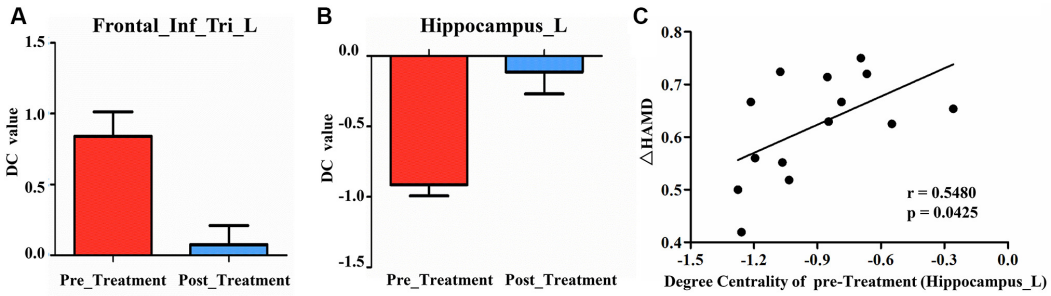

FIGURE 6 | (A) Post-treatment, adolescents exhibited decreased DC in the triangular part of the left inferior frontal gyrus (Frontal_Inf_Tri_L). **(B)** Post-treatment, adolescents exhibited increased DC in the left hippocampus (Hippocampus_L). **(C)** Our correlation analysis showed that △HAMD was positively correlated with the DC value of Hippocampus_L at baseline.

prefrontal cortex (Zheng et al., 2020), but did not discuss SI. Shen et al. (2015) found that 2 weeks of pharmacological therapy could alter DC in the middle frontal gyrus and precuneus; however, this study also lacked focus on SI. Post-ECT, our present study found changed brain function in the precentral gyrus, hippocampus, and the triangular part of the inferior frontal gyrus, which may indicate the mechanism of action behind the efficacy of ECT in adolescents with MDD and SI.

Studies have demonstrated that the hippocampus has been linked to mood disorders that begin during adolescence, which show major cognitive and emotional disturbances (Masi and Brovedani, 2011; Hueston et al., 2017). Other previous studies have found that ECT induces structural changes in the hippocampus (Redlich et al., 2016; Sartorius et al., 2016). The most consistent finding from previous studies on the hippocampus depicted substantial reductions in hippocampal volume in MDD patients compared to healthy controls, which increased following ECT (Boccia et al., 2015; Arnone et al., 2016; Peng et al., 2016). Tendolkar et al. (2013) found bilateral volume increases in the hippocampus after ECT, which was further verified to occur in the right hippocampus by Abbott et al. (2014). Smaller hippocampal volumes were found in patients with MDD and a history of SA compared to those without SA (Colle et al., 2015). Therefore, this may indicate that a potential mechanism underlying ECT in MDD is through the increase in hippocampal volume.

Additional previous studies have found that DC differed between in psychiatric disorders; One study demonstrated that DC changes in the hippocampus are related to delayed encephalopathy after carbon monoxide poisoning (DEACMP). Compared with healthy controls, DEACMP patients with cognition disturbances displayed significantly decreased DC values in the right hippocampus but increased DC values in the right inferior frontal gyrus, which is inconsistent with our results (Wu et al., 2020). This inconsistency may be related to differences in characteristics or diseases, but can also indicate that abnormal brain function in the hippocampus may present as changed DC. An additional study found that decreased DC values in the frontoparietal network could distinguish patients who had experienced SA from those with SI, but it focused on adults and lacked longitudinal data (Wagner et al., 2021). A 2-week pharmacological therapy for MDD patients found correlations in baseline DC with changes in the HAMD scores, including in the precuneus, supramarginal gyrus, middle temporal, but not in the hippocampus, this might be due to different treatment compared with our study (Shen et al., 2015). In the present study, we also found decreased DC in the inferior frontal gyrus post-ECT, which was consistent with previous studies demonstrating that patients with past SA had abnormal brain activity and DC values were found in the inferior frontal gyrus (Makris et al., 2007; Wagner et al., 2021). Wu et al. (2021) found patients with MDD showed abnormal DC in the prefrontal cortex (PFC), and the DC of PFC was negatively correlated with the course of the disease, not with the HAMD scores, however, these results should be interpreted cautiously with ours. Therefore, further studies are needed.

Previous studies found that patients with MDD have altered ALFF/fALFF in various regions, such as the precentral gyrus. Wang et al. (2012) found that patients with MDD demonstrated increased ALFF in the right fusiform gyrus, but no change in the precentral gyrus; however, the fALFF in patients was significantly increased in the right precentral gyrus compared to healthy controls. For MDD patients with SI, Chen et al. (2021) found higher mfALFF of the right middle temporal pole gyrus in the SI group compared with the NS group, similar results were not found in the precentral gyrus, but a positive correlation between depression score and mfALFF was found in the right postcentral gyrus, showed high HAMD scores correlated with higher mfALFF, which was similar with our study. Kong et al. (2017) found that older patients with MDD administered ECT demonstrated decreased ALFF values in the precentral gyrus compared to pre-treatment, which is consistent with our results. We suggest that lower ALFF/fALFF in the precentral gyrus may indicate better outcomes for patients with MDD.

Several studies have focused on the changes of ALFF/fALFF in adolescents with MDD pre/post-treatment, with treatment options being pharmacotherapy, psychotherapy, or pharmacotherapy combined with psychotherapy. Kim et al. (2018) found behavioral difficulties in adolescent bullies with

depressed mood, and after cognitive behavioral therapy (CBT), decreased fALFF in the inferior parietal lobule and the lingual, interior frontal, and middle occipital gyri were demonstrated. Shu et al. (2020) found that in young patients with MDD and SA after CBT and antidepressant co-therapy, fALFF in the left middle occipital cortex and left precuneus were significantly increased in the CBT group compared with the healthy control group. Fan et al. (2013) found SA patients had increased ALFF in the right superior temporal gyrus relative to non-suicidal patients. Cao et al. (2016) found the SA group showed increased zALFF in the right superior temporal, left middle temporal, and left middle occipital gyri in young patients with MDD aged 15–29 years, but additional research is lacking.

These aforementioned studies are only partly consistent with our current research. This may be related to different treatment options, methods of patient evaluation, the severity of disease, and diagnosis. Notably, it can be difficult to distinguish unipolar from bipolar depression in adolescents. There are limited studies that aim to understand the efficacy of ECT using fMRI in adolescents with MDD and SI; our results suggest that changes in ALFF/fALFF and DC after ECT in various brain regions may be a potential mechanism behind the efficacy of ECT in adolescents with MDD and SI.

Limitations

Several limitations of our current study should be noted. First, our sample size was small, possibly due to concerns about ECT side effects. Second, there was a lack of healthy controls to compare the brain function with the patient group at baseline; therefore, further research is needed.

CONCLUSION

We found decreased ALFF/fALFF in the right precentral gyrus, decreased DC in the triangular part of the left inferior frontal gyrus and increased DC in the left hippocampus in adolescents with MDD and SI after ECT. ALFF in the right precentral gyrus at baseline and DC in the left hippocampus at baseline, changes in fALFF in the right precentral gyrus were correlated with treatment outcome. We suggest that these brain regions may be potential indicators of ECT response in adolescents with MDD and SI.

DATA AVAILABILITY STATEMENT

The raw data supporting the conclusions of this article will be made available by the authors, without undue reservation.

ETHICS STATEMENT

The studies involving human participants were reviewed and approved by Human Research and Ethics Committee of the First Affiliated Hospital of Chongqing Medical University (no. 2017-157). Written informed consent to participate in this study was provided by the participants' legal guardian/next of kin.

AUTHOR CONTRIBUTIONS

XL conceived the structure of the manuscript and wrote the manuscript. RY and QH prepared the samples and did fMRI. XC, YZ, LD, and XQ analyzed the data. MA and LK critically reviewed the manuscript. All authors have read and approved the final manuscript. All authors contributed to the article and approved the submitted version.

FUNDING

This work was supported by the National Natural Science Foundation of China (No.: 81971286).

ACKNOWLEDGMENTS

We sincerely appreciate all the participants and their families for participating in our study.

REFERENCES

Abbott, C. C., Jones, T., Lemke, N. T., Gallegos, P., McClintock, S. M., Mayer, A. R., et al. (2014). Hippocampal structural and functional changes associated with electroconvulsive therapy response. *Transl. Psychiatry* 4:e483. doi: 10.1038/tp.2014.124

Angst, J., Hengartner, M. P., Gamma, A., von Zerssen, D., and Angst, F. (2013). Mortality of 403 patients with mood disorders 48 to 52 years after their psychiatric hospitalisation. *Eur. Arch. Psychiatry Clin. Neurosci.* 263, 425–434. doi: 10.1007/s00406-012-0380-1

Arnone, D., Job, D., Selvaraj, S., Abe, O., Amico, F., Cheng, Y., et al. (2016). Computational meta-analysis of statistical parametric maps in major depression. *Hum. Brain Mapp.* 37, 1393–1404. doi: 10.1002/hbm.23108

Beck, A. T., Kovacs, M., and Weissman, A. (1979). Assessment of suicidal intention: the scale for suicide ideation. *J. Consult. Clin. Psychol.* 47, 343–352. doi: 10.1037//0022-006x.47.2.343

Boccia, M., Acierno, M., and Piccardi, L. (2015). Neuroanatomy of Alzheimer's disease and late life depression: a coordinate-based meta-analysis of MRI studies. *J. Alzheimers Dis.* 46, 963–970. doi: 10.3233/JAD-142955

Bu, X., Hu, X., Zhang, L. Q., Li, B., Zhou, M., Lu, L., et al. (2019). Investigating the predictive value of different resting-state functional MRI parameters in obsessive-compulsive disorder. *Transl. Psychiatry* 9:17. doi: 10.1038/s41398-018-0362-9

Buckner, R. L., Sepulcre, J., Taludar, T., Krienen, F. M., Liu, H., Hedden, T., et al. (2009). Cortical hubs revealed by intrinsic functional connectivity: mapping, assessment of stability, and relation to Alzheimer's disease. *J. Neurosi.* 29, 1860–1873. doi: 10.1523/JNEUROSCI.5062-08.2009

Cao, J., Chen, X. R., Chen, J. M., Ai, M., Gan, Y., Wang, W., et al. (2016). Resting-state functional MRI of abnormal baseline brain activity in young depressed patients with and without suicidal behavior. *J. Affect. Disord.* 205, 252–263. doi: 10.1016/j.jad.2016.07.002

Chen, V. C.-H., Chou, Y.-S., Tsai, Y.-H., Huang, Y.-C., Mclntyre, R. S., and Weng, J.-C. (2021). Resting-state functional connectivity and brain network abnormalities in depressive patients with suicidal ideation. *Brain Topogr.* 34, 234–244. doi: 10.1007/s10548-020-00817-x

Chen, Y. W., and Dilsaver, S. C. (1996). Lifetime rates of suicide attempts among subjects with bipolar and unipolar disorders relative to subjects with other Axis I disorders. *Biol. Psychiatry* 39, 896–899. doi: 10.1016/0006-3223(95)00295-2

Colle, R., Chupin, M., Cury, C., Vandendrie, C., Gressier, F., Hardy, P., et al. (2015). Depressed suicide attempters have smaller hippocampus than depressed patients without suicide attempts. *J. Psychiatr. Res.* 61, 13–18. doi: 10.1016/j.jpsychires.2014.12.010

Du, L., Qiu, H., Liu, H., Zhao, W., Tang, Y., Fu, Y., et al. (2016). Changes in problem-solving capacity and association with spontaneous brain activity after a single electroconvulsive treatment in major depressive disorder. *J. ECT* 32, 49–54. doi: 10.1097/YCT.0000000000000269

Egeland, J. A., Hostetter, A. M., Pauls, D. L., and Sussex, J. N. (2000). Prodromal symptoms before onset of manic-depressive disorder suggested by first hospital admission histories. *J. Am. Acad. Child Adolesc. Psychiatry* 39, 1245–1252. doi: 10.1097/00004583-200010000-00011

Fan, T. T., Wu, X., Yao, L., and Dong, J. (2013). Abnormal baseline brain activity in suicidal and non-suicidal patients with major depressive disorder. *Neurosci. Lett.* 534, 35–40. doi: 10.1016/j.neulet.2012.11.032

Gao, C. H., Liu, W. H., Liu, Y. L., Ruan, X. H., Chen, X., Liu, L. L., et al. (2016). Decreased subcortical and increased cortical degree centrality in a nonclinical college student sample with subclinical depressive symptoms: a resting-state fMRI study. *Front. Hum. Neurosci.* 10:617. doi: 10.3389/fnhum.2016.00617

Ghaziuddin, N., Shamseddeen, W., Gettys, G., and Ghaziuddin, M. (2020). Electroconvulsive therapy for the treatment of severe mood disorders during adolescence: a retrospective chart review. *J. Child Adolesc. Psychopharmacol.* 30, 235–243. doi: 10.1089/cap.2019.0054

Hamilton, M. (1960). A rating scale for depression. *J. Neurol. Neurosurg. Psychiatry* 23, 56–62. doi: 10.1136/jnnp.23.1.56

Horesh, N., Orbach, I., Gothelf, D., Efrati, M., and Apter, A. (2003). Comparison of the suicidal behavior of adolescent inpatients with borderline personality disorder and major depression. *J. Nerv. Ment. Dis.* 191, 582–588. doi: 10.1097/01.nmd.0000087184.56009.61

Huang, Q., Xiao, M., Ai, M., Chen, J., Wang, W., Hu, L., et al. (2021). Disruption of neural activity and functional connectivity in adolescents with major depressive disorder who engage in non-suicidal self-injury: a resting-state fMRI study. *Front. Psychiatry* 12:571532. doi: 10.3389/fpsyt.2021.571532

Hueston, C. M., Cryan, J. F., and Nolan, Y. M. (2017). Stress and adolescent hippocampal neurogenesis: diet and exercise as cognitive modulators. *Transl. Psychiatry* 7:e1081. doi: 10.1038/tp.2017.48

Kessler, R. C., Chiu, W. T., Demler, O., Merikangas, K. R., and Walters, E. E. (2005). Prevalence, severity, and comorbidity of 12-month DSM-IV disorders in the National Comorbidity Survey Replication. *Arch. Gen. Psychiatry* 62, 617–627. doi: 10.1001/archpsyc.62.6.617

Kim, J. I., Kang, Y.-H., Lee, J. M., Cha, J.-H., Park, Y.-H., Kweon, K.-J., et al. (2018). Resting-state functional magnetic resonance imaging investigation of the neural correlates of cognitive-behavioral therapy for externalizing behavior problems in adolescent bullies. *Prog. Neuropsychopharmacol. Biol. Psychiatry* 86, 193–202. doi: 10.1016/j.pnpbp.2018.05.024

Klonsky, E. D., May, A. M., and Safer, B. Y. (2016). Suicide, suicide attempts, and suicidal ideation. *Annu. Rev. Clin. Psychol.* 12, 307–330. doi: 10.1146/annurev-clinpsy-021815-093204

Kong, X.-M., Xu, S.-X., Sun, Y., Wang, K.-Y., Wang, C., Zhang, J., et al. (2017). Electroconvulsive therapy changes the regional resting state function measured by regional homogeneity (ReHo) and amplitude of low frequency fluctuations (ALFF) in elderly major depressive disorder patients: an exploratory study. *Psychiatry Res. Neuroimaging* 264, 13–21. doi: 10.1016/j.pscychresns.2017.04.001

Lan, M. J., Rizk, M. M., Pantazatos, S. P., Falcone, H. R., Miller, J. M., Sublette, M. E., et al. (2019). Resting-state amplitude of low-frequency fluctuation is associated with suicidal ideation. *Depress Anxiety* 36, 433–441. doi: 10.1002/da.22888

Lee, H.-J., Kim, S.-H., and Lee, M.-S. (2019). Understanding mood disorders in children. *Adv. Exp. Med. Biol.* 1192, 251–261. doi: 10.1007/978-981-32-9721-0_12

Levi-Belz, Y., Gavish-Marom, T., Barzilay, S., Apter, A., Carli, V., Hoven, C., et al. (2019). Psychosocial factors correlated with undisclosed suicide attempts to significant others: findings from the adolescence seyle study. *Suicide Life Threat. Behav.* 49, 759–773. doi: 10.1111/sltb.12475

Li, X. Y., Phillips, M. R., Tong, Y. S., Li, K. J., Zhang, Y. L., Zhang, Y. P., et al. (2010). Reliability and validity of the Chinese version of Beck Suicide Ideation Scale (BSI-CV) in adult community residents. *Chin. Ment. Health J.* 24, 250–255. doi: 10.3969/j.issn.1000-6729.2010.04.003

Liu, Y., Du, L., Li, Y., Liu, H., Zhao, W., Liu, D., et al. (2015). Antidepressant effects of electroconvulsive therapy correlate with subgenual anterior cingulate activity and connectivity in depression. *Medicine* 94:e2033. doi: 10.1097/MD.0000000000002033

Makris, N., Papadimitriou, G. M., Sorg, S., Kennedy, D. N., Caviness, V. S., and Pandya, D. N. (2007). The occipitofrontal fascicle in humans: a quantitative, *in vivo*, DT-MRI study. *NeuroImage* 37, 1100–1111. doi: 10.1016/j.neuroimage.2007.05.042

Marzuk, P. M., Hartwell, N., Leon, A. C., and Portera, L. (2005). Executive functioning in depressed patients with suicidal ideation. *Acta Psychiatr. Scand.* 112, 294–301. doi: 10.1111/j.1600-0447.2005.00585.x

Masi, G., and Brovedani, P. (2011). The hippocampus, neurotrophic factors and depression: possible implications for the pharmacotherapy of depression. *CNS Drugs* 25, 913–931. doi: 10.2165/11595900-000000000-00000

Meyer, J. P., Swetter, S. K., and Kellner, C. H. (2020). Electroconvulsive therapy in geriatric psychiatry: a selective review. *Clin. Geriatr. Med.* 36, 265–279. doi: 10.1016/j.cger.2019.11.007

Miller, A. B., McLaughlin, K. A., Busso, D. S., Brueck, S., Peverill, M., and Sheridan, M. A. (2018). Neural correlates of emotion regulation and adolescent suicidal ideation. *Biol. Psychiatry Cogn. Neurosci. Neuroimaging* 3, 125–132. doi: 10.1016/j.bpsc.2017.08.008

Mitchell, S., Hassan, E., and Ghaziuddin, N. (2018). A follow-up study of electroconvulsive therapy in children and adolescents. *J. ECT* 34, 40–44. doi: 10.1097/YCT.0000000000000452

Nock, M. K., Green, J. G., Hwang, I., McLaughlin, K. A., Sampson, N. A., Zaslavsky, A. M., et al. (2013). Prevalence, correlates and treatment of lifetime suicidal behavior among adolescents: results from the National Comorbidity Survey Replication Adolescent Supplement. *JAMA Psychiatry* 70, 300–310. doi: 10.1001/2013.jamapsychiatry.55

Nugent, A. C., Martinez, A., D'Alfonso, A., Zarate, C. A., and Theodore, W. H. (2015). The relationship between glucose metabolism, resting-state fMRI BOLD signal, and $GABA_A$-binding potential: a preliminary study in healthy subjects and those with temporal lobe epilepsy. *J. Cereb. Blood Flow Metab.* 35, 583–591. doi: 10.1038/jcbfm.2014.228

Pacilio, R. M., Livingston, R. K., and Gordon, M. R. (2019). The use of electroconvulsive therapy in eating disorders: a systematic literature review and case report. *J. ECT* 35, 272–278. doi: 10.1097/YCT.0000000000000599

Pagnin, D., de Queiroz, V., Pini, S., and Battista Cassano, G. (2004). Efficacy of ECT in depression: a meta-analytic review. *J. ECT* 20, 13–20. doi: 10.1097/00124509-200403000-00004

Peng, W., Chen, Z. Q., Yin, L., Jia, Z. Y., and Gong, Q. Y. (2016). Essential brain structural alterations in major depressive disorder: a voxel-wise meta-analysis on first episode, medication-naïve patients. *J. Affect. Disord.* 199, 114–123. doi: 10.1016/j.jad.2016.04.001

Porta-Casteràs, D., Cano, M., Camprodon, J. A., Loo, C., Palao, D., Soriano-Mas, C., et al. (2020). A multimetric systematic review of fMRI findings in patients with MDD receiving ECT. *Prog. Neuropsychopharmacol. Biol. Psychiatry* 108:110178. doi: 10.1016/j.pnpbp.2020.110178

Puffer, C. C., Wall, C. A., Huxsahl, J. E., and Frye, M. A. (2016). A 20-year practice review of electroconvulsive therapy in adolescents. *J. Child Adolesc. Psychopharmacol.* 26, 632–636. doi: 10.1089/cap.2015.0139

Redlich, R., Opel, N., Grotegerd, D., Dohm, K., Zaremba, D., Burger, C., et al. (2016). Prediction of individual response to electroconvulsive therapy *via* machine learning on structural magnetic resonance imaging data. *JAMA Psychiatry* 73, 557–564. doi: 10.1001/jamapsychiatry.2016.0316

Sanghani, S. N., Petrides, G., and Kellner, C. H. (2018). Electroconvulsive therapy (ECT) in schizophrenia: a review of recent literature. *Curr. Opin. Psychiatry* 31, 213–222. doi: 10.1097/YCO.0000000000000418

Sartorius, A., Demirakca, T., Bohringer, A., Clemm von Hohenberg, C., Aksay, S. S., Bumn, J. M., et al. (2016). Electroconvulsive therapy increases temporal gray matter volume and cortical thickness. *Eur. Neuropsychopharmacol.* 26, 506–517. doi: 10.1016/j.euroneuro.2015.12.036

Shen, Y., Yao, J., Jiang, X., Zhang, L., Xu, L., Feng, R., et al. (2015). Sub-hubs of baseline functional brain networks are related to early improvement following

two-week pharmacological therapy for major depressive disorder. *Hum. Brain Mapp.* 36, 2915–2927. doi: 10.1002/hbm.22817

Shu, Y. P., Kuang, L., Huang, Q. K., and He, L. H. (2020). Fractional amplitude of low-frequency fluctuation (fALFF) alterations in young depressed patients with suicide attempts after cognitive behavioral therapy and antidepressant medication cotherapy: a resting-state fMRI study. *J. Affect. Disord.* 276, 822–828. doi: 10.1016/j.jad.2020.07.038

Szanto, K., Mulsant, B. H., Houck, P., Dew, M. A., and Reynolds, C. F. (2003). Occurrence and course of suicidality during short-term treatment of late-life depression. *Arch. Gen. Psychiatry* 60, 610–617. doi: 10.1001/archpsyc.60.6.610

Tendolkar, I., Van Beek, M., Van Oostrom, I., Mulder, M., Janzing, J., Voshaar, R. O., et al. (2013). Electroconvulsive therapy increases hippocampal and amygdala volume in therapy refractory depression: a longitudinal pilot study. *Psychiatry Res.* 214, 197–203. doi: 10.1016/j.pscychresns.2013.09.004

Wagner, G., Li, M., Sacchet, M. D., Turecki, G., Gotlib, I. H., Walter, M., et al. (2021). Functional network alterations differently associated with suicidal ideas and acts in depressed patients: an indirect support to the transition model. *Transl. Psychiatry* 11:100. doi: 10.1038/s41398-021-01232-x

Wang, L., Dai, W. J., Su, Y. N., Wang, G., Tan, Y. L., and Jin, Z. (2012). Amplitude of low-frequency oscillations in first-episode, treatment-naive patients with major depressive disorder: a resting-state functional MRI study. *PLoS One* 7:e48658. doi: 10.1371/journal.pone.0048658

Wilkinson, S. T., Sanacora, G., and Bloch, M. H. (2017). Hippocampal volume changes following electroconvulsive therapy: a systematic review and meta-analysis. *Biol. Psychiatry Cogn. Neurosci. Neuroimaging* 2, 327–335. doi: 10.1016/j.bpsc.2017.01.011

Wu, K. F., Liu, M., He, L. C., and Tan, Y. M. (2020). Abnormal degree centrality in delayed encephalopathy after carbon monoxide poisoning: a resting-state fMRI study. *Neuroradiology* 62, 609–616. doi: 10.1007/s00234-020-02369-0

Wu, Z., Zhong, Y., Dai, Y. L., Xiao, C. Y., Zhang, N., and Wang, C. (2021). Differential patterns of dynamic functional connectivity variability in major depressive disorder treated with cognitive behavioral therapy. *J. Affect. Disord.* 291, 322–328. doi: 10.1016/j.jad.2021.05.017

Zang, Y.-F., He, Y., Zhu, C.-Z., Cao, Q.-J., Sui, M.-Q., Liang, M., et al. (2007). Altered baseline brain activity in children with ADHD revealed by resting-state functional MRI. *Brain Dev.* 29, 83–91. doi: 10.1016/j.braindev.2006.07.002

Zang, Y., Jiang, T., Lu, Y., He, Y., and Tian, L. (2004). Regional homogeneity approach to fMRI data analysis. *NeuroImage* 22, 394–400. doi: 10.1016/j.neuroimage.2003.12.030

Zhang, Z., Zhou, X., Liu, J. P., Qin, L., Yu, L., Pan, X. M., et al. (2020). Longitudinal assessment of resting-state fMRI in temporal lobe epilepsy: atwo-year follow-up study. *Epilepsy Behav.* 103:106858. doi: 10.1016/j.yebeh.2019.106858

Zhao, J. P., and Zheng, Y. P. (1992). Reliability and validity of hamilton depression scale assessed in 329 chinese depression patients. *Chin. Ment. Health J.* 5, 214–216.

Zheng, A., Yu, R., Du, W., Liu, H., Zhang, Z., Xu, Z., et al. (2020). Two-week rTMS-induced neuroimaging changes measured with fMRI in depression. *J. Affect. Disord.* 270, 15–21. doi: 10.1016/j.jad.2020.03.038

Zou, Q.-H., Zhu, C.-Z., Yang, Y., Zuo, X.-N., Long, X.-Y., Cao, Q.-J., et al. (2008). An improved approach to detection of amplitude of low-frequency fluctuation (ALFF) for resting-state fMRI: fractional ALFF. *J. Neurosci. Methods* 172, 137–141. doi: 10.1016/j.jneumeth.2008.04.012

Zuo, X.-N., Ehmke, R., Mennes, M., Imperati, D., Castellanos, F. X., Sporns, O., et al. (2012). Network centrality in the human functional connectome. *Cereb. Cortex* 22, 1862–1875. doi: 10.1093/cercor/bhr269

Conflict of Interest: The authors declare that the research was conducted in the absence of any commercial or financial relationships that could be construed as a potential conflict of interest.

Publisher's Note: All claims expressed in this article are solely those of the authors and do not necessarily represent those of their affiliated organizations, or those of the publisher, the editors and the reviewers. Any product that may be evaluated in this article, or claim that may be made by its manufacturer, is not guaranteed or endorsed by the publisher.

frontiers | Frontiers in Human Neuroscience

ORIGINAL RESEARCH
published: 07 April 2022
doi: 10.3389/fnhum.2022.838181

Distinct Brain Dynamic Functional Connectivity Patterns in Schizophrenia Patients With and Without Auditory Verbal Hallucinations

Yao Zhang[1†], Jia Wang[2†], Xin Lin[2†], Min Yang[3†], Shun Qi[4], Yuhan Wang[5], Wei Liang[6], Huijie Lu[6], Yan Zhang[6], Wensheng Zhai[2], Wanting Hao[1], Yang Cao[6], Peng Huang[6], Jianying Guo[1]*, Xuehui Hu[7]* and Xia Zhu[6]**

[1] Military Medical Center, Xijing Hospital, Fourth Military Medical University, Xi'an, China, [2] School of Biomedical Engineering, Fourth Military Medical University, Xi'an, China, [3] Fundamentals Department, Air Force Engineering University, Xi'an, China, [4] Department of Radiology, Fourth Military Medical University, Xi'an, China, [5] School of Basic Medicine, Fourth Military Medical University, Xi'an, China, [6] Department of Medical Psychology, Fourth Military Medical University, Xi'an, China, [7] Department of Nursing, Xijing Hospital, Fourth Military Medical University, Xi'an, China

Schizophrenia patients with auditory verbal hallucinations (AVHs) are diseased groups of serious psychosis with still unknown etiology. The aim of this research was to identify the neurophysiological correlates of auditory verbal hallucinations. Revealing the neural correlates of auditory hallucination is not merely of great clinical significance, but it is also quite essential to study the pathophysiological correlates of schizophrenia. In this study, 25 Schizophrenia patients with AVHs (AVHs group, 23.2 ± 5.35 years), 52 Schizophrenia patients without AVHs (non-AVHs group, 25.79 ± 5.63 years) and 28 healthy subjects (NC group, 26.14 ± 5.45 years) were enrolled. Dynamic functional connectivity was studied with a sliding-window method and functional connectivity states were then obtained with the k-means clustering algorithm in the three groups. We found that schizophrenia patients with AVHs were characterized by significant decreased static functional connectivity and enhanced variability of dynamic functional connectivity (non-parametric permutation test, Bonferroni correction, $p < 0.05$). In addition, the AVHs group also demonstrated increased number of brain states, suggesting brain dynamics enhanced in these patients compared with the non-AVHs group. Our findings suggested that there were abnormalities in the connection of brain language regions in auditory verbal hallucinations. It appears that the interruption of connectivity from the language region might be critical to the pathological basis of AVHs.

Keywords: schizophrenia, auditory verbal hallucinations, dynamic functional connectivity, static functional connectivity, k-means clustering

OPEN ACCESS

Edited by:
Yongbin Wei,
VU Amsterdam, Netherlands

Reviewed by:
Zhiqiang Sha,
Max Planck Institute for Psycholinguistics, Netherlands
Ji Chen,
Zhejiang University, China

***Correspondence:**
Peng Huang
huangpeng@fmmu.edu.cn
Jianying Guo
jyguo@fmmu.edu.cn
Xuehui Hu
466980356@qq.com
Xia Zhu
zhuxia@fmmu.edu.cn

† These authors have contributed equally to this work

Specialty section:
This article was submitted to Brain Imaging and Stimulation, a section of the journal Frontiers in Human Neuroscience

Received: *17 December 2021*
Accepted: *11 March 2022*
Published: *07 April 2022*

Citation:
Zhang Y, Wang J, Lin X, Yang M, Qi S, Wang Y, Liang W, Lu H, Zhang Y, Zhai W, Hao W, Cao Y, Huang P, Guo J, Hu X and Zhu X (2022) Distinct Brain Dynamic Functional Connectivity Patterns in Schizophrenia Patients With and Without Auditory Verbal Hallucinations. Front. Hum. Neurosci. 16:838181. doi: 10.3389/fnhum.2022.838181

INTRODUCTION

Schizophrenia is a mental illness, but its harm has been seriously underestimated due to its low incidence and small number of direct deaths. In fact, schizophrenia is highly disabling, has a significant impact on families and society, and is prone to relapse. Clinically, it is often manifested as different syndromes with different symptoms, involving various disorders in perception, thinking, emotion, behavior and other aspects, as well as the disharmony between psychological activities and the environment. Among the above-mentioned symptoms, auditory verbal hallucinations probably occurred among 60–80% of schizophrenia patients (Saha et al., 2005; Petrolini et al., 2020; Sun et al., 2021). Auditory verbal hallucinations (AVHs) is one of the main symptoms of schizophrenia and serves as an important clinical index for the diagnosis of schizophrenia. It refers to hearing without corresponding external sound stimulation acting on the auditory organs. Twenty-five percent of auditory verbal hallucinations patients are chronic and difficult to cure (Allen et al., 2012; Koops et al., 2016). It has been confirmed that schizophrenia patients have structural abnormalities of the brain, but the nature of abnormalities is not consistent (Cui et al., 2017b; Nakahara et al., 2018; Wei Y. et al., 2018).

The content of AVHs often involves threatening or commanding to the patient, or talking about the patient's thoughts, or commenting on the patient's behavior, which brings great mental suffering to the patient (Garwood et al., 2015). Especially when under the control of commanding auditory hallucinations, patients may break out strong aggressive or destructive behaviors, thus endangering themselves, families or even the social surroundings due to some sudden self-injury or wounding violence. Auditory verbal hallucinations in schizophrenia are serious psychosis with still unknown etiology. Although after more than 20 years of neuroimaging research, people still do not know the neurophysiological mechanism of auditory verbal hallucinations. Revealing the neural mechanism of AVHs is not only of great clinical significance, but also of great importance as to explore the pathophysiological mechanism of schizophrenia. In recent years, various neuroimaging technologies have been used in the research related to AVHs, and many breakthroughs have been made, which not only provide important bases for the diagnosis and treatment of schizophrenia with AVHs, but also provide vital support in revealing the mechanism of AVHs. Through a series of studies, the neural mechanism of AVHs has also made fruitful progresses. It is found that AVHs are highly correlated with the structural and functional changes in brain regions related to speech generation and perception (Barber et al., 2021). Relevant research results have proved that the formation of AVHs is mainly related to the left middle temporal gyrus, the left temporal parietal lobe, and the left inferior frontal lobe (Zhang et al., 2017; Zhuo et al., 2021). Recent studies have also shown that the cortical thickness in the frontal and temporal cortical areas of patients with AVHs is thinner. Voxel-based morphological studies reported that the severity of auditory hallucinations was associated with the temporal lobe, including the primary and secondary auditory cortex. FMRI studies found that AVHs were related to the over activation of left inferior frontal cortex and left middle temporal cortex. Meta analysis also showed that AVHs were highly correlated with left inferior frontal gyrus and left inferior parietal lobe (Kühn and Gallinat, 2012; Cui et al., 2016, 2018).

The cause of auditory hallucination is much more complex than regional brain abnormalities. Many neuroimaging studies suggest that cognitive dysfunction could not simply be attributed to the structural lesions and functional disorders in a single brain region or several brain regions (Karnath et al., 2018; Herbet and Duffau, 2020). Cognitive dysfunction is often caused by abnormal connections between brain regions. Therefore, it is not enough just to understand the pathogenesis of auditory hallucinations by merely studying the abnormalities in specific brain regions of schizophrenia patients with AVHs (Diederen et al., 2012; Sehatpour et al., 2020).

Most fMRI studies (Chang et al., 2017; Mallikarjun et al., 2018; Geng et al., 2020) investigating functional connectivity (FC) in schizophrenia and hallucinations have employed a static connectivity approach, whereby FC is averaged over scan time. There is substantial evidence for abnormal FC in schizophrenia, but findings vary widely. Dynamic functional connectivity is an extension of traditional static functional connectivity, as this analysis allows exploration of temporal changes in connectivity. Weber et al. (2020) found that hallucination severity did not show a significant relationship with dynamic FC.

Although previous studies have shown that the emergence of AVHs is related to the changes in the connectivity of brain language networks, there are only a few systematic studies on how the changes in the structural and functional connections of brain language regions in schizophrenia patients lead to AVHs, as well as whether these abnormalities have their internal relationship. In this study, static connectivity analysis and dynamic connectivity analysis were complemented. We believe that studying the connectivity of brain language network might shed light on the revelation of the neuropathological mechanism of auditory hallucinations, which is also of great significance in the diagnosis and treatment of schizophrenia patients with auditory verbal hallucinations.

MATERIALS AND METHODS

Participants

Twenty-five schizophrenia patients with auditory verbal hallucinations, 52 schizophrenia patients without auditory verbal hallucinations and 28 healthy subjects were enrolled. All subjects participated in the experiment voluntarily and signed the informed consent form before the experiment. Two weeks before the scan, the patients stopped taking psychotropic drugs. The experiment was approved by the Ethics Committee of the Fourth Military Medical University. All patients were diagnosed by two senior clinical psychiatrists in the Department of Psychosomatics, Xijing Hospital of the Fourth Military Medical University according to DSM-IV standards. Participants' information is shown in **Table 1**.

TABLE 1 | Demographic data of the three groups.

	AVHs	Non-AVHs	NC	p
No.	25	52	28	–
Age	23.20	25.79	26.14	0.06
Gender (male/female)	15/10	28/24	15/13	0.283

AVHs, Schizophrenia patients with auditory verbal hallucinations; non-AVHs, Schizophrenia patients without auditory verbal hallucinations; NC, Healthy subjects without schizophrenia.

Data Acquisition

The MRI data were collected from a 3.0-Tesla SIEMENS Magnetom Trio Tim scanner in Xijing Hospital. Resting-state fMRI images were acquired with an echo planar imaging (EPI) sequence using the following parameters: repetition time (TR) = 2,000 ms, echo time (TE) = 30 ms, flip angle (FA) = 90°, matrix = 64 × 64, slice thickness = 4 mm, slice number = 33, and field of view (Fov) = 220 mm × 220 mm. The subjects were told to lie still in the scanner, eyes closed, but not to fall asleep. We collected 240 fMRI scans for each subject.

Data Preprocessing

fMRI images were preprocessed with the statistical parametric mapping software package (SPM12)[1] and the Gretna toolbox.[2] Due to magnetic field instability, the first ten functional images were discarded and the remaining 230 scans from each subject were excluded in further analyses. Slice timing and realignment were first performed to correct for differences in acquisition time of slices and head motion, respectively. One patient without AVHs and one healthy control were excluded from further analyses due to excessive head motion (>3 mm translation or 3°rotation). fMRI images were then normalized into standard MNI space with a T1 unified segmentation strategy and then spatially smoothed with a Gaussian kernel filter of 6 mm full-width half-maximum (FWHM). After temporally detrending, nuisance signals including head motion profiles (using Friston-24 parameters), as well as signals from the white matter and cerebrospinal fluid (CSF) were regressed out. Since previous studies were controversial on whether the global signal should be regressed out, two preprocessing strategies were used, and we investigated functional connectivity both with and without global signal regression. Then, a band-pass filter was applied to remove low-frequency (<0.01 HZ) drift and high-frequency (>0.1 HZ) physiological noises. Finally, data scrubbing was performed to reduce the impact of head motion on the fMRI data. In specific, frames with frame-wise displacement (FD) greater than 0.5 were interpolated with data from one previous time point and two subsequent time points.

Dynamic Functional Connectivity Analysis

Dynamic functional connectivity analysis was performed by using a sliding-window algorithm with the DynamicBC toolbox.[3] After preprocessing, the brain was parcellated into 246 regions of interest (ROIs) according to the Brainnetome atlas.[4] Mean time course of each ROI was obtained and we then investigated whole-brain functional connectivity by calculating the correlation between time courses of any pair of ROIs within each time window. In specific, functional connectivity within a time window whose length was 50 TR was first calculated. This window was then slid and functional connectivity matrix within each of a series of consecutive windows was obtained. Two different settings of the overlap between two neighboring windows were adopt in the current study. We first used the default setting of 0.6 (according to a step of 20 TR) provided by the DynamicBC toolbox. This step has also been conducted in previous studies (Shakil et al., 2016; Wei L. et al., 2018; Guo et al., 2020). Totally 10 time windows under this setting were obtained. In addition, another setting of the overlap (0.9) and obtained 37 time windows were also employed, benefiting with a better time resolution for researchers to investigate the dynamics in functional connectivity. In addition to dynamic functional connectivity matrices, a static functional connectivity matrix for each subject was also calculated by setting the window width to be 230 TR. Non-parametric permutation test was used to compare the static and dynamic functional connectivity maps in AVHs patients, non-AVHs patients, and healthy subjects. Bonferroni correction was used to correct for multiple comparison.

Dynamic Functional Connectivity States

Dynamic functional connectivity states were obtained by the k-means clustering algorithms. The distance between two brain functional connectivity patterns was measured by the correlation between them. The maximum number of states was set as 10, and the optimal number of states then automatically estimated by the DynamicBC toolbox which averaged the optimal number of states estimated according to silhouette, Calinski-Harabasz, and Davies-Bouldin values.

RESULTS

Static Functional Connectivity

We used a permutation test to compare static functional connectivity patterns among AVHs patients, non-AVHs patients, and healthy subjects. Without global signals regression, there were 2 connections with significant difference between the AVHs group and the non-AVHs group, 59 connections with significant difference between the AVHs group and the NC group, and 9 connections with significant difference between the non-AVHs group and the NC group ($p < 0.05$, Bonferroni corrected; **Table 2** and **Figure 1**). With global signal regression, there were 5 connections with significant difference between AVHS and non-AVHs group, 23 connections with significant difference between AVHs and NC group, and 36 connections with significant difference between non-AVHs and NC group ($p < 0.05$, Bonferroni corrected; **Table 3** and **Figure 2**).

[1] http://www.fil.ion.ucl.ac.uk/spm/software/spm12/

[2] https://www.nitrc.org/projects/gretna/

[3] https://guorongwu.github.io/DynamicBC/

[4] http://atlas.brainnetome.org/brainnetome.html

TABLE 2 | Differences in static functional connectivity without global signal regression.

AVHs and non-AVHs		AVHs and NC						Non-AVHs and NC	
Region 1	**Region 2**	**Region 1**	**Region 2**	**Region 1**	**Region 2**	**Region 1**	**Region 2**	**Region 1**	**Region 2**
IPL_R_6_4	LOcC_L_4_2	OrG_L_6_4	PrG_L_6_3	STG_R_6_6	PoG_R_4_2	OrG_L_6_4	Hipp_L_2_1	MFG_L_7_7	PrG_L_6_4
MFG_R_7_3	Hipp_R_2_1	OrG_R_6_4	PrG_L_6_4	MTG_L_4_4	PoG_R_4_2	OrG_R_6_4	Hipp_L_2_1	OrG_L_6_4	ITG_L_7_3
–	–	OrG_L_6_4	STG_L_6_1	STG_L_6_5	PoG_L_4_3	SFG_L_7_1	BG_L_6_1	PrG_L_6_4	ITG_L_7_3
–	–	OrG_R_6_4	STG_L_6_1	OrG_L_6_2	PoG_L_4_4	LOcC_L_4_3	BG_R_6_1	MFG_R_7_2	SPL_R_5_5
–	–	OrG_L_6_4	STG_R_6_1	OrG_R_6_4	PoG_R_4_4	SFG_L_7_1	BG_L_6_2	OrG_R_6_2	PoG_L_4_4
–	–	OrG_R_6_4	STG_R_6_1	STG_L_6_5	INS_R_6_5	OrG_L_6_4	BG_L_6_3	STG_L_6_5	LOcC_R_4_2
–	–	ITG_R_7_1	ITG_R_7_5	IFG_L_6_4	MVOcC_L_5_3	SFG_R_7_1	BG_L_6_4	IFG_L_6_3	LOcC_L_4_2
–	–	OrG_R_6_5	PhG_L_6_1	PrG_L_6_1	MVOcC_L_5_3	SFG_R_7_5	BG_L_6_4	STG_L_6_1	BG_L_6_3
–	–	MFG_R_7_3	IPL_R_6_2	SPL_L_5_3	MVOcC_L_5_3	CG_L_7_5	BG_L_6_4	PhG_L_6_1	BG_R_6_3
–	–	SFG_R_7_4	IPL_R_6_3	SPL_L_5_5	MVOcC_L_5_3	CG_R_7_5	BG_L_6_4	–	–
–	–	ITG_L_7_5	IPL_L_6_4	IPL_L_6_3	MVOcC_L_5_3	CG_L_7_5	BG_R_6_4	–	–
–	–	MTG_R_4_4	PCun_L_4_3	PoG_L_4_1	MVOcC_L_5_3	CG_R_7_5	BG_R_6_4	–	–
–	–	OrG_L_6_4	PoG_L_4_1	PoG_L_4_3	MVOcC_L_5_3	CG_L_7_5	BG_L_6_5	–	–
–	–	MTG_L_4_2	PoG_L_4_1	STG_L_6_5	LOcC_L_4_2	SFG_L_7_5	BG_L_6_6	–	–
–	–	MTG_L_4_4	PoG_L_4_1	STG_L_6_6	LOcC_L_4_2	SFG_R_7_5	BG_L_6_6	–	–
–	–	IFG_L_6_3	PoG_R_4_1	STG_R_6_6	LOcC_L_4_2	PoG_L_4_4	BG_L_6_6	–	–
–	–	STG_L_6_6	PoG_R_4_1	STG_L_6_6	LOcC_R_4_2	SFG_L_7_5	BG_R_6_6	–	–
–	–	MTG_L_4_4	PoG_R_4_1	SPL_L_5_5	LOcC_R_4_3	PrG_R_6_4	BG_R_6_6	–	–
–	–	STG_L_6_6	PoG_L_4_2	OrG_L_6_4	Amyg_L_2_2	PoG_L_4_4	BG_R_6_6	–	–
–	–	STG_L_6_4	PoG_R_4_2	OrG_R_6_5	Amyg_L_2_2	–	–	–	–

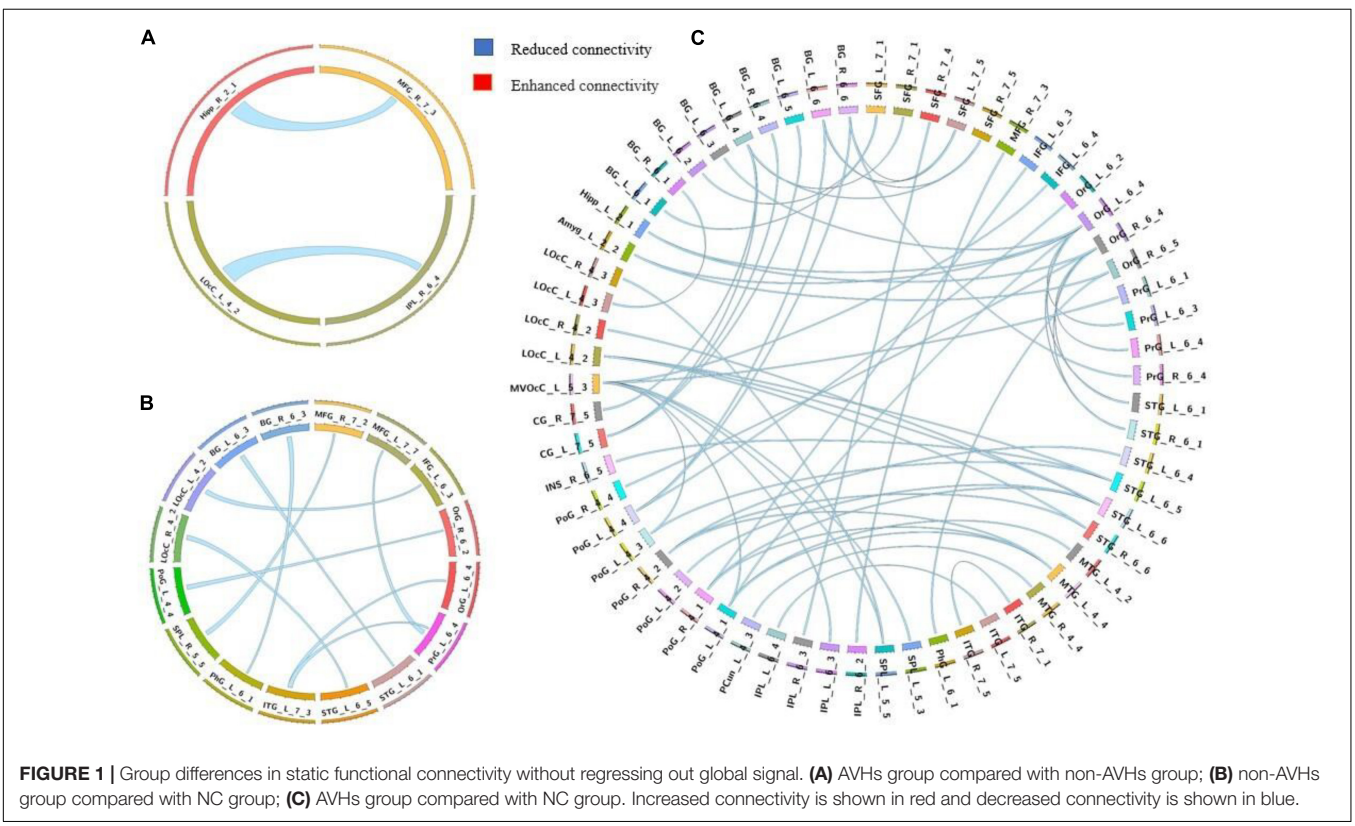

FIGURE 1 | Group differences in static functional connectivity without regressing out global signal. **(A)** AVHs group compared with non-AVHs group; **(B)** non-AVHs group compared with NC group; **(C)** AVHs group compared with NC group. Increased connectivity is shown in red and decreased connectivity is shown in blue.

Although the between group differences with and without global signal regression consistently suggested mainly reduced static functional connectivity in patients with AVHs, compared to SZ patients without AVHs. Interestingly, without global signal regression, patients with AVHs only demonstrated reduced static functional connectivity compared with the other two groups. The

TABLE 3 | Differences in static functional connectivity with global signal regression.

AVHs and non-AVHs		AVHs and NC				Non-AVHs and NC			
Region 1	**Region 2**	**Region 1**	**Region 2**	**Region 1**	**Region 2**	**Region 1**	**Region 2**	**Region 1**	**Region 2**
OrG_R_6_4	SPL_R_5_5	SFG_R_7_6	IFG_L_6_2	pSTS_L_2_1	Tha_L_8_2	MFG_L_7_6	MFG_L_7_7	MFG_R_7_2	CG_L_7_7
SPL_R_5_5	IPL_L_6_6	IFG_R_6_2	PrG_R_6_2	STG_R_6_1	Tha_R_8_7	SFG_L_7_3	MFG_R_7_7	STG_L_6_1	LOcC_R_4_2
SPL_R_5_5	IPL_R_6_6	PrG_R_6_5	STG_L_6_5	MTG_L_4_3	Tha_L_8_8	MFG_L_7_6	MFG_R_7_7	STG_L_6_5	LOcC_R_4_2
MTG_R_4_4	PCun_L_4_3	OrG_R_6_2	ITG_R_7_7	–	–	MFG_R_7_6	MFG_R_7_7	MFG_R_7_1	Amyg_L_2_1
SPL_L_5_4	BG_R_6_2	MFG_L_7_3	IPL_L_6_2	–	–	MFG_R_7_1	STG_L_6_1	MFG_R_7_5	Amyg_L_2_1
–	–	SFG_R_7_4	IPL_R_6_3	–	–	SFG_L_7_4	STG_L_6_2	ITG_L_7_3	Amyg_L_2_1
–	–	SFG_L_7_3	IPL_R_6_4	–	–	MFG_R_7_7	ITG_R_7_6	INS_L_6_1	Amyg_R_2_1
–	–	IFG_L_6_3	PoG_R_4_1	–	–	SFG_R_7_2	PhG_L_6_5	MFG_R_7_6	Amyg_L_2_2
–	–	STG_L_6_4	PoG_L_4_2	–	–	MFG_L_7_4	PhG_R_6_6	STG_L_6_5	Amyg_L_2_2
–	–	STG_L_6_4	PoG_R_4_2	–	–	MFG_R_7_2	SPL_R_5_5	LOcC_R_4_2	Amyg_L_2_2
–	–	STG_L_6_5	PoG_R_4_2	–	–	MFG_R_7_5	SPL_R_5_5	MFG_R_7_1	Hipp_L_2_1
–	–	STG_L_6_6	PoG_R_4_2	–	–	MFG_R_7_7	IPL_R_6_2	MVOcC_R_5_5	BG_L_6_1
–	–	MTG_L_4_4	PoG_R_4_2	–	–	OrG_R_6_2	PCun_L_4_3	STG_L_6_1	BG_L_6_3
–	–	IPL_L_6_1	INS_L_6_4	–	–	SPL_R_5_1	PoG_L_4_2	Hipp_L_2_2	BG_L_6_3
–	–	STG_L_6_5	INS_L_6_5	–	–	OrG_R_6_2	PoG_L_4_4	PhG_L_6_1	BG_R_6_3
–	–	STG_L_6_5	INS_R_6_5	–	–	PrG_L_6_5	INS_R_6_2	MFG_L_7_3	BG_R_6_5
–	–	OrG_L_6_4	Hipp_L_2_1	–	–	STG_L_6_3	INS_R_6_2		
–	–	CG_L_7_5	BG_L_6_4	–	–	STG_L_6_5	INS_L_6_5		
–	–	CG_R_7_5	BG_L_6_4	–	–	STG_R_6_5	INS_L_6_5		
–	–	CG_L_7_5	BG_R_6_4	–	–	STG_L_6_5	INS_R_6_5		

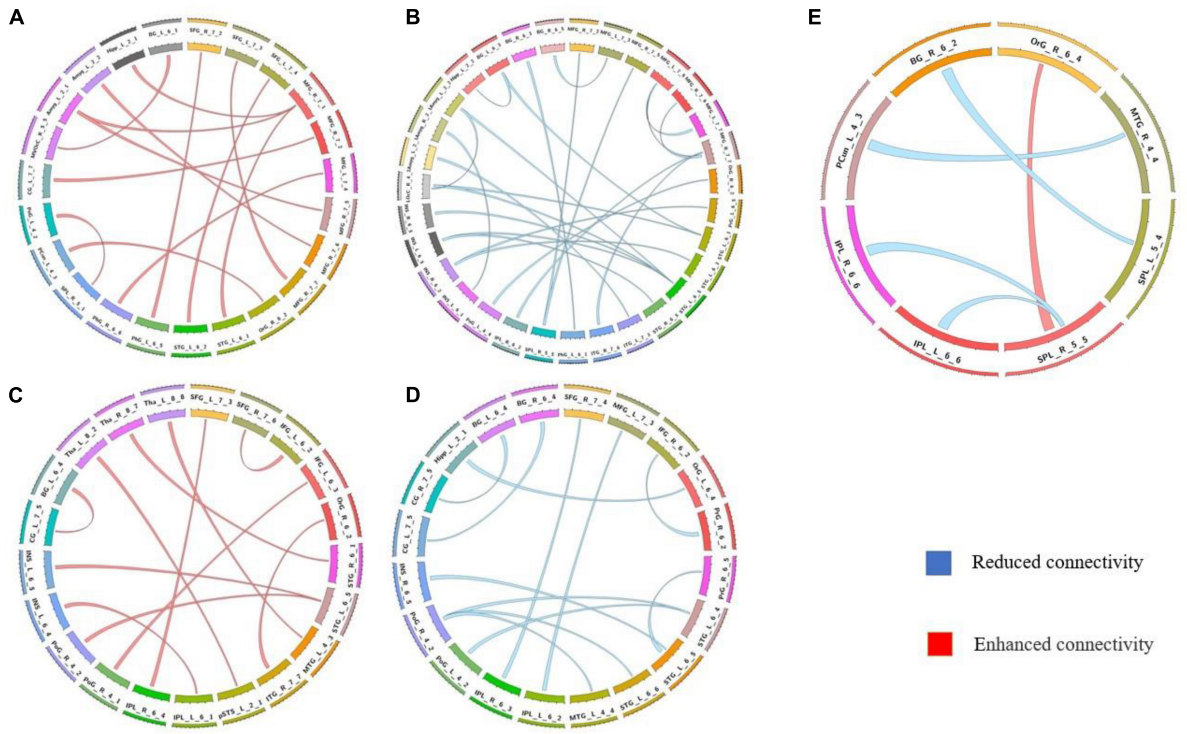

FIGURE 2 | Comparison of the static functional connectivity of the three groups after global signal regression. **(A)** Static functional connections with enhanced connectivity in the non-AVHs group compared with the NC group; **(B)** Static functional connections with reduced connectivity in the non-AVHs group compared to the NC group; **(C)** Static connections with enhanced connectivity in AVHs group compared with NC group; **(D)** Static connections with reduced connectivity in AVHs group compared with NC group; **(E)** Compared with non-AVHs group, static connections with significant differences in AVHs group. Red represents increased connectivity and blue represents decreased connectivity.

TABLE 4 | Significant differences in variances of the dynamic functional connectivity matrices obtained without regressing out global signal (overlap = 0.6).

AVHs and non-AVHs		AVHs and NC		Non-AVHs and NC	
Region 1	**Region 2**	**Region 1**	**Region 2**	**Region 1**	**Region 2**
SFG_R_7_7	MFG_R_7_3	OrG_R_6_2	PrG_L_6_3	SFG_L_7_7	STG_L_6_5
OrG_R_6_4	CG_L_7_3	STG_R_6_4	ITG_L_7_7	ITG_L_7_3	INS_L_6_1
–	–	MFG_L_7_4	FuG_R_3_2	MVOcC_R_5_1	Hipp_R_2_2
–	–	STG_L_6_1	IPL_L_6_2	–	–
–	–	SFG_R_7_2	MVOcC_L_5_2	–	–
–	–	OrG_R_6_3	Amyg_L_2_1	–	–
–	–	FuG_R_3_2	BG_R_6_6	–	–

involvement of global signal regression seemed to result in more enhanced connectivity in the AVHs group when compared with patients without AVHs and healthy controls.

Dynamics of Functional Connectivity

The differences in the dynamics of whole-brain functional connectivity between the three groups were accessed by comparing the variance of dynamic functional connectivity matrices. For each connection, we calculated the variance of this connection over all the sliding windows to quantify its variability. Then a non-parametric permutation test was used to compare dynamics of functional connectivity of the three groups ($P < 0.05$; Bonferroni correction; **Tables 4**–**7** and **Figures 3**–**6**). As shown in **Figures 3**–**6**, SZ patients with and without AVHs showed differences in functional connectivity compared with the healthy controls. The AVHs group consistently demonstrated enhanced dynamics in functional connectivity compared with the non-AVHs group under different settings of overlap between neighboring windows, as well as with different data preprocessing strategies.

Dynamic Functional Connectivity States

The optimal number of dynamic function connection states estimated by k-means algorithm is 3 for AVHs group, 2 for non-AVHs group, and 3 for NC group. **Figure 7** shows the spatial patterns of these three groups of brain states. From **Figure 7** we observed that the number of optimal states estimated in the AVH group was higher than that in the non-AVH group. This observation is also robust under different setting of overlap (overlap = 0.9) seen in **Supplementary Figure 1–3**, suggesting that the resting-sate functional connectivity of the AVHs group seems to be alternating among more brain states than that of the non-AVHs group. This finding is also in line with our observation of increased variance of dynamic functional connectivity matrices, suggesting enhanced brain dynamics in patients with AVHs.

TABLE 5 | Significant differences in variances of the dynamic functional connectivity matrices obtained without regressing out global signal (overlap = 0.9).

AVHs and non-AVHs		AVHs and NC		Non-AVHs and NC	
Region 1	**Region 2**	**Region 1**	**Region 2**	**Region 1**	**Region 2**
SFG_R_7_7	MFG_R_7_3	OrG_R_6_2	PrG_L_6_3	MTG_L_4_3	PhG_R_6_1
OrG_R_6_1	OrG_R_6_6	MFG_L_7_4	FuG_R_3_2	ITG_L_7_3	INS_L_6_1
ITG_L_7_7	INS_L_6_5	IFG_L_6_1	FuG_R_3_2	ITG_L_7_3	INS_R_6_2
OrG_R_6_4	*CG_L_7_3*	PrG_L_6_6	LOcC_R_4_1	MTG_L_4_4	INS_L_6_5
OrG_R_6_4	CG_R_7_7	INS_L_6_5	Amyg_L_2_2	ITG_L_7_7	INS_L_6_5
OrG_R_6_1	Tha_L_8_4	–	–	OrG_R_6_4	BG_L_6_5
–	–	–	–	OrG_R_6_1	Tha_L_8_7

DISCUSSION

In this study, we examined the differences in static FC. Importantly, we also examined the differences in dynamic FC. The results showed that compared with NC, both AVHs group and non-AVHs group showed only decreased static functional connectivity when without global signal regression. Instead, resulting in increasing connectivity between the two groups with global signal regression, most of the static functional connectivity in the AVHs group showed decreased connectivity compared to the non-AVHs group.

In general, The AVHs group consistently demonstrated enhanced dynamics in functional connectivity compared with the non-AVHs group under different settings of overlap between neighboring windows, as well as with different data preprocessing strategies (with/without global regression; overlap=0.6/0.9). These findings suggested that patients with AVHs are characterized by reduced strength of static functional connectivity, accompanied with enhanced dynamics of functional connectivity.

From the analysis of functional connectivity, we found that auditory hallucinations in patients with schizophrenia may be related to abnormal functional connectivity among the frontal lobe, temporal regions and parietal regions. In fact, auditory verbal hallucinations are considered to be a disease caused by the patient's inability to recognize the internal language generated by the brain (Anthony, 2004; Zhuo et al., 2021). This loss of cognitive internal language ability is highly correlated with the frontal cortex of speech generation and the temporal and parietal regions of sensory processing (Frith, 2005). With the proposal of "abnormal connection hypothesis," the connection between these language brain regions is becoming ever more important in the study of auditory hallucinations (Li et al., 2017). In this study, we studied and compared the whole

TABLE 6 | Significant differences in variances of the dynamic functional connectivity matrices obtained with global signal regression (overlap = 0.6).

AVHs and non-AVHs		AVHs and NC		Non-AVHs and NC	
Region 1	**Region 2**	**Region 1**	**Region 2**	**Region 1**	**Region 2**
SFG_R_7_2	IPL_R_6_1	OrG_R_6_3	MVOcC_L_5_5	PrG_L_6_1	ITG_L_7_2
SFG_R_7_2	PoG_R_4_3	OrG_R_6_3	MVOcC_R_5_5	MFG_L_7_3	ITG_L_7_3
ITG_R_7_4	MVOcC_L_5_2	IFG_R_6_4	Amyg_L_2_1	IFG_R_6_5	PhG_L_6_6
–	–	ITG_L_7_7	Tha_L_8_1	FuG_L_3_2	PoG_L_4_3
–	–	INS_L_6_1	Tha_L_8_1	MFG_L_7_3	Hipp_R_2_1
–	–	INS_L_6_1	Tha_L_8_2	PoG_L_4_3v	BG_L_6_2
–	–	MFG_L_7_6	Tha_R_8_4	INS_R_6_3	BG_L_6_2

TABLE 7 | Significant differences in variances of the dynamic functional connectivity matrices obtained with global signal regression (overlap = 0.9).

AVHs and non-AVHs		AVHs and NC		Non-AVHs and NC	
Region 1	**Region 2**	**Region 1**	**Region 2**	**Region 1**	**Region 2**
SFG_R_7_2	IPL_R_6_1	IFG_R_6_4	Amyg_L_2_1	IFG_R_6_2	PoG_R_4_2
SFG_R_7_2	PoG_R_4_3	OrG_R_6_3	Amyg_L_2_1	FuG_L_3_2	PoG_L_4_3
ITG_R_7_4	MVOcC_L_5_2	LOcC _R_4_3	BG_R_6_4	OrG_L_6_6	LOcC_L_4_4
–	–	ITG_L_7_7	Tha_L_8_1	MFG_L_7_3	Hipp_R_2_1
–	–	–	–	INS_R_6_3	BG_L_6_2

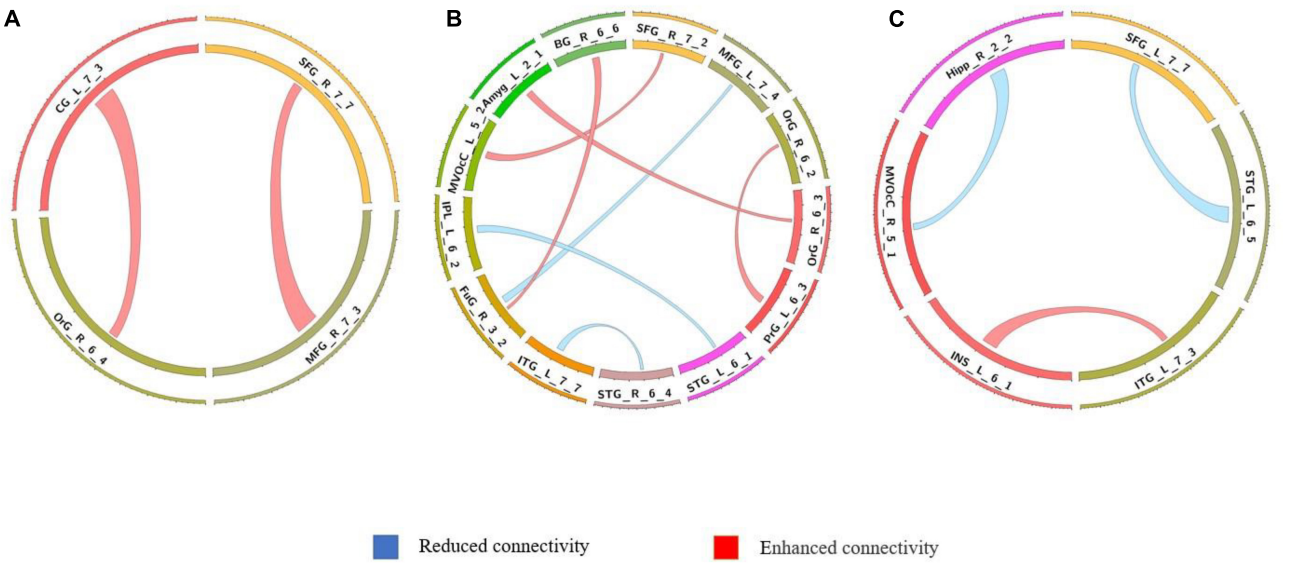

FIGURE 3 | Comparison of dynamic differences in functional connectivity without global signal regression (overlap = 0.6). **(A)** AVHs group compared with the non-AVHs group; **(B)** AVHs group compared with the NC group; **(C)** non-AVHs group compared with the NC group. Increased connectivity shown in red and decreased shown in blue.

brain functional connectivity and patterns of schizophrenia patients with and without auditory hallucinations and normal subjects.

Compared with non-AVHs group, the AVHs group were characterized by significantly enhanced static functional connectivity among Frontal Gyrus, Inferior Parietal Lobule, and Hippocampus. The above brain areas are related to language acquisition and language understanding, which further imply that there were abnormalities in the connection of brain language regions in auditory hallucinations (Vercammen et al., 2010; Clos et al., 2014). FMRI study found that the decrease of functional connection between temporal and parietal lobes in patients with AVHs was positively correlated with the severity of auditory hallucinations (Vercammen et al., 2010). This study also revealed that many of the connections demonstrated increased variability in the AVHs group compared with the non-AVHs group. The above findings are consistent with some research results (Cui et al., 2017a; Barber et al., 2021), indicating that AVHs

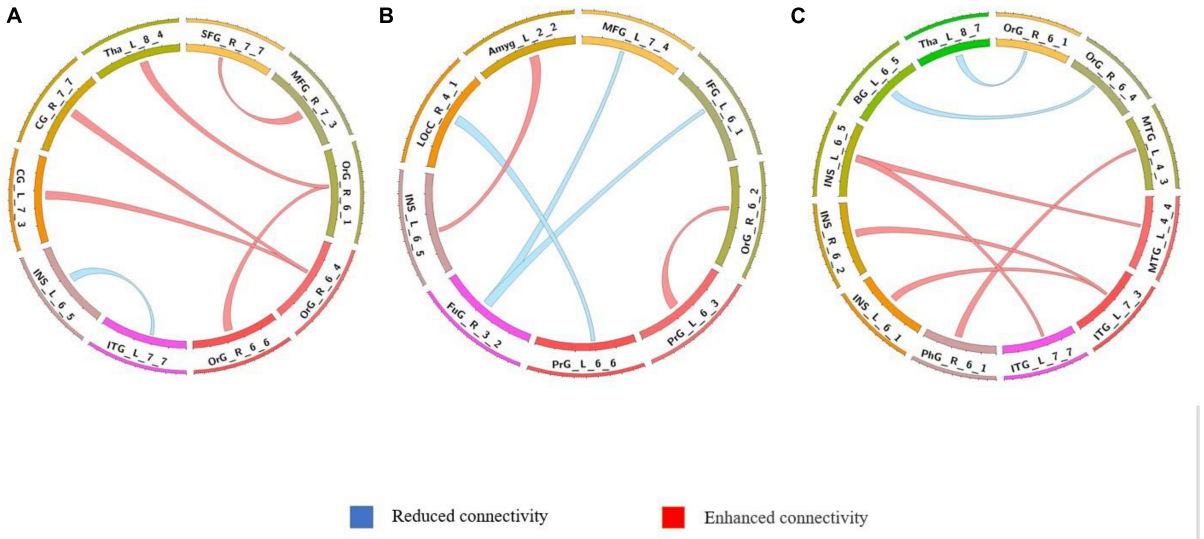

FIGURE 4 | Comparison of dynamic functional connectivity without global signal regression (overlap = 0.9). **(A)** AVHs group compared with the non-AVHs group; **(B)** AVHs group compared with the NC group; **(C)** non-AVHs group compared with the NC group. Increased connectivity was shown in red and decreased shown in blue.

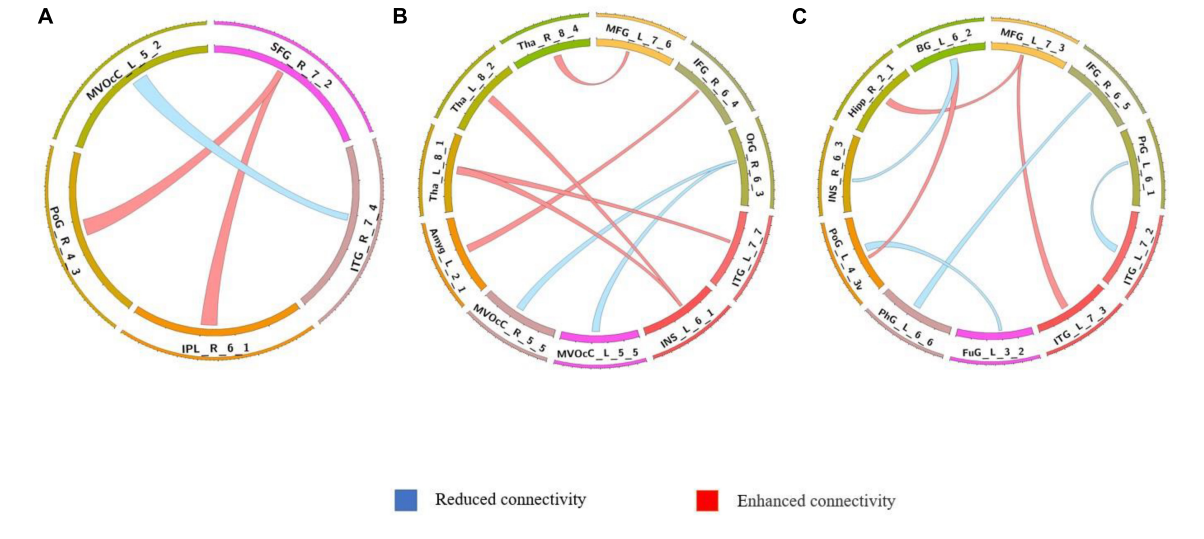

FIGURE 5 | Comparison of dynamic differences in functional connectivity with global signal regression (overlap = 0.6). **(A)** AVHs group compared with the non-AVHs group; **(B)** AVHs group compared with the NC group; **(C)** non-AVHs group compared with the NC group.

have something to do with dysfunction of the regions involving speech imagery, production, and monitoring, and schizophrenia patients with AVHs showed deficit communication between the brain network.

Our findings are a little different from previous results. These contradictory results may be related to the heterogeneity of schizophrenia and the sample size. The characteristic of this study is to directly compare AVHs and non-AVHs and reveal the pathophysiological basis of auditory hallucinations intuitively.

There are several potential limitations of the current study. First, schizophrenia patients with AVHs may hallucinate or fall asleep during the scan, thus losing control over the design of the resting state. Second, small sample sizes may lead to reduced reliability of inter-group differences. The correlation strength between auditory hallucination phenotype and language-related regions in schizophrenia patients has yet to be studied by expanding the sample size.

CONCLUSION

The results showed that the connectivity of most static functional connections was significantly reduced, and the dynamic of

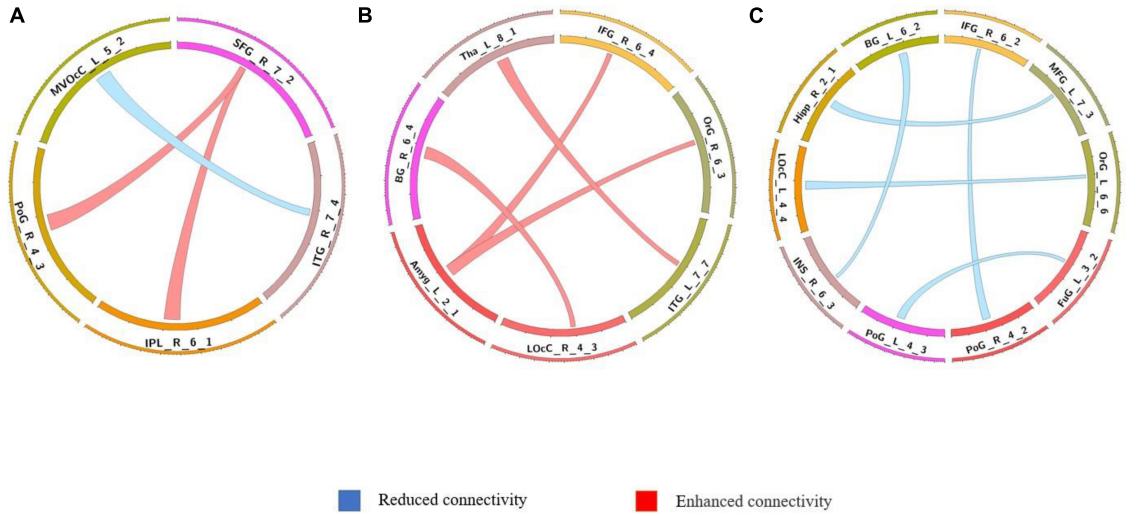

FIGURE 6 | Comparison of dynamic differences in functional connectivity with global signal regression (overlap = 0.9). **(A)** AVHs group compared with the non-AVHs group; **(B)** AVHs group compared with the NC group; **(C)** non-AVHs group compared with the NC group. Increased connectivity shown in red and decreased shown in blue.

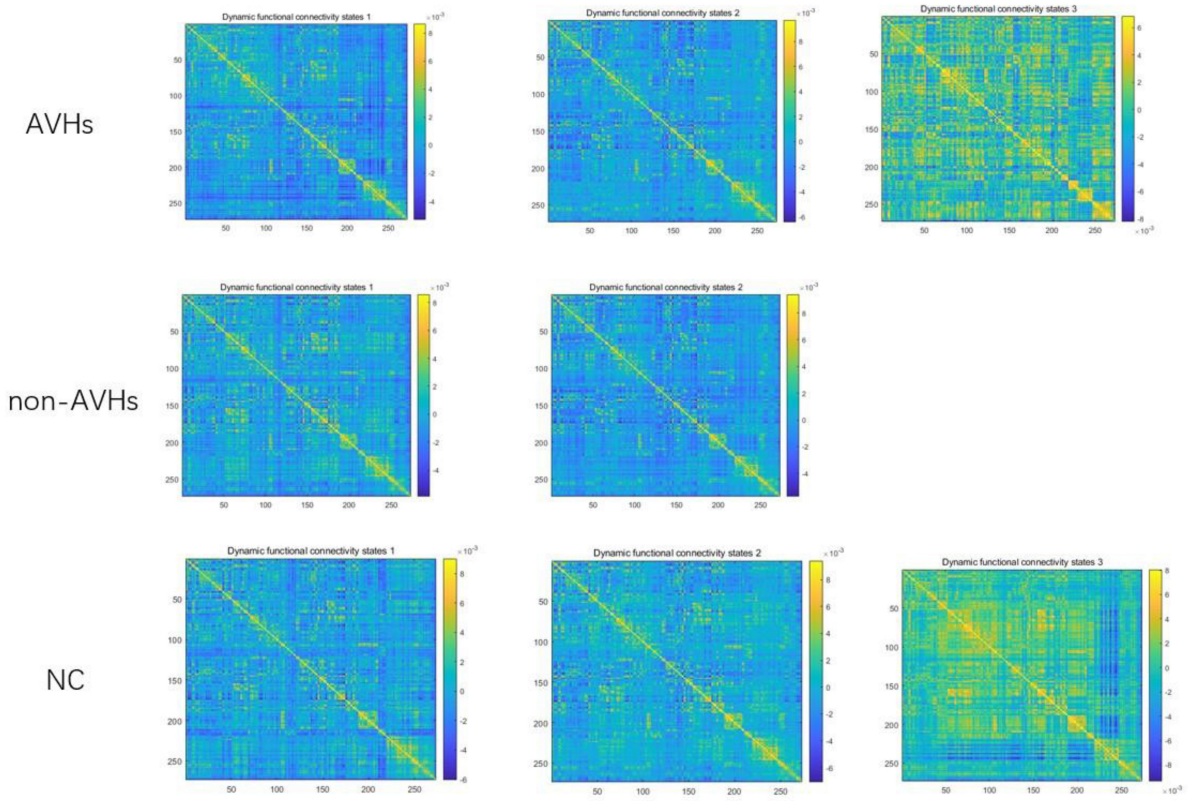

FIGURE 7 | Patterns of dynamic functional connectivity states in the AVHs, non-AVHs groups and NC groups without global signal regression (overlap = 0.6).

functional connections was significantly increased in the AVHs group under the two preprocessing strategies. In a cluster analysis of the two groups based on the dynamic nature of functional connectivity, schizophrenia patients with AVHs shifted between more brain states. The results suggest that significant changes in functional connectivity of the brain may contribute to the study of pathophysiological mechanisms of schizophrenia patients with AVHs and the diagnosis of AVHs.

DATA AVAILABILITY STATEMENT

The raw data supporting the conclusions of this article will be made available by the authors, without undue reservation.

ETHICS STATEMENT

The experiment was approved by the Ethics Committee of the Fourth Military Medical University. The patients/participants provided their written informed consent to participate in this study. Written informed consent was obtained from the individual(s) for the publication of any potentially identifiable images or data included in this article.

AUTHOR CONTRIBUTIONS

YaZ and PH conceptualized and designed the research. SQ and HL collected demographics and MRI data. JW, XL, and PH analyzed MRI data and undertook statistical analysis with WL. PH, JW, YnZ, WH, YC, YW, and MY wrote the first draft. PH, JG, XH, XZ, JW, WZ, and YaZ contributed to the final manuscript including editing figures, tables, and format. All authors critically reviewed the content and approved the final version for publication.

FUNDING

This work was supported by the Military Medical Science and Technology Youth Top-Notch Project (Grant No. 21QNPY091) and the Key R&D Plan of Shaanxi Province (Grant No. 2022SF-023).

SUPPLEMENTARY MATERIAL

The Supplementary Material for this article can be found online at: https://www.frontiersin.org/articles/10.3389/fnhum.2022.838181/full#supplementary-material

REFERENCES

Allen, P., Chaddock, C. A., Howes, O. D., Egerton, A., Seal, M. L., Fusar-Poli, P., et al. (2012). Abnormal relationship between medial temporal lobe and subcortical dopamine function in people with an ultra high risk for psychosis. *Schizophr. Bull.* 38, 1040–1049. doi: 10.1093/schbul/sbr017

Anthony, D. (2004). The cognitive neuropsychiatry of auditory verbal hallucinations: an overview. *Cogn. Neuropsychiatry* 9, 107–123. doi: 10.1080/13546800344000183

Barber, L., Reniers, R., and Upthegrove, R. (2021). A review of functional and structural neuroimaging studies to investigate the inner speech model of auditory verbal hallucinations in schizophrenia. *Transl. Psychiatry* 11:582. doi: 10.1038/s41398-021-01670-7

Chang, X., Collin, G., Xi, Y., Cui, L., Scholtens, L. H., Sommer, I. E., et al. (2017). Resting-state functional connectivity in medication-naïve schizophrenia patients with and without auditory verbal hallucinations: a preliminary report. *Schizophr. Res.* 188, 75–81. doi: 10.1016/j.schres.2017.01.024

Clos, M., Diederen, K. M., Meijering, A. L., Sommer, I. E., and Eickhoff, S. B. (2014). Aberrant connectivity of areas for decoding degraded speech in patients with auditory verbal hallucinations. *Brain Struct. Funct.* 219, 581–594. doi: 10.1007/s00429-013-0519-5

Cui, L.-B., Liu, L., Guo, F., Chen, Y.-C., Chen, G., Xi, M., et al. (2017b). Disturbed brain activity in resting-state networks of patients with first-episode schizophrenia with auditory verbal hallucinations: a cross-sectional functional MR imaging study. *Radiology* 283, 810–819. doi: 10.1148/radiol.2016160938

Cui, L.-B., Chen, G., Xu, Z.-L., Liu, L., Wang, H.-N., Guo, L., et al. (2017a). Cerebral blood flow and its connectivity features of auditory verbal hallucinations in schizophrenia: a perfusion study. *Psychiatry Res. Neuroimaging* 260, 53–61. doi: 10.1016/j.pscychresns.2016.12.006

Cui, L.-B., Liu, K., Li, C., Wang, L.-X., Guo, F., Tian, P., et al. (2016). Putamen-related regional and network functional deficits in first-episode schizophrenia with auditory verbal hallucinations. *Schizophr. Res.* 173, 13–22. doi: 10.1016/j.schres.2016.02.039

Cui, Y., Liu, B., Song, M., Lipnicki, D., Li, J., Xie, S., et al. (2018). Auditory verbal hallucinations are related to cortical thinning in the left middle temporal gyrus of patients with schizophrenia. *Psychol. Med.* 48, 115–122. doi: 10.1017/S0033291717001520

Diederen, K. M. J., Van Lutterveld, R., and Sommer, I. (2012). Neuroimaging of voice hearing in non-psychotic individuals: a mini review. *Front. Hum. Neurosci.* 6:111. doi: 10.3389/fnhum.2012.00111

Frith, C. (2005). The neural basis of hallucinations and delusions. *C. R. Biol.* 328, 169–175. doi: 10.1016/j.crvi.2004.10.012

Garwood, L., Dodgson, G., Bruce, V., and McCarthy-Jones, S. (2015). A preliminary investigation into the existence of a hypervigilance subtype of auditory hallucination in people with psychosis. *Behav. Cogn. Psychother.* 43, 52–62. doi: 10.1017/S1352465813000714

Geng, H., Xu, P., Sommer, I. E., Luo, Y.-J., Aleman, A., and Ćurčić-Blake, B. (2020). Abnormal dynamic resting-state brain network organization in auditory verbal hallucination. *Brain Struct. Funct.* 225, 2315–2330. doi: 10.1007/s00429-020-02119-1

Guo, X., Duan, X., Chen, H., He, C., Xiao, J., Han, S., et al. (2020). Altered inter-and intrahemispheric functional connectivity dynamics in autistic children. *Hum. Brain Mapp.* 41, 419–428. doi: 10.1002/hbm.24812

Herbet, G., and Duffau, H. (2020). Revisiting the functional anatomy of the human brain: toward a meta-networking theory of cerebral functions. *Physiol. Rev.* 100, 1181–1228. doi: 10.1152/physrev.00033.2019

Karnath, H.-O., Sperber, C., and Rorden, C. (2018). Mapping human brain lesions and their functional consequences. *Neuroimage* 165, 180–189. doi: 10.1016/j.neuroimage.2017.10.028

Koops, S., Dellen, E. V., Schutte, M. J., Nieuwdorp, W., Neggers, S. F., and Sommer, I. E. (2016). Theta burst transcranial magnetic stimulation for auditory verbal hallucinations: negative findings from a double-blind-randomized trial. *Schizophr. Bull.* 42, 250–257. doi: 10.1093/schbul/sbv100

Kühn, S., and Gallinat, J. (2012). Quantitative meta-analysis on state and trait aspects of auditory verbal hallucinations in schizophrenia. *Schizophr. Bull.* 38, 779–786. doi: 10.1093/schbul/sbq152

Li, B., Cui, L.-B., Xi, Y.-B., Friston, K. J., Guo, F., Wang, H.-N., et al. (2017). Abnormal effective connectivity in the brain is involved in auditory verbal hallucinations in schizophrenia. *Neurosci. Bull.* 33, 281–291. doi: 10.1007/s12264-017-0101-x

Mallikarjun, P. K., Lalousis, P. A., Dunne, T. F., Heinze, K., Reniers, R. L., Broome, M. R., et al. (2018). Aberrant salience network functional connectivity in auditory verbal hallucinations: a first episode psychosis sample. *Transl. Psychiatry* 8:69. doi: 10.1038/s41398-018-0118-6

Nakahara, S., Matsumoto, M., and van Erp, T. G. (2018). Hippocampal subregion abnormalities in schizophrenia: a systematic review of structural and physiological imaging studies. *Neuropsychopharmacol. Rep.* 38, 156–166. doi: 10.1002/npr2.12031

Petrolini, V., Jorba, M., and Vicente, A. (2020). The role of inner speech in executive functioning tasks: schizophrenia with auditory verbal hallucinations and autistic spectrum conditions as case studies. *Front. Psychol.* 11:2452. doi: 10.3389/fpsyg.2020.572035

Saha, S., Chant, D., Welham, J., and McGrath, J. (2005). A systematic review of the prevalence of schizophrenia. *PLoS Med.* 2:e141. doi: 10.1371/journal.pmed.0020141

Sehatpour, P., Avissar, M., Kantrowitz, J. T., Corcoran, C. M., De Baun, H. M., Patel, G. H., et al. (2020). Deficits in pre-attentive processing of spatial location and negative symptoms in subjects at clinical high risk for schizophrenia. *Front. Psychiatry* 11:629144. doi: 10.3389/fpsyt.2020.629144

Shakil, S., Lee, C.-H., and Keilholz, S. D. (2016). Evaluation of sliding window correlation performance for characterizing dynamic functional connectivity and brain states. *Neuroimage* 133, 111–128. doi: 10.1016/j.neuroimage.2016.02.074

Sun, Q., Fang, Y., Shi, Y., Wang, L., Peng, X., and Tan, L. (2021). Inhibitory top-down control deficits in schizophrenia with auditory verbal hallucinations: a Go/NoGo Task. *Front. Psychiatry* 12:544746. doi: 10.3389/fpsyt.2021.544746

Vercammen, A., Knegtering, H., den Boer, J. A., Liemburg, E. J., and Aleman, A. (2010). Auditory hallucinations in schizophrenia are associated with reduced functional connectivity of the temporo-parietal area. *Biol. Psychiatry* 67, 912–918. doi: 10.1016/j.biopsych.2009.11.017

Weber, S., Johnsen, E., Kroken, R. A., Løberg, E.-M., Kandilarova, S., Stoyanov, D., et al. (2020). Dynamic functional connectivity patterns in schizophrenia and the relationship with hallucinations. *Front. Psychiatry* 11:227. doi: 10.3389/fpsyt.2020.00227

Wei, L., Jiao, L., Xujun, D., Qian, C., Heng, C., and Huafu, C. (2018). Static and dynamic connectomics differentiate between depressed patients with and without suicidal ideation. *Hum. Brain Mapp.* 39, 4105–4118. doi: 10.1002/hbm.24235

Wei, Y., Collin, G., Mandl, R. C., Cahn, W., Keunen, K., Schmidt, R., et al. (2018). Cortical magnetization transfer abnormalities and connectome dysconnectivity in schizophrenia. *Schizophr. Res.* 192, 172–178. doi: 10.1016/j.schres.2017.05.029

Zhang, L., Li, B., Wang, H., Li, L., Liao, Q., Liu, Y., et al. (2017). Decreased middle temporal gyrus connectivity in the language network in schizophrenia patients with auditory verbal hallucinations. *Neurosci. Lett.* 653, 177–182. doi: 10.1016/j.neulet.2017.05.042

Zhuo, C., Fang, T., Chen, C., Chen, M., Sun, Y., Ma, X., et al. (2021). Brain imaging features in schizophrenia with co-occurring auditory verbal hallucinations and depressive symptoms—Implication for novel therapeutic strategies to alleviate the reciprocal deterioration. *Brain Behav.* 11:e01991. doi: 10.1002/brb3.1991

Conflict of Interest: The authors declare that the research was conducted in the absence of any commercial or financial relationships that could be construed as a potential conflict of interest.

Publisher's Note: All claims expressed in this article are solely those of the authors and do not necessarily represent those of their affiliated organizations, or those of the publisher, the editors and the reviewers. Any product that may be evaluated in this article, or claim that may be made by its manufacturer, is not guaranteed or endorsed by the publisher.

frontiers | Frontiers in Human Neuroscience

TYPE Original Research
PUBLISHED 19 January 2023
DOI 10.3389/fnhum.2022.925543

OPEN ACCESS

EDITED BY
Long-Biao Cui,
Fourth Military Medical University, China

REVIEWED BY
Sarael Alcauter,
National Autonomous University of Mexico, Mexico
Fu Yufei,
Fourth Military Medical University, China

*CORRESPONDENCE
Xiaoming Hou
houxiaoming11111@hotmail.com

†These authors have contributed equally to this work and share first authorship

SPECIALTY SECTION
This article was submitted to Brain Imaging and Stimulation, a section of the journal Frontiers in Human Neuroscience

RECEIVED 21 April 2022
ACCEPTED 07 December 2022
PUBLISHED 19 January 2023

CITATION
Li B, Zhang S, Li S, Liu K and Hou X (2023) Aberrant resting-state regional activity in patients with postpartum depression.
Front. Hum. Neurosci. 16:925543.
doi: 10.3389/fnhum.2022.925543

Aberrant resting-state regional activity in patients with postpartum depression

Bo Li[1†], Shufen Zhang[2†], Shuyan Li[3], Kai Liu[1] and Xiaoming Hou[4*]

[1]Department of Radiology, The 960th Hospital of the PLA Joint Logistics Support Force, Jinan, China, [2]Department of Obstetrics, Shandong Second Provincial General Hospital, Jinan, China, [3]Foreign Languages College, Shandong University of Traditional Chinese Medicine, Jinan, Shandong, China, [4]Department of Pediatrics, Provincial Hospital Affiliated to Shandong First Medical University, Jinan, Shandong, China

Background: Postpartum depression (PPD) is a common disorder with corresponding cognitive impairments such as depressed mood, memory deficits, poor concentration, and declining executive functions, but little is known about its underlying neuropathology.

Method: A total of 28 patients with PPD and 29 healthy postpartum women were recruited. Resting-state functional magnetic resonance imaging (rs-fMRI) scans were performed in the fourth week after delivery. Individual local activity of PPD patients was observed by regional homogeneity (ReHo) during resting state, and the ReHo value was computed as Kendall's coecient of concordance (KCC) and analyzed for differences between voxel groups. Correlations between ReHo values and clinical variables were also analyzed.

Result: Compared with healthy postpartum women, patients with PPD exhibited significantly higher ReHo values in the left precuneus and right hippocampus. ReHo value was significantly lower in the left dorsolateral prefrontal cortex (dlPFC) and right insula. Furthermore, ReHo values within the dlPFC were negatively correlated with the Edinburgh PPD scale (EPDS) score. The functional connectivity (FC) of the right hippocampus to the left precuneus and left superior frontal gyrus (SFG) was stronger in patients with PPD than that in controls.

Conclusion: The present study provided evidence of aberrant regional functional activity and connectivity within brain regions in PPD, and it may contribute to further understanding of the neuropathology underlying PPD.

KEYWORDS

postpartum depression, regional functional connectivity, ReHo, fMRI, functional connectivity

1. Introduction

Postpartum depression (PPD) has been reported in 10–20% of new mothers within the first 4 weeks following delivery, which is a major public health concern that has significant consequences for mothers, their children, and their families (Gress-Smith et al., 2012). Rates of hospitalization, self-harm, and maternal suicide are increased among depressed women during the peripartum period (Lindahl et al., 2005). Infants with mothers affected by PPD are more likely to suffer infant abuse or infanticide, less

infant weight gain, and increased rates of hospitalization (Gress-Smith et al., 2012). PPD further harms infants in their subsequent development of cognition, emotion, and behavior during childhood and adolescence (Gress-Smith et al., 2012).

Although the devastating sequelae of PPD have been comprehensively studied, the diagnosis and pathophysiology of this disease, especially its neuropathology, are not well defined (Duan et al., 2017). Findings from clinical studies and laboratory rodent models highlight that alterations in activation of brain areas during PPD likely alter key neural networks associated with women's maternal care, empathy, stress, motivation, emotional reaction to stimulus valence, learned reward, and executive functioning (Pawluski et al., 2017). As the most important and useful tool to noninvasively study the functions of the brain, functional magnetic resonance imaging (fMRI) has become more commonly used. Physicians use fMRI to detect cerebral blood-oxygenation-level dependent (BOLD) activity in response to changes in neural activity (Logothetis et al., 2001) either with activation or at rest. The studies using fMRI with activation were to investigate differences in mothers' brain responses to infant and non-infant cues. Neural activation between PPD and healthy mothers differs in response to infant- and non-infant-related cues, such that activity in the specific brain regions will increase in response to a non-infant emotional cue but decrease in response to an infant-related emotional cue (Moses-Kolko et al., 2010; Silverman et al., 2011; Barrett et al., 2012; Laurent and Ablow, 2012b; Wonch et al., 2016).

The other studies used resting-state fMRI (rs-fMRI) to analyze women's brain resting state. An advantage of rs-fMRI is that it can clarify how PPD may affect a mother's baseline brain activity at rest and provide a comprehensive understanding of neural circuitry dysfunction in mothers with PPD. Rs-fMRI has been applied to detect spontaneous neural brain activity and functional connectivity (FC) in PPD using the resting-state functional connectivity (RSFC) (Deligiannidis et al., 2013, 2019; Chase et al., 2014), the dynamic amplitude of low-frequency fluctuations ALFF analysis (Cheng et al., 2022b), regional homogeneity (ReHo) analysis (Xiao-Juan et al., 2011), voxel-mirrored homotopic connectivity (Zhang et al., 2020), dynamic functional connectivity (FC) (Cheng et al., 2022b), functional connectivity density (FCD) (Cheng et al., 2021), and functional connectivity strength (FCS) (Cheng et al., 2022a). At rest, women with PPD showed decreased corticocortical and corticolimbic connectivity. More specifically, the women with PPD showed significantly weaker connectivity among the amygdala (AMG), anterior cingulate cortex (ACC), dorsal lateral prefrontal cortex (dlPFC), and the hippocampus compared with non-depressed postpartum women (Deligiannidis et al., 2013). In addition, they showed negative connectivity between the posterior cingulate cortex (PCC) and AMG (Chase et al., 2014). The area of the dorsomedial prefrontal cortex (dmPFC) has greater connectivity with the rest of the default mode network (DMN) and reduced connectivity with the precuneus, posterior cingulate cortex, and supramarginal gyrus/angular gyrus regions in women with PPD (Deligiannidis et al., 2019). PPD mothers exhibited increased FC between the subgenual anterior cingulate cortex (sgACC) and ventral anterior insula and disrupted FC between the sgACC and middle temporal gyrus. The changes in dynamic FC between the sgACC and superior temporal gyrus could differentiate PPD and HCs (Cheng et al., 2022b). Patients with PPD showed specifically weaker long-range FCD in the right lingual gyrus (L.G.R), functional couplings between LG.R and dmPFC, and left precentral gyrus and specifically stronger functional coupling between LG.R and right angular. Moreover, the altered FCD and RSFC were closely associated with depression and anxiety symptoms load (Cheng et al., 2021). PPD group showed specifically higher FCS in right parahippocampus, and perceived social support mediated the influence of FCS in the right cerebellum posterior lobe on depression and anxiety symptoms (Cheng et al., 2022a). Compared with healthy controls (HCs), mothers with PPD showed significantly increased posterior cingulate and medial frontal gyrus and decreased temporal gyrus ReHo (Xiao-Juan et al., 2011). Patients with PPD exhibited significantly decreased voxel-mirrored homotopic connectivity values in the bilateral dmPFC, dorsal anterior cingulate cortex (dACC), and orbitofrontal cortex (Zhang et al., 2020). Compared to the relative wealth of data available for major depression, fMRI studies of PPD were limited in number and design. It seems reasonable to conduct studies using a variety of rs-fMRI techniques to help identify neuroimaging signatures for PPD.

In this study, we focused on the homogeneity of regional activity by investigating changes in ReHo, which is distinct from mainstream methods of measuring long-range connections using the amplitude of low-frequency fluctuations. ReHo is a highly sensitive, reproducible, and reliable index of local activity and can reflect functional similarities in brain activities among neighboring voxels located within a short range (Ji et al., 2020). Decreases or increases in ReHo are thought to, respectively, reflect spontaneous neural hypoactivity or hyperactivity in a given regional brain area (Jiang and Zuo, 2016). Here, we collected a dataset from 57 participants, including 28 patients with PDD and 29 HCs. We calculated individual local activity by ReHo and explored their potential correlations with the clinical symptoms. We further used the brain areas with abnormal ReHo values in PPD as the region of interest (ROI) and conducted FC analysis. We tested the following hypotheses: (1) the PPD group showed abnormal ReHo in DMN and limbic system compared to HCs; (2) the alterations of ReHo would be related to Edinburgh postpartum depression scale (EPDS) score; and (3) the brain regions with abnormal ReHo in DMN and the limbic system showed the aberrant FC.

2. Material and methods

2.1. Participants

This study included 57 participants (28 patients with PDD and 29 HCs) who were recruited from the Department of Obstetrics of Shandong Second Provincial General Hospital and the Department of Obstetrics of the 960th Hospital of the PLA Joint Logistics Support Force. Two experienced senior associate chief physicians of neurology confirmed their diagnoses by using the Structured Clinical Interview for Diagnostic and Statistical Manual of Mental Disorders, Fifth Edition (DSM-5) and Chinese Classification and Diagnostic Criteria of Mental Disorders, 3rd edition (CCMD-3). Inclusion criteria for patients were as follows: new mothers (a) whose age ranged from 21 to 38 years, in the fourth week after delivery; (b) with first-episode, treatment-naive PPD patients; (c) with EPDS score of $\geqq$ 13; (d) with no other medical or mental illness history; (e) with no substance abuse or substance dependent; (f) with no contraindications of an MR examination; and (g) with no organic abnormalities for MRI routine series. The EPDS score was assessed 1 h before the image acquisition. Inclusion criteria for HCs were as follows: new mothers (a) whose age ranges from 21 to 38 years, in the fourth week after delivery; (b) with no current or previous history of depressive episodes; (c) with EPDS score < 3; and (d)–(g) were same to the PPD group. This study was approved by the ethics committee of the Shandong Second Provincial General Hospital and all participants provided written informed consent.

2.2. Image acquisition

All fMRI data were acquired on a 3.0T MR system (Discovery MR750, General Electric, Milwaukee, USA) with a standard eight-channel head coil. During scanning, all participants were instructed to lie quietly and remain still with their eyes closed and heads fixed in place by foam pads to minimize head movement.

High-resolution structural T1-weighted scans (Three-dimensional Brain Volume, 3D BRAVO) were performed using the following parameters: time repetition (TR) = 8.2 ms, time echo (TE) = 3.2 ms, flip angle = 12°, the field of view (FOV) = 240 mm × 240 mm, slices = 115, voxel size = 1 mm, and thickness = 1.0 mm. Resting-state BOLD MR images were acquired with the following parameters: TR = 2,000 ms, TE= 40 ms, flip angle = 90°, FOV = 240 mm × 240 mm, resolution = 64 × 64, voxel size = 3.75 mm, thickness = 4.0 mm, no interspace, slices = 41, gradient echo-planar volumes = 200, and duration was 6 min 40 s. In addition, routine MRI data were collected to exclude anatomic abnormality among all participants.

2.3. Data preprocessing

The fMRI data preprocessing was conducted using the Data Processing Assistant for rs-fMRI (DPARSF) and rs-MRI data analysis toolkit (REST) (http://www.restfmri.net), which are based on Statistical Parametric Mapping (SPM12; http://www.fil.ion.ucl.ac.uk/spm). First, the first ten volumes were discarded. Second, the slice-time corrected images were realigned to the first volume for slice-timing correction. For head motion correction, all subjects with a head motion > 1.5° rotation and 1.5 mm translation were excluded. For the frame-wise displacement estimates, we used a volume censoring technique ("scrubbing") (Power et al., 2012) to eliminate the potential impact of sudden motions or moderate motions on the FC. We normalized motion-corrected functional images to a standard EPI template in the Montreal Neurological Institute space by applying the parameters of structural image normalization and resampling the normalized images to 3 mm isotropic voxels. After linear detrend, the data were band-pass filtered (0.01–0.08 Hz) to eliminate physiological noise. Several sources of spurious covariates along with their temporal derivatives, including the six head motion parameters, global mean, white matter, and cerebrospinal fluid, were removed.

2.4. ReHo analysis

The ReHo value was computed as KCC in rs-fMRI (Zang et al., 2004). A KCC was assigned to a given voxel by calculating the KCC of the time series of this voxel with 26 nearest neighbors. A higher KCC indicates a higher synchronization. We obtained the standardized KCC value by dividing the KCC value of each voxel by the average value of the whole brain. The KCC program was coded in MATLAB (The MathWorks, Inc., Natick, MA). Thus, an individual ReHo map was generated for each subject. Finally, we smoothed all individual ReHo maps by using a 4-mm full-width at half-maximum Gaussian kernel.

The variables, including age and clinical symptom scores between PPD and the control group, were analyzed by the Mann–Whitney *U*-test in SPSS version 18.0 (SPSS Inc., Chicago, IL, USA). The differences in the delivery method were determined using chi-square tests. The threshold was set at $p < 0.05$. With age as a covariate, a two-sample *t*-test was performed using the REST1.8 software to determine significant voxel-based differences in ReHo value between the two groups. The resulting statistical map was set at $q < 0.05$ for multiple comparisons (FDR corrected, cluster size > 55 voxels) using the REST1.8 software.

2.5. FC analysis

We used the brain clusters with significantly different ReHo values between PPD and HCs as the ROIs. FC analyses were

TABLE 1 Demographic factors and clinical data.

Characteristic	Healthy control (HC, $n = 29$)		Postpartum depressed (PPD, $n = 28$)		p-value
	Mean (SD)	Percent (%)	Mean (SD)	Percent (%)	
Age (years)	28.56 (4.57)		29.27 (4.72)		0.82
Right handedness	29	100	20	100	
Socioeconomic status (thousand RMB)	181.64 (4.60)		182.84 (3.26)		0.26
Education (years)	11.28 (3.74)		11.85 (3.26)		0.60
Cesarean	10	34.5	11	39.2	0.87
Breastfeeding	29	100	28	100	
Primi para	14	48.3	15	53.6	0.90
EPDS	0.79 (0.96)		14.97 (1.66)		0.00

SD, standard deviation; RMB, Renminbi; EPDS, Edinburgh postpartum depression scale.

performed using the default FC processing pipeline in the REST toolbox. In this processing pipeline, white matter, cerebral spinal fluid noise, and global mean signal were removed through regression after spatially smoothing (4-mm full-width at half-maximum). The mean time series from each ROI was calculated by averaging the time series of all the voxels within that region. The seed-based FC analysis was computed between the seed reference time course and that of each voxel in the brain in a voxel-wise way. Finally, the Fisher r-to-Z transformation was used to transform correlation coefficients to Z values. FDR correction ($q < 0.05$) was performed for multiple comparisons.

2.6. Correlation analysis between the brain and clinical characteristics

In this study, we performed a correlation analysis between clinical characteristics and brain functional metrics, including ReHo and FC strength. The mean ReHo in each between-group significant cluster was extracted for each subject. After seed-based FC analysis, the mean FC within each between-group significant cluster was extracted. Finally, Pearson correlation analyses were performed between the mean ReHo or FC strength in each cluster and the EPDS scores in the PPD with HCs group using the SPSS version 18.0 software with significance at $p < 0.05$.

3. Results

3.1. Demographic and clinical characteristics

A total of 28 PPD patients and 29 HCs were enrolled in the final analyses of this study. All the participants were right-handed. We found no significant differences in age, educational level, delivery method, delivery time, or feed options among the PPDs and controls. Patients with PPD showed significantly higher EPDS scores than HCs ($t = 36.514$, $p < 0.001$), as shown in Table 1.

3.2. Intergroup differences in ReHo values

The PPD group exhibited higher ReHo in the left precuneus and right hippocampus. ReHo was significantly lower in the left dlPFC and right insula (Figure 1). Specific ReHo values of the PDD groups are listed in Table 2.

3.3. Correlations between ReHo and clinical characteristics

The ReHo values within the left dlPFC were significantly negatively correlated with EPDS scores in the PPD group ($r = -0.513$, $p = 0.005$) (Figure 2). There were no significant correlations among the ReHo values in any other regions and EPDS scores in PPD and HC groups.

3.4. Seed-based FC analysis

We used four brain regions (left dlPFC, left precuneus, right hippocampus, and right insula) with significantly different ReHo values between PPD and HCs as seeds in the FC analysis of the whole brain. In the PPD group, the right hippocampus (seed region) showed increased FC with the left precuneus and left superior frontal gyrus (SFG) compared with HCs. The left precuneus (seed region) showed increased FC with the right hippocampus compared with HCs (Figure 3 and Table 3). There

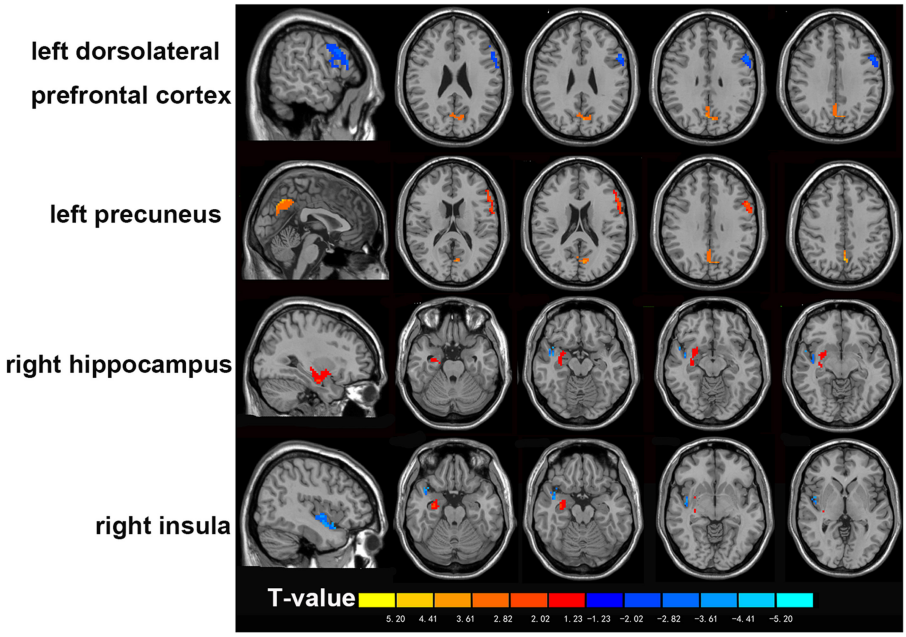

FIGURE 1
Comparisons of rs ReHo values between patients with PPD and HCs. The PPD group exhibited higher ReHo in left precuneus and right hippocampus. ReHo was significantly lower in left dlPFC and right insula. Warm color represents significantly increased ReHo, and cool color represents significantly decreased ReHo. dlPFC, dorsolateral prefrontal cortex; HCs, healthy controls.

TABLE 2 Regional homogeneity values in brain regions showing significant group differences.

Brain region	Peak MNI coordinates			Cluster size (mm^3)	Peak *T*-value	ReHo direction
	x	y	z			
Left dorsolateral prefrontal cortex	−54	12	30	190	−3.07	PPD < HC
Right insula	42	−3	−15	55	−3.75	PPD < HC
Left precuneus	−1	−63	42	120	4.52	PPD > HC
Right hippocampus	33	−12	−18	89	2.23	PPD > HC

MNI, Montreal Neurological Institute.

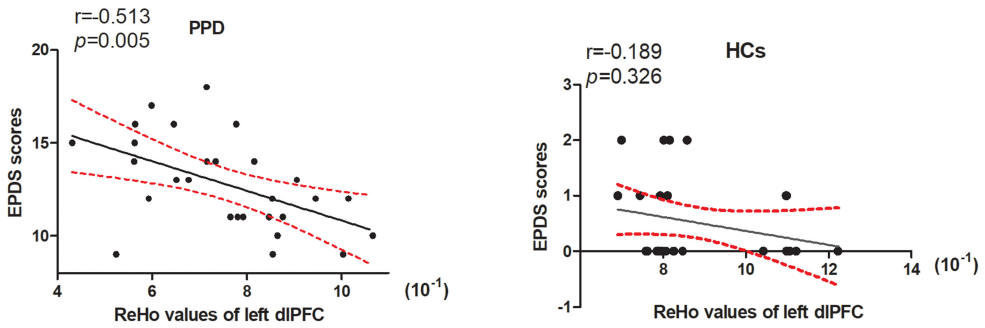

FIGURE 2
The ReHo values within the left dlPFC were significantly negatively correlated with the EPDS scores in the PPD group ($r = -0.513$, $p = 0.005$). There were no significant correlations between the ReHo values within the left dlPFC and EPDS scores in HCs group ($r = -0.189$, $p = 0.326$). dlPFC, dorsolateral prefrontal cortex; EPDS, Edinburg postpartum depression scale; HCs, healthy controls.

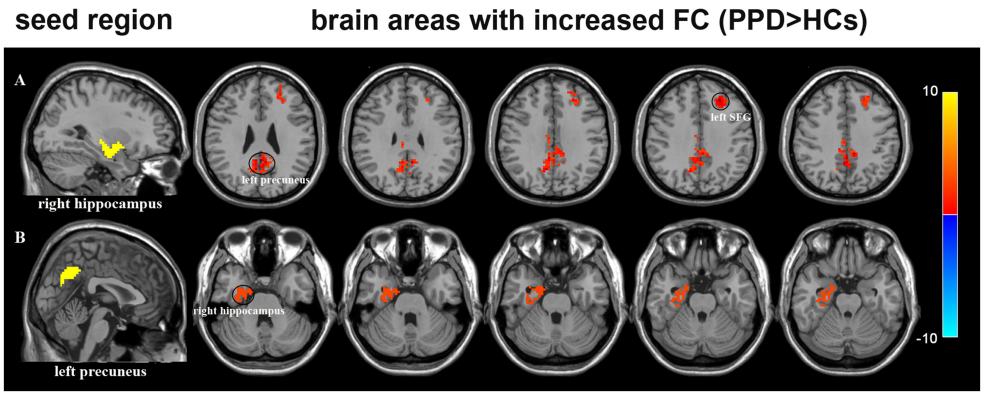

FIGURE 3
(A) Brain regions showing aberrant FC with right hippocampus (seed region) in the PPD group compared with HCs. Warm color represents significantly increased FC. The FC of the right hippocampus to the left precuneus and left SFG was stronger in patients with PPD than in HCs. **(B)** Brain regions showing FC with left precuneus (seed region) in the PPD group compared with HCs. Warm color represents significantly increased FC. The FC of the left precuneus to right hippocampus was stronger in patients with PPD than in controls. FC, functional connectivity; HCs, healthy controls; SFG, superior frontal gyrus.

TABLE 3 Significant differences in FC between PPD and HCs.

Seed region	Area with altered FC	Peak MNI coordinates			Cluster size (mm^3)	Peak *T*-value	FC direction
		x	y	z			
Right hippocampus	Left precuneus	−6	−51	30	268	4.35	PPD > HC
	Left superior frontal gyrus	−24	33	36	104	4.03	PPD > HC
Left precuneus	Right hippocampus	26	−5	−23	109	4.67	PPD > HC

were no other significantly different FCs in any ROIs with the whole brain between the two groups.

3.5. Correlations between FC and clinical characteristics

There were no significant correlations among the FC values in any regions and EPDS scores in PPD and HC groups.

4. Discussion

This study measured the ReHo value using rs-fMRI and correlations among abnormal ReHo values within regions and clinical characteristics in patients with PPD. In this study, we observed the following: (1) ReHo value was higher in the left precuneus and right hippocampus and lower in the left dlPFC and the right insula in the PPD group; (2) ReHo value within the left dlPFC was significantly negatively correlated with EPDS scores in the PPD group, with age as covariates; and (3) the right hippocampus showed increased FC with the left precuneus and left SFG compared with HCs.

The precuneus is a key component of the DMN (Utevsky et al., 2014) and a critical hub with dense and widespread connectivity in human whole-brain structural and functional networks. The precuneus plays a pivotal role in a wide spectrum of functions, including cognition, memory retrieval, self-consciousness, visuospatial imagery, emotional judgment, and self-referential processing (Cavanna and Trimble, 2006). The alterations in the precuneus might be associated with thought-action fusion disturbance, self-referential processing ruminations, and the dysregulation of the sensory part of the fear network, which might be the putative biomarker for depression and anxiety (Lai, 2018). The higher ReHo in the left precuneus and the stronger FC between the precuneus and hippocampus were found in patients with major depressive disorder (MDD) (Yang et al., 2015; Cheng et al., 2018; Xiao et al., 2021). In this study, we found higher ReHo in the left precuneus and stronger connectivity between the left precuneus and right hippocampus in patients with PPD. The earlier fMRI studies of PPD showed a negative coupling between the precuneus and right AMG region and dmPFC (Chase et al., 2014; Deligiannidis et al., 2019). The abnormal function and connectivity in the left precuneus might explain depression and anxiety among PPD.

As the core region in the limbic system and DMN, the hippocampus plays a very important role in memory,

regulation of motivation, stress, and emotion (Eichenbaum, 2013). Patients with MDD have shown to have impaired FCs of the hippocampus, which might explain the memory deficits and depression experienced by patients with MDD (Hao et al., 2020). We observed decreased FC in the left hippocampal-ROI to the bilateral middle frontal gyrus, as well as in the right hippocampal-ROI to the right inferior parietal cortex (IPC) and the cerebellum in patients with MDD compared to the HCs (Cao et al., 2012). Here, we found higher ReHo in the right hippocampus in PPD and stronger connectivity between the left precuneus and right hippocampus. Subjects with PPD had already shown the attenuation of connectivity between the dlPFC and hippocampus (Deligiannidis et al., 2013). The abnormal activity and functional connections of the hippocampus might also be evidence of the depression experienced by patients with PDD.

It is worth noting that both the left precuneus and right hippocampus are important regions in DMN (Zhang et al., 2021). Altered spontaneous neural activities and altered FC between the left precuneus and right hippocampus indicate DMN dysfunction in patients with PPD. It is known that depression symptoms are associated with excessive self-focus, a tendency to engage oneself in self-referential processing (Mor and Winquist, 2002). DMN is responsible for spontaneous cognition, self-referential processing, and emotional regulation (Ho et al., 2015). After taking this evidence into consideration, it is hypothesized that aberrant DMN function may lead to self-referential processing abnormally integrating with biased emotional memory in PPD. Failure of DMN deactivation during emotional or cognitive tasks has been proposed as a possible mechanism acting in PPD.

In the frontal lobe, the dlPFC acts as a key node of the brain networks, including the extrinsic mode network (Hugdahl et al., 2015) and cognitive control network (Cole and Schneider, 2007). It has been implicated in cognitive, affective, sensory processing, and emotional regulation, such as attention, value encoding (Liu et al., 2016), working memory, creativity (Liu et al., 2015), decision-making (Rahnev et al., 2016), reappraisal, expectation, and desire for relief (Sevel et al., 2016). Functional imaging studies have shown decreases in regional cerebral blood flow and metabolism in dlPFC, especially on the left side among patients with depression (Dolan et al., 1993). SFGs are a crucial part of the dlPFC (Xiong et al., 2019). The SFG is generally considered a core brain region in the cognitive control system (Niendam et al., 2012) for emotion regulation-related processes (Frank et al., 2014), which are influential factors for depressive symptoms. In this study, we reported that patients with PPD had lower ReHo in left dlPFC than HCs and stronger connectivity between left SFG and right hippocampus. Previous studies have shown that women with PPD showed significantly weaker connectivity among the AMG, ACC, dlPFC, and hippocampus than HCs (Deligiannidis et al., 2013). We also found significant correlations between ReHo values in dlPFC regions and EPDS scores in the PPD group. Higher EPDS scores correlated with lower ReHo values in dlPFC regions. Based on the previous studies (Mayberg, 1997; Mayberg et al., 1999), depression is associated with increased activation in the subcortical and ventral frontal system (subgenual cingulate, ventral insula, hippocampus, ventral frontal, and hypothalamus implicating in the production of normal and abnormal affective states) and relatively decreased activation in the dorsal frontoparietal system (e.g., dlPFC, dorsal ACC, IPL, and PCC implicating in the cognition and regulating the parameters of affective states) (Xiong et al., 2019). This process may be derived from the bottom-up pathway from the limbic areas, through the cingulate and subcortical regions, to the PFC and frontal lobe finally (Disner et al., 2011). Although we have observed stronger connectivity between left SFG and right hippocampus in PPD, inhibited activations of high-order regions (specifically in dlPFC) attenuate the cognitive control of the top-down system and allow the bottom-up hyperactivation (hippocampus) preserved. In addition, the hypoactivation of the dlPFC has been related to an impairment of cognitive control that may favor rumination, which is considered one of the key factors in the onset and maintenance of depression. All results suggested that many symptom profiles of patients with PPD, such as depression and impaired concentration, might be due to the hypofunction of the left dlPFC.

The human insula is implicated as a major multimodal network hub with connections to the frontal, parietal, temporal, and limbic areas (Dionisio et al., 2019). It is a key component of the fronto-limbic circuit and involves a large variety of complex functions, including pain, cognition, memory, emotion, and self-recognition (Augustine, 1996; Nieuwenhuys, 2012). The right insula is involved in sensory function, pain, and saliency processing (Dionisio et al., 2019). The altered functional activity and connectivity of the insula have been observed in patients with depression (Iwabuchi et al., 2014). Patients with MDD have been shown to have reduced ReHo in the right insula (Liu et al., 2010), which correlated with anxiety and hopelessness (Yao et al., 2009). We found lower ReHo in the right insular of patients with PPD. This is the first study that has found the reduced activity of the right insula in PPD by rs-fMRI. In task-based fMRI studies, the mothers with PPD showed decreased insula activation in response to cries (vs. non-cry control and other infant cries), emotional faces (vs. cries/emotional faces of other infants) (Laurent and Ablow, 2012a), and expressions of joy (Fiorelli et al., 2015). These patients showed increased insular activity, especially on the right side, when exposed to negative words or negative stimuli (Silverman et al., 2007). It was also observed that mothers with PPD had decreased AMG-right insular cortex connectivity when viewing their infants compared to other infants (Duan et al., 2017). Therefore, the PPD group may have impaired function in this region.

Due to the insula's wide range of functions regarding pain, emotional processing, memory, attention, and cognition, the decline of right insular activity might be related to the PPD's diverse symptoms.

Many brain regions such as the hypothalamus, AMG, anterior cingulate, orbitofrontal cortex, and dlPFC, as well as the insula and striatum, have been shown to be involved in the pathogenesis of PPD and are also linked to mothering (Stickel et al., 2019). Our study showed abnormal activities in the left dlPFC, left precuneus, right hippocampus, and right insula in patients with PPD, which were in accordance with the reported regions. We also noticed an earlier study that showed different brain regions with abnormal ReHo including the posterior cingulate, medial frontal, and temporal gyrus (Xiao-Juan et al., 2011). Our study was conducted with sample sizes over two times larger than the earlier study (10 patients with PPD). Furthermore, we conducted the seed-based FC analysis and found the right hippocampus showed increased FC with the left precuneus and left SFG in the PPD group compared with HCs. All our results point to a plausible underlying functional foundation of the neural mechanism in the course of PPD. The four regions with abnormal ReHo values and the altered FC were associated with many brain networks including DMN, fronto-limbic circuit system, and cognitive control network. Our results might suggest the abnormal neuro-activity in these brain networks in patients with PPD, which might help better understand the underlying neuropathology of the disease. However, the present study had some limitations. First, we need additional recruitment and further exploration to verify our results. Second, the study lacked the comparison between the pre- and post-treatment of PPD patients and could not provide the imaging change of the above brain areas after treatment. Third, the study lacked participants' other demographic factors that might influence the results of the study, such as smoking, number of pregnancies, and the presence of underlying diseases. In conclusion, our study provided evidence of aberrant ReHo and FC within brain regions in PPD, and it may contribute to identifying the neuroimaging signatures of patients with PPD for diagnosis and a better understanding of the neuropathology underlying PPD.

Data availability statement

The raw data supporting the conclusions of this article will be made available by the authors, without undue reservation.

Ethics statement

The studies involving human participants were reviewed and approved by the Ethics Committee of the Shandong Second Provincial General Hospital. The patients/participants provided their written informed consent to participate in this study.

Author contributions

BL and XH: conception and study design. SZ, BL, and KL: data collection or acquisition. SZ and BL: statistical analysis. XH: interpretation of results and drafting the manuscript work or revising it critically for important intellectual content. SL: revising the manuscript. All authors contributed to the article and approved the submitted version.

Funding

This study was supported by the Shandong Provincial Medical and Health Science and Technology Development Plan Project (grant number 20210520733), the Key Basic Research Projects of the Foundation Strengthening Plan (grant number 2019-JCJQ-ZNM-02), the Clinical Medical Science and Technology Innovation Program (grant number 202019022), and the President's Foundation of the 960th Hospital of the Chinese People's Liberation Army Joint Service Support Force (grant number 2021MS04).

Acknowledgments

The research was conducted in accordance with The Code of Ethics of the World Medical Association (Declaration of Helsinki) for experiments involving humans. The manuscript was in line with the Recommendations for the Conduct, Reporting, Editing, and Publication of Scholarly Work in Medical Journal. Informed consent was obtained from all individual participants included in the study.

Conflict of interest

The authors declare that the research was conducted in the absence of any commercial or financial relationships that could be construed as a potential conflict of interest.

Publisher's note

References

Augustine, J. R. (1996). Circuitry and functional aspects of the insular lobe in primates including humans. *Brain Res. Brain Res. Rev*. 22, 229–244. doi: 10.1016/S0165-0173(96)00011-2

Barrett, J., Wonch, K. E., Gonzalez, A., Ali, N., Steiner, M., Hall, G. B., et al. (2012). Maternal affect and quality of parenting experiences are related to amygdala response to infant faces. *Soc. Neurosci*. 7, 252–268. doi: 10.1080/17470919.2011.609907

Cao, X., Liu, Z., Xu, C., Li, J., Gao, Q., Sun, N., et al. (2012). Disrupted resting-state functional connectivity of the hippocampus in medication-naive patients with major depressive disorder. *J. Affect Disord*. 141, 194–203. doi: 10.1016/j.jad.2012.03.002

Cavanna, A. E., and Trimble, M. R. (2006). The precuneus: a review of its functional anatomy and behavioural correlates. *Brain* 129, 564–83. doi: 10.1093/brain/awl004

Chase, H. W., Moses-Kolko, E. L., Zevallos, C., Wisner, K. L., and Phillips, M. L. (2014). Disrupted posterior cingulate-amygdala connectivity in postpartum depressed women as measured with resting BOLD fMRI. *Soc. Cogn. Affect Neurosci*. 9, 1069–1075. doi: 10.1093/scan/nst083

Cheng, B., Roberts, N., Zhou, Y., Wang, X., Li, Y., Chen, Y., et al. (2022a). Social support mediates the influence of cerebellum functional connectivity strength on postpartum depression and postpartum depression with anxiety. *Transl. Psychiatry*. 12, 54. doi: 10.1038/s41398-022-01781-9

Cheng, B., Wang, X., Roberts, N., Zhou, Y., Wang, S., Deng, P., et al. (2022b). Abnormal dynamics of resting-state functional activity and couplings in postpartum depression with and without anxiety. *Cereb. Cortex*. 32, 5597–5608. doi: 10.2139/ssrn.3881726

Cheng, B., Zhou, Y., Kwok, V. P. Y., Li, Y., Wang, S., Zhao, Y., et al. (2021). Altered functional connectivity density and couplings in postpartum depression with and without anxiety. *Soc. Cogn. Affect Neurosci*. 17, 756–766. doi: 10.1093/scan/nsab127

Cheng, W., Rolls, E. T., Ruan, H., and Feng, J. (2018). Functional connectivities in the brain that mediate the association between depressive problems and sleep quality. *JAMA Psychiatry*. 75, 1052–1061. doi: 10.1001/jamapsychiatry.2018.1941

Cole, M. W., and Schneider, W. (2007). The cognitive control network: Integrated cortical regions with dissociable functions. *Neuroimage* 37, 343–360. doi: 10.1016/j.neuroimage.2007.03.071

Deligiannidis, K. M., Fales, C. L., Kroll-Desrosiers, A. R., Shaffer, S. A., Villamarin, V., Tan, Y., et al. (2019). Resting-state functional connectivity, cortical GABA, and neuroactive steroids in peripartum and peripartum depressed women: a functional magnetic resonance imaging and spectroscopy study. *Neuropsychopharmacology* 44, 546–554. doi: 10.1038/s41386-018-0242-2

Deligiannidis, K. M., Sikoglu, E. M., Shaffer, S. A., Frederick, B., Svenson, A. E., Kopoyan, A., et al. (2013). GABAergic neuroactive steroids and resting-state functional connectivity in postpartum depression: a preliminary study. *J. Psychiatr Res*. 47, 816–828. doi: 10.1016/j.jpsychires.2013.02.010

Dionisio, S., Mayoglou, L., Cho, S. M., Prime, D., Flanigan, P. M., Lega, B., et al. (2019). Connectivity of the human insula: a cortico-cortical evoked potential (CCEP) study. *Cortex* 120, 419–442. doi: 10.1016/j.cortex.2019.05.019

Disner, S. G., Beevers, C. G., Haigh, E. A., and Beck, A. T. (2011). Neural mechanisms of the cognitive model of depression. *Nat. Rev. Neurosci*. 12, 467–477. doi: 10.1038/nrn3027

Dolan, R. J., Bench, C. J., Liddle, P. F., Friston, K. J., Frith, C. D., Grasby, P. M., et al. (1993). Dorsolateral prefrontal cortex dysfunction in the major psychoses; symptom or disease specificity? *J. Neurol. Neurosurg. Psychiatry*. 56, 1290–1294. doi: 10.1136/jnnp.56.12.1290

Duan, C., Cosgrove, J., and Deligiannidis, K. M. (2017). Understanding peripartum depression through neuroimaging: a review of structural and functional connectivity and molecular imaging research. *Curr. Psychiatry Rep*. 19, 70. doi: 10.1007/s11920-017-0824-4

Eichenbaum, H. (2013). Hippocampus: remembering the choices. *Neuron*. 77, 999–1001. doi: 10.1016/j.neuron.2013.02.034

Fiorelli, M., Aceti, F., Marini, I., Giacchetti, N., Macci, E., Tinelli, E., et al. (2015). Magnetic resonance imaging studies of postpartum depression: an overview. *Behav. Neurol*. 2015, 913843. doi: 10.1155/2015/913843

Frank, D. W., Dewitt, M., Hudgens-Haney, M., Schaeffer, D. J., Ball, B. H., Schwarz, N. F., et al. (2014). Emotion regulation: quantitative meta-analysis of functional activation and deactivation. *Neurosci. Biobehav. Rev*. 45, 202–211. doi: 10.1016/j.neubiorev.2014.06.010

Gress-Smith, J. L., Luecken, L. J., Lemery-Chalfant, K., and Howe, R. (2012). Postpartum depression prevalence and impact on infant health, weight, and sleep in low-income and ethnic minority women and infants. *Matern Child Health J*. 16, 887–893. doi: 10.1007/s10995-011-0812-y

Hao, Z. Y., Zhong, Y., Ma, Z. J., Xu, H. Z., Kong, J. Y., Wu, Z., et al. (2020). Abnormal resting-state functional connectivity of hippocampal subfields in patients with major depressive disorder. *BMC Psychiatry*. 20, 71. doi: 10.1186/s12888-020-02490-7

Ho, T. C., Connolly, C. G., and Henje Blom, E. (2015). Emotion-dependent functional connectivity of the default mode network in adolescent depression. *Biol. Psychiatry*. 78, 635–646. doi: 10.1016/j.biopsych.2014.09.002

Hugdahl, K., Raichle, M. E., Mitra, A., and Specht, K. (2015). On the existence of a generalized non-specific task-dependent network. *Front Hum. Neurosci*. 9, 430. doi: 10.3389/fnhum.2015.00430

Iwabuchi, S. J., Peng, D., Fang, Y., Jiang, K., Liddle, E. B., Liddle, P. F., et al. (2014). Alterations in effective connectivity anchored on the insula in major depressive disorder. *Eur. Neuropsychopharmacol*. 24, 1784–1792. doi: 10.1016/j.euroneuro.2014.08.005

Ji, L., Meda, S. A., Tamminga, C. A., Clementz, B. A., Keshavan, M. S., Sweeney, J. A., et al. (2020). Characterizing functional regional homogeneity (ReHo) as a B-SNIP psychosis biomarker using traditional and machine learning approaches. *Schizophr. Res*. 215, 430–438. doi: 10.1016/j.schres.2019.07.015

Jiang, L., and Zuo, X. N. (2016). Regional homogeneity: a multimodal, multiscale neuroimaging marker of the human connectome. *Neuroscientist*. 22, 486–505. doi: 10.1177/1073858415595004

Lai, C. H. (2018). The regional homogeneity of cingulate-precuneus regions: the putative biomarker for depression and anxiety. *J. Affect Disord*. 229, 171–176. doi: 10.1016/j.jad.2017.12.086

Laurent, H. K., and Ablow, J. C. (2012a). The missing link: mothers' neural response to infant cry related to infant attachment behaviors. *Infant Behav Dev*. 35, 761–772. doi: 10.1016/j.infbeh.2012.07.007

Laurent, H. K., and Ablow, J. C. A. (2012b). cry in the dark: depressed mothers show reduced neural activation to their own infant's cry. *Soc. Cogn. Affect Neurosci*. 7, 125–134. doi: 10.1093/scan/nsq091

Lindahl, V., Pearson, J. L., and Colpe, L. (2005). Prevalence of suicidality during pregnancy and the postpartum. *Arch. Womens Ment. Health*. 8, 77–87. doi: 10.1007/s00737-005-0080-1

Liu, S., Erkkinen, M. G., Healey, M. L., Xu, Y., Swett, K. E., Chow, H. M., et al. (2015). Brain activity and connectivity during poetry composition: toward a multidimensional model of the creative process. *Hum. Brain Mapp*. 36, 3351–3372. doi: 10.1002/hbm.22849

Liu, Y., Bengson, J., Huang, H., Mangun, G. R., and Ding, M. (2016). Top-down modulation of neural activity in anticipatory visual attention: control mechanisms revealed by simultaneous EEG-fMRI. *Cereb. Cortex*. 26, 517–529. doi: 10.1093/cercor/bhu204

Liu, Z., Xu, C., Xu, Y., Wang, Y., Zhao, B., Lv, Y., et al. (2010). Decreased regional homogeneity in insula and cerebellum: a resting-state fMRI study in patients with major depression and subjects at high risk for major depression. *Psychiatry Res*. 182, 211–215. doi: 10.1016/j.pscychresns.2010.03.004

Logothetis, N. K., Pauls, J., Augath, M., Trinath, T., and Oeltermann, A. (2001). Neurophysiological investigation of the basis of the fMRI signal. *Nature* 412, 150–157. doi: 10.1038/35084005

Mayberg, H. S. (1997). Limbic-cortical dysregulation: a proposed model of depression. *J. Neuropsychiatry Clin. Neurosci*. 9, 471–481. doi: 10.1176/jnp.9.3.471

Mayberg, H. S., Liotti, M., Brannan, S. K., McGinnis, S., Mahurin, R. K., Jerabek, P. A., et al. (1999). Reciprocal limbic-cortical function and negative mood: converging PET findings in depression and normal sadness. *Am. J. Psychiatry*. 156, 675–682. doi: 10.1176/ajp.156.5.675

Mor, N., and Winquist, J. (2002). Self-focused attention and negative affect: a meta-analysis. *Psychol Bull*. 128, 638–662. doi: 10.1037/0033-2909.128.4.638

Moses-Kolko, E. L., Perlman, S. B., Wisner, K. L., James, J., Saul, A. T., Phillips, M. L., et al. (2010). Abnormally reduced dorsomedial prefrontal cortical activity and effective connectivity with amygdala in response to negative emotional faces in postpartum depression. *Am. J. Psychiatry*. 167, 1373–1380. doi: 10.1176/appi.ajp.2010.09081235

Niendam, T. A., Laird, A. R., Ray, K. L., Dean, Y. M., Glahn, D. C., Carter, C. S., et al. (2012). Meta-analytic evidence for a superordinate cognitive control network

subserving diverse executive functions. *Cogn. Affect Behav. Neurosci*. 12, 241–268. doi: 10.3758/s13415-011-0083-5

Nieuwenhuys, R. (2012). The insular cortex: a review. *Prog. Brain Res*. 195, 123–163. doi: 10.1016/B978-0-444-53860-4.00007-6

Pawluski, J. L., Lonstein, J. S., and Fleming, A. S. (2017). The neurobiology of postpartum anxiety and depression. *Trends Neurosci*. 40, 106–120. doi: 10.1016/j.tins.2016.11.009

Power, J. D., Barnes, K. A., Snyder, A. Z., Schlaggar, B. L., and Petersen, S. E. (2012). Spurious but systematic correlations in functional connectivity MRI networks arise from subject motion. *Neuroimage* 59, 2142–2154. doi: 10.1016/j.neuroimage.2011.10.018

Rahnev, D., Nee, D. E., Riddle, J., Larson, A. S., and D'Esposito, M. (2016). Causal evidence for frontal cortex organization for perceptual decision making. *Proc. Natl. Acad. Sci. U. S. A*. 113, 6059–6064. doi: 10.1073/pnas.1522551113

Sevel, L. S., Letzen, J. E., Staud, R., and Robinson, M. E. (2016). Interhemispheric dorsolateral prefrontal cortex connectivity is associated with individual differences in pain sensitivity in healthy controls. *Brain Connect*. 6, 357–364. doi: 10.1089/brain.2015.0405

Silverman, M. E., Loudon, H., Liu, X., Mauro, C., Leiter, G., Goldstein, M. A., et al. (2011). The neural processing of negative emotion postpartum: a preliminary study of amygdala function in postpartum depression. *Arch. Womens Ment. Health*. 14, 355–359. doi: 10.1007/s00737-011-0226-2

Silverman, M. E., Loudon, H., Safier, M., Protopopescu, X., Leiter, G., Liu, X., et al. (2007). Neural dysfunction in postpartum depression: an fMRI pilot study. *CNS Spectr*. 12, 853–862. doi: 10.1017/S1092852900015595

Stickel, S., Wagels, L., Wudarczyk, O., Jaffee, S., Habel, U., Schneider, F., et al. (2019). Neural correlates of depression in women across the reproductive lifespan - An fMRI review. *J. Affect Disord*. 246, 556–570. doi: 10.1016/j.jad.2018.12.133

Utevsky, A. V., Smith, D. V., and Huettel, S. A. (2014). Precuneus is a functional core of the default-mode network. *J. Neurosci*. 34, 932–940. doi: 10.1523/JNEUROSCI.4227-13.2014

Wonch, K. E., de Medeiros, C. B., Barrett, J. A., Dudin, A., Cunningham, W. A., Hall, G. B., et al. (2016). Postpartum depression and brain response to infants: differential amygdala response and connectivity. *Soc. Neurosci*. 11, 600–617. doi: 10.1080/17470919.2015.1131193

Xiao, H., Yuan, M., Li, H., Li, S., Du, Y., Wang, M., et al. (2021). Functional connectivity of the hippocampus in predicting early antidepressant efficacy in patients with major depressive disorder. *J. Affect Disord*. 291, 315–321. doi: 10.1016/j.jad.2021.05.013

Xiao-Juan, W., Jian, W., Zhi-Hong, L., Yan, M., and Shi-Wei, Z. (2011). Increased posterior cingulate, medial frontal and decreased temporal regional homogeneity in depressed mothers. a resting-state functional magnetic resonance study. *Procedia. Environ. Sci*. 8, 737–43. doi: 10.1016/j.proenv.2011.10.112

Xiong, G., Dong, D., Cheng, C., Jiang, Y., Sun, X., He, J., et al. (2019). State-independent and -dependent structural alterations in limbic-cortical regions in patients with current and remitted depression. *J Affect Disord*. 258, 1–10. doi: 10.1016/j.jad.2019.07.065

Yang, X., Ma, X., Li, M., Liu, Y., Zhang, J., Huang, B., et al. (2015). Anatomical and functional brain abnormalities in unmedicated major depressive disorder. *Neuropsychiatr Di.s Treat*. 11, 2415–2423. doi: 10.2147/NDT.S93055

Yao, Z., Wang, L., Lu, Q., Liu, H., and Teng, G. (2009). Regional homogeneity in depression and its relationship with separate depressive symptom clusters: a resting-state fMRI study. *J. Affect Disord*. 115, 430–438. doi: 10.1016/j.jad.2008.10.013

Zang, Y., Jiang, T., Lu, Y., He, Y., and Tian, L. (2004). Regional homogeneity approach to fMRI data analysis. *Neuroimage* 22, 394–400. doi: 10.1016/j.neuroimage.2003.12.030

Zhang, B., Qi, S., Liu, S., Liu, X., Wei, X., Ming, D., et al. (2021). Altered spontaneous neural activity in the precuneus, middle and superior frontal gyri, and hippocampus in college students with subclinical depression. *BMC Psychiatry*. 21, 280. doi: 10.1186/s12888-021-03292-1

Zhang, S., Wang, W., Wang, G., Li, B., Chai, L., Guo, J., et al. (2020). Aberrant resting-state interhemispheric functional connectivity in patients with postpartum depression. *Behav. Brain Res*. 382, 112483. doi: 10.1016/j.bbr.2020.112483

Frontiers in
Human Neuroscience

Bridges neuroscience and psychology to understand the human brain

The second most-cited journal in the field of psychology, that bridges research in psychology and neuroscience to advance our understanding of the human brain in both healthy and diseased states.

Discover the latest Research Topics

See more →

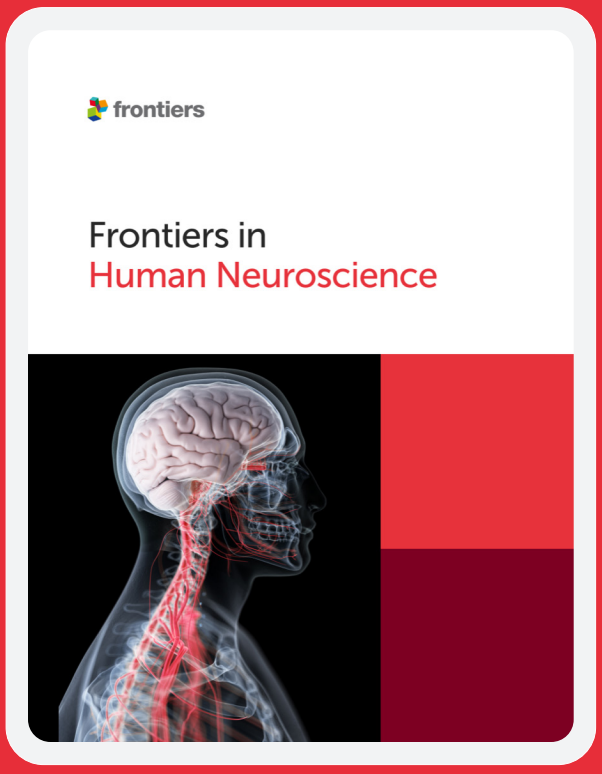

Frontiers

Avenue du Tribunal-Fédéral 34
1005 Lausanne, Switzerland
frontiersin.org

Contact us

+41 (0)21 510 17 00
frontiersin.org/about/contact